Third International Conference of Mathematics and its Applications

(TICMA 2022)

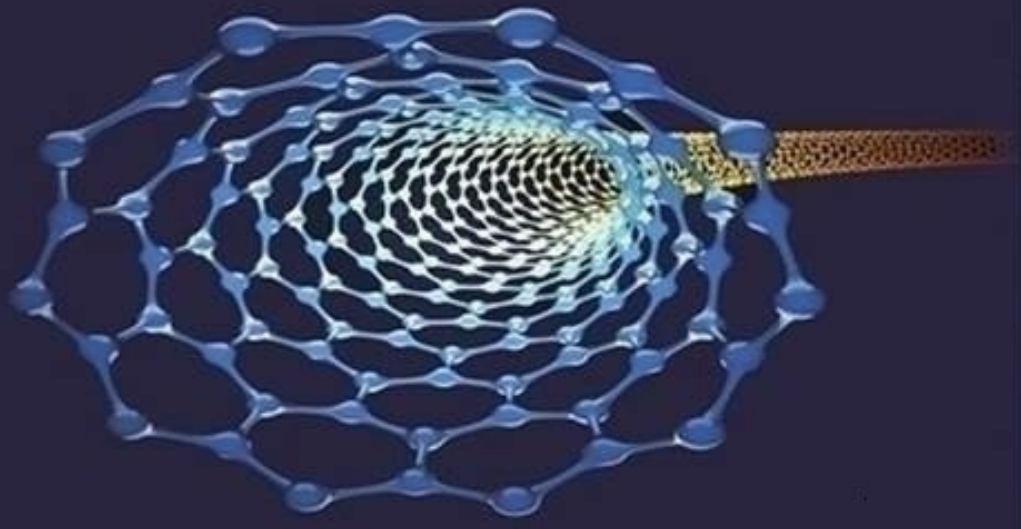

زانکۆی سەلاحەدین - هەولێر
Salahaddin University-Erbil

College of science / Mathematics Department

29-31 August 2022

ZANCO Journal of Pure and Applied Sciences

ZANCO

Journal of Pure and Applied Sciences

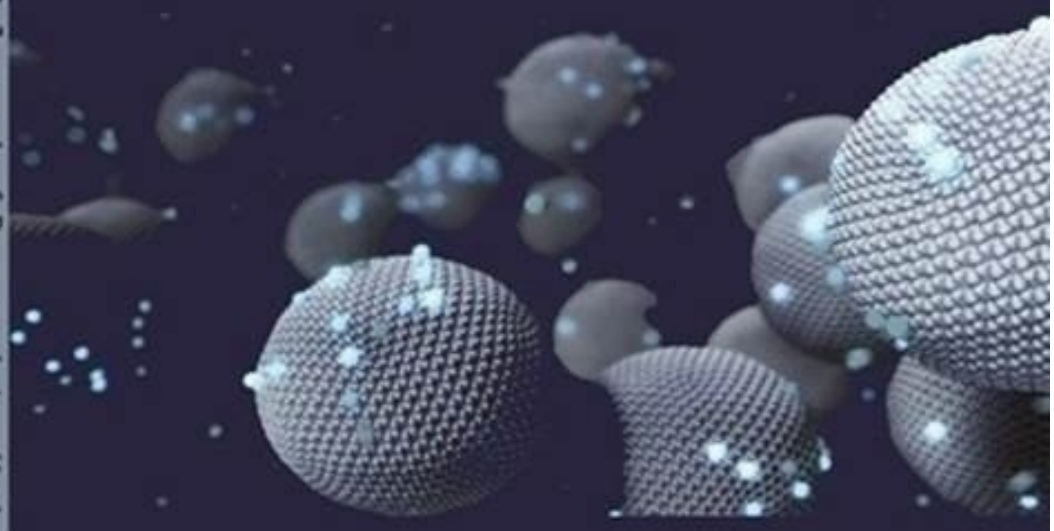

زانکۆی سەلاحەدین - هەولێر
Salahaddin University-Erbil

College of science / Mathematics Department

29-31 August 2022

Proceeding of 3rd International Conference of Mathematics and its Applications TICMA2022
https://conferences.su.edu.krd/su/ticma2022/
DOI: https://doi.org/10.31972/ticma2022

RESEARCH PAPER

Extended-Cyclic Operators

Nareen Bamerni*
Department of Mathematics, University of Duhok, Kurdistan Region, Iraq

A B S T R A C T:
In this paper, we study new classes of operators on separable Banach spaces which are called extended-cyclic operators and extended-transitive operators. We study some properties of their vectors which are called extended-cyclic vectors. We show that if x is an extended-cyclic vector for T, then $T^n x$ is also an extended-cyclic vector for T for all $n \in \mathbb{N}$. Then, we show the extended-cyclicity is preserved under qsuasi-similarity. Moreover, we prove that an operator is extended-cyclic if and only if it is extended-transitive. As a consequence, the set of all extended-cyclic vectors is a dense and G_δ set. Finally, we find some spectral properties of these operators. Particularly, the point spectrum of the adjoint of an extended-cyclic operator has at most one element of modules greater than one. Moreover, if the spectrum of an operator has a connected component subset of $B_0(1)$, then T is not extended-cyclic.

KEY WORDS: Extended-Cyclic, Banach spaces, G_δ set.
DOI: https://doi.org/10.31972/ticma22.01

1. INTRODUCTION:

Nowadays the area of linear dynamics is being interested by many researchers due to its connection with the two of the biggest open problems in mathematics which are invariant subspace problem and invariant subset problem. This connection will be clarified in the sequel.

In this paper, we use X to denote a separable infinite dimensional Banach space over scalar field $\mathbb{C}$ unless otherwise stated. Moreover, we use $\mathcal{B}(X)$ to denote the operator algebra consisting of all continuous linear operators $T: X \to X$.

A vector x is said to be cyclic for an operator $T \in \mathcal{B}(X)$ if the linear span of the orbit $span\text{Orb}\,(T,x) = \text{span}\{T^n x: n \in \mathbb{N}\}$ is dense in X , and T is called cyclic if it has a cyclic vector.

A vector x is said to be hypercyclic for an operator $T \in \mathcal{B}(X)$ if the orbit $\text{Orb}\,(T,x) = \{T^n x: n \in \mathbb{N}\}$ is dense in$X$, and T is called hypercyclic it has a hypercyclic vector. The study of hypercyclic operators can be traced back to the work of Birkhoff [1] in 1922 on the Frechet space $H(\mathbb{C})$ of entire functions. However, the first example of hypercyclic operators on Banach spaces was constructed by Rolewicz [2] who showed that if T is the unilateral backward shift on the sequence space $\ell^p(\mathbb{N})$ and if c is a scalar with $|c| \leq 1$, then cT is not hypercyclic.

Note that T has no nontrivial closed invariant subspace (resp. subset) if and only if every nonzero vector is cyclic (resp. hypercyclic) for T. This establishes the connection between these concepts and invariant subspace (resp. subset) problem and invariant subset problem.

The supercyclicity origin goes back to 1972 paper of Hilden and Wallen, [3] and it has widely studied since then. A vector x is said to be supercyclic if the scaled orbit $\mathbb{C}Orb(T,x) = \{\alpha T^n x: \alpha \in \mathbb{C}, n \in \mathbb{N}\}$ is dense in X, and T is called supercyclic if it has a supercyclic vector.

*** Corresponding Author: Nareen Bamerni**
E-mail: nareen_bamerni@yahoo.com
Article History:
Received: 01/08/2022
Accepted: 15/09/2022
Published: 07/12/2022

DOI: https://doi.org/10.31972/ticma2022

Based on Rolewicz example the disk cyclicity notion was defined by Zeana in 2002 by the same manner [4]. A vector $x \in X$ is called diskcyclic if the disk orbit $\mathbb{D}Orb(T,x) = \{\alpha T^n x : \alpha \in \mathbb{D}, n \geq \mathbb{N}\}$ is dense in X and in this case T is called diskcyclic operator. Good references to learn about hypercyclicity, supercyclicity and disk cyclicity are [5], [6], [7] and [8].

In this paper, we extend the disk cyclicity concept; that is, instead of the closed unit disk we use the closed disk $D_r(0)$ of radius $r \geq 1$ and centered at zero, and we call it extended-cyclic.

First, we find some basic properties of extended-cyclic operators and their vectors. We show that the positive integer powers of an extended-cyclic operator T are also extended-cyclic. We study the extended-cyclicity of similar and quasi-similar operators.

Second, we define extended-transitivity concept and prove that extended-transitive operators are equivalent to extended-cyclic ones. Moreover, we establish an extended-cyclic criterion for an operator to be extended-transitive. Then, we use this result to find an example of an extended-cyclic operator which is not diskcyclic.

Finally, we study the spectral properties of these operators. We show that if T is extended-cyclic, then T^* has at most one eigenvalue of modules greater than 1. On the other hand, the spectrum of an extended-cyclic operator cannot have a component in the open unit ball.

2.MAIN RESULTS:

First, we define extended-cyclicity notion which is an intermediate concept between diskcyclicity and supercyclicity.

Definition 1. Let $T \in \mathcal{B}(X)$, then T is called extended-cyclic operator if there exist $x \in X$ such that the extended- orbit (E-orbit, for short) of x, EOrb $(T,x) = \{\alpha T^n(x) : \alpha \in D_r(0), n \in \mathbb{N}\}$ is dense in X. In this case, x is called extended-cyclic vector for T.

In what follows, we denote the set of all extended-cyclic vectors for T by $EC(T)$ and the set of all extended-cyclic operators on $\mathcal{B}(X)$ by $EC(X)$.

Remark:

1. Every diskcyclic operator is extended-cyclic;
2. Every extended-cyclic is supercyclic.

We need the following lemma to prove the next proposition.

Lemma 1. If x is an extended-cyclic vector for T, then

$$inf\{\lambda\|T^n x\| : n \geq 0, \lambda \in D_r(0)\} = 0$$
$$\sup\{\|T^n x\| : n \geq 0\} = \infty$$

Proof: We have $\lambda \in D_r(0)$, then it follows that $\inf\{\lambda\|T^n x\| : n \geq 0\} = 0$. First we will show that $\sup\{\lambda\|T^n x\| : n \geq 0, \lambda \in D_r(0)\} = \infty$. By contradiction, suppose that

$$\sup\{\lambda\|T^n x\| : n \geq 0, \lambda \in D_r(0)\} = k, k \in \mathbb{R}$$

and $z \in X$ such that $\| z \| > k$. Since $T \in EC(X)$, then there exist two sequences $\{n_k\} \in \mathbb{N}$ and $\{\lambda_k\} \in D_r(0)$ such that $\lambda_k T^{n_k} x \to z$. It follows that $\| z \| \leq k$ which is contradiction. Now, we have

$$\begin{aligned} \infty &= \sup\{\lambda\|T^n x\| : n \geq 0, \lambda \in D_r(0)\} \\ &\leq r\sup\{\|T^n x\| : n \geq 0\} \end{aligned}$$

It follows that

$$\sup\{\|T^n x\| : n \geq 0\} = \infty.$$

Proposition 1. Let $T \in \mathcal{B}(X)$ and $\| T \| < 1$, then T is not extended-cyclic.

Proof: Suppose that T is an extended-cyclic operator and $x_0 \in EC(T)$. By Lemma 1, we have $\sup\{\|T^n x_0\| : n \geq 0\} = \infty$ that is $\|T^m x_0\| > k$ for some $m \in \mathbb{N}$ and all $k \in \mathbb{R}^+$. Since $\| T \| < 1$ then,

$$k \leq \|T^m x_0\| \leq \|T^m\|\|x_0\| \leq \| T \|^m \|x_0\| \leq \|x_0\|$$

for all $k \in \mathbb{R}^+$which means that $\|x_0\| = \infty$ a contradiction to the assumption that $x_0 \in EC(T)$. Therefore, T is not extended-cyclic.

https://conferences.su.edu.krd/su/ticma2022/
DOI: https://doi.org/10.31972/ticma2022

Example 1. If $T \in \ell^p(\mathbb{N})$ is the backward shift operator. Then αT is not extended-cyclic for all $\alpha \in \mathbb{C}; |\alpha| \leq 1$.
Proof: Since $\| T \| \leq 1$ then $\| \alpha T \| \leq |\alpha| < 1$. It follows that αT is not extended-cyclic.

Proposition 2. If $T \in EC(X)$ and $S \in \mathcal{B}(X)$ be an operator with dense range. If T commutes with S and $x \in EC(T)$ then $Sx \in EC(T)$
Proof: Since $x \in EC(T)$, then

$$\begin{aligned}\overline{\text{EOrb}\,(T, Sx)} &= \overline{\{\alpha T^n Sx : \alpha \in D_r(0), n \geq 0\}} \\ &= \overline{\{\alpha S T^n x : \alpha \in D_r(0), n \geq 0\}} \\ &= \overline{S\{\alpha T^n x : \alpha \in D_r(0), n \geq 0\}} \\ &\supseteq S\left(\overline{\{\alpha T^n x : \alpha \in D_r(0), n \geq 0\}}\right) \\ &= S(X).\end{aligned}$$

Thus $E\text{Orb}\,(T, Sx)$ is dense in X and hence $Sx \in EC(T)$. From the last proposition one can easily deduce that if an operator has one extended-cyclic vector, then it has many extended-cyclic vectors. In other words, we have the following two corollaries

Corollary 1. If x is an extended-cyclic vector for T, then $T^n x$ is also an extended-cyclic vector for T for all $n \in \mathbb{N}$.

Corollary 2. If T is an extended-cyclic operator, then it has a dense range.

Let $T \in \mathcal{B}(X)$ and $S \in \mathcal{B}(Y)$, then T and S are called quasi-similar if there exists an operator $f: X \to Y$ with dense range such that $Sf = fT$. If f is a homeomorphism, then T and S are called similar. The following proposition shows that the extended-cyclicity is preserved under quasi-similarity.

Proposition 3. Let T and S be quasi-similar, and let $T \in EC(X)$ then $S \in EC(Y)$. Moreover, $f(EC(T)) \subset EC(S)$.
Proof: Since T and S are quasi-similar, then there exists an operator $f: X \to Y$ with dense range such that $Sf = fT$. Let A be a non-empty subset of Y, then $f^{-1}(A)$ is also open and non-empty.

Now, let $x \in EC(T)$, then there exists $\alpha \in D_r(0), n \in \mathbb{N}$ such that $\alpha T^n x \in f^{-1}(A)$ which means that $\alpha f(T^n x) \in A$. It follows that $\alpha S(fx) = \alpha f(Tx) \in A$; that is, $\text{EOrb}\,(S, fx)$ intersects every open sets in Y and so it is dense in Y. It follows that $S \in EC(Y)$ and $fx \in EC(S)$.

Corollary 3. Let T and S be similar, then $T \in EC(X)$ if and only if $S \in EC(Y)$. Moreover, $f(EC(T)) \subset EC(S)$.

Proposition 4. Let $\{X_i\}_{i=1}^n$ be a family of Banach spaces and $T_i \in \mathcal{B}(X_i)$ for all $1 \leq i \leq n$. If $\oplus T_i$ is extended-cyclic in $\oplus X_i$ then T_i is extended-cyclic in X_i for all $1 \leq i \leq n$.
Proof: Since $\oplus T_i$ is quasi-similar to $T_k; 1 \leq k \leq n$ then the proof follows by Proposition 3.
The following theorem shows that the set of all extended-cyclic vectors for an operator can be written as a countable intersection of open sets.

Theorem 1. Let T be an extended-cyclic operator, then

$$EC(T) = \bigcap_k \left(\bigcup_{\lambda \in D_r(0)} \bigcup_n T^{-n}\left(\frac{1}{\lambda} B_k\right) \right)$$

where $\{B_k\}$ is a countable open basis for X. Moreover, $EC(T)$ is a G_δ set.

DOI: https://doi.org/10.31972/ticma2022

Proof: First, we will show that $EC(T) \subseteq \bigcap_k \left(\bigcup_{\lambda\in D_r(0)} \bigcup_n T^{-n}\left(\frac{1}{\lambda}B_k\right)\right)$. Let $x \in EC(T)$ then $\{\lambda T^n x : n \geq 0, \lambda \in D_r(0)\}$ is dense in X and so for each $k > 0$, there exist $\lambda \in D_r(0)$, and $n \in \mathbb{N}$ such that $\lambda T^n x \in B_k$. It follows that $x \in \bigcap_k \left(\bigcup_{\lambda\in D_r(0)} \bigcup_n T^{-n}\left(\frac{1}{\lambda}B_k\right)\right)$ and so $EC(T) \subseteq \bigcap_k \left(\bigcup_{\lambda\in D_r(0)} \bigcup_n T^{-n}\left(\frac{1}{\lambda}B_k\right)\right)$. The proof of the second inclusion is just the reverse of the former. Therefore, we get

$$EC(T) = \bigcap_k \left(\bigcup_{\lambda\in D_r(0)} \bigcup_n T^{-n}\left(\frac{1}{\lambda}B_k\right)\right)$$

Since $EC(T)$ can be written as a countable intersection of open sets, then $EC(T)$ is a G_δ set.

Now, we define extended-transitive operators. Then we find its relation with extended-cyclic operators in order to find some more properties of extended-cyclic operators.

Definition 2. A bounded linear operator $T: X \to X$ is called extended-transitive if for any pair U, V of nonempty open subsets of X, there exist $\lambda \in D_r(0)$, and $n \geq 0$ such that $T^n(\lambda U) \cap V \neq \phi$ or equivalently, $T^{-n}(\frac{1}{\lambda}U) \cap V \neq \phi$.

Proposition 5. An operator T is extended-transitive if and only if $EC(T)$ is dense in X.

Proof: By Theorem 1, we have $EC(T) = \bigcap_k \left(\bigcup_{\lambda\in D_r(0)} \bigcup_n T^{-n}(\lambda B_k)\right)$. Suppose that $G_k = \bigcup_{\lambda\in D_r(0)} \bigcup_n T^{-n}(\lambda B_k)$, then by Baire Theorem $EC(T)$ is dense if and only if each open set $G_k = \bigcup_{\lambda\in D_r(0)} \bigcup_n T^{-n}(\lambda B_k)$ is dense; i.e, if and only if for each non-empty open set U and any $k \in \mathbb{N}$ there exist n and $\lambda \in D_r(\mathbf{0})$ such that $U \cap T^{-n}(\lambda B_k) \neq \phi$ if and only if T is extended-transitive.

Theorem 2. An operator $T \in \mathcal{B}(X)$ is extended-cyclic if and only if it is extended-transitive.

Proof: Let T be extended-transitive. By Proposition 5, EC (T) is a dense set and so T is extended-cyclic. Conversely, let T be extended-cyclic, and let U and V be two open sets. By the density of the E-orbit of T there exist an $\lambda \in D_r(0)$ and $p \in \mathbb{N}$ such that $\lambda T^p x \in U$. Also one can find $\beta \in D_r(0), s \in \mathbb{N}$, such that $s \geq p, |\beta| \leq r|\lambda|$ and $\beta T^s x \in V$. Thus, $(\beta/\lambda)T^{s-p}U \cap V \neq \phi$. It follows that T is extended-transitive.

The following two propositions give some necessary and sufficient conditions for an operators to be extended-transitive.

Proposition 6. Let $T \in \mathcal{B}(X)$. The following statements are equivalent.

1 T is extended-transitive.
2 For each $x, y \in X$, there exist sequences $\{x_k\}$ in $X, \{n_k\}$ in $\mathbb{N}$, and $\{\alpha_k\}$ in $D_r(0)$ such that $x_k \to x$ and $T^{n_k}\alpha_k x_k \to y$.
3 For each $x, y \in X$ and each neighborhood W of 0, there exist $z \in X, n \in \mathbb{N}$, and $\alpha \in D_r(0)$ such that $x - z \in W$ and $T^n \alpha z - y \in W$.

Proof: $1 \Rightarrow 2$: Let $x, y \in X$. For all $k \geq 1$, let $U_k = \mathbb{B}(x, 1/k), V_k = \mathbb{B}(y, 1/k)$. Then both U_k and V_k are non-empty open sets in X. Since T is extended-transitive, there exist $n_k \in \mathbb{N}, \alpha_k \in D_r(0)$ such that $\alpha_k T^{n_k} U_k \cap V_k \neq \phi$. So, for all $k \geq 1$ there exists $x_k \in U_k$ such that $\alpha_k T^{n_k} x_k \in V_k$ which means that $\|x_k - x\| < 1/k$ and $\|T^{n_k}\alpha_k x_k - y\| < 1/k$ for all $k \geq 1$. It follows that $x_k \to x$ and $T^{n_k}\alpha_k x_k \to y$.

$2 \Rightarrow 3$: Follows directly by taking $z = x_k$ for a large enough $k \in \mathbb{N}$.

$3 \Rightarrow 1$: Let U and V be two non-empty open subsets of X, and let $x \in U$ and $y \in V$. Suppose that $W_k = B\left(0, \frac{1}{k}\right)$ is a neighborhood for 0 for all $k \geq 1$. Then, there exist $z_k \in X, n_k \in \mathbb{N}, \alpha_k \in D_r(0)$ such that $x - z_k \in W_k$ and $T^{n_k}\alpha_k z_k - y \in W_k$. This implies that $z_k \in U$ and $T^{n_k}\alpha_k z_k \in V$ which follows $T^{n_j}\alpha_j z_j U \cap V \neq \phi$ for some $j \in \mathbb{N}$ and so T is extended-transitive.

Proposition 7. An operator $T \in \mathcal{B}(X)$ is extended-cyclic if and only if the set $\{(x, \lambda T^n x) : x \in X, n \geq 0, \lambda \in D_r(0)\}$ is dense in $X \oplus X$.

https://conferences.su.edu.krd/su/ticma2022/
DOI: https://doi.org/10.31972/ticma2022

Proof: Let $(a,b) \in X \oplus X$ and $\epsilon > 0$. Since $T \in EC(X)$, then there exist $c \in X, m \geq 0$ and $\lambda \in D_r(0)$ such that $\| c - a \| \leq \frac{\epsilon}{2}$ and $\|\lambda T^n c - b\| \leq \frac{\epsilon}{2}$. It follows that

$$\|(c, \lambda T^n c) - (a,b)\| = \|(c-a, \lambda T^n c - b)\| = \| (c-a) \| + \|(\lambda T^n c - b)\| \leq \epsilon$$

Conversely: Let $a, b \in X$. By hypothesis, there exist sequences $c_k \in X, \lambda_k \in D_r(0)$ and $n_k \in \mathbb{N}$ such that $(c_k, \lambda_k T^{n_k} c_k) \to (a,b)$ as $k \to \infty$. Therefore, there exist a large number $m \in \mathbb{N}$ and $\epsilon > 0$ such that $\|(c_k, \lambda_k T^{n_k} c_k) - (a,b)\| \leq \epsilon$ for all $k \geq m$ which means $\|c_k - a\| \leq \epsilon$ and $\|\lambda_k T^{n_k} c_k - b\| \leq \epsilon$ that is $c_k \to a$ and $\lambda_k^{n_k} c_k \to b$ as $k \to \infty$, Hence T is extended-cyclic.

Proposition 8. Let $T \in \mathcal{B}(X)$ and W be a 0-neighborhood in X, and let U and V be two nonempty open sets in X. If there exist $n \geq 0, \lambda \in D_r(0)$ such that $\lambda T^n U \cap W \neq \phi$ and $\lambda T^n W \cap V \neq \phi$, then T is extended-cyclic.
Proof: Let $x, y \in X$, and let $A_k = B_{\frac{1}{k}}(x)$ and $B_k = B_{\frac{1}{k}}(y)$ for all $k \geq 1$. By hypothesis, there exist sequences $n_k \in \mathbb{N}, \lambda_k \in D_r(0)$ and $w_k \in W$ such that $z_k \in A_k$ and $\lambda_k T^{n_k} z_k \in W$ and $\lambda_k T^{n_k} w_k \in B_k$ for all $k \geq 1$. Therefore,

$$z_k \to x, \text{ and } \lambda_k T^{n_k} z_k \to 0$$

and

$$w_k \to 0, \text{ and } \lambda_k T^{n_k} w_k \to y$$

By taking $x_k = z_k + w_k$ the proof is completed.

Definition 3. An operator $T \in \mathcal{B}(X)$ is said to be satisfied extended-cyclic criterion if there exist two dense sets A and B in X, a sequence n_k of positive integers, a sequence $\lambda_k \in D_r(0)$ and a map $S: B \to X$ such that

1 $\lambda_k T^{n_k} x \to 0$ for all $a \in A$,
2 $\frac{1}{\lambda_k} S^{n_k} y \to 0$ for all $b \in B$,
3 $T^{n_k} S^{n_k} y \to y$ for all $b \in B$

The following theorem gives a sufficient condition for an operator to be extended-cyclic. Then, we use this theorem to find an example of an extended-cyclic operator.

Theorem 3. If $T \in \mathcal{B}(X)$ satisfies extended-cyclic criterion, then T is extended-cyclic.
Proof: Let U and V be two nonempty open sets. Since A and B are dense sets then there exist a and b in X such that $a \in A \cap U$ and $b \in B \cap V$. Consider the sets

$$c_k = a + \frac{1}{\lambda_k} S^{n_k} b \ldots . (1)$$

for all $k \geq 1$. By hypothesis, we have $\frac{1}{\lambda_k} S^{n_k} b \to 0$ as $k \to \infty$ and so $c_k \to a$ which follows that $c_k \in G$ for all $k \geq k_1; k_1 \in \mathbb{N}$. Using Equation (1), we get $\lambda_k T^{n_k} c_k = \lambda_k T^{n_k} a + T^{n_k} S^{n_k} b$. Again, by hypothesis, we have $\lambda_k T^{n_k} c_k \to b$ as $k \to \infty$. It follows that $\lambda_k T^{n_k} c_k \in V$ for all $k \geq k_2; k_2 \in \mathbb{N}$; and so, $\lambda_k T^{n_k} U \cap V \neq \phi$ for some $k \geq \max\{k_1, k_2\}$. Therefore, T is extended-transitive and so extended-cyclic.

We have seen in Example 1 if $T \in \ell^p(\mathbb{N})$ is the backward shift operator, then αT is not extended-cyclic whenever $\alpha \in \mathbb{C}; |\alpha| \leq 1$. However, the next example shows different thing when $|\alpha| > 1$.

Example 2. If $T \in \ell^p(\mathbb{N})$ is the backward shift operator. Then αT is extended-cyclic for all $\alpha \in \mathbb{C}; |\alpha| > 1$.
Proof: We will verify extended-cyclic criterion. Let $A = B$ be the dense sets in $\ell^p(\mathbb{N})$ consisting of all points with only finitely many non-zero coordinates. Let $n_k = n$ be the set of all nonnegative integers, $F \in \ell^p(\mathbb{N})$ be the unilateral forward shift operator and $\lambda_k = \frac{r}{\alpha} \in D_r(0)$ for some $r \in \mathbb{C}; |r| > 1$. Consider the map $S = \frac{1}{\alpha} F: B \to X$ and $T_1 = \alpha T$ then

1 $\lambda_k T_1^k x = \frac{r^k}{\alpha^k} \alpha^k T^k x \to 0$ for all $x \in A$,
2 $\frac{1}{\lambda_k} S^k y = \frac{\alpha^k}{r^k} \frac{1}{\alpha^k} F y \to 0$ for all $y \in B$,
3 $T_1^k S^k y = (\alpha T)^k \frac{1}{\alpha^k} F^k y = y$ for all $y \in B$.

https://conferences.su.edu.krd/su/ticma2022/
DOI: https://doi.org/10.31972/ticma2022

By Theorem 3, αT is extended-cyclic. The following example shows that not every extended-cyclic operator is diskcyclic

Example 3. Let $F: \ell^2(\mathbb{Z}) \to \ell^2(\mathbb{Z})$ be the bilateral forward weighted shift with the weight sequence

$$w_n = \begin{cases} 2 & \text{if } n \geq 0 \\ 5 & \text{if } n < 0 \end{cases}$$

Let $p \in \mathbb{N}; p > 2$, and let

$$\lambda_n = \begin{cases} 4^n & \text{if } n \leq p \\ \dfrac{1}{4^n} & \text{if } n > p \end{cases}$$

Then F is extended-cyclic but not diskcyclic with respect to the sequence λ_n.
Proof: We will verify extended-cyclic criterion. It is clear that $\lambda_n \in B_r(0)$ for some $r > 4^p$ and all $n \geq 1$. Let $A = \{x \in \ell^2(\mathbb{Z}): x \text{ has only finitely many non-zero coordinates }\}$ and (n) be the sequence of all non-negative integers. Let $\{e_n\}_{n\in\mathbb{Z}}$ be the canonical basis of $\ell^2(\mathbb{Z})$, and let $x \in A$. Suppose that $S = F^{-1}$ be the bilateral backward weighted shift such that $Se_n = (1/w_{n-1})e_{n-1}$. Then S has the weight sequence

$$\frac{1}{w_{n-1}} = \begin{cases} \dfrac{1}{2} & \text{if } n > 0 \\ \dfrac{1}{5} & \text{if } n \leq 0 \end{cases}$$

Without loss of generality, we will suppose that $x = e_0$ then by [b, Lemma 3.1.], if $F^n e_0 \to 0$ as $n \to \infty$ then $F^n e_k \to 0$ for all $k \in \mathbb{Z}$ and so by triangle inequality, $F^n x \to 0$. Since

$$\lim_{n\to\infty} \|\lambda_n F^n e_0\| = \lim_{n\to\infty} \left(\frac{1}{4^n} \prod_{k=1}^{n} 2 \right) = \lim_{n\to\infty} \frac{2^n}{4^n} = 0$$

Then

$$\lambda_n F^n x = 0 \text{ as } n \to \infty \text{ .....(1)}$$

Again, by [2, Lemma 3.1.], if $S^n e_0 \to 0$ as $n \to \infty$ then $S^n e_k \to 0$ for all $k \in \mathbb{Z}$ and so by triangle inequality, $S^n x \to 0$.

Now, since $\lim_{n\to\infty} \left\| \frac{1}{\lambda_n} S^n e_0 \right\| = \lim_{n\to\infty} 4^n \prod_{i=1}^{n} (1/5) = \lim_{n\to\infty} (4^n/5^n) = 0$ then

$$\frac{1}{\lambda_n} S^n x \to 0 \text{ as } n \to \infty \text{ .....(2)}$$

Then by equations (1) and (2), and the fact that $F^n S^n x = x, F$ satisfies extended-cyclic criterion with respect to the sequence λ_n and so T is extended-cyclic.

On the other hand, since $\lambda_n \notin \mathbb{D}$ then by [5, Theorem 2.6.] T is not diskcyclic with respect to λ_n. In what follows, we will suppose that X is an infinite dimensional separable Hilbert space. First, we need the following lemma.

Lemma 2. Let x be an extended-cyclic vector for T and $z \in X$. Then the set $A = \{\langle \alpha T^n x, z\rangle: n \geq 0, \alpha \in D_0(r)\}$ is dense in $\mathbb{C}$.
Proof: Let $c \in \mathbb{C}$. It is clear that the vector $\frac{cz}{\|z\|^2} \in X$. Since $T \in EC(X)$, then there exists a sequence $\alpha_k T^{n_k} x \in$ E Or $b(T, x)$ such that

$$\alpha_k T^{n_k} x \to \frac{cz}{\| z \|^2}$$

Which follows that

$$\langle \alpha_k T^{n_k} x, z\rangle \to \left\langle \frac{cz}{\| z \|^2}, z \right\rangle = \frac{c}{\| z \|^2} \langle z, z\rangle = c.$$

Therefore, the set A is dense in $\mathbb{C}$.

Theorem 4. Let T is extended-cyclic. Then T^* has at most one eigenvalue of modules greater than 1.

https://conferences.su.edu.krd/su/ticma2022/
DOI: https://doi.org/10.31972/ticma2022

Proof: Since T is extended-cyclic then it is supercyclic and so either $\sigma_p(T^*)$ contains at most one non-zero eigenvalue [9, Proposition 3.1.]. Suppose that $\sigma_p(T^*) = \{\lambda\}$. Hence, there is a unit vector $z \in X$ such that $T^*z = \lambda z$. Let $x \in EC(T)$, then by Lemma 2 it is easy to show that

$$A = \{|\langle \alpha T^n x, z\rangle| : n \geq 0, \alpha \in D_0(r)\}$$

is dense in $\mathbb{R}^+ \cup \{0\}$.

Now, suppose that $|\lambda| < 1$. Then for all $|\langle \alpha T^n x, z\rangle| \in A$, we have

$$\begin{aligned} |\langle \alpha T^n x, z\rangle| &= |\alpha| \langle T^n x, z\rangle \\ &\leq r\langle T^n x, z\rangle = r\langle x, T^{*n} z\rangle \\ &= r\lambda^n \langle x, z\rangle \\ &< r\langle x, z\rangle \end{aligned}$$

which contradicts (2) since $r\langle x, z\rangle$ is a constant. Therefore, $|\lambda| \geq 1$.

Proposition 9. Let T be extended-cyclic, then either the Weyl-spectrum $\sigma_w(T) = \sigma(T)$ or $\sigma_w(T) = \sigma(T) \setminus \{\alpha\}; |\alpha| > 1$

Proof: For any $T \in \mathcal{B}(X)$, we have

$$\sigma(T^*) \setminus \sigma_w(T^*) \subseteq \sigma_p(T^*)$$

By Theorem 4, we get

$$\sigma_w(T^*) = \sigma(T^*) \text{ or } \sigma_w(T^*) = \sigma(T^*) - \{\lambda\}; |\lambda| > 1$$

So, either,

$$\sigma_w(T) = \overline{\sigma_w(T^*)} = \overline{\sigma(T^*)} = \sigma(T)$$

$$\sigma_w(T) = \overline{\sigma_w(T^*)} = \overline{\sigma(T^*) - \{\lambda\}} = \sigma(T) - \{\bar{\lambda}\}; |\bar{\lambda}| > 1$$

From equations (3) and (4), we get the desired result.

Proposition 10. Let $T \in \mathcal{B}(X)$. If $\sigma(T)$ has a connected component σ such that $\sigma \subset B_0(1)$, then T is not extended-cyclic.

Proof: Suppose that σ is a connected component $\sigma(T)$ such that $\sigma \subset B_0(1)$. Then, by Riesz decomposition Theorem, $T = T_1 \oplus T_2$ such that $\sigma(T_1) = \sigma$. It follows that $\lim_{n\to\infty} \|T^n x\| \to 0$ for all $x \in X$ which means that $\sup\{\|T^n x\| : n \geq o\} \neq \infty$ a contradiction to Lemma 1. Therefore T is not extended-cyclic.

Corollary 4. Let T be an extended-cyclic operator, then $\sigma(T) \cap D_p(0)$ is connected for all $p \leq 1$.

Proof: Suppose that $\sigma(T) \cap D_p(0)$ is not connected for some $p \leq 1$. Then there exists a closed and open set $\sigma \subseteq \sigma(T) \cap D_p(0)$. Since $p \leq 1$, then $\sigma \subseteq B_0(1)$. Then by Proposition10, T is not extended-cyclic which contradicts the hypothesis. Therefore $\sigma(T) \cap D_p(0)$ is connected for all $p \leq 1$.

3.CONCLUSIONS

We defined and studied two new types of operators which are called extended-cyclic operators and extended-transitive operators. Also, we studied their corresponding vectors and investigated their properties. Moreover, various results regarding spectral properties were derived.

REFERENCES

[1] Birkhoff, G.D., 1922. Surface transformations and their dynamical applications. *Acta Mathematica*, 43,1-119.
[2] Rolewicz, S., 1969. On orbits of elements. *Studia Mathematica*, 32(1),17-22.
[3] Hilden, H.M. and Wallen, L.J., 1974. Some cyclic and non-cyclic vectors of certain operators. *Indiana University Mathematics Journal*, 23(7),557-565.
[4] Zeana, Z.J., 2002. *Cyclic Phenomena of operators on Hilbert space* (Doctoral dissertation, Thesis, University of Baghdad).
[5] Bamerni, N., Kılıçman, A. and Noorani, M.S.M., 2016. A review of some works in the theory of diskcyclic operators. *Bulletin of the Malaysian Mathematical Sciences Society*, 39(2),723-739.
[6] Bayart, F. and Matheron, É., 2009. *Dynamics of linear operators* (No. 179). Cambridge university press.
[7] Grosse-Erdmann, K.G. and Manguillot, A.P., 2011. *Linear chaos*. Springer Science & Business Media.
[8] Kitai, C., 1982. Invariant closed sets for linear operators. ProQuest LLC. *Ann Arbor, MI*.
[9] Herrero, D.A., 1991. Limits of hypercyclic and supercyclic operators. *Journal of functional analysis*, 99(1),179-190.

Proceeding of 3rd International Conference of Mathematics and its Applications TICMA2022
https://conferences.su.edu.krd/su/ticma2022/
DOI: https://doi.org/10.31972/ticma2022

RESEARCH PAPER

Purely Semismall Compressible Modules

Mukdad Qaess Hussain[1,a,*]
Zahraa jawad kadhim[2,b]
Shahad Jasim Mahmood[3,c]

[1]*College of Education for pure science, Diyala University*
[2]*Computer Engineering, Al-mansur University College*
[3]*College of science, Diyala University*

[a]*mukdadqaess2016@yahoo.com*
[b]*zahraa.jawad@muc.edu.iq*
[c]*shahadjasim@uodiyala.edu.iq*

A B S T R A C T:
Let R be a ring with 1 and D be unitary left Module over R. In this paper, we present purely semi small compressible Modules. Also, we give remarks and examples, many properties of such Modules are investigated.

KEY WORDS: Semi small Submodule, prime Modules, pure Modules, semi small compressible Module.
DOI: https://doi.org/10.31972/ticma22.02

1. INTRODUCTION:

A Submodule W of an R-Module D is small Submodule ($W \ll D$) if $W + U = D$ for any Submodule U of D then $U = D$[1]. A proper Submodule W of an R-Module D is semismall of D ($W \ll_S D$) if $W = 0$ or $W/U \ll D/U$ $\forall$ nonzero Submodule U of W [2]. An R-Module D is semismall compressible (S.S.C.) if D embedded in all its non-zero semismall Submodule. That is, D is S.S.C. if $\exists$ a monomorphism f: $D \longrightarrow W$ whenever $0 \neq W \ll_s D$[3]. A ring R is S.S.C. if R as R-Module is S.S.C. [3]. In this paper, we give purely semismall compressible Modules as a generalization of semismall compressible Modules.

An R-Module D is purely semismall compressible (P.S.S.C.) if D embedded in all its non-zero pure semismall Submodule. Equivalently, D is P.S.S.C. if $\exists$ a monomorphism $f : D \to W$ whenever $0 \neq W$ is a pure semismall Submodule of D. A ring R is P.S.S.C. if R as R-Module is P.S.S.C. Clearly, every S.S.C. Module is P.S.S.C. The converse is not true.

For example:

- Z_4 as a Z-Module is P.S.S.C. which is not S.S.C.
- An R-Module D is purely semismall simple if pure semismall Submodules of D are (0) and D.
- Every purely semismall simple Module is P.S.S.C.
- Every integral domain R is a P.S.S.C. R-Module.
- A ring R is regular ring if for every $r \in R$ $\exists$ $w \in R$ such that $r = rwr$[4].
- An R-Module D is regular Module if for every $u \in D$ and $\forall$ $r \in R$, $\exists$ $w \in R$ such that $ru = rwru$[5].
- Every regular Module D is S.S.C. iff D is P.S.S.C.
- Every Module D over regular ring R is S.S.C. iff D is P.S.S.C.

*** Corresponding Author: Mukdad Qaess Hussain**
E-mail: **mukdadqaess2016@yahoo.com**
Article History:
Received: 01/08/2022
Accepted: 15/09/2022
Published: 07/12/2022

DOI: https://doi.org/10.31972/ticma2022

Proposition 1. Let D_1 and D_2 be two isomorphic Modules. Then D_1 is P.S.S.C. iff D_2 is P.S.S.C.
Proof: Assume D_1 is P.S.S.C. and an isomorphism $\varphi: D_1 \to D_2$. Let $0 \neq W$ be a pure semismall Submodule of D_2. Put $K = \varphi^{-1}(W)$, thus K is a semismall submodule of D_1. Claim K is pure in D_1. Let j be an ideal of R. But f is a monomorphism gives $\varphi(jD_1 \cap K) = \varphi(jD_1) \cap \varphi(K) = j\varphi(D_1) \cap \varphi\varphi^{-1}(W) = jD_2 \cap W = jW = j\varphi(K) = \varphi(jK)$. But φ is an isomorphism, then $jD_1 \cap K = jK$. Hence K is pure in D_1. Let $f: D_1 \to K$ be a monomorphism and let $g = = \varphi\big|_K$ thus $g: K \to D_2$ is a monomorphism and $g(K) = \varphi(\varphi^{-1}(W)) = W$, hence $g: K \to W$ is a monomorphism. Now, we have the composition $D_2 \xrightarrow{\varphi^{-1}} D_1 \xrightarrow{f} K \xrightarrow{g} W$. Let $Y = gf\varphi^{-1}$ is a monomorphism. Thus D_2 is P.S.S.C.

Proposition 2. Every non-zero pure semismall Submodule of a P.S.S.C. Module is P.S.S.C.
Proof: Assume W be a non-zero pure semismall Submodule of P.S.S.C. Module D. Assume U be a pure semismall Submodule of W. Thus, by [6, Remarks 1.2.8] U is pure in D. Then there is a monomorphism $f: W \to U$ and hence $if: U \to W$ is a monomorphism where $i: U \to W$ be inclusion homomorphism. Thus W is P.S.S.C.

Corollary 3. Every direct summand of P.S.S.C. Module is P.S.S.C.

Corollary 4. Assume D Regular Module. Every non-zero semismall Submodule of P.S.S.C. Module D is P.S.S.C.

Corollary 5. Let R be a regular ring. Every non-zero semismall Submodule of P.S.S.C. is P.S.S.C.

Remark 6. A homomorphic image (quotient) of P.S.S.C. Module is not always be P.S.S.C. For example, Z as Z-Module is P.S.S.C., but $Z/6Z \simeq Z_6$ is not a P.S.S.C. Z-Module.

Remark 7. The direct sum of P.S.S.C. Modules is not P.S.S.C.

Example 8. Let $D = Z_4 \oplus Z_2$ as a Z-Module. Clearly Z_4 and Z_2 is P.S.S.C. Z-Module. Since D is not P.S.S.C. But $D = \{(\bar{0}, \bar{0}), (\bar{0}, \bar{1}), (\bar{1}, \bar{0}), (\bar{1}, \bar{1}), (\bar{2}, \bar{0}), (\bar{2}, \bar{1}), (\bar{3}, \bar{0}), (\bar{3}, \bar{1})\}$,$F = Z(\bar{1}, \bar{1}) = \{(\bar{0}, \bar{0}), (\bar{1}, \bar{1}), (\bar{2}, \bar{0}), (\bar{3}, \bar{1})\}$, and $G = Z(\bar{2}, \bar{1}) = \{(\bar{0}, \bar{0}), (\bar{2}, \bar{1})\}$. Clearly, $D = F \oplus G$ .Thus, F and G is a pure semismall Submodule of D, since D cannot be embedded in F (or in G). Thus D is not P.S.S.C.

An R-Module D is purely semismall prime (P.S.S.P.) if $ann(D) = ann(W)$ for each pure semismall Submodule $0 \neq W$ of D.

A Submodule W of a Module D is P.S.S.P. Submodule if $wz \in W$ with $s \in R, z \in D$ and (z) is pure semismall in D implies either $z \in W$ or $s \in [W: D]$.

Example 9. Let $D = Z_6$ as a Z-Module and $W = (\bar{2})$. W is pure semismall in Z_6 and W is P.S.S.P. Submodule of D.

Lemma 10. An R-Module D is P.S.S.P. iff (0) is a P.S.S.P. Submodule of D.
Proof: ($\Longrightarrow$) Suppose $wz = 0$ with $w \in R, z \in D$ and (z) is pure in D. Assume $z \neq 0$. Since D is P.S.S.P. then $annD = ann(z)$ and hence $w \in annD = [0: D]$ .Thus (0) is a P.S.S.P. Submodule of D.
($\Longleftarrow$) Assume (0) is a P.S.S.P. Submodule of D and $0 \neq W$ be a pure semismall Submodule of D . Let $w \in annW$. Thus $wz = 0$ for all $z \in W$, and hence $wz \in (0)$. Assume that $z \neq 0$, then $w \in [0: D] = annD$, thus $annW \subseteq annD$, so $annD = annW$, then D is P.S.S.P.

Lemma 11. Let D be a Module and every Submodule of a pure Module is pure. If W is P.S.S.P. Module, then annW is a pure semismall ideal of R for each non-zero pure semismall Submodule W of D.

DOI: https://doi.org/10.31972/ticma2022

Proof: Assume $0 \neq W$ be a pure Submodule of D. let $a, b \in R$ and $ab \in annW$. Thus $abW = 0$. Suppose that $bW \neq 0$. Since $bW \leq W$ and W is pure in D then bW is pure in D. Since D is P.S.S.P. and $a \in annbW$, then $a \in annD$, on the other hand $annD = annW$, so $a \in annW$ and hence annW is a semismall prime ideal of R. The converse of Lemma 11 is not true.

Example 12. Z_6 is not P.S.S.P. Z-Module, however $ann_z(\bar{2}) = 3Z$ and $ann_z(\bar{3}) = 2Z$ which are both prime ideals in Z and that $(\bar{2}), (\bar{3})$ are pure Submodule of Z_6.

Proposition 13. Every P.S.S.C. Module is P.S.S.P.
Proof: Assume D be P.S.S.C. Module and $0 \neq W$ be a pure semismall Submodule of D. To show $annD = annW$. Let $x \in annW$. Thus $xW = 0$. Let $f: D \to W$ be a monomorphism, thus $f(xD) = xf(D) \subseteq xW = 0$ implies that $xD = 0$, then $x \in annW$ and hence $annD = annW$.

2. CONCLUSIONS

In this paper, we give purely semismall compressible Modules. Also, we give remarks and examples, many properties of such Modules

- D_1 is purely semismall compressible. iff D_2 is purely semismall compressible, where D_1 and D_2 be two isomorphic Modules**.**
- Every non-zero pure semismall Submodule of purely semismall compressible Module is purely semismall compressible.
- Every direct summand of purely semismall compressible Module is purely semismall compressible.
- Every non-zero semismall Submodule of regular purely semismall compressible Module is purely semismall compressible.
- Every non-zero semismall Submodule of purely semismall compressible in regular ring is purely semismall compressible.
- A homomorphic image (quotient) of purely semismall compressible Module is not always be purely semismall compressible.
- The direct sum of purely semismall compressible Modules is not purely semismall compressible.
- Every purely semismall compressible Module is purely semismall prime.

References

[1] Kasch, F., 1982. *Modules and rings* (Vol. 17). Academic press.
[2] Ali, I.M. and Mahmood, L.S., 2009, March. Semismall submodules and semi-lfting modules. In *Proceeding of 3 rd scientific conference of the college of science, Univ. of Baghdad* (pp. 24-26).
[3] Kadhim, Z.J., Dheyab, A.H., Abdulkareem, D.J. and Hussain, M.Q., 2020. Semismall compressible and semismall retractable modules. *Journal of Discrete Mathematical Sciences and Cryptography*, 23(7),1395-1398.
[4] Rotman, J.J. and Rotman, J.J., 2009. *An introduction to homological algebra* (Vol. 2). New York: Springer.
[5] N. H. Garib., 1989.Some Generalizations of Lifting Modules. M. Sc. thesis, Mosul University.
[6] Sahera Yasen Mahmoo., 1993. on F-regular modules, Msc Thesis. Baghdad university.

Proceeding of 3rd International Conference of Mathematics and its Applications TICMA2022
https://conferences.su.edu.krd/su/ticma2022/
DOI: https://doi.org/10.31972/ticma2022

RESEARCH PAPER

Comparison Between Factor Analysis and Cluster Analysis to Determine the Most Important Affecting Factors for Students' Admission and Their Interests in The Specializations: A Sample of Salahaddin University-Erbil

Mohammed O ABDULLAH[1,a], Rizgar M AHMED[2,b,*], Yener ALTUN[3,c]
[1] *STATISTICS DEPARTMENT, INSTITUTE OF NATURAL AND APPLIED SCIENCES, YUZUNCU YIL UNIVERSITY, Van,Turkey.*
[2] *STATISTICS DEPARTMENT, ADMINISTRATOR AND ECONOMICS,, SALAHADDIN UNIVERSITY- ERBIL, Iraq.*
[3] *STATISTICS DEPARTMENT, INSTITUTE OF NATURAL AND APPLIED SCIENCES, YUZUNCU YIL UNIVERSITY, Van, Turkey.*

[a] muhamad91m91@gmail.com
[b] rizgar.ahmed@su.edu.krd
[c] yeneraltun@yyu.edu.tr

A B S T R A C T:

The main goal of this thesis is to determine the most important effective factors for student admission and his/her interests in the specialization by using multivariate methods. Therefore, it focused on using factor analysis by identifying a number of the obtained factors and cluster analysis by classifying them into five clusters. Furthermore, the factor analysis and cluster analysis results will be compared to each other. Moreover, this study depends on the analysis of 350 questionnaire forms, distributed by random stratified sample method on students in the first stage of three different colleges, including Scientific colleges and Humanity colleges of Salahaddin University in Northern Iraq for the academic year 2018-2019.

Thus, the IBM SPSS Statistics V: 25 software programs have been used in data analysis. Additionally, the results have demonstrated that Reliability is accepted, and also in factor analysis, the rate of the total variance interpretation is %62.157. Moreover, the most common variables between the factor analysis and cluster analysis can be considered the most important and influential variables for student admission and their interests in choosing a specialization. Consequently, the first factor and the first cluster have five significant variables in common; they are V1, V2, V3, V4 and V5 (the system is helpful for student admission to colleges to get their desired professions). The second factor and the second cluster have four influential variables in common they are V24, V32, V35 and V37 (the new system may help master's and PhD students to be admitted to colleges and get competitive results by utilizing their accounts). In the fourth factor and the fourth cluster, there is one variable in common, which is V18 (decreasing the number of students admitted in the parallel system by using the graduated students who must not be able to refill admission forms). Ultimately, the conclusion has shown a kind of approach and similarity between factor analysis and cluster analysis.

KEY WORDS: Factor Analysis, Cluster Analysis, Cluster Analysis.
DOI: https://doi.org/10.31972/ticma22.03

1. INTRODUCTION:

One of the important topics in the student's life is Admission to universities or institutes according to their interests. In Iraq and northern Iraq, the students finish the study period for (12) years until they reach their future in university or institute. Previously the admission system at the university was based on filling out various admission forms in (the central Admission) department, which links the ministry of education with higher education for the admission of the students in universities and institutes.

*** Corresponding Author: Rizgar M AHMED[2]**
E-mail: rizgar.ahmed@su.edu.krd
Article History:
Received: 01/08/2022
Accepted: 15/09/2022
Published: 07/12/2022

DOI: https://doi.org/10.31972/ticma2022

Nowadays, the Ministry of Higher Education in northern Iraq depends on the new system, which depends on filling the forms of Admission on the internet to extract the results according to the interests with a reasonable proportion. Student admissions are vital to any university's running because universities can stay alive with students. The admission system is an influential activity that helps the universities survive with the student's contribution. Then, lack of knowledge by the students and poor admission system are serious problems that cause fewer students to be admitted to the universities because of the system's slow response, which leads the students to make mistakes. Therefore, students are not able to get to their desired universities. For these reasons, there must be good educated information about the online admission system; it can be achieved only by choosing the best method for Admission [1].

Although the admission system can widely consider the process when a student gets more interested in reaching higher education until Admission in a particular course and university happens [2]. The admission process at the university is an entrance process in a university. It generally influences all the resources of the universities and their quality restraints [3]. The Ministry of Higher Education and Scientific Research in the north of Iraq has introduced a new system for Admission to colleges and institutes in the region for the academic year (2011-2012). Furthermore, this system has a great success since its inception. Also, this system has been used to accept all students in the region from its inception until now.

This research studies the new student admission system for attending colleges and institutes with their interests in the specialization. The new admission system includes four methods (Zankoline, Credit, Parallel, and Evening study). The student introduces many requests to more than one university by filling a form online in a specialized system for student admission. The current admission system gives them acceptance into one university, giving many chances to other students. The proposed system accepts only one request from each student in all universities. On the other hand, it helps the universities have only one place to receive the students' requisitions. The problem is that there are some deficiencies or imperfections in this system, which (include delaying the time to receive results, not taking the interest of students as regarded, and lack of trust of the student in the system…etc.). The vital aim of this topic lies in several aspects: it is related to a student's future in their life, and there are several problems facing the student in this system, such as the chosen department may not be his/her interest or sometimes some students' names might be missed. In this thesis, all the important aspects of this system are studied and processed using an advanced statistical method; it includes two types of multivariate analysis: cluster analysis and factor analysis. In addition, some recommendations are considered an essential effective service to the students to achieve the departments in which they are interested.

2. METHODOLOGY:

Factor analysis (FA) is a strategy used in Statistics that is applied to a solo set of variables by statistical researchers interested in finding which variables are related to others and which one is independent in the set of the variables. Therefore, those variables associated with other variables but not correlated with different subsets of variables are linked into factors. In addition, factors are accustomed to reflecting on the process, which has built the correlation between variables [4]. Moreover, factor analysis is a set of methods for clarifying the correlations between variables in the form of basic entities called factors. Additionally, the model' factor analysis' is broadly comprehended to refera collection of nearly associated forms intended to clarify or create a co-relational structure between the observed random variables [5].

One of the central assumptions of the factor analysis is that it is not normal to observe the factors directly; the variables rely on the factors, also they are reasons for random errors. Thus, the assumption is especially well-organized to the forms like psychology, where it is not suited to measure the concepts which one is interested in directly, for instance, 'intelligence'. Then it is mainly ambiguous to define the concepts [6]. Furthermore, the utilization of factor analysis methods has been enlarged in many scientific research eras such as psychological, educational, athletic, marketing, behavioural, social, medicine, economics, and geography as a result of the technological development of computers. Factor analysis aims to explain the number of basic impacts underlying a domain of variables, count the amount of the variable associated with the factors, and gain enough instruction about their nature to observe the contribution of each factor with its variables.

https://conferences.su.edu.krd/su/ticma2022/
DOI: https://doi.org/10.31972/ticma2022

Likewise, the specific target of the subject is to describe the patterns of correlations between observed variables briefly; this way, a large number of the observed variables will be reduced to a smaller number of factors. The final aim which to recognize the observed reasons that illuminate the data variation. Moreover, to reach this goal, the relation of the factors and original variables should be checked, then give them an explanation in the framework of how the data were generated. Lastly, the aim generally is to demonstrate a few important common factors [7,8,9].

3. Type of Factor Analysis:

Exploratory Factor Analysis (EFA) and Confirmatory Factor Analysis (CFA) are two fundamental kinds of factor analysis. Usually, a difference is made between Exploratory and Confirmatory factor analysis. The exploratory analysis aims to demonstrate the factor structure for a collection of variables. It mostly includes the identification how a lot of the factor loadings. However, most EFA programs permit the number of factors to be particularized in advance. Moreover, the variables could not be forced to load just on some specific characteristics. Therefore, EFA is usually identified to be more of a theory-generating than a theory-testing program. Conversely, Confirmatory Factor Analysis is normally built on a powerful theoretical and empirical organization that permits the scientific researcher to identify accurate factor models in advance. Therefore, the model generally identifies which variables will load on which factors. Likewise, whichh factors are associated. Furthermore, Confirmatory Factor Analysis is an academic testing program more than a procedure EFA. Practically, the research may include aspects of both Exploratory and Confirmatory analysis. It is beneficial to differentiate between both techniques in their situational form[10,11,12,13].

4. The Orthogonal Factor Model:

The observable random vectors X with ρ components have mean μ and covariance matrix Σ. Moreover, the factor model postulates, which X is linearly reliant on a small number of unobservable random variables such as F1, F2,…, Fm, which are called common factors, and ρ extra sources of variation such as ε1, ε2, …, εp, which are called errors, or sometimes certain factors. Significantly, the factor analysis model is

$$\mathbf{X_1} = \boldsymbol{\mu_1} + \boldsymbol{\ell_{11}}\,\mathbf{F_1} + \boldsymbol{\ell_{12}}\,\mathbf{F_2} + \cdots + \boldsymbol{\ell_{1m}}\,\mathbf{F_m} + \varepsilon_1 \qquad (1)$$

$$\mathbf{X_2} = \boldsymbol{\mu_2} + \boldsymbol{\ell_{21}}\,\mathbf{F_1} + \boldsymbol{\ell_{22}}\,\mathbf{F_2} + \cdots + \boldsymbol{\ell_{2m}}\,\mathbf{F_m} + \varepsilon_2 \qquad (2)$$

$$\mathbf{X_p} = \boldsymbol{\mu_p} + \boldsymbol{\ell_{p1}}\,\mathbf{F_1} + \boldsymbol{\ell_{p2}}\,\mathbf{F_2} + \cdots + \boldsymbol{\ell_{pm}}\,\mathbf{F_m} + \varepsilon_p \qquad (3)$$

The form for the P variables can be joined in the solo matrix expression; the public factor form can be penned as

$$\mathbf{X_{(p\times 1)}} = \boldsymbol{\mu_{(p\times 1)}} + \mathbf{L_{(p\times m)}}\,\mathbf{F_{(m\times 1)}} + \varepsilon_{(p\times 1)} \qquad (4)$$

X: vector of observable random variables. μ: mean of variables. L: matrix of factor loadings. F: common factors. ε: errors or specific factors from time to time.
Or in matrix data.

$$\mathbf{X} = \mathbf{L}\underline{\mathbf{F}} + \underline{\varepsilon} \qquad (5)$$

[14][15].

5. Cluster Analysis:

Cluster analysis is a multivariate statistical method, a technique of categorization utilizing an evaluation of similarity or distance given for a random couple of objects. Thus, objects divided into groups are similar

DOI: https://doi.org/10.31972/ticma2022

among pair objects inside a group, which ought to be a big number, and similarity among two groups ought to be small. By the way, the distance measured inside a group should be small, and the distance among groups should be a big number [16]. The goal of cluster analysis is to find a structure in an arranged data collection-clusters. Furthermore, objects inward a cluster ought to be similar to one another and be dissimilar from the objects of other clusters [17]. The target of cluster analysis is to the division an arranged data set or objects into clusters or its term such as (subsets, groups, and classes). The mentioned division should have the following properties: A- Homogeneity inside the clusters. Data belonging to the same cluster ought to be similarly possible. B- Heterogeneity among clusters means data belonging to dissimilar clusters that ought to be differently possible [18]. Therefore, put into a system of cluster analysis, which is a collection of objects for categorization and similarity (or distance) among a couple of objects; output from cluster analysis means several groups that shape a partition, or a family of partitions, of the collection objects[16].

The cluster analysis methods were applied broadly to the collection in several eras, like medicine, psychiatry, sociology, criminology, anthropology, archaeology, geology, geography, remote sensing, market research, economics, and engineering.[19]. Depending on the clustering objective, cluster analysis could be defined in several ways. Usually, one of its definitions is one may agree that a cluster is a collection of objects, which are more similar to one another than to participants of other clusters. Subsequently, it also could be elucidated as set of homogenous observation [20][21]. Methods of cluster analysis can be divided into two categories of hierarchical clustering and nonhierarchical clustering.

6. Hierarchical Clustering:

Hierarchical techniques are between the long-established methods of cluster analysis. Moreover, hierarchical clustering consists of successive aggregation or partition of the observations and their separations. Concluding from this sort of procedure, there is a form of a tree structure, considered a dendrogram [22]. Techniques of hierarchical cluster analysis are divided to a couple of classes; (agglomerative techniques - a succeeding pooling of divisions of the collection of objects and divisive techniques- succeeding partitions of the collection of objects). Hierarchical cluster analysis or agglomerative hierarchical cluster analysis is a technique to generate a family of categorization of a limited collection of objects built on a measure of resemblance identified on a couple of objects. Therefore, the method applies to different fields in natural and social sciences [16,23]. The agglomerative methods begin with the collection of observations, which is a divided cluster. In addition, groups are combined in accordance with the lessening quantity of similarity (or the rising amount of dissimilarity) until one cluster is recognized [22]. Hierarchical classifications shaped by cluster methods, such as the agglomerative or divisive techniques, may be characterized by a two-dimensional diagram, which is recognized as a dendrogram that elucidates the fusions or separations created at each phase of the analysis.[16]. A dendrogram can recognize the resemblance of variables and groups of variables.

7. Dendrogram:

A dual-dimensional diagram mainly demonstrates the hierarchical structure, so it is named a tree diagram or dendrogram. Therefore, the dendrogram is a graphical demonstration of the results of hierarchical cluster analysis. Besides, it emerges in the shape of a tree as plot, where each pace of hierarchical clustering is demonstrated as a fusion of a couple of branches of the tree solution into a single one. By the way, the branches demonstrate clusters obtained at each pace of hierarchical clustering. [24]. A dendrogram is a tree diagram in which the (X) axis demonstrates the objects while the lower *Y* axis displays distances. Besides, the tree branches show the order of the (n-1) links; the fork explains the primer link. In addition, the second fork shows the second link continually until all link together at the trunk. Thus, the dendrogram could be utilized to build a new distance matrix among the objects [6]. Additionally, the tree is mainly shown upside down. By the way, the tree's root is located at the bottom, and the branches are at the top. On the other hand, when a computer creates trees, it is most suitable to print them out, and the tree is on its side with the branches on the left [25,23].

DOI: https://doi.org/10.31972/ticma2022

8. Non-Hierarchical Clustering:

Non-hierarchical clustering has a point to begin with: the specification of the number of clusters. Sometimes it identifies the number, and the objects are assigned to groups. So, it is a couple-phase process. Firstly, the cluster seed is particularized. Thus, it is a beginning point, which can be illustrated by the researcher as either a systematic or random choice. Furthermore, observations are assigned according to their similarities to the pre-defined seed [26]. In addition, nonhierarchical clustering methods are shaped to group items rather than variables into a set of K clusters, so the number of clusters, which is named *K*, may either be particularized in a developed way or verified as part of the clustering procedure because the dissimilarities of a matrix do not have to be determined and the 16 fundamental data does not be stored throughout the computer run. Nonhierarchical techniques begin from either (1) the first division of items into groups or (2) a primary collection of seed points that will shape the nuclei of clusters. God's selections for beginning configurations ought to be liberated of apparent biases. One of the paths to begin is to choose seed points randomly from among the items in the first group [14]. Besides, the nonhierarchical group of algorithms is the K-means. The K-means works by separating the data into a pre-specified number and systematically assigning observations to the clusters. Nonhierarchical techniques can be applied to a large number of data collections. The K-means technique is apt for big samples (n > 1000) since it does not figure the closeness matrix among all cases [26].

9. RESULTS AND DISCUSSIONS:

To better understand the action of students' Admission and those problems facing students in the new system in northern Iraq, with excellent and scannable solutions for the preferred system, by using statistical data that had been analyzed through cluster analysis and factor analysis. Therefore, a statistical Mechanism will be applied to get the data. A set of questions is prepared in questionnaire form; the questions will be prepared according to the admission system strategy, which focuses on age, gender, specialization, interest, average score, and 39 variables related to the student admission system and their interests in the fields. Then, this questionnaire form is distributed among 350 students of the first stage at Salahaddin University-Erbil for the academic year 2018-2019 in 3 scientific colleges and humanity colleges at ten different departments. Moreover, Stratified Random Sampling has been used. Thus, they are 251 students in Administrator and Economics College, 74 in Science College, and 25 in Education College. Profoundly, the data is collected manually and entered into (statistical package for the social sciences) IBM SPSS statistics V: 25 programs for analyzing them.

10. Reliability Test:

Reliability is one of the most important and fundamental countenances in evaluating any measurement instrument or tool for good research, for an exploratory or pilot study[27]. George and Mallery had provided the rules of thumb e. i. if the value of alpha is >0.9 = Excellent, >0.8 = Good, >0.7 = Acceptable, >0.6 = Questionable, >0.5 =Poor, and <0.5 = Unacceptable[28]. Accordingly, in this study, the reliability test is conducted by means of Chronbach's alpha using SPSS software before applying (factor and cluster) analysis; it has summarized the results i' the following table.

TABLE 1. Reliability Statistics

Cronbach's Alpha	N of Items
.70	39

The reliability analysis shows that Cronbach's Alpha is 0.70 for 39 items. Therefore, the data is good to analyze.

11. Factor Analysis:

Factor analysis has been used to construct the new affective factors for student admission and their interests in the specialization. Moreover, factor analysis aims to reduce the redundancy among the variables by using

DOI: https://doi.org/10.31972/ticma2022

a smaller number of factors. Principal component methods are used to analyze the correlation matrix to show the significance of each variable based on the relationship between the variables. A correlation matrix should be used in the process of factor analysis; it displays the correlation or relationships between a single variable and every other variable in the investigation.

The first step of the factor analysis is to measure the adequacy of the data, Kaiser-Meyer-Olkin (KMO), which measures the appropriateness of the data for the factor analysis; the value of (KMO) is greater than 0.5, the more appropriate data for factor analysis. Additionally, the (KMO) is the partial correlation between the questions to ensure a strong association between all or most of the questions, not only among a few. Bartlett's test of Sphericity will be used to test the strength of these correlations. The null hypothesis of this test is that there are no correlations between the questions. Therefore, the factor analysis requires the rejection of this hypothesis to make the data suitable for this analysis.

KMO and Bartlett's Test for our data summarized the results in the following table:

TABLE 2. KMO and bartlett's test

Kaiser-Meyer-Olkin Measure of Sampling Adequacy.		.713
Bartlett's Test of Sphericity	Approx. Chi-Square	1985.241
	Df	741
	Sig.	.000

The Kaiser-Meyer-Olkin (KMO) measure should be greater than 0.50 and is inadequate if less than 0.50. The KMO test tells us whether or not each factor predicts enough questions. Therefore, for these data, the value is 0.713, which is acceptable and reasonable. Furthermore, there is a test called the Bartlett test of Sphericity that ought to be significant (i.e., a significance value of less than .05); it means that the questions are correlated adequately to give a logical basis for factor analysis. In addition, the data is suitable for factor analysis in this case (the p-value is less than .05, demonstrating that the correlation matrix is significantly unlike an identity matrix).

TABLE 3. Communalities

Variables	**Extraction**	**Variables**	**Extraction**
V1	.604	V21	.568
V2	.658	V22	.609
V3	.651	V23	.673
V4	.664	V24	.611
V5	.553	V25	.722
V6	.492	V26	.575
V7	.647	V27	.591
V8	.624	V28	.634
V9	.757	V29	.643
V10	.675	V30	.710
V11	.714	V31	.552
V12	.624	V32	.609
V13	.722	V33	.581
V14	.643	V34	.441
V15	.648	V35	.501
V16	.582	V36	.656
V17	.538	V37	.519
V18	.638	V38	.609
V19	.647	V39	.666
V20	.688		

The communalities table shows the initial commonalities before rotation. Table 3. Is a table of communalities, which shows how much of the Variance in the variables has been accounted for by the extracted factors.

Note: that the initial communalities are higher than .50, which is good.

https://conferences.su.edu.krd/su/ticma2022/
DOI: https://doi.org/10.31972/ticma2022

The Total Variance Explained table shows how the Variance is divided among the 39 possible factors. It is noted that the tables have shown the Eigenvalue of the fifteen and sixteen Components, which is less than one. The first sixteen Components depend on the interpretation variance ratio. The extraction window is not based on Eigenvalue; it is based on a fixed number of the factors divided into sixteen factors, in terms of the variable's worth of each one of the variance explanations. So, the first Components show almost. Note: that the firs' component explains 7.818% of the Variance after rotation (as much Variance as in five variables). The seco'd component explains 6.683% of the Variance, 3.849% of the Variance is explained by the third component, 3.828 % of the Variance is defined by the fourth component, the fifth component explains 3.789% of the Variance,

Thus, when the sixteen components depend on the interpretation variance ratio, the component explains less information than a single variable would have defined. The following figure illustrates this.

TABLE 4. Total Variance

	Initial Eigenvalues			Rotation Sums of Squared Loadings		
Component	**Total**	**% of Variance**	**Cumulative %**	**Total**	**% of Variance**	**Cumulative %**
1	3.742	9.595	9.595	3.049	7.818	7.818
2	3.418	8.764	18.359	2.606	6.683	14.501
3	1.578	4.045	22.405	1.501	3.849	18.351
4	1.524	3.908	26.313	1.493	3.828	22.178
5	1.430	3.668	29.981	1.478	3.789	25.967
6	1.367	3.506	33.487	1.446	3.707	29.674
7	1.327	3.403	36.890	1.432	3.672	33.346
8	1.296	3.324	40.214	1.388	3.559	36.906
9	1.228	3.149	43.363	1.328	3.405	40.310
10	1.153	2.955	46.318	1.286	3.299	43.609
11	1.098	2.815	49.134	1.281	3.285	46.894
12	1.088	2.789	51.922	1.233	3.161	50.055
13	1.045	2.680	54.603	1.220	3.127	53.182
14	1.017	2.607	57.210	1.217	3.120	56.302
15	.983	2.521	59.731	1.157	2.967	59.269
16	.946	2.426	62.157	1.126	2.888	62.157

The Scree plot demonstrates that after the first sixteen components are different with the Eigenvalues decline (the curve flattens) and they are less than (0.946) or dependent on the interpretation variance ratio decline (the curve flattens). This again supports a sixteen-component solution. Moreover, it notes that both the Scree plot and the sixteen values support the conclusion that these (39) variables could be reduced to sixteen components. It states that the Scree plot flattens out after the sixteen components.Each component accounts for the cumulative Percent of Variance between variables. Before and after rotation, 62.157% of the Variance is accounted for by the first sixteen components.

So, those components that are rotated are easier to interpret. Thus, the rotation makes it as much as possible; the different variables are explained or predicted by different underlying components. So, it is the aim of rotation. It is not usually gained. In the Rotated Component of the factor loadings matrix, there is one thing to look for: the extent to which simple structure is achieved. It summarizes the results in the following table:

DOI: https://doi.org/10.31972/ticma2022

TABLE 5. Rotated Component Matrix[a]

	Components				
	1	2	3	4	5
V3	.771				
V2	.728				
V1	.707				
V4	.667				
V5	.655				
V24		.667			
V35		.608			
V37		.527			
V32		.504			
V22			.713		
V19			-.616		
V18				.716	
V16				.624	
V7					.724
V10					.620

Extraction Method: Principal Component Analysis. Rotation Method: Varimax with Kaiser Normalization. [a]

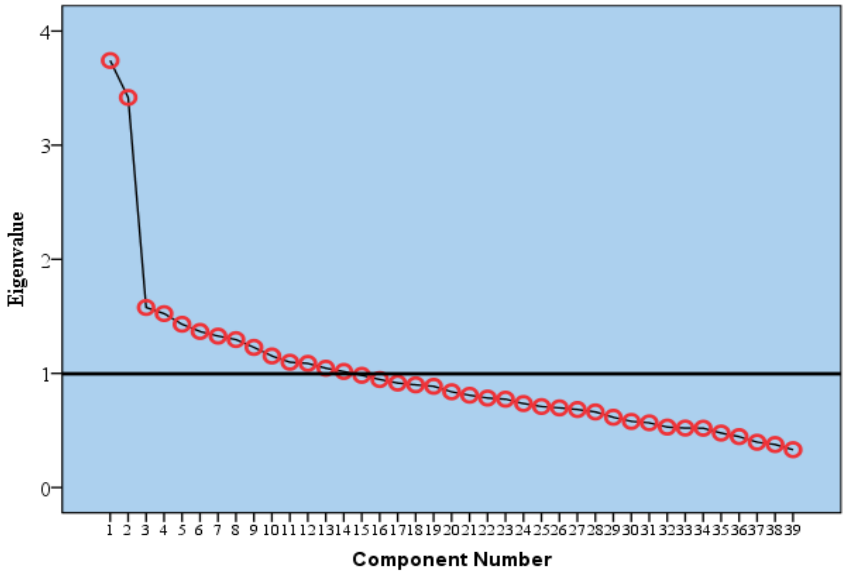

FIGURE 1. Scree plot.

12. Rotation converged in 21 iterations.

The variables are sorted in the table (5.) because the variable has the highest loading (not considering whether the correlation is positive or negative). Every variable has some loading from every component, but we requested loadings less than |.50| to be excluded from the output, so there are blanks where low loadings exist. (|.50| means the absolute value or value without considering the sign).

The first five components are the most fundamental; they have been chosen. Thus, The first component explains the largest variance ratio containing five variables they are (V3: It helps the students be accepted in college and the specialization they like.V2: The students can trust this system. V1: I prefer the system. V4: It has a good effect on the student's future. V5: It facilitates for the students to choose the department that he/she wants.), with loadings (.771, .728, .707, .667, .655). The second component contains four variables respectively (V24: I prefer the Permission of students in master and PhD degrees to be done by using the new system.V35: I suggest daily the students be aware of the results when the competition is done in the system by using their account. V37: The changes and guides must be given to all high schools before starting a new academic year.V32: I like all students to be accepted at the same time.), with loadings (.667, .608, .527, .504).

DOI: https://doi.org/10.31972/ticma2022

The third component contains two variables respectively (V22: My low marks didn't let me study in the department and specialization I desired. V19: The department and specialization that I am studying in is %100 my interest), with loadings (.713, -.616). The fourth component contains two variables respectively (V18: In the parallel system, the graduated students must not be able to refill the admission forms. V16: I like the number of students in the parallel system to be decreased), with loadings (.716, .624). The fifth component contains two variables respectively (V7: It doesn't account for the economic status of the student. V10: Employing the geographic area dependent method affects choosing colleges and specializations), with loadings (.724, .620). Every variable has a loading or a weight within every factor, but in a 'clean' factor analysis, mostly the loadings are not selected. Therefore, we have drawn that the Rotated Factor Matrix will be low (blank or less than .50).

13. Cluster Analysis:

Cluster analysis has been applied in this study. It is one of the most important statistical methods used to classify variables into homogeneous groups. Further, it depends on the differences and similarities between the data. Using average linkage (between groups) and rescaled distance cluster combines to find the distance matrix and relationship between clusters, dividing the number of sets into five discrete clusters using the fragmentation style. The degree of homogeneity is strong or weak between different groups, as the results are shown below:

TABLE 6. Cluster analysis for our data

5 clusters	Membership	Variables
1	10	V1,V2,V3,V4,V5,V6,V12,V19,V20,V27
2	22	V7,V8,V9,V10,V13,V15,V16,V17,V21,V22,V24,V25 ,V26,V30,V31,V32,V34,V35,V36,V37,V38,V39
3	4	V11,V14,V28,V33
4	2	V18, V29
5	1	V23

Note: the variables were classified into five clusters of the thirty-nine variables are Analyzed by cluster analyses, the first cluster includes ten variables at the rate of 25.656%, the second cluster consists of 22 variables for a large percentage 56.410%, the third cluster contains four variables in the rate of 10.256%, the fourth cluster includes two variables in the rate of 5.128, and the last cluster includes one variable by the rate 2.564. A common way to show the cluster analysis is a dendrogram. Figure 2. Displays the dendrogram by using the average ward linkage. The number of clusters will be chosen into five discrete clusters based on 39 variables, showing the variables and the distance between them.

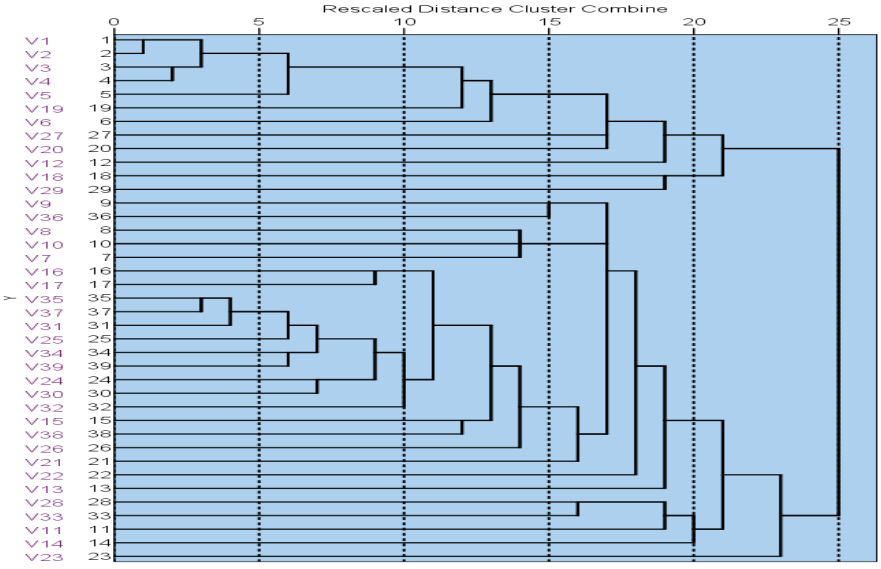

FIUGRE 2. Dendrogram using average linkage (between Groups).

DOI: https://doi.org/10.31972/ticma2022

14. Comparison Between Results of The Factor Analysis And The Cluster Analysis:

After applying factor and cluster analysis to the variables, a table has been created to compare their results. Thus, the following table illustrates the comparison.

TABLE 7. Comparison between results of the factor analysis and cluster analysis

Factor analysis		**Cluster analysis**	
Factor	Variables	Cluster	Variables
1	V1,V2,V3,V4,V5	1	V1,V2,V3,V4,V5,V6,V12,V19,V20,V27
2	V24 ,V32 ,V35,V37	2	V7,V8,V9,V10,V13,V15,V16,V17,V21,V22,V24,V25,V26,V30,V31,V32,V34,V35,V36,V37,V38,V39
3	V22, V19	3	V11,V14,V28,V33
4	V16,V18	4	V18,V29
5	V7,V10	5	V23

Note**:** the first factor and the first cluster have five variables in common, which are V1: I prefer the system. V2: The students can trust this system. V3: It helps the students be accepted in colleges and the specializations they like. V4: It has a good effect on the student's future. V5: It facilitates the students to choose the department they want. The second factor and the second cluster have four variables in common, which are V24: I prefer the admission of students with master's and PhD degrees; it must be done by using the new system. V32: I like all students to be accepted at the same time. V35: I suggest that the students be aware daily of the results when the competition is done in the system (by using their account). V37: The changes and guides must be given to all high schools before starting a new academic year. And the fourth row has one variable in common, which is V18: In a parallel system, the graduated students must not be allowed to refill admission forms.

15. CONCLUSIONS

The questionnaire items' answers agree on all variable paragraphs where the rates of total agreements are %67.199. The variable 25th (It is better if counting the average grade of 10th and 11th is optional) has the highest agreement ratio, reaching %83.943. Variable 37th (The changes and guides must be given to all high schools before starting a new academic year) has the second high agreement in the rate of %83.029; these two variables are more important for students.

Factor analysis has produced sixteen components affecting the students' Admission and their interests in the specialization. The first five components are fundamental in the results: the first component is more influential, representing the five variables (the system is helpful for students' Admission to college to get their desired professions), and the total effect of this component is %7.818. Furthermore, the second component (the new system may help the master's and PhD students to be admitted to the colleges and get competitive results by utilizing their accounts) and the total effect of this component is % 6.683. Moreover, in the third component (the student's desired professions need a higher mark to be admitted to the departments), the total effect of this component is % 3.849. The fourth component (decreasing the number of students' Admission in a parallel system by using the graduated students must not be able to refill admission forms) its rate interpretation is %3.828. The fifth component (geographic area and economic status), its rate interpretation is %3.789.

The Cluster analysis presents the number of clusters used to analyze five clusters. Therefore, the 39 variables that have been obtained were divided into these five clusters. Thus, the first cluster (the system is helpful for students' Admission to college to get their desired professions) involves ten variables with a rate of %25.656. The second cluster (the new system may help the master's and PhD students to be admitted to the colleges and get competitive results by utilizing their accounts) includes 22 variables with a significant percentage %56.410. The third cluster (the chance of Admission will be the same in private and government universities with filling a form suitable for the student's ability) involves four variables in the rate %10.256.

In addition, the fourth cluster (in a parallel system, the graduated and employee students cannot refill the admission form) includes two variables in the rate of %5.128. The last cluster contains one variable by the rate %2.564, which is (I like the order, and the choices will be decreased to 25 options).

There is a significant rapprochement and similarity between factor analysis and cluster analysis because the first cluster and component have the same variables in common. It confirms that both cluster and component analyses in the situational variable are classified in the study. Additionally, the results show that the most mutual variables between the factor analysis and cluster analysis can be considered the essential and influential variables for the student's Admission and their interests in their specializations. Consequently, in the first, five variables are in common: V1, V2, V3, V4, and V5. In the second, four variables are in common: V24, V32, V35, and V37. In the third, one is not in common, but in the fourth, one variable is in common: the V18: In a parallel system, the graduated students must not be allowed to refill admission forms.

ACKNOWLEDGMENTS

The authors would like to thank the yuzuncu yil university and salahaddin university.

REFERENCES

[1] R. Kumar, P. Desale, C. G. Puri., 2013. International Journal of Emerging Technology and Advanced Engineering **3,** 634-639.
[2] Harman, G., 1994. Student selection and admission to higher education: Policies and practices in the Asian region. *Higher Education*, 27(3),313-339.
[3] Kaur, A. and Hasija, S., 2015. A conceptual model of admission system and performance evaluation for a university. *International Journal of Computer Applications*, *125*(4).
[4] Tabachnick, B.G., Fidell, L.S. and Ullman, J.B., 2007. *Using multivariate statistics* (Vol. 5, pp. 481-498). Boston, MA: pearson.
[5] Tabachnick, B.G., Fidell, L.S. and Ullman, J.B., 2007. *Using multivariate statistics* (Vol. 5, pp. 481-498). Boston, MA: pearson.
[6] Basilevsky, A.T., 2009. *Statistical factor analysis and related methods: theory and applications*. John Wiley & Sons.
[7] Sánchez, J., 1982. MARDIA, KV, JT KENT, JM BIBBY: Multivariate Analysis. Academic Press, London-New York-Toronto-Sydney-San Francisco 1979. xv, 518.
[8] Tinsley, H.E. and Brown, S.D. eds., 2000. *Handbook of applied multivariate statistics and mathematical modeling*. Academic press.
[9] Härdle, W.K. and Hlávka, Z., 2015. *Multivariate statistics: exercises and solutions*. Springer.
[10] G. Singh, M. Kumar., 2014. *Global Journal of Management and Business Research* **14,** 39-48.
[11] J. P. Stevens., 2009. "Eploratory and Confirmatory Factor Analysis" in *Applied Multivariate Statistics For The Social Sciences*. (Fifth edition)(Taylor, New York),329-381.
[12] Ellis, J.L., 2017. Factor analysis and item analysis. *Applying Statistics in Behavioural Research*,11-59.
[13] Kenny, D.A., Kashy, D.A. and Cook, W.L., 2006. Dyadic Data Analysis (Methodology in the Social Sciences) The Guilford Press. *New York, NY, USA*.
[14] Matsunaga, M., 2010. How to Factor-Analyze Your Data Right: Do's, Don'ts, and How-To's. *International journal of psychological research*, 3(1),97-110.
[15] Johnson, R.A. and Wichern, D.W., 2002. Prentice hall Englewood Cliffs. *Applied multivariate statistical analysis. 5th ed. New Jersy: Prentice hall Englewood Cliffs*.
[16] Comrey, A.L. and Lee, H.B., 2013. *A first course in factor analysis*. Psychology press.
[17] Miyamoto, S., 2012. *Fuzzy sets in information retrieval and cluster analysis* (Vol. 4). Springer Science & Business Media.
[18] Zakharov, K., 2016. Application of k-means clustering in psychological studies. *Tutorials in Quantitative Methods for Psychology*, *12*(2), pp.87-100.
[19] Hoppner, F., Klawonn, F., Kruse, R. and Rankler, T., 1999. Fuzzy Cluster Analysis: Methods for Classification Data Analysis and Image Recognition John Wiley & Sons Inc. *Bew York*.
[20] Rencher, A.C. and Christensen, W.F., 2002. Méthods of multivariate analysis. a john wiley & sons. *Inc. Publication*, *727*.
[21] Abonyi, J. and Feil, B., 2007. *Cluster analysis for data mining and system identification*. Springer Science & Business Media.
[22] Burns, R.P. and Burns, R., 2008. *Business research methods and statistics using SPSS*. Sage.
[23] Wierzchoń, S.T. and Kłopotek, M.A., 2018. *Modern algorithms of cluster analysis* (Vol. 34). Springer International Publishing.
[24] Everitt, B.S., Landau, S., Leese, M. and Stahl, D., 2011. Cluster analysis: Wiley series in probability and statistics. *Southern Gate, Chichester, West SussexUnited Kingdom: John Wiley & Sons*.

DOI: https://doi.org/10.31972/ticma2022

[25] Meena, L.K., Sen, C. and Kushwaha, S., 2017. Cluster analysis to form similarity for major selected crops in rajasthan, India. *International Journal of Current Microbiology and Applied Sciences*, 6(4),2673-2682.
[26] C. Chatfield, A. J. Collins.,1980 "Cluster Analysis" in *Introduction To Multivariate Analysis* (First edition)(chapman and hall, Boca raton),212-229
[27] Figueiredo Filho, D.B., da Rocha, E.C., da Silva Júnior, J.A., Paranhos, R., da Silva, M.B. and Duarte, B.S.F., 2014. Cluster analysis for political scientists. *Applied Mathematics*, *2014*.
[28] Namdeo, S.K. and Rout, S.D., 2016. Calculating and interpreting Cronbach's alpha using Rosenberg assessment scale on paediatrician's attitude and perception on self esteem. *International Journal of Community Medicine and Public Health*, 3(6),1371-1374.
[29] Mohajan, H., 2017. Two criteria for good measurements in research: Validity and reliability. *Annals of Spiru Haret University Economics Series*, (4).

Proceeding of 3rd International Conference of Mathematics and its Applications TICMA2022
https://conferences.su.edu.krd/su/ticma2022/
DOI: https://doi.org/10.31972/ticma2022

RESEARCH PAPER

Practical Analysis of IEEE 802.11ax Wireless Protocol in Wi-Fi Boosters Environments

Ghassan A. QasMarrogy*
Author Affiliations
(*College of Engineering, Department of Communication and Computer Engineering, Cihan University-Erbil, Kurdistan Region, Iraq*
ghassan.qasmarrogy@cihanuniversity.edu.iq

A B S T R A C T:
All the world now is depending on networks to share information between the users, where different data types are transferred wirelessly from network to network. Using wireless LANs are important to connect the users and share the data, these Wireless LANs have different types of obstacles that affect the data sharing or the wireless signal, such as, compatibility wireless protocol types, range coverage, walls penetration, moving devices, different routing protocols, data transferred types, weak signal, and many more. In this paper a practical analysis will be made to the latest IEEE 802.11ax wireless protocol to be compared with two types of Wi-Fi booster's networks, Mesh and Extender Wi-Fi, while transferring 4k video size data rate, inside a room and on different rooms for wall penetration analysis, while measuring the throughput, delay, and signal strength metrics. The main importance of this paper is to give a more practical understanding and avoid the main problems of using the wireless protocol 802.11ax in different network types.

KEY WORDS: IEEE 802.11ax, Wi-Fi Boosters, Signal Strength, Mesh Network, Extender Network.

DOI: https://doi.org/10.31972/ticma22.04

1. I NTRODUCTION:

When the WLAN signal is not performing at best due to dropped connections, slow speeds, dead Wi-Fi spots, etc. [1]. A solution must be done to enhance the network connection for the WLAN users with the best Wi-Fi wireless protocol. The IEEE 802.11 wireless protocols became very popular in recent wireless devices as they give the standards of data transmission speed rate and coverage distance [2]. These standards made it possible to share large amounts of data between the users in the same network or through different networks with different rooms. The upgrades in IEEE wireless protocols of 802.11 made it possible to enhance the mobility, flexibility, increasing data rates, penetrating walls, reducing the time of maintenance and installation, and the ease of use between networks, as it results in large scale WLAN deployment enhancement for different areas, interior, and exterior with different types of applications [3].

These deployments can be used for Wi-Fi booster networks such as in both mesh and Wi-Fi extenders. In mesh, all devices can work as one system connected through the entire area, the main device called a mesh router, while other devices are called nodes that are connected through different areas with a triple or double connection between all devices. While in Wi-Fi extenders, is a device that extends the Wi-Fi signal through different areas to help far devices to connect to the main device, as shown in figure (1) [4].

*** Corresponding Author: Ghassan A. QasMarrogy**
E-mail: *ghassan.qasmarrogy@cihanuniversity.edu.iq*
Article History:
Received: 01/08/2022
Accepted: 15/09/2022
Published: 07/12/2022

DOI: https://doi.org/10.31972/ticma2022

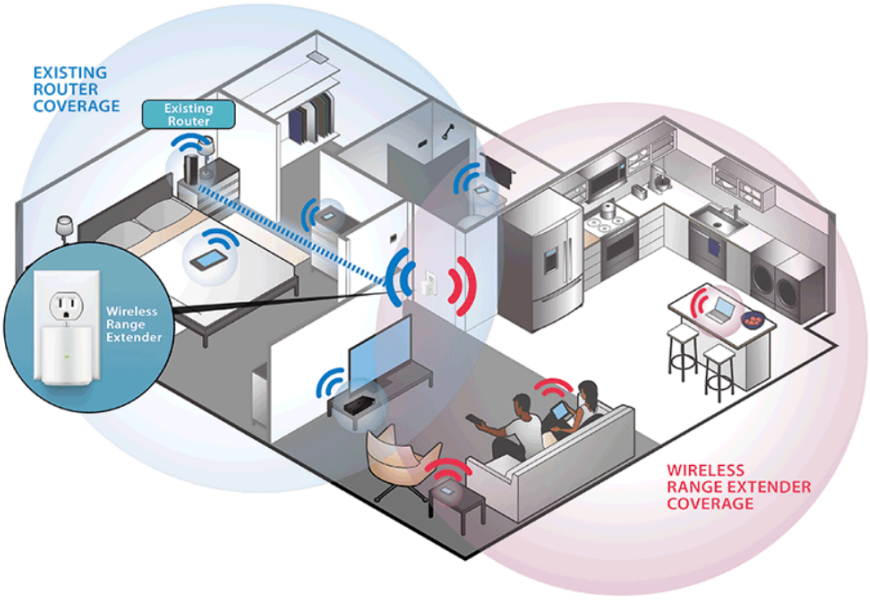

Figure (1): Wi-Fi Boosters in Home Wireless Networks [4].

These new Wi-Fi Boosters use the new IEEE 802.11ax wireless protocol, as it gives huge improvements from the old IEEE 802.11 wireless standards as shown in table 1 [5].

Table 1: IEEE 802.11 Wireless Protocols Standards [5].

IEEE 802.11 Wireless Standards	Frequency	Maximum Data Rate
802.11a	5GHz	54 Mbps
802.11b	2.4GHz	11 Mbps
802.11g	2.4GHz	54 Mbps
802.11n	2.4GHz, 5GHz	600 Mbps
802.11ac	2.4GHz, 5GHz	1.3 Gbps
802.11ax	2.4GHz, 5GHz, 6GHz	10-12 Gbps

The increase in data rate was done using different and faster coding schemes and modulation with wider channels and the implementation of (MIMO) Multiple Input Multiple Output technique [6].

Still, further data rate upgrades need newer channel access techniques rather than giving wider channels, therefore it's more difficult to upgrade the wireless protocols frequently [6].

The latest IEEE 802.11 wireless protocol used recently is the 802.11ax protocol, this protocol is the successor of the IEEE 802.11ac, also known as WIFI 6E that operates in 6 GHz frequency as it operates from 1 and 7.125 GHz, including the 2.4 and 5 GHz bands, this protocol was created mainly to enhance the throughput of the data transmission between the devices for small and medium areas and offices [7].

The main contribution of this paper is to measure the practical performance of the latest IEEE 802.11ax wireless protocol with real-life scenarios for the best user environment to see the best usage with the highest throughput and lowest delay.

In this paper the performance of IEEE 802.11ax wireless protocol will be measured with real devices and simulated with two types of Wi-Fi boosted networks, mesh and Wi-Fi extenders, with a 4k video transmission

DOI: https://doi.org/10.31972/ticma2022

to capture the highest throughput between the devices, end to end delay, and signal strength of the transmitted video.

The rest of the paper will be organized as follows, section 2 will give short-related work information, while section 3 will provide a deep background of the IEEE 802.11ax with related network design, and section 4 will give the scenario simulations parameters and the final result will be discussed, finally, in section 5 the conclusion and future work of the paper will be presented.

2. Related work:

As IEEE 802.11ax is the latest wireless protocol in the market many researchers tried to analyze, simulate and enhance these protocols. In [8] the important techniques of IEEE 802.11ax such as OFDMA random access, spatial reuse, UL MU-MIMO, and OFDMA PHY were discussed and overview, highlighting the main principal design to give smart environmental opportunities. In [9], the author explains briefly the different breakthroughs of the 802.11ax protocol with the new orthogonal FDM technique, with newer frequency reuse method. The results show an enhancement in the protocol of more than 20% than the default one. In [10] the research paper surveys the evaluation of 802.11ax performance and by using technology SLISP platform, as the result shows that the 802.11ax highly improves large scale networks end-user experience and achieving higher throughput for data rates transmission. Also, in [11] the author gives an overview of the 802.11ax key features such as MU-MIMO, OFDMA PHY, UL, OFDMA random access, spatial reuse, and power-saving, also the paper highlights the principal design to give better scenarios to be used. Finally, in [12] the author shows the 802.11ax and 802.11ac comparison while using 5GHz frequency with NS3 simulator with measuring the throughput and delay for both protocols, the result shows that 802.11ax gives better throughput with a large number of uses but with a higher delay that the 802.11ac wireless protocol.

3. IEEE 802.11ax Wireless Protocol and Network Boosters:

As Wi-Fi upgrading, more devices are created to support the latest IEEE 802.11 wireless protocols, and with more connected devices to the same routers, they need a huge bandwidth for heavy traffic applications, therefore future networks will demand more bandwidth reliability and capacity to support and maintains reliability for all connected users [13].

4. IEEE 802.11ax Wireless Protocol:

Upgrading Wi-Fi standards gives more improvement in both performance and stability, therefore the latest 802.11ax gives a significant boost to the performance of Wi-Fi with a maximum data rate of 10-12 Gbps and longer coverage distance. This wireless protocol is the new enhanced version of the previews 802.11ac wireless protocol, with newer features that support scalability and flexibility with less power consumption for more traffic demanding applications.

The new IEEE 802.11ax gives a higher level of service to the new and old applications, which makes it very desirable to be used and replace the old IEEE 802.11 wireless protocols. The IEEE 802.11ax can support more users in a large environment with enhanced user experience in different wireless networks, with more reliable performance for highly advanced applications such as UHD, IoT, 4K videos, gaming, transferring large files, and many more.

It can achieve better performance by maximizing the main dimensions, firstly, with denser modulation using 1024 QAM (Quadrature Amplitude Modulation) that can give more than 35% of speed data rate, secondly, by using OFDMA based scheduling to decrease the latency and overhead as shown in figure (2), and finally, very powerful and highly efficient signal broadcasting for minimum received signal strength indication (RSSI) [14].

DOI: https://doi.org/10.31972/ticma2022

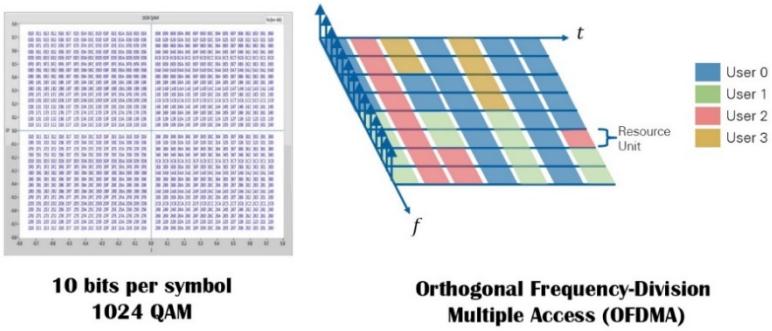

Figure (2): 1024 QAM / OFDMA enhancement Techniques for 802.11ax [14].

The OFDMA technology in IEEE 802.11ax supports eight spatial streams and gives approximately up to 10-12 Gbps data rate at the physical layer. Therefore, all users will achieve higher data transmission at the MAC layer, with the best user experience. Also, with the support of dual-band frequency of 2.4GHz and 5GHz different devices can connect for a longer range and faster data rate [15].

The new IEEE 802.11ax works by using a higher number of QAM modulations that achieve a faster data rate by permitting more data packets to be sent over the channel. Also, it can give higher spectrum utilization efficiently by creating broader channels and splitting them into sub narrow channels, which increase the available number of total channels, which make it easier for the users to find and connect to a clear channel to the router, as shown in figure (3) [16].

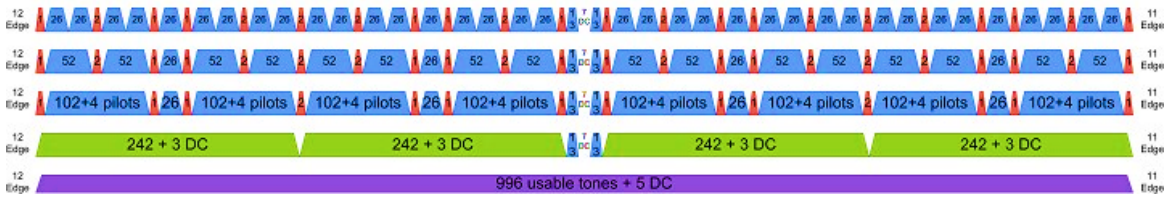

Figure (3): Sub-Channels of Different Resource Unit sizes [16].

The other basic IEEE 802.11 standard wireless protocols allow only one transmission per time between the user and the access point router, while the new standards such as 802.11ac with the integration of Multi-Input, Multiple Output (MU-MIMO), allows the wireless access point router to connect up to four connections simultaneously, while the 802.11ax can give up to eight connections in the same time while using an explicit beamforming technique, also to aim those connections more accurately at the receiver's antenna, as shown in figure (4) [17].

DOI: https://doi.org/10.31972/ticma2022

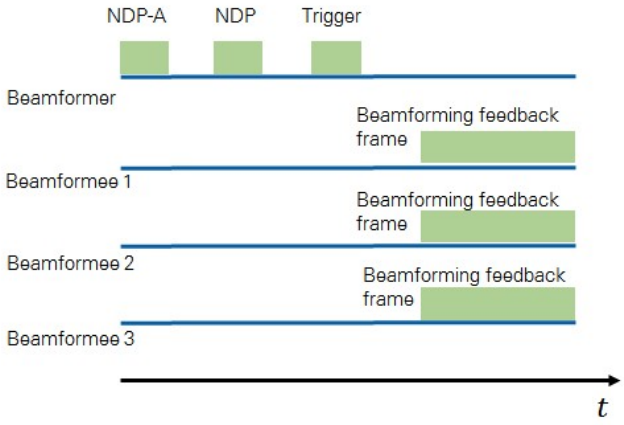

Figure (4): MU-MIMO operation requesting channel information using a beamformer router [17].

Furthermore, to increase the speed of 802.11ax four times the existing speed, the OFDMA technology was piggybacked on MU-MIMO channels, which allows each MU-MIMO connection to be divided into four additional connections, thus boosting the data transfer rates, as shown in figure (5) [17].

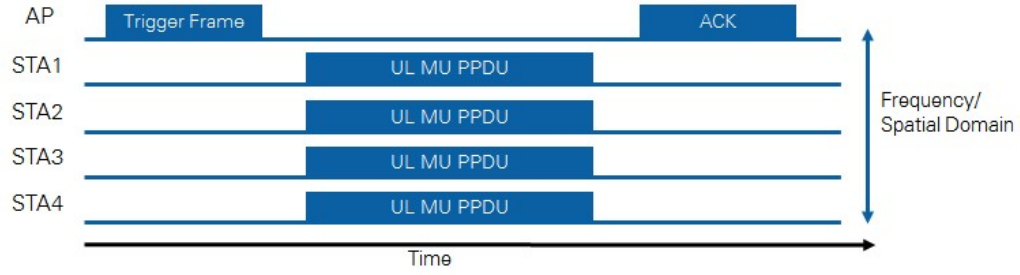

Figure (4): Acknowledge Message in MU-MIMO channels [17].

As the 802.11ax wireless protocol supports 2.4GHz, 5GHz, and 6GHz frequencies, it can determine frequency ranges of 20MHz, 40MHz, 80MHz, and 160MHz channels, which means it can give more channels that are not interfering with each other, hence giving more data rates speed and longer-range coverage without interference.

5. Wi-Fi Boosters Networks:

WLANs are a form of networks that transfer data without using any cables, but still, it cannot transmit for longer distance, therefore wireless devices will be used to strengthen the signal for longer distances [18], these devices called Wi-Fi boosters.

These boosters can extend the network wireless coverage over a specific area, they can be used as signal extenders, by rebroadcasting the weak Wi-Fi signal to other areas with the same name or with different names. Unfortunately, rebroadcasting the same signal more than one time weakens the signal strengths and quality [19]. Also, Wi-Fi boosters can use a newer technology called mesh Wi-Fi networks, these networks consist of several nodes that are connected, while all the users will connect to any node directly, the main advantage is that the signal does not weaken during rebroadcasting as each node is connected directly with other nodes while all nodes are connected in a mesh topology.

Mesh networks can be suited best for high-performance networks, while Wi-Fi extenders are suited best for local and small range networks, figure (5) shows the Wi-Fi boosters types [20].

DOI: https://doi.org/10.31972/ticma2022

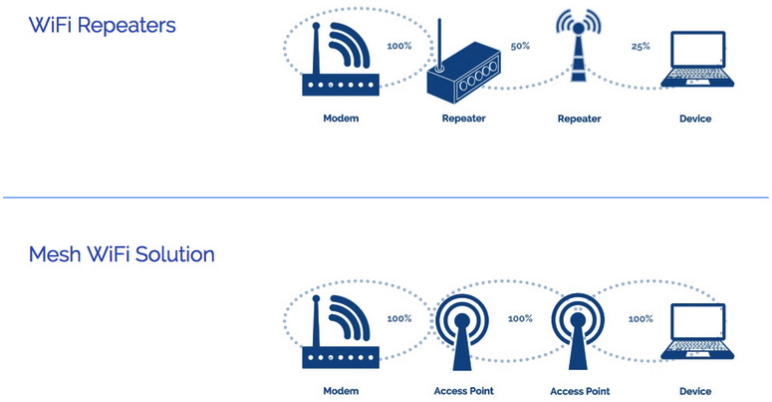

Figure (5): Wi-Fi Boosters Types [20].

6. Practical Scenarios Analysis and Results:

To analyze the IEEE 802.11ax wireless protocol performance in real-life scenarios, two practical scenarios were designed and implemented, the first scenario with a group of 6 wireless routers that support the 802.11ax wireless protocol are connected in a mesh topology with 2 802.11ax supported laptops that transferring a 4k 10 min video with a total size of (8.35 GB), while the second scenario connects 6 wireless routers in an extender signal design while connecting the 2 two laptops while transferring the 4k video. Both scenarios were implemented inside one room (10x10) m^2 and between rooms (20x20) m^2 to measure the wall penetration effect on the performance of the network, as shown in table (2).

Table (2): Practical Simulation Parameters.

Parameters	Metrics
IEEE Wireless Protocol	802.11ax
Network Topologies	Wi-Fi Mesh, Extender
Area size (No Walls, Walls)	10x10 m^2, 20x20 m^2
No. of wireless devices connected	6 routers, 2 laptops
Video format, Size, Duration	4K, 8.35 GB, 5 Min
No. of Walls used	1, 2 Walls
Wi-Fi Frequencies measured	2.4GHz, 5GHz

Figure (6) shows the practical throughput (Gbps) performance of both network boosters, mesh, and extender. The best performance was found in mesh 5GHz frequency with no walls as it gives the highest throughput compared to others, unfortunate with walls the performance drops down heavy as the 5GHz frequency as its path loss is much higher than the 2.4GHz which fades the signal faster through walls [21].

Mesh networks give better performance in throughput as the nodes communicate together in different channels than transmitted data channels, which gives the best performance through walls also.

DOI: https://doi.org/10.31972/ticma2022

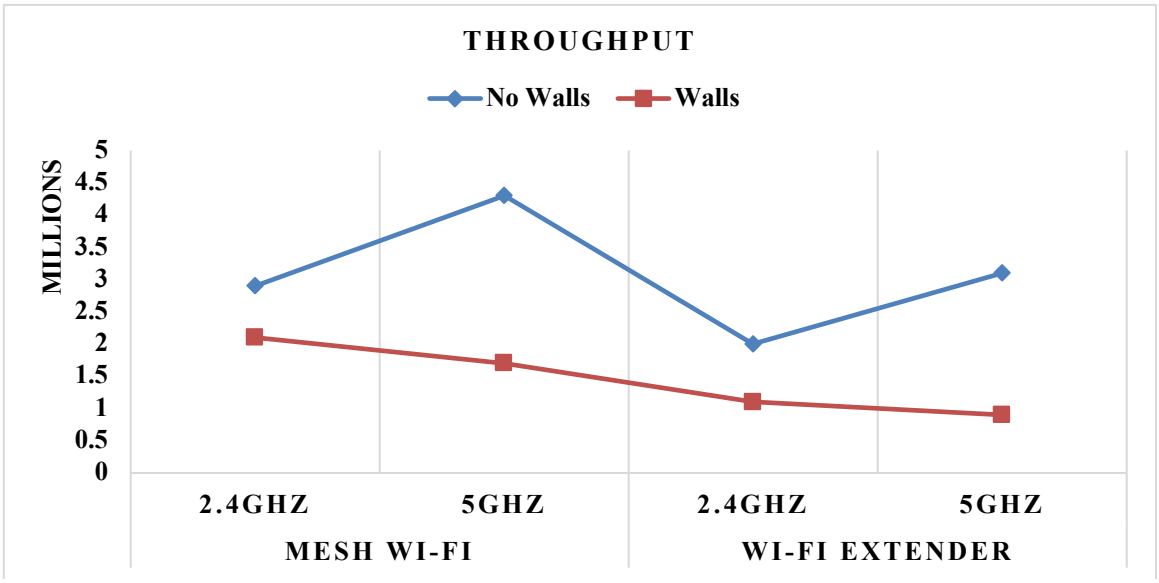

Figure (6): Throughput (Gbps) of Both Mesh and Extender network with and without walls

Figure (7) demonstrates the highest delay (seconds) in 5GHz extender Wi-Fi networks as its signal fades through walls with also rebroadcasting fading, which gives a very high delay in receiving the packets. The lowest delay can also be seen in the 5GHz no walls scenario as it's connected directly to the user with maximum transmission rate.

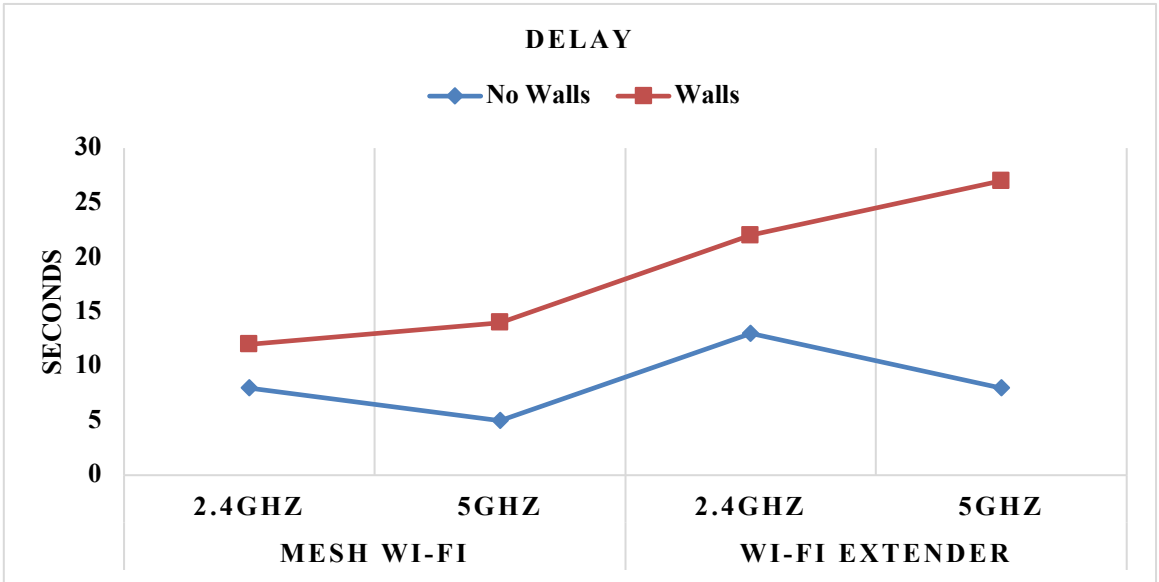

Figure (7): Delay (seconds) of Both Mesh and Extender network with and without walls

Finally, figure (8) shows the signal strength of the two networks, where the 2.4GHz shows the best result for both with and without walls, as it has lower path loss which gives more distance coverage. Unfortunately, 5GHz gives the lowest signal strength as it has short-range coverage.

DOI: https://doi.org/10.31972/ticma2022

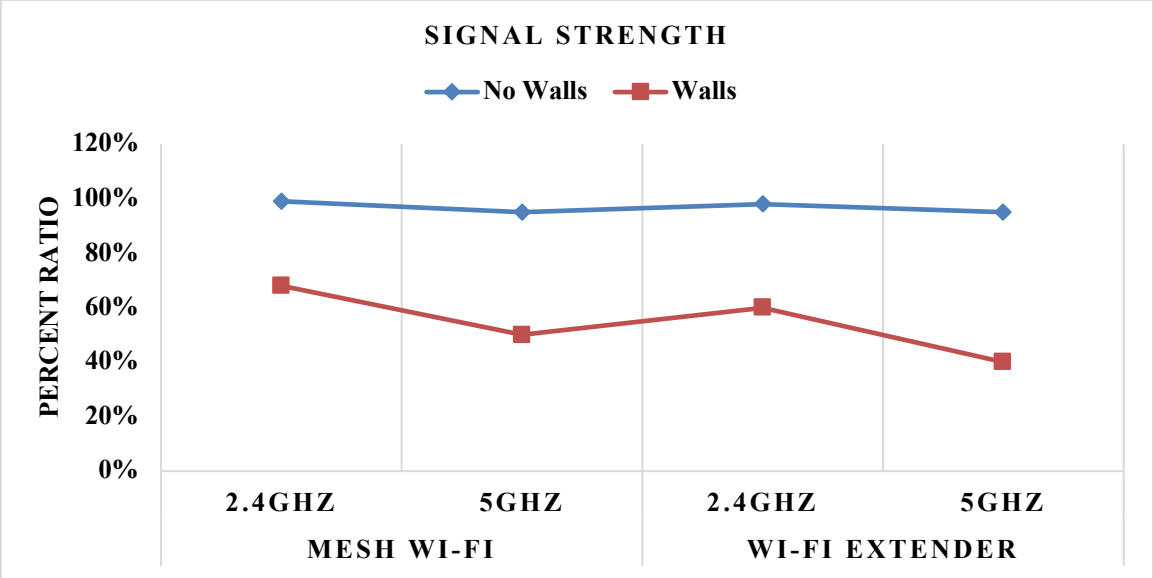

Figure (6): Signal Strength of Both Mesh and Extender network with and without walls

7. CONCLUSIONS

The IEEE 802.11ax wireless protocol gives remarkable improvement to the old wireless protocols in data transmission performance for different user environments, as it is implemented with advanced mechanisms to support more users and higher data transmission with reliable data transfer nowadays.

In this paper, a comprehensive practical analysis was done using real IEEE 802.11ax wireless routers connected with two scenarios Wi-Fi mesh and Wi-Fi extenders that broadcast two types of frequencies 2.4GHz and 5GHz in one room and two rooms separated with walls, to measures the throughput, delay and signal strength of the received signal.

The result shows that the best Wi-Fi booster for IEEE 802.11ax is Wi-Fi mesh connection as it keeps the signal strength as high as possible in both 5GHz and 2.4GHz, while 5GHz gives the lowest performance through walls. For Wi-Fi extenders, it gives lower performance compared to Wi-Fi mesh networks as it's suited for very short coverage with lower walls as possible.

For future work, it's recommended to test more result and metrics for the IEEE 802.11ax and comparing it with the older version in the different user environment, also its recommended to use more advance varying technology such as MANET, VANET, and FANET to measure the fast-changing topology impact of the IEEE 802.11ax performance.

REFERENCES

[1] Liu, B., Yi, X., Yang, K., Liang, Z., Feng, G., Choi, P., Boon, C.C. and Li, C., 2019. A carrier aggregation transmitter front end for 5-GHz WLAN 802.11 ax application in 40-nm CMOS. *IEEE Transactions on Microwave Theory and Techniques*, 68(1),264-276.

[2] Deng, C., Fang, X., Han, X., Wang, X., Yan, L., He, R., Long, Y. and Guo, Y., 2020. IEEE 802.11 be Wi-Fi 7: New challenges and opportunities. *IEEE Communications Surveys & Tutorials*, 22(4),2136-2166.

[3] Chen, C., Kedem, O., da Silva, C.R. and Cordeiro, C., 2019. Millimeter-wave fixed wireless access using IEEE 802.11 ay. *IEEE Communications Magazine*, 57(12),98-104.

[4] QasMarrogy, G.A. and Fadhil, A.J., 2022. A Comparative Study of Different FANET 802.11 Wireless Protocols with Different Data Loads. *Polytechnic Journal*, 12(1),61-66.

[5] Deng, C., Fang, X., Han, X., Wang, X., Yan, L., He, R., Long, Y. and Guo, Y., 2020. IEEE 802.11 be Wi-Fi 7: New challenges and opportunities. *IEEE Communications Surveys & Tutorials*, 22(4),2136-2166.

DOI: https://doi.org/10.31972/ticma2022

[6] Muhammad, S., Zhao, J. and Refai, H.H., 2021, March. An empirical analysis of IEEE 802.11 ax. In *2020 International Conference on Communications, Signal Processing, and their Applications (ICCSPA)* (1-6). IEEE.
[7] Naik, G., Bhattarai, S. and Park, J.M., 2018, May. Performance analysis of uplink multi-user OFDMA in IEEE 802.11 ax. In *2018 IEEE International Conference on Communications (ICC)* (1-6). IEEE.
[8] Deng, D.J., Lin, Y.P., Yang, X., Zhu, J., Li, Y.B., Luo, J. and Chen, K.C., 2017. IEEE 802.11 ax: highly efficient WLANs for intelligent information infrastructure. *IEEE Communications Magazine*, 55(12),52-59.
[9] Khorov, E., Kiryanov, A., Lyakhov, A. and Bianchi, G., 2018. A tutorial on IEEE 802.11 ax high efficiency WLANs. *IEEE Communications Surveys & Tutorials*, 21(1),197-216.
[10] Qu, Q., Li, B., Yang, M., Yan, Z., Yang, A., Deng, D.J. and Chen, K.C., 2019. Survey and performance evaluation of the upcoming next generation WLANs standard-IEEE 802.11 ax. *Mobile Networks and Applications*, 24(5),1461-1474.
[11] Deng, D.J., Lin, Y.P., Yang, X., Zhu, J., Li, Y.B., Luo, J. and Chen, K.C., 2017. IEEE 802.11 ax: highly efficient WLANs for intelligent information infrastructure. *IEEE Communications Magazine*, 55(12),52-59.
[12] Rochim, A.F., Harijadi, B., Purbanugraha, Y.P., Fuad, S. and Nugroho, K.A., 2020, February. Performance comparison of wireless protocol IEEE 802.11 ax vs 802.11 ac. In *2020 International Conference on Smart Technology and Applications (ICoSTA)* (1-5). IEEE.
[13] QasMarrogy, G., 2021. Evaluation of Flying Ad Hoc Network Topologies, Mobility Models, and IEEE Standards for Different Video Applications. *Aro-the Scientific Journal of Koya University*, 9(1),77-88.
[14] Weller, D., Mensenkamp, R.D., van der Vegt, A., van Bloem, J.W. and de Laat, C., 2020, June. Wi-Fi 6 performance measurements of 1024-QAM and DL OFDMA. In *ICC 2020-2020 IEEE International Conference on Communications (ICC)* (1-7). IEEE.
[15] Karthik, R.M. and Palaniswamy, S., 2018, September. Resource Unit (RU) based OFDMA Scheduling in IEEE 802.11 ax system. In *2018 International Conference on Advances in Computing, Communications and Informatics (ICACCI)* (1297-1302). IEEE.
[16] Lanante, L., Uwai, H.O.T., Nagao, Y., Kurosaki, M. and Ghosh, C., 2017, May. Performance analysis of the 802.11 ax UL OFDMA random access protocol in dense networks. In *2017 IEEE international conference on communications (ICC)* (1-6). IEEE.
[17] Kwon, D. and Kim, J., 2018, October. Opportunistic medium access for hyper-dense beamformed IEEE 802.11 ax wireless networks. In *2018 International Conference on Information and Communication Technology Convergence (ICTC)* (198-200). IEEE.
[18] QasMarrogy, G.A., 2021. Improving VoIP transmission for IEEE 802.11 n 5GHz MANET. , 33(1),157-162.
[19] QasMarrogy, G.A., 2021. FANET Drone's 4K Data Applications, Mobility Models and Wi-Fi IEEE802. 11n Standards. *Journal of Telecommunications and Information Technology,* (1),51-55.
[20] Ho, L., Garcia-Rodriguez, A., Giordano, L.G. and López-Pérez, D., 2020, May. Next generation Wi-Fi mesh for indoor residential deployments. In *2020 IEEE 91st Vehicular Technology Conference (VTC2020-Spring)* (1-5). IEEE.
[21] Adame, T., Carrascosa, M. and Bellalta, B., 2019, April. The TMB path loss model for 5 GHz indoor WiFi scenarios: On the empirical relationship between RSSI, MCS, and spatial streams. In *2019 Wireless Days (WD)* (1-8). IEEE.

Proceeding of 3rd International Conference of Mathematics and its Applications TICMA2022
https://conferences.su.edu.krd/su/ticma2022/
DOI: https://doi.org/10.31972/ticma2022

RESEARCH PAPER

Improving Prediction Accuracy of Lasso and Ridge Regression as an Alternative to LS Regression to Identify Variable Selection Problems

Pareekhan Abdulla Omer*
[1] Statistics department- College of Administration and Economics - Salahaddin University - Erbil / Iraq
Pareekhan.omer@su.edu.krd

A B S T R A C T:

This paper introduces the Lasso and Ridge Regression methods, which are two popular regularization approaches. The method they give a penalty to the coefficients differs in both of them. L1 Regularization refers to Lasso linear regression, while L2 Regularization refers to Ridge regression. As we all know, regression models serve two main purposes: explanation and prediction of scientific phenomena. Where prediction accuracy will be optimized by balancing each of the bias and variance of predictions, while explanation will be gained by constructing interpretable regression models by variable selection. The penalized regression method, also known as Lasso regression, adds bias to the model's estimates and reduces variance to enhance prediction. Ridge regression, on the other hand, introduces a minor amount of bias in the data to get long-term predictions. In the presence of multicollinearity, both regression methods have been offered as an alternative to the least square approach (LS). Because they deal with multicollinearity, they have the appropriate properties to reduce numerical instability caused by overfitting. As a result, prediction accuracy can be improved. For this study, the Corona virus disease (Covid-19) dataset was used, which has had a significant impact on global life. Particularly in our region (Kurdistan), where life has altered dramatically and many people have succumbed to this deadly sickness. Our data is utilized to analyze the benefits of each of the two regression methods. The results show that the Lasso approach produces more accurate and dependable or reliable results in the presence of multicollinearity than Ridge and LS methods when compared in terms of accuracy of predictions by using NCSS10, EViews 12 and SPSS 25.

KEY WORDS: Methodology, Regularization, Lasso regression, Ridge regression, multicollinearity.
DOI: https://doi.org/10.31972/ticma22.05

1. INTRODUCTION:

Multiple regression is frequently used to build a model for predicting future responses or to look into the link between the response variable and the predictor factors. The model's prediction accuracy is critical for the first aim, but the model's complexity is more relevant for the second goal. The least squares (LS) regression is notorious for underperforming in terms of model complexity and prediction accuracy. Ridge regression (Hoerl & Kennard, 1970), the Garotte (Breiman, 1995), Bridge regression (Frank and Friedman, 1993) and the Lasso (Tibshirani, 1996) were among the regularized regression approaches created in the last few decades to solve the faults of (LS) regression (see Van der Kooij and Meulman, 2006). The (LS) provides the coefficients that best fit to the data, with the additional criterion of finding unbiased coefficients. In this case, unbiased means that LS does not take into account which of the independent variables is more relevant than the others. It finds the coefficients for a given data set; there is just one set of betas to find Residual sum of squares (RSS). The intriguing question becomes, "Is the model with the smallest RSS truly the optimal mode?" The answer to the preceding question is (not really). It must also take into account (Bias), as implied by the word unbiased. Bias refers to how equally concerned a model is with its predictors.

This investigation will take a variety of approaches. This research will take a variety of techniques, using a variety of phrases and figures. There are two things that you should always keep in our mind. The first thing is that we always favor a model that catches the general patterns.

*** Corresponding Author: Pareekhan Abdulla Omer**
E-mail: Pareekhan.omer@su.edu.krd
Article History:
Received: 01/08/2022
Accepted: 15/09/2022
Published: 07/12/2022

DOI: https://doi.org/10.31972/ticma2022

The other is that we would forecast it based on new data rather than specific data. As a result, evaluation of model should be based on new data (testing set), rather than data that has already been collected (training set). Then, by adding a penalty term to the best fit produced from the trained data, regularization is a key concept used to avoid overfitting of the data, especially when the trained data are highly variable. Regularization is used to reduce volatility in the tested data, as well as to limit the influence of predictor factors on the output variable by compressing their coefficients. In statistics, the Lasso method is widely used to improve the model's prediction accuracy and interpretability. It was created in 1989 and is a regression strategy or approach that includes selection and regularization.

Lasso regression is a shrinkage-based extension of linear regression. The Lasso constrains the sum of the absolute values of the model parameters, with an upper bound of a specified constant. As a result of this constraint, the regression coefficients for some variables to shrink towards zero, i.e. (shrinkage). When there is automatic feature or variable selection, the Lasso regression is fairly simple (very easy). It's also useful when dealing with high-correlation predictors, as standard regression will usually have large regression coefficients. The Lasso regression technique can be applied in three different ways: (stepwise, backward, and forward) techniques. Feature selection is an important step in machine learning to avoid overfitting, and it's the same in regression.

If there are too many features in Lasso, some of them are completely removed, Setting the coefficients to zero completes the process. In machine learning jargon (vocab), this technique is referred to as (L1 Regularization). The Ridge regression was the most widely used technique for enhancing (improving) accuracy of prediction at the time. Ridge regression lowers prediction error by reducing overfitting by lowering the sum of the squares of the regression coefficients to be smaller than a specified value. However, it does not perform covariate selection and so does not help to the model's interpretability. The Lasso regression achieves both of these goals by reducing the total of the absolute values of the regression coefficients to be less than a fixed value, effectively driving certain coefficients to zero and removing them from the prediction process. This notion is identical to Ridge regression, which decreases the size of the coefficients as well, however Ridge regression tends to zero out many fewer coefficients.

2. METHODOLOGY:

A methodology of relationship between variables known as the regression studies, Functions are generally used to approximate the data. In the late 1880s, Francis Galton wondered if he could forecast men's height based on the height of their fathers. He proposed that men's heights are determined by the heights of their fathers, i.e., the taller the parent, the taller the son. Galton (1889) attempted to fit a straight line across the data set by plotting the heights of 14 fathers and their sons (Al-Nasser, 2017). In this case the relation between two variables Y and X can be written as:

$$y = \beta_0 + \beta_1 x_i + \varepsilon_i \quad , \quad \varepsilon_i \sim N(0, \sigma_\varepsilon^2) \tag{1}$$

This equation refers to simple linear regression model where Y is called a dependent variable, X is called a predictor variable and ε is called a random error, other symbols β0, β1 are called the regression coefficients (parameters). In general, a multiple linear regression model studies the relationship between dependent variable and several predictors' variables or features $X_i = (X_{i1}, X_{i2}, \dots, X_{ik})$ for a given (n) samples $(x_i, y_i)_{i=1}^{n}$. This model can be written as the form:

$$Y_i = \beta_0 + \beta_1 X_{i1} + \beta_2 X_{i2} + \cdots + \beta_k X_{ik} + \varepsilon_i \qquad j = 1,2, \dots, k \quad , \quad \varepsilon_i \sim N(0, \sigma_\varepsilon^2) \tag{2}$$

DOI: https://doi.org/10.31972/ticma2022

Where: Y_i: the dependent variable, X_j: the jth predictor variables. β_j: the average effect on response variable Y a one-unit increase in X_j, all other predictors held constant and ε_i: the error term. The least square approach (LS), which minimizes the Residual sum of squares (RSS), is used to determine the values of these parameters $\beta_0, \beta_1, \beta_2, \dots, \beta_k$:

$$RSS = \sum_{i=1}^{n}(y_i - \hat{y}_i)^2 \tag{3}$$

Where:

y_i: represents the actual response value for the i^{th} observation, and $\hat{y}_i$: represents the predicted response value based on the multiple linear regression model. If the data consists of n observations, then the following linear regression model is considered:

$$y_i = x_i^T \beta + \varepsilon_i \tag{4}$$

where β is a vector of parameters and ε_i are scalar random errors, the matrix form (4) can be represented as (a general linear model)

$$\underline{Y} = X\underline{\beta} + \underline{\varepsilon} \quad , \quad \varepsilon_i \sim N(0, \sigma_\varepsilon^2) \tag{5}$$

$\underline{Y}$: represents a vector of the response variable of order $(n \times 1)$.

X: represents the matrix of the observation of the explanatory variables of order $(n \times p)$, where $p = k + 1$

$\underline{\beta}$: vector parameters are estimated from the class $(p \times 1)$.

$\underline{\varepsilon}$: random error vector of class $(n \times 1)$.

In form (4) and (5), the errors are assumed to have zero mean and a constant variance: $E(\varepsilon) = 0$, $Var(\varepsilon) = \sigma^2 I_n$ (see Bager, Mohammed, & Odah, 2017), As a result, the OLS assumptions are met, and the following estimations of β are obtained:

$$\hat{\beta} = (X^T X)^{-1} X^T Y \tag{6}$$

And the fitted values of the response variable are:

$$\hat{Y} = X\hat{\beta} = X(X^T X)^{-1} X^T Y \tag{7}$$

Multicollinearity can be a concern when the predictor variables are highly correlated. This can make the model's coefficient estimations incorrect (unreliable) and have a lot of variances.

DOI: https://doi.org/10.31972/ticma2022

3. REGULARIZATION METHODS

Regularization works by adding a penalty, complexity term, or shrinkage term to the complicated model using Residual sum of squares (RSS).

$$RSS = \sum_{i=1}^{n}\left(y_i - \beta_0 - \sum_{j=1}^{k}\beta_j x_{ij}\right)^2 \quad (8)$$

Regularization solves the overfitting problem, which has an impact on the model's accuracy. It is carried out by adding the penalty term to the best fit equation derived from the trained data. This strategy can be used to reduce the number of variables in the model while still keeping them in the model. Regularization can be used for a variety of purposes, including deciphering (understanding) simpler models such as sparse and group structure models. Ridge Regression and Lasso Regression are two major regularization techniques that are used to reduce the model's complexity. Except for the penalty term, which is different since lasso regression uses absolute weights and ridge regression uses the square of weights (see Melkumova & Shatskikh, 2017).

4. LASSO REGRESSION

Lasso was developed by Tibshirani (1996), which is widely used in the construction of prediction models. Hastie, Tibshirani, and Wainwright (2015) provide a great introduction to the Lasso's physics and use as a prediction tool (Tibshirani and Taylor, 2011). The full form of Lasso is the least Absolute Shrinkage and Selection Operation. The Lasso regression is a regularization technique. it is used over regression methods for a more accurate prediction. The "shrinkage" strategy is used in the lasso model to generate coefficients, which are then shrunk toward the center point as the mean or median. Data values are shrunk towards a central point known as the mean in shrinkage. In regularization, lasso regression is based on simple models with fewer parameters (models with fewer parameters). Because of the shrinkage process, we can get a better interpretation of the models. The shrinking procedure also allows for the detection of variables that are tightly linked to variables that correspond to the target. Penalized regression is another name for Lasso regression. In machine learning, this strategy is commonly used to pick a subset of variables. When compared to other regression models, it has a greater prediction accuracy. Model interpretation is increased by lasso regularization. The lasso regression penalizes the dataset's less important features. This dataset's coefficients are set to zero, resulting in their removal. For lasso regression, a dataset with high dimensions and correlation is well suited (Flexeder, 2010).

The Lasso method has been popularly used for variable selection problems. In a regression model, the Lasso method uses a L_1 penalty to shrink the coefficients associated with covariates towards zero and set some unimportant covariate coefficients to zero, such that important covariates are selected and unimportant covariates are left out. The Lasso method was originally developed to model the quantitative response variables (see Bak, 2017). A linear regression model (2) can be considered as:

$$y_i = \beta_0 + \sum_{j=1}^{k}\beta_j X_{ij} + \varepsilon_i \qquad \varepsilon_i \sim N(0, \sigma^2) \quad (9)$$

Where $Y_i \in R$ is the response variable and $X_i = (X_{i1}, X_{i2}, \dots, X_{ik})$ is a vector that has (k) predictor values for subject (i) and $i = 1,2, \dots, n$, for a given sample size of n. The Lasso seeks out a model that minimizes the sum of squares of residuals $\sum_{i=1}^{n}\varepsilon_i^2$, subject to a constraint $\sum_{j=1}^{k}|\beta_j| \leq t$ where $t > 0$ is a parameter that determines the amount of shrinkage applied to the coefficients and allows the model to be cleaned up (irrelevant variables from the model) by setting some βs to zero.

DOI: https://doi.org/10.31972/ticma2022

The Lasso estimate of $\hat{\beta} = (\hat{\beta}_0, \hat{\beta}_1, \dots, \hat{\beta}_k)$ is given by

$$\hat{\beta} = arg\min_{\beta}\{\sum_{i=1}^{n}(y_i - \beta_0 - \sum_{j=1}^{k}\beta_j X_{ij})^2\} \quad s.t\ \sum_{j=1}^{k}|\beta_j| \le t \tag{10}$$

Here, the smaller value of t will shrink coefficients more toward the origin and make more of the coefficients to be zero. Therefore, the Lasso penalty performs variable selection continuously as the t continuously increases or decreases. Note that the optimization problem in equation (2) can be rewritten in Lagrange function that the Lasso estimates of $\hat{\beta} = (\hat{\beta}_0, \hat{\beta}_1, \dots, \hat{\beta}_k)$ minimize a penalized Residual sum of squares is provided by

$$\hat{\beta}^{Lasso} = arg\min_{\beta}\{\sum_{i=1}^{n}(y_i - \beta_0 - \sum_{j=1}^{k}\beta_j X_{ij})^2 + \lambda\sum_{j=1}^{k}|\beta_j|\} = RSS + \lambda\sum_{j=1}^{k}|\beta_j| \tag{11}$$

Reversely, the larger value of the tuning parameter λ, the greater amount of shrinkage, more coefficient is set to zero, and thus a more parsimonious model is achieved. The choice of λ that optimizes the predictability of the fitted model by Lasso is obtained by the cross-validation procedure (Bak, 2017).

5. RIDGE REGRESSION

Ridge regression is not a new concept in the field of education .It has been used as an alternative prediction weighting technique to non-ordinary least squares (OLS) (see Walker, 2004) .Ridge regression is a technique for analyzing and treating multicollinearity after testing multicollinear data in multiple regression models .When predictor variables have a correlation among themselves, this is known as multicollinearity. Ridge regression seeks to reduce the standard error by adding some bias to the fisher information matrix .The reliability of regression estimates is greatly improved when the standard error is reduced .Ridge regression is a type of linear regression in which we introduce a little amount of bias, known as the Ridge regression penalty, so that we can get better long-term predictions, it's known as the L2 -norm in statistics.

When there are more predictor variables in a data set than there are observations, or when there is multicollinearity, least squares estimates are unbiased, but their variances are enormous, therefore they may be far off the true value .Ridge regression reduces standard errors by adding a degree of bias to the regression estimates .It is hoped that the net effect will be to provide more dependable estimates .The covariates (the columns of X) are super-collinear when the design matrix is high-dimensional .In regression analysis, multicollinearity refers to the situation where two (or more) covariates are highly linearly connected .As a result, the collinear subspace may not be (or may be close to not being) of full rank .Consequently, the subspace spanned by collinear may not be (or close to not being) of full rank. The function is changed in this method by including a penalty term (shrinkage term), which multiplies the lambda by the squared weight of each unique feature .As a result, the optimization function becomes:

$$\hat{\beta}^{Ridge} = arg\min_{\beta}\{\sum_{i=1}^{n}(y_i - \beta_0 - \sum_{j=1}^{k}\beta_j X_{ij})^2 + \lambda\sum_{j=1}^{k}\beta_j^2\} = RSS + \lambda\sum_{j=1}^{k}\beta_j^2 \tag{12}$$

Which is equivalent to minimization of RSS subject to, for some $c > 0$, $\sum_{j=1}^{k}\beta_j^2 < c$. constraining the sum of the squared coefficients. Writing this criterion in matrix form we have:

$$RSS(\lambda) = (Y - X\beta)^T(Y - X\beta) + \lambda\beta^T\beta$$

Then the result is the Ridge regression estimator as: $\hat{\beta}^{Ridge} = (X^TX + \lambda I)^{-1}X^TY$ (13)

DOI: https://doi.org/10.31972/ticma2022

6. LASSO REGRESSION VERSUS RIDGE REGRESSION

Lasso regression and Ridge regression are used to reduce the model's complexity .Ridge regression is also known as L2 Regularization and Lasso linear regression is known as L1 Regularization .But first, let's distinguish between ridge and lasso regression .To obtain long-term forecasts, ridge regression introduces a modest amount of bias. By adding the penalty term, this amount of bias is known as the Ridge regression penalty .The absolute weights are contained in the penalty term in Lasso regression .As a result of the use of absolute values, the Lasso might decrease closer to the slope than ridge regression, which shrinks towards zero.

One variable is kept in Lasso linear regression, while the other correlated variables are set to zero . As a result of the loss of information, accuracy suffers .Ridge regression is frequently referred to as a Lasso regression example .As a result, it's clear that Lasso and ridge regression each have their own set of benefits .With the help of automatic variable selection for the models, Lasso eliminates the coefficients (shrinks to zero), whereas ridge regression is unable to do so .Both strategies, however, deal with over-fitting, which is a problem in realistic statistical models .The availability of data for machine learning is critical to the effectiveness of these techniques .Ridge regression is more efficient than Lasso regression, but Lasso is successful in eliminating the unwanted parameters present in the model (Melkumova and Shatskikh, 2017).

the Figure 1. helps us to understand better, where we will assume a hypothetical dataset with only two features. Using the constrain for the coefficients of Lasso and Ridge regression, the constraint regions for Lasso and Ridge regression are plotted with cyan and green colors for a two-dimensional feature space .Linear regression is responsible for the elliptical contours (eq. 4 and 5). If the coefficients are relaxed, the constrained region can expand and eventually reach the ellipse's center .When the findings of Lasso and Ridge regression resemble those of linear regression, this is the case .Otherwise, both approaches calculate coefficients by finding the first point where the elliptical contours intersect the constraint region .In contrast to the disk, the diamond (Lasso) has corners on the axes, and whenever the elliptical region hits such a point, one of the features completely vanishes. For higher dimensional feature space, there can be many solutions on the axis with Lasso regression, and thus only the most important features are selected.

Now we'll compare the shrinkage methods by examining the geometry of Lasso and Ridge regression. The estimation problem for both methods is shown in the figure below, when just two predictors are available .The circular outlines centered around the OLS estimate show locations where the RSS is constant, and the figure displays the constraint region from equations (7 and 8) .The location where the elliptical contour intersects the constraint region is found by both regression methods. Lasso has a diamond-shaped constraint region given by $|\beta_1| + |\beta_2| \leq t$. whereas Ridge regression has a circle-shaped constraint region defined by $\beta_1^2 + \beta_2^2 \leq c$. In the case of Lasso, one of the coefficients β_j is equal to zero if the contour crosses the diamond at a corner (Matthias & Emmert-Streib, 2019)

TABLE 1. Overview of regularization or penalty and methods

Methods	Regularization Term
Ridge regression	L_2 norm: $\|\beta\|_2$
Lasso regression	L_1 norm: $\|\beta\|_1$

Proceeding of 3rd International Conference of Mathematics and its Applications
TICMA2022
https://conferences.su.edu.krd/su/ticma2022/
DOI: https://doi.org/10.31972/ticma2022

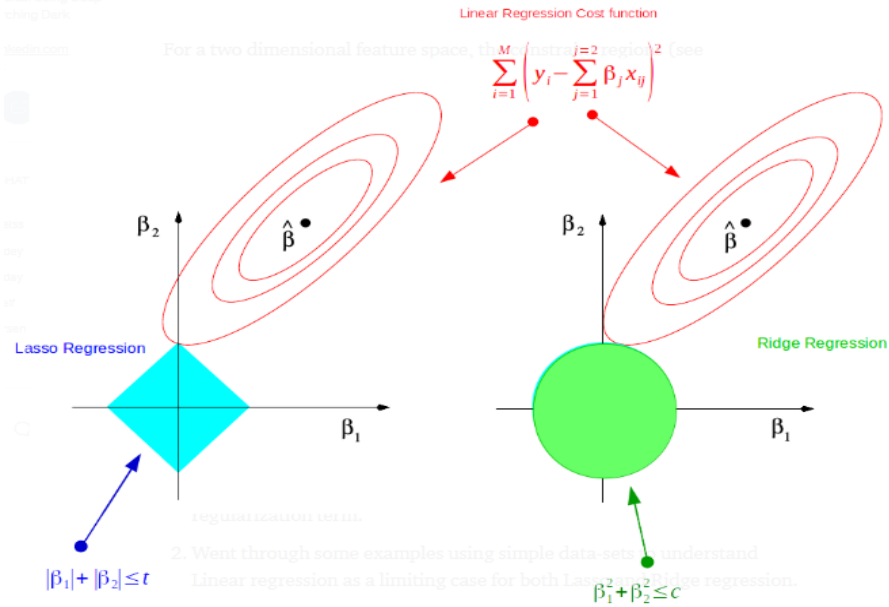

FIGURE 1. Lasso and Ridge geometrical interpretation: elliptical contours as the contours of errors and constraints for Lasso $|\beta_1| + |\beta_2| \leq t$ and Ridge $\beta_1^2 + \beta_2^2 \leq c$ (Matthias & Emmert-Streib, 2019)

7. DATA COLLECTION

The dataset of Corona virus epidemic (Covid-19) was taken for this study, which has affected on the world life totally. Especially in our region (Kurdistan), where life has changed in unexpected significantly way and millions of people have suffered from this dangerous disease. So, Influenza and the Covid-19 virus both display a similar disease presentation. In other words, they both cause respiratory disease, which can present as a variety of illnesses ranging from asymptomatic or mild to severe disease and death .Both viruses can spread through touch, droplets, and spores .As a result, everyone may prevent infection by practicing the same public health precautions, such as hand washing and proper respiratory hygiene (coughing into your elbow or into a tissue and throwing the tissue away right away) are important actions all can take to prevent infection. So, the speed of transmission is only important point of difference between the two viruses. When compared to Covid-19, influenza has a shorter median incubation period (the gap between infection and the onset of symptoms) and serial interval (the space between subsequent occurrences). Used the data of (263) case and have been taken in 2020, the information of each person gathered individually who suffered from this dangerous disease during this year. The dependent variable was (duration or number of sick daily injured and the independent variables were (Gender, Age, causes, does has other disease, in what way (he or she) got the disease, take the treatment, the result of disease (dead or alive)).

8. APPLICATION, RESULTS AND DISCUSSION

The Lasso regression analysis is a technique used in statistics and machine learning that performs both variable selection and regularization to improve the predictability accuracy and understandability of the resulting statistical model .When the subspace (which Y is projected) is close to rank deficient. It is almost impossible to separate the contribution of the individual covariates. The fit of the linear regression model to the data is frequently characterized by a significant inaccuracy in the estimates of the regression parameters corresponding to the collinear covariates, which reflects the uncertainty regarding the covariate responsible for the variance explained in Y. (Wieringen, 2015) .In regularization, we typically maintain the same number of features while reduce the coefficients' magnitudes .By using a variety of regression techniques that make use of regularization, we can reduce the magnitude of the coefficients.

Variables	Regular LS Coeffici.	Standardized LS Coeffici.	LS Standard Error	Regular Ridge Coeffici.	Standardized Ridge Coeffici.	Ridge Standard Error	Regular Lasso Coeffici.	Standardized Lasso Coeffici.	Lasso Standard Error
Intercept	9.093963	-------	6.139416	9.19879	------	--------			
Gender- X_1	-1.32163	-0.0491	1.67572	-1.31357	-0.0488	1.667189	-1.26287	-0.046940	1.679153
Age - X_2	0.090004	0.1018	0.058112	0.08929	0.1010	0.057751	0.12730	0.143983	0.052496
Cause -X_3	0.710753	0.0451	1.004914	0.70845	0.0449	0.999360	1.182839	0.075045	0.955255
Other disease- X_4	-1.44385	-0.0460	2.207817	-1.43019	-0.0455	2.191664	-1.14771	-0.036531	2.203867
In what way- X_5	1.908793	0.1112	1.2426	1.89172	0.1102	1.23242	2.606488	0.151813	1.152546
take treatment - X_6	3.447485	0.1199	2.068082	3.41144	0.1186	2.05126	4.486400	0.155996	1.950047
Result- X_7	5.201583	0.0777	4.514616	5.17289	0.0772	4.485531	9.868086	0.147326	3.241224

TABLE 2. Least Squares vs Ridge and Lasso regression comparison

Table 2. shows the results of fitting a multiple linear regression model of LS, Ridge and Lasso regression to describe the relationship between the duration (number of sick days) and (7) of independent variables which describing them in the data collection part above, these three methods provide different results. it illustrates the Regular estimated values of the regression of each method. Additionally, it provides the estimated Standardized Regression Coefficient values for each method .The coefficients that would result from standardizing each independent and dependent variable are the standardized regression coefficients for each method .Here, standardization is described as dividing by the standard deviation of a variable and subtracting the mean from it .These standardized coefficients would yield from a regression study on these standardized variables. The formula for the standardized regression coefficient is:

$$\hat{\beta}_j^{std.} = \hat{\beta}_j \left(\frac{S_{x_j}}{S_y}\right) \tag{14}$$

Where S_y and S_{x_j} are the standard deviations for the dependent variable and the corresponding j^{th} independent variable. Also, in the table above shows the estimated error of the regression coefficient $S.E(\hat{\beta}_j)$, it is the standard deviation of the estimate, whoever the standard error of the estimate reduces, it makes the estimates more precise. Here, Lasso standard error of the estimates (yellow color column) has the values less than Ridge and LS standard error of the estimates in table 2.

TABLE 3. the testing hypotheses and dependency problem in the explanatory variables

Variables	VIF	VIF	VIF

https://conferences.su.edu.krd/su/ticma2022/
DOI: https://doi.org/10.31972/ticma2022

	LS	Ridge	Lasso
Gender- X_1	1.0323	1.0214	1.89057
Age - X_2	1.3996	1.3749	8.04846 (*)
Cause -X_3	1.0456	1.0343	5.59775 (*)
Other disease - X_4	1.4436	1.4177	1.69566
In what way - X_5	1.5317	1.5017	11.0564 (*)
take treatment - X_6	1.5700	1.5380	1.77009
Result - X_7	1.1991	1.1833	14.6705 (*)

(*): represents the existence of multicollinearity when the value of VIF Lasso higher than (5).

To check the presence of dependency between the independent variables look the table 5. of correlation matrix and used VIF, in table 3. expresses three models for regression and tested their multicollinearity problem, shows that the Lasso model under investigation has this issue (problem). The Variance Inflation Factor (VIF), which assesses the inflation of the parameter estimates for all explanatory variables in the model, was used to identify the causal variables (see Farrar & Glauber, 1967), the VIF measures the presence of multicollinearity, and computed as follows:

$$VIF_j = \frac{1}{1-R_j^2} = \frac{1}{Tolerance} \quad , \quad VIF = (1 - R_j^2)^{-1} \quad , \; j = 1,2, \dots, k \tag{15}$$

using the VIF_j is one method for detecting multicollinearity in regression data. Where the more likely of multicollinearity among the variables is indicated by a lower tolerance. When $VIF_j = 1$, it represents that the independent variables are not correlated with one another. if the value of $1 < VIF_j < 5$, It indicates that there is a moderate correlation between the variables. The difficult range for VIF_j is between 5 and 10, which indicates the range of highly correlated variables .It means $VIF_j \geq 5 \; to \; 10$, there will be multicollinearity among the regression model's predictors, and if $VIF_j > 10$ the regression coefficients for the regression matrix X are only tentatively estimated in the presence of multicollinearity (see Shrestha, N., 2020). In our results of analyzing these three methods the variables suffer from inflation in the variance of their parameters variables as showed in table (3) of (VIF Lasso), the explanatory variables (X_2, X_3, X_5, X_7) have high value of VIF, where X_2, X_3 have value between $5 < VIF_j < 10$, and X_5 , X_7 have a VIF value greater than 10 for large datasets indicates a multicollinearity problem.

https://conferences.su.edu.krd/su/ticma2022/
DOI: https://doi.org/10.31972/ticma2022

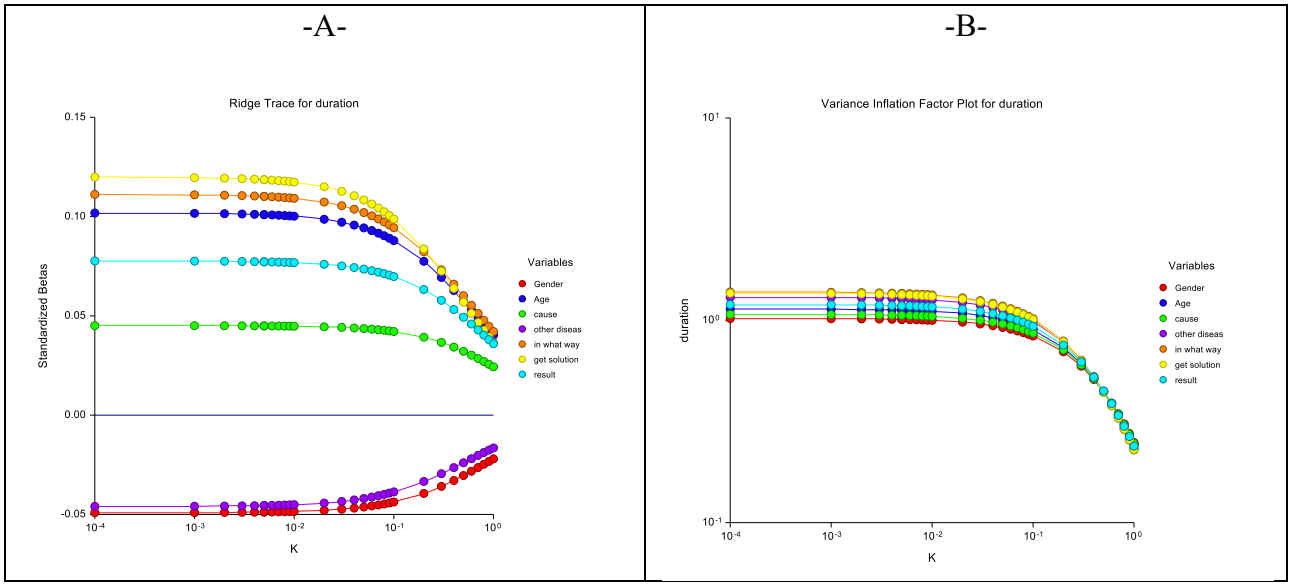

FIGURE 2. Ridge coefficient path for the data set found in NCSS

Choosing an acceptable value of K, is one of the key challenges in using Ridge regression (see Hoerl, and Kennard,1970). The Ridge Trace, a diagram created by the Ridge regression's creators, was recommended. The Ridge regression coefficients are plotted here as a function of K. The analyst selects a value of k for which the regression coefficients have stabilized while looking at the Ridge Trace (see figure 2.). Often, for low values of k, the regression coefficients frequently exhibit large fluctuations before stabilizing. Select the least value of k that results in the smallest amount of bias and causes the regression coefficients have seem to remain constant .Be aware that as k increases, eventually drive the regression coefficients to zero.

The figure (2. -A-) shows that these lines are for different explanatory variables and which of them are significant predictors of Y in above dataset. Additionally gives the standardized regression coefficients for Ridge parameter values in the range of 0.0 to 0.1. These are the regression model's coefficients when the variables are expressed in standardized form. The coefficients frequently shift considerably at first as the Ridge parameter is increased from zero but subsequently tend to stabilize. The smallest value after which the estimates shift gradually (change slowly) is a good value for the Ridge parameter. Your coefficients will be penalized by the ridge regression, and those that you estimate to be least useful (effective) will decrease the quickest.

The variance inflation factors for each of the regression model's coefficients are displayed in Figure (2. -B-). In comparison to the case in which all independent variables are uncorrelated, the variance inflation factors quantify how much the variance of the predicted coefficients is inflated. The VIFs frequently decline sharply (decrease dramatically) when the ridge parameter is increased from 0, but after that they tend to stabilize. The smallest value after which the VIFs change slowly is a suitable value for the ridge parameter. Press the alternative mouse button and choose Analysis Options to alter the range of ridge parameters investigated .When there is a multicollinearity problem between the independent variables, the Ridge regression model is based on estimation of the model parameters. If the value of (k=0), the same estimators as in the LS are obtained, where the Ridge regression coefficients are (k) .But, when the value of (k) increases away from zero, we observe the stability of the estimators as their values change. At (k=0.005), the results demonstrate that the level of the VIF of Ridge model for the explanatory variables are shown as in the figure above.

DOI: https://doi.org/10.31972/ticma2022

TABLE 4. the results of three estimation procedures

Methods	Std. Error of the Estimate	F-Ratio test	p-value	Adj R^2	MES
LS regression	13.4022	0.4850	0.8433	0.48094 %	170.0295
Ridge regression	13.2406	0.4898	0.8448	0.580893%	170.0563
Lasso regression	13.1766	3.691	0.0440(*)	0.601661%	167.9220

(*) indicate significant of Lasso regression model at the 5%

Table 4. expresses standard deviation of estimate, F-test, P-value, Adjusted R2 and MSE values. The results of applied OLS and Ridge and Lasso method are shown above, these techniques provide different outcomes, and the approach we suggest provide the smallest value by minimizing the sum squared of errors using the value of k rather than LS, which results in the value of MSE. it can be seen that the P-value of LS method and Ridge method are greater than 0.05, it means not significant statistically relationship between the variables at the 95% or higher confidence level. Consequently, the researcher should consider removing variable that is not significant from the model. The adjusted R^2 statistic is more suitable for comparing different multiple models with different numbers of independent variables. The adjusted $R^2 = 0.60166$ of Lasso regression model shows that 60.166% gives how effectively the model generalizes in comparison to other models. The value of F ratio test of measures the statistical significance of the Lasso model equal to (3.691) and MSE of Lasso has small value equal to (167.9220), F-test value is statistically significant at $(p - value < 0.05)$, $(0.044 < 0.05)$ and it can be observed that from the table above. Totally, the results of analyzing data by Lasso regression model obtained better than two other models.

TABLE 5. Correlations matrix

		Gender	Age	Cause	Other disease	In.what.way	take treatment	Result
Gender- X_1	Pearson Correlation	1	.046	.001	.090	.017	.006	.079
Age - X_2	Pearson Correlation	.046	1	.124*	.312**	-.116	.009	-.150*
Cause -X_3	Pearson Correlation	.001	.124*	1	.161**	-.028	.126*	-.189**
Other disease - X_4	Pearson Correlation	.090	.312**	.161**	1	-.277**	.284**	-.283**

DOI: https://doi.org/10.31972/ticma2022

In what way - X_5	Pearson Correlation	.017	-.116	-.028	-.277**	1	-.467**	.288**
take treatment - X_6	Pearson Correlation	.006	.009	.126*	.284**	-.467**	1	-.224**
Result - X_7	Pearson Correlation	.079	-.150*	-.189**	-.283**	.288**	-.224**	1
*. Correlation is significant at the 0.05 level (2-tailed).								
**. Correlation is significant at the 0.01 level (2-tailed).								

9. CONCLUSIONS

The statistical analysis of Lasso and Ridge regression estimation as an alternative method to LS regression estimation for the data leads to the following conclusions:

1. whoever the standard error of the estimate reduces, it makes the estimates more precise. As it seen in standard error of the estimates of Lasso has the smallest values when compared with Ridge and LS standard error of the estimates.

2. In presence of multicollinearity used VLF measurement, shows that Lasso regression method has more powerful to checking this problem between explanatory variables while the other methods haven't this power because in Lasso method found 5 explanatory variables with high dependency value of VIF among 7 of explanatory variables, Lasso method is investigated the relationship between variables for the real dataset. this problem could be improved by adding more cases in to the data, increasing the sample size of the data set.

3. The estimators used in the LS regression are the same as those found in the Ridge regression coefficients if the value of (k=0). But when the value of (k) moves away from zero, we observe that the estimators' stability increases. At (k=0.005) the results indicate the level of the VIF of Ridge model for the explanatory variables, at this value of (k) found it the best estimates of the model.

4. It observed that the proposed Lasso method is more significant than the classical LS method and Ridge method, depend on the value of p-value of the F-test and decrease value of MSE.

5. Increase the value of Adj R2 of Lasso method leads that it will be more appropriate method than the other for this data.

6. The estimation method of LS and Ridge regression method provides almost similar results, while the Lasso estimation method is able to produce consistent and more efficiency coefficients results depend on that criterion used in this study.

ACKNOWLEDGMENTS

Most of all I thanks "almighty Allah" with countless and gratitude, for all this blessing, who gave me this great opportunity to complete this research. I'm very grateful and thankful to my family for their support.

We should also thank everyone who participated in my research and to all the people I remembered who helped me.

REFERENCES

[1] AlNasser, H., 2017. *On ridge regression and least absolute shrinkage and selection operator* (Doctoral dissertation).
[2] Bak, S., 2017. *Generalized linear regression model with LASSO, group LASSO, and sparse group LASSO regularization methods for finding bacteria associated with colorectal cancer using microbiome data* (Doctoral dissertation, University of Guelph).
[3] BAGER, A.S.M., Mohammed, B.K. and Odah, M.H., 2017. Ridge Regression Analysis On The Influential Factors Of Fdi In Iraq. In *Proceedings of the INTERNATIONAL MANAGEMENT CONFERENCE* (Vol. 11, No. 1, pp. 19-25). Faculty of Management, Academy of Economic Studies, Bucharest, Romania.
[4] Flexeder, C., 2010. *Generalized lasso regularization for regression models* (Doctoral dissertation, Institut für Statistik).
[5] Farrar, D.E. and Glauber, R.R., 1967. Multicollinearity in regression analysis: the problem revisited. *The Review of Economic and Statistics*,92-107.
[6] Melkumova, L.E. and Shatskikh, S.Y., 2017. Comparing Ridge and LASSO estimators for data analysis. *Procedia engineering*, 201,746-755.
[7] Emmert-Streib, F. and Dehmer, M., 2019. High-dimensional LASSO-based computational regression models: Regularization, shrinkage, and selection. *Machine Learning and Knowledge Extraction*, 1(1),359-383.
[8] Pereira, J.M., Basto, M. and da Silva, A.F., 2016. The logistic lasso and ridge regression in predicting corporate failure. *Procedia Economics and Finance*, 39,634-641.
[9] Shrestha, N., 2020. Detecting multicollinearity in regression analysis. *American Journal of Applied Mathematics and Statistics*, 8(2),39-42.
[10] Shariff, N.S.M. and Duzan, H.M.B., 2018. An application of proposed Ridge Regression Methods to real data problem. *International Journal of Engineering & Technology*.
[11] Tibshirani, R.J. and Taylor, J., 2011. The solution path of the generalized lasso. *The annals of statistics*, 39(3),1335-1371.
[12] Flexeder, C., 2010. *Generalized lasso regularization for regression models* (Doctoral dissertation, Institut für Statistik).
[13] Walker, D.A., 2004. Ridge regression as an alternative to ordinary least squares: Improving prediction accuracy and the interpretation of beta weights. *The AIR Professional File*, 92,1-12.
[14] van Wieringen, W.N., 2015. Lecture notes on ridge regression. *arXiv preprint arXiv:1509.09169*.
[15] Van der Kooij, A.J. and Meulman, J.J., 2008. Regularization with ridge penalties, the lasso, and the elastic net for regression with optimal scaling transformations. *Submitted for publication*.

Proceeding of 3rd International Conference of Mathematics and its Applications TICMA2022
https://conferences.su.edu.krd/su/ticma2022/
DOI: https://doi.org/10.31972/ticma2022

RESEARCH PAPER

Assessment of natural radionuclides in cooking salts available in Kurdistan region-Iraq

Adeeb O. Jafir[a,*] , Hallo M. Abdullah[b], Ali H. Ahmed[c]
Department of physics, College of Science, Salahaddin University-Hawler, Kurdistan Region, Iraq.
[a]adeeb.jafir@su.edu.krd
[b]hallo.sallay@su.edu.krd
[c]*ali.ahmed@su.edu.krd*

A B S T R A C T:
Eighteen local and imported salt samples were collected in markets of Kurdistan region. The cooking salt as an essential foodstuff element in meals of population in all over the world has been examined for radioactivity assessment. Gamma ray spectroscopy of NaI (Tl) was used to obtain the spectra and measuring the specific radionuclide activities of 226Ra, 232Th and 40K in salt samples. The related radiological indices of radium equivalent (Raeq), indoor absorbed dose, indoor annual effective dose equivalent (Ein), the internal index (Hin), annual committed effective dose (Eing) and excess life time cancer (ELCR) were calculated which were below the world safety recommendation values declared by UNSCEAR2000 and WHO. Statistics of Pearson correlation were applied to the obtained data to establish the correlation between primordial radionuclide's and radiological hazards.

KEY WORDS: RADIOACTIVITY, NAI(TL) DETECTOR, SALT, CANCER RISK, ANNUAL DOSE
DOI: https://doi.org/10.31972/ticma22.06

1. INTRODUCTION:

The environmental radioactive material can be divided into natural and man-made radionuclides. The former is caused by cosmic and terrestrial radiation, while the latter are a result of nuclear worldwide tests and accidents. Natural primordial radionuclides are exposed to humans and are present in the environment with varying abundances and non-identical distributions [1]. According to [2], there are four different ways that radioactive materials can enter the human body: inhalation from breathing radioactive aerosols or dust particles; ingestion from radioactivity being transferred to the mouth; absorption from entry through intact skin; and injection from an object puncturing the skin with radioactive materials. The nature, the geology, and the location of food production are just a few of the many variables that might affect the presence of radionuclides in food. The common radionuclides in food are the long lived ^{40}K, ^{232}Th and ^{238}U with their associated progeny. According to [3], the primary sources of the internal dose that is continuously exposed inside the human body as a result of eating are the single decay scheme of potassium-40 and the decay series of thorium-232 and uranium-238 with their daughters. Mines and the ocean floor both contain salt that can be extracted. Different industries use salt and the components it produces for human use [4]. The measurement of radioactivity in cooking salt has been examined by numerous researchers from around the world [5]; [6]; [7]; [8]; [4]; [9]; [10]; [11]. The purpose of the current work is to determine the level of natural primordial radionuclides and the associated radiological hazard index in local and imported cooking salt available in Kurdistan markets.

*** Corresponding Author: Adeeb O. Jafir**
E-mail: adeeb.jafir@su.edu.krd
Article History:
Received: 01/08/2022
Accepted: 15/09/2022
Published: 07/12/2022

https://conferences.su.edu.krd/su/ticma2022/
DOI: https://doi.org/10.31972/ticma2022

2.Materials and method:

Sampling From Kurdistan's local markets, 18 samples of various cooking salts were gathered. For the salt samples, the drying and sieving processes were carried out, and 1 kg of each was placed inside a sealed Marinelli beaker and stored for at least 30 days in order to acquire the secular equilibrium between the parent and progeny radionuclides. Different kinds of local and imported cooking salts are displayed in Table 1.

Here we provide some basic advice for formatting your mathematics, but we do not attempt to define detailed styles or specifications for mathematical typesetting. You should use the standard styles, symbols, and conventions for the field/discipline you are writing about.

TABLE 1. Type and origin of the studied salt samples.

Name	Code	Production Country
Khosh	S1	Turkey
Almaeda	S2	Iraq
Alnima	S3	Turkey
Altabaq	S4	Iraq
Altunsa	S5	Turkey
Altunsara	S6	Iraq
Awagrd	S7	Iraq
Bilbak	S8	Turkey
Cihan	S9	Turkey
Dolfin see	S10	Turkey
Golha	S11	Iran
Hakan	S12	Turkey
Nawras	S13	Turkey
Raz	S14	Turkey
Sevan	S15	Turkey
Salt	S16	Iraq
Surdash	S17	Iraq
Zer	S18	Turkey

3. Gamma Ray Spectrometry Analysis

Gamma ray spectrometry of NaI (Tl) with the crystal size of 3″×3″ (SILENA type model 3S3), was used to determine the specific activity of primordial radionuclides in eighteen salt samples. The system consists of preamplifier, amplifier, multi-channel analyzer of 512 channels and a high voltage power supply (521681 LYBOLD) with the range and operating voltage of 0-1500 (800 Volt).

The detector resolution was 7.4KeV at 662KeV photo peak gamma line of ^{137}Cs. Two different materials of lead (10 cm) and copper (20mm) were used to reduce the background and attenuated the x-ray fluorescence respectively. A CASSY software program was used to acquire and identify the spectrum. The point source of ^{226}Ra and its descendants, ^{214}Pb (242, 295, and 352 KeV) and ^{214}Bi (609 and 1120 KeV), were used to calibrate the energy for NaI (Tl) gamma ray spectrometry, and the three famous activity sources of ^{137} Cs, ^{60}Co, and ^{152}Eu were used to calibrate the complete peak efficiency. The salt samples were counted within the calibrated spectrometer for 21600 sec. The obtained net salt spectra (after subtracting the background) have been analyzed using the indirect methods to measure the specific activities of ^{226}Ra and ^{232}Th. The activities of ^{40}K, ^{226}Ra and ^{232}Th with the unit of Bq/Kg was estimated from the photo peak energy of 1460 KeV, 352 (^{214}Pb) KeV and 911 (^{228}Ac) KeV, respectively. The following formula was used to determine the specific activity in salt samples[12].

DOI: https://doi.org/10.31972/ticma2022

$$A_s = \frac{Ns}{\varepsilon_\gamma I_\gamma \, t \, m_c} (Bq \; Kg^{-1}) \quad (1)$$

4. Results and Discussion

4.1 Activity concentration

The specific activity for primordial radionuclide in the cooking salt samples have been reported in Table 2. and shown in Figures. 1 and 2.

TABLE 2. Specific activities of primordial radionuclides in salt samples.

Sample Code	Specific Activity (Bq / Kg)		
	^{226}Ra	^{232}Th	^{40}K
S1	0.304±0.023	ND	1.235±0.176
S2	0.256±0.021	1.556±0.102	8.774±0.47
S3	0.313±0.023	0.253±0.042	11.623±0.541
S4	0.366±0.025	ND	2.118±0.231
S5	0.413±0.027	0.387±0.052	13.173±0.576
S6	0.360±0.025	0.803±0.075	39.557±0.999
S7	0.339±0.024	0.408±0.054	11.093±0.529
S8	0.356±0.025	ND	3.555±0.299
S9	ND	0.641±0.067	4.815±0.348
S10	0.430±0.027	ND	13.236±0.578
S11	0.241±0.020	ND	2.067±0.228
S12	0.453±0.028	ND	17.182±0.658
S13	0.463±0.028	ND	17.371±0.662
S14	0.497±0.029	0.781±0.074	19.035±0.693
S15	0.523±0.030	0.472±0.058	27.178±0.828
S16	0.466±0.028	0.338±0.049	29.006±0.855
S17	0.359±0.025	ND	13.942±0.593
S18	0.432±0.027	0.394±0.053	9.719±0.495

*ND: Not Detection

DOI: https://doi.org/10.31972/ticma2022

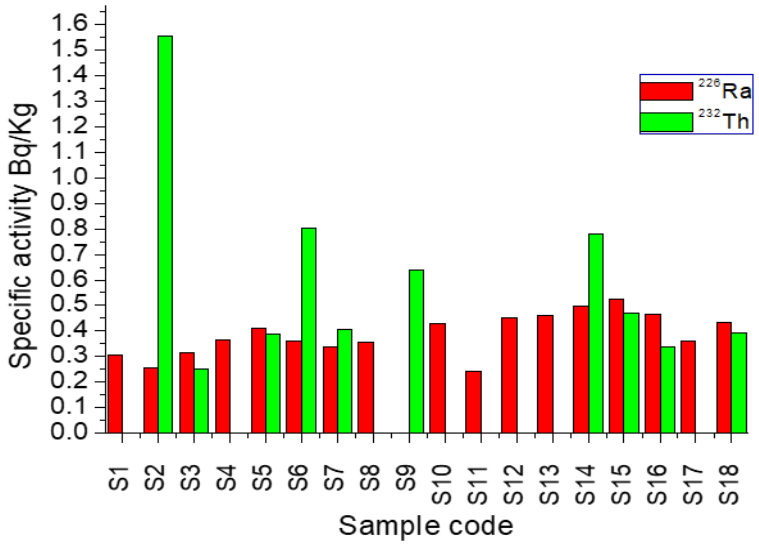

FIGURE 1. Specific activities of ^{226}Ra and ^{232}Th in salt samples.

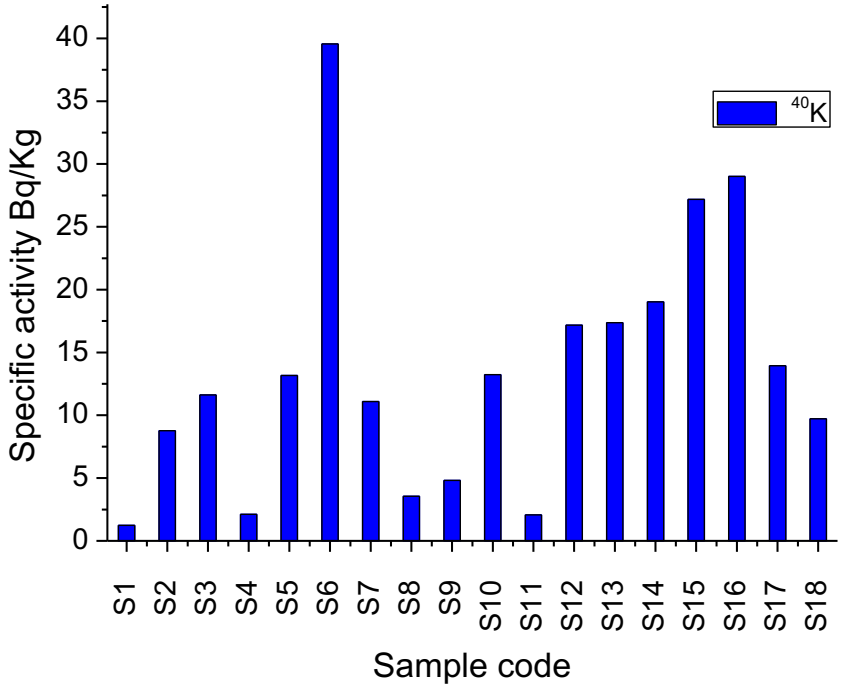

FIGURE 2. Specific activities of ^{40}K in salt samples.

Radium (^{226}Ra) was detected in all salt samples (except S9) and measured with a minimum of not detectable (ND) in S9, a maximum of 0.523±0.030 in S15 and the average specific activities was 0.387±0.026 Bq.kg^{-1}. Thorium (^{232}Th) was detected in salt samples with a minimum ND value, a maximum of 1.556±0.102 in S2, and the arithmetic mean of 0.693±0.063 Bq.kg^{-1}. Potassium (^{40}K) was detected in all salt samples with a minimum value of 1.235±0.176 in S1, a maximum of 39.556±0.999 in S6 with an average of 13.593±0.542 Bq.kg^{-1}.

The wider variation in the level of primordial radionuclides present in salt samples could be linked to the geological and geographical variation in mining or sea origin in which the salts are produced.

The recorded specific activity of ^{226}Ra has lower value in compare to both ^{232}Th and ^{40}K. Similarly the measured activity of ^{232}Th was lower than the value reported in Iraq [5]; [6]. The higher ^{40}K activity returned

DOI: https://doi.org/10.31972/ticma2022

to the hyposodic iodized salt with low Na and a high content of KCl, K3C6H5O7, KI (potassium iodide) with the ratio of (31.3%) [4]. The obtained ^{40}K activity lied below the permitted world average of (400Bq. kg^{-1}). Table 3. Presents a comparison between the obtained salt activities with others published in different countries.

TABLE 3. Comparison of salt samples specific activities with those of other countries.

Country	Specific activity Bq/Kg			Reference
	^{226}Ra	^{232}Th	^{40}K	
Iraq	5.6±2.1	9.0±2.8	16.6±5.2	[5]
Iraq	0.508±0.359-19.577±2.230	4.790±0.670-9.674±0.953	64.216±4.216-239.981±8.150	[6]
Turkey	ND -3±0.4	4.1 ± 0.7- 7.3 ± 1.1	ND- 34.0 ± 5.3	[7]
Italy	-------	--------	2.61±0.12	[4]
Iraq	4.161-32.138	1.426-12.456	334.4-3864.1	[8]
Turkey	7.32±0.9	2.72±0.7	488.53±21.61	[9]
Pakistan	ND	ND	10 - 69	[13]
Egypt	0.46±0.02-32.6±1.6	0.2±0.01-10.5±0.5	0.42±0.02-158.6±7.8	[11]
Kurdistan-Iraq	ND-0.523±0.03	ND-1.556±0.102	1.235±0.176-39.556±0.999	Present study

4.2 Radium Equivalent

The effect of primordial radionuclide of ^{226}Ra, ^{232}Th and ^{40}K can be combined in a single physical quantity known as radium equivalent and obtained from the following equation [14].

$$Ra_{eq} = A_{Ra} + 1.43A_{Th} + 0.077A_K \quad (2)$$

The quantities $\boldsymbol{A_{Ra}}$, $\boldsymbol{A_{Th}}$ and $\boldsymbol{A_K}$ in eq.2 can be defined as specific activities of ^{226}Ra, ^{232}Th and ^{40}K in a unit of Bq.kg^{-1}, Ra_{eq} represents that 370 Bq/kg of ^{226}Ra, 259 Bq/kg of ^{232}Th and 4810 Bq/kg of ^{40}K generates the same external and internal gamma dose rate [14]. The obtained values are presented in Table 4, column 2. It was ranged from 0.339 to 4.554 with an algebraic mean value of 1.891 Bq/kg; all obtained values are under the action limit of (370 Bq/kg) declared by [1].

4.3 Indoor Absorbed Gamma Dose Rate (D_{in})

In order to convert the specific activities to an indoor dose rate (D_{in}) the conversion factors of 0.92, 1.1 and 0.081 nGyh-1/Bq.kg^{-1} are used for ^{226}Ra, ^{232}Th and 40K respectively, thus it can be obtained using the following equation [15].

$$D_{in}(nGyh^{-1}) = 0.926A_{Ra} + 1.1A_{Th} + 0.081A_K \quad (3)$$

The calculated D_{in} for salt samples are tabulated in Table 4, column 3. The measured range of D_{in} varied from minimum 0.38 (S1) to maximum 4.418(S6) with arithmetic mean of 1.806 nGyh^{-1}. The calculated values are below the indoor dose reference limit of 84 nGyh^{-1} declared by [1].

DOI: https://doi.org/10.31972/ticma2022

4.4 Indoor Annual Effective Dose Rate (E_{in}):

The indoor annual effective dose rate can be obtained from the indoor dose in air using the conversion factor of 0.7 Sv Gy^{-1} and the individuals remain in the indoor building with an average life of 80% during one year. The calculation of Ein was done using:

$$E_{in}(mSv\ y^{-1}) = D_{in}(nGyh^{-1}) \times 8760h \times 0.8 \times 0.7Sv\ Gy^{-1} \times 10^{-6} \quad (4)$$

The calculated Ein for the salt samples are presented in Table 4 column 4 and ranges from a minimum of 0.002 (S1) to a maximum of 0.022 (S6) with algebraic mean of 0.009 $mSv.y^{-1}$ which is well below the safety recommendation value of 0.41 $mSv.y^{-1}$ declared by [1].

4.5. Internal hazards index (H_{in}):

Internal hazards index can be used to determine the effect of alpha particles emitted from radon and its progenies that affects the respiratory organs especially lungs, which can be obtained from [16]; [14]:

$$H_{in} = \frac{A_{Ra}}{185} + \frac{A_{Th}}{259} + \frac{A_K}{4810} \quad (5)$$

The evaluated H_{in} values are shown in Table 4, column 5. The internal hazard index varies from a minimum of 0.002 to a maximum of 0.013 with the average values were found to be 0.006. The calculated values are under the action limit of one. It can be concluded that, all the studied salt samples do not create radioactive risk to residents.

4.6. Annual Committed Effective Dose E_{ing}:

Annual effect dose arises from ingestion of food over a lifetime, it depends on the amount of food consumption during every day and the specific radionuclides involved and can be calculated as:

$$E_{ing}(Sv\ y^{-1}) = I \times A \times C \quad (6)$$

Where I: is the average amount of salts intake by adults (3.65kg/year) for one year) [17], A is the specific activities of salt samples in Bq/kg and C represents the ingestion dose factor which used to convert the activity to ingestion dose rate with values of 4.5×10^{-8}, 2.3×10^{-7} and 6.2×10^{-9} Sv/y for ^{226}Ra, ^{232}Th and ^{40}K respectively[18].

The (E_{ing}) calculated for the salt samples are presented in Table 4, column 6. It changes from minimum of 0.028 to a maximum of 2.287 with a mean value of 0.649 $\mu Sv.y^{-1}$, which is below the recommended of 1000 $\mu Sv.y^{-1}$ [1].

TABLE 4. The radiological indices for ^{226}Ra, ^{232}Th and ^{40}K in salt samples.

Code	$Ra_{eq.}$ Bq/kg	D_{in} ($nGyh^{-1}$)	E_{in} (mSv/y)	H_{in}	E_{ing} µ sv/y	$ELCR_{ing}$ $*10^{-3}$
S1	0.399	0.380	0.002	0.002	0.078	0.0003
S2	3.157	2.658	0.013	0.009	1.547	0.0051
S3	1.570	1.508	0.007	0.005	0.527	0.0017
S4	0.529	0.508	0.002	0.002	0.108	0.0004
S5	1.981	1.873	0.009	0.006	0.691	0.0023
S6	4.554	4.418	0.022	0.013	1.628	0.0054
S7	1.777	1.660	0.008	0.006	0.650	0.0021
S8	0.630	0.615	0.003	0.003	0.139	0.0005

DOI: https://doi.org/10.31972/ticma2022

S9	1.287	1.095	0.005	0.003	0.647	0.0021
S10	1.449	1.468	0.007	0.005	0.370	0.0012
S11	0.400	0.389	0.002	0.002	0.086	0.0003
S12	1.776	1.809	0.009	0.006	0.463	0.0015
S13	1.800	1.833	0.009	0.006	0.469	0.0015
S14	3.081	2.859	0.014	0.010	1.169	0.0039
S15	3.291	3.202	0.016	0.010	1.097	0.0036
S16	3.183	3.150	0.015	0.010	1.017	0.0034
S17	1.433	1.460	0.007	0.005	0.375	0.0012
S18	1.744	1.618	0.008	0.006	0.622	0.0021
Min	0.399	0.380	0.002	0.002	0.078	0.0003
Max	4.554	4.418	0.022	0.013	1.628	0.0054
Average	1.891	1.806	0.009	0.006	0.649	0.0021

Excess Life Time Cancer Risk (ELCR)

The excess life time cancer can be defined as the probability of occurring and appearing cancer from ingestion doses and can be estimated by:

$$(ELCR)_{ing} = E_{ing} \times LE \times RF \quad (7)$$

Where (Eing), LE and RF(Sv^{-1}) are the annual effective doses, individual expected life time (66 years) and fatal risk factor per Sievert (0.05), respectively [19] .

The results are presented in Table 3, column 7. The range of $ELCR_{ing}$ varies from a minimum of 0.0003 $\times 10^{-3}$ (S1) to a maximum 0.0054×10^{-3} with an algebric mean of 0.0021 $\times 10^{-3}$. The obtained values are well below the average recommendation worldwide value of 1.45×10^{-3} declared by [1].

Statistics of Pearson correlation coefficient

(SPSS) is a statistical useful tool used to determine the correlation relationship between the activities of primordial radionuclide and the derived radiological index. This relationship was established on the basis of using the Pearson correlation coefficient analysis and tabulated in Table 5.

The calculated coefficients show that there is a negative correlation between ^{238}U and ^{232}Th which indicates to different sources of the two radionuclides. On the other hand, there was a weak and positive relation between ^{226}Ra and ^{40}K revealing their same origin and contribution to the derived doses. The strong relationship between all indices with both ^{232}Th and ^{40}K certifies that the calculated doses are controlled by both radionuclides, while a weak positive relation for ^{226}Ra indicates its less contribution to the total doses.

TABLE 4. Pearson correlation coefficients between natural radionuclides and derived radiological indices.

Variables	**^{226}Ra**	**^{232}Th**	**^{40}K**	**$Ra_{eq.}$**	**D_{in}**	**E_{in}**	**H_{in}**	**E_{ing}**	**$ELCR_{ing}$**
^{226}Ra	1								
^{232}Th	-0.205	1							
^{40}K	0.512*	0.281	1						
$Ra_{eq.}$	0.352	0.687**	0.886**	1					

DOI: https://doi.org/10.31972/ticma2022

D_{in}	0.405	0.609**	0.928**	0.995**	1				
E_{in}	0.411	0.605**	0.928**	0.993**	0.999**	1			
H_{in}	0.463	0.624**	0.901**	0.989**	0.991**	0.991**	1		
E_{ing}	0.143	0.867**	0.720**	0.957**	0.923**	0.921**	0.923**	1	
$ELCR_{ing}$	0.199	0.834**	0.731**	0.954**	0.923**	0.922**	0.924**	0.983**	1

5. CONCLUSIONS

The specific activities of three primordial radionuclides in cooking salt samples available in local markets of Kurdistan region have been determined. The highest radium equivalent is found in Altunsara produced in Iraq while the lowest found in Khosh produced in Turkey. Fortunately, all obtained values are well below the recommendation values declared by WHO and UNSCEAR and are in the limit of safe consumption. Statistics of multivariate analysis of Pearson correlation has been performed. Statistically, the strong positive correlation between the derived indices and primordial radionuclides indicates that the doses produced are dependent on three radionuclides, especially loaded on both ^{232}Th and ^{40}K. It was recommended that individuals prepare their meals every day using the khosh salt varieties.

References

[1] Unscear, S., 2000. effects of Ionizing Radiation. *United Nations, New York*,453-487.

[2] Podgoršak, E.B., 2006. *Radiation physics for medical physicists* (Vol. 1). Berlin: Springer.

[3] Morino, Y., Ohara, T. and Nishizawa, M., 2011. Atmospheric behavior, deposition, and budget of radioactive materials from the Fukushima Daiichi nuclear power plant in March 2011. *Geophysical research letters*, *38*(7).

[4] Caridi, F., Messina, M., Belvedere, A., D'Agostino, M., Marguccio, S., Settineri, L. and Belmusto, G., 2019. Food salt characterization in terms of radioactivity and metals contamination. *Applied Sciences*, *9*(14), p.2882.

[5] Jasim, M.H., Ramadan, A.E. and Hussain, N.A., 2021. Measurement and Analysis of Natural Radioactive Elements in Salty Sediments from Central and Southern Iraq. *Iraqi Journal of Science*, 62(11),3911-3920.

[6] Alhous, S.F., Kadhim, S.A., Alkufi, A.A. and Kadhim, B.A., 2020, November. Measuring the level of Radioactive contamination of selected samples of Sugar and Salt available in the local markets in Najaf governorate/Iraq. In *IOP Conference Series: Materials Science and Engineering* (Vol. 928, No. 7, p. 072097). IOP Publishing.

[7] A. Hançerlio\ugullari and K. Eyübo\uglu.,2020. Int. J. Environ. Anal. Chem.

[8] Alaboodi, A.S., Hassan, A.M. and Muhmood, A.A., 2019, July. Study the Health risk of Radioisotopes in different samples of salt in markets of Iraq. In *Journal of Physics: Conference Series* (Vol. 1279, No. 1, p. 012032). IOP Publishing.

[9] Yüksel, Z. and Tufan, M.Ç., 2018. Determination of radioactivity levels of salt minerals on the market. *Canadian Journal of Physics*, 96(7),784-785.

[10] Shafik, S.S., 2013. Specific Activity and Effective Dose Measurements for Different Potassium Salts Which Used by Iraqi Costumers. *journal of kerbala university*, 11(3),304-308.

[11] El-Bahi, S.M., 2003. Radioactivity levels of salt for natural sediments in the northwestern desert and local markets in

Egypt. *Applied Radiation and Isotopes*, 58(1),143-148.

[12] . H. Al-Sulaiti, N. Alkhomashi, N. Al-Dahan, M. Al-Dosari, D. A. Bradley, S. Bukhari, M. Matthews, P. H. Regan, and T. Santawamaitre, Nucl.,2011. Instruments Methods Phys. Res. Sect. A Accel. Spectrometers, Detect. Assoc. Equip. 652, 915.

[13] Baloch, M.A., Qureshi, A.A., Waheed, A., Ali, M., Ali, N., Tufail, M., Batool, S., Akram, M., Iftikhar, P., Qayyum, H. and Manzoor, S., 2012. A study on natural radioactivity in Khewra Salt Mines, Pakistan. *Journal of radiation research*, 53(3),411-421.

[14] Beretka, J. and Matthew, P.J., 1985. Natural radioactivity of Australian building materials, industrial wastes and by-products. *Health physics*, 48(1),87-95.

[15] U. C. 1999 E. Commission and others, Nucl. Saf. Civ. Prot. (n.d.).

[16] A. O. Taiwo, D. J. Adeyemo, U. Sadiq, and I. A. Bappah.,2014. Arch. Appl. Sci. Res. 6, 23.

[17] Lidz, C.W., Mulvey, E.P. and Gardner, W., 1993. The accuracy of predictions of violence to others. *Jama*, 269(8),1007-1011.

[18] Eckerman, K., Harrison, J., Menzel, H.G. and Clement, C.H., 2012. ICRP publication 119: compendium of dose coefficients based on ICRP publication 60. *Annals of the ICRP*, 41,1-130.

[19] Al-Mashhadani, A.H., Yas, R.M., z Majeed, W., Saeed, A.A., Naje, N.B. and Hadi, W.A., 2020, March. Estimation the cancer risk due to ingestion the food spices commonly used in Iraqi kitchen. In *IOP Conference Series: Materials Science and Engineering* (Vol. 757, No. 1, p. 012014). IOP Publishing.

Proceeding of 3rd International Conference of Mathematics and its Applications TICMA2022
https://conferences.su.edu.krd/su/ticma2022/
DOI: https://doi.org/10.31972/ticma2022

RESEARCH PAPER

Integer-valued polynomials and binomially Noetherian rings

Shadman Kareem*
Department of Mathematic, Faculty of Science and Healthy, Koya University. University Park Danielle Mitterrand Boulevard Koya, Erbil, Iraq.
College of Information Technology and Computer Sciences, Catholic University in Erbil, Erbil, Iraq.

A B S T R A C T:
A torsion free as a $\mathbb{Z}-$ module ring R with unit is said to be a binomial ring if it is preserved as binomial symbol

$$\binom{a}{i} \coloneqq \frac{a(a-1)(a-2)\dots(a-(i-1))}{i!},$$

for each $a \in R$ and i ≥ 0. The polynomial ring of integer-valued in rational polynomial $\mathbb{Q}[X]$ is defined by Int $(\mathbb{Z}^X) := \{h \in \mathbb{Q}[X]: h(\mathbb{Z}^X) \subset \mathbb{Z}\}$ an important example for binomial ring and is non-Noetherian ring. In this paper the algebraic structure of binomial rings has been studied by their properties of binomial ideals. The notion of binomial ideal generated by a given set has been defined. Which allows us to define new class of Noetherian ring using binomial ideals, which we named it binomially Noetherian ring. One of main result the ring Int $(\mathbb{Z}^{\{x,y\}})$ over variables x and y present as an example of that kind of class of Noetherian. In general the ring Int$(\mathbb{Z}^X)$ over the finite set of variables X and for a particular F subset in $\mathbb{Z}$ the rings Int$\left(F^{\{x_1,x_2,\dots,x_i\}},\mathbb{Z}\right) = \{h \in \mathbb{Q}[x_1,x_2,\dots,x_i]: h(F^{\{x_1,x_2,\dots,x_i\}}) \subseteq \mathbb{Z}\}$ both are presented as examples of that kind of class of Noetherian.

KEY WORDS: Binomial ring, Integer-valued polynomial, Binomial ideal, Noetherian rings, binomially Noetherian rings.
DOI: https://doi.org/10.31972/ticma22.07

1. INTRODUCTION:

Binomial rings first introduced by Hall [3] in his work on nilpotent groups theory. He uses elements of a binomial ring to describe a type of generalized exponentiation of elements of any nilpotent group. There original definition is a unity torsion-free (as a Z-module) ring R is said to be binomial ring if R preserved by the binomial symbol

$$\binom{a}{i} = \frac{a(a-1)(a-2)\dots\dots\dots(a-(i-1))}{n} \in (R \otimes \mathbb{Q})$$

In fact, it in R for each $a \in R$ and $i \geq 0$.

Binomial rings have several useful applications in many contexts. In algebraic topology, Wilkerson [4] show that where each Adams operations over binomial rings are trivial. Then it well be a specific class of λ-rings (where λ-rings R is class of commutative with identity, equipped with operation $\lambda^i: R \to R$, for $i \geq 0$, satisfying some axioms that are satisfied by the binomial coefficients [15]) with λ-operations are presented by binomial symbol as

* **Corresponding Author:** ***Shadman Kareem***
E-mail: :shadman.rahman@koyauniversity.org
Article History:
Received: 01/08/2022
Accepted: 15/09/2022
Published: 07/12/2022

DOI: https://doi.org/10.31972/ticma2022

$$\lambda^i(a) = \binom{a}{i},$$

for all $a \in R$ and $i \geq 0$. Also shows that on a $\mathbb{Z}$-module torsion free $\psi -$ ring R there exists a λ-ring construction that satisfy the condition (Fermat's Little Theorem)

$$\psi^P(r) \equiv r^P(\ mod\ pR).$$

Yau [14] Use above condition to see that the λ-rings are preserved under most sensible operations such as localization and completion. Also, for a binomial ring, he gives ring isomorphism between universal λ-ring $\Lambda(R)$ of R and Necklace ring $Nr(R)$ of R.

Kareem [8] as special class of λ-rings, he proves that the binomial rings are closed under localization. Applied this result to show that P −local integers $\mathbb{Z}_{(P)}$ of the ring $\mathbb{Z}$ of integers, is another example of binomial ring.

Knutson [12] built an isomorphism of ring come from a binomial ring R with a special kind of generator subset

$$R \cong \mathbb{Z}$$

Actually, that result lead to the interesting result in the topological K –theory filed. It shows the $\mathrm{K}^0(X)$ ring with a particular type of space Y is binomial ring, It gives

$$\mathrm{K}^0(Y) \cong \mathbb{Z}.$$

Similarly in representation theory if the ring $R(G)$ of representation ring is binominal ring, then G must be identity group, that is

$$R(G) \cong \mathbb{Z}.$$

In category theory Elliott in [5] As a special class of λ-rings they study the connection between λ-rings and particular type of binomial rings. He presents characterizations of binomial ring by their homomorphic image and called it quasi-binomial.

By same manner, we can introduce the new class of ideal call binomial ideal I of binomial ring R as a way we defined a class of binomial ring. A usual ideal I of binomial ring R is said to be a binomial ideal if it is preserved by binomial symbol.

$$\binom{k}{i} \in I$$

for each $k \in I$ and $i \geq 1$. Indeed there is inadequate amount of work on this kind of class of ideal (binomial ideal) to presented here . Xantcha [11] introduce a brief survey on binomial ideal.

The standard ring of polynomials of integer-valued ring with rational coefficients that send $\mathbb{Z}$ to $\mathbb{Z}$, is denote by

$$\mathrm{Int}(\mathbb{Z}^X) = \{h(X) \in \mathbb{Q}[X] : h(\mathbb{Z}^X) \subset \mathbb{Z}\}$$

where X is set of variables. Actually, it is subring of $\mathbb{Q}[X]$, where the condition that $h \in \mathbb{Q}[X]$ been integer-valued polynomial clarify as follows. First $\mathbb{Z}^X$ for each $x \in X$ set of functions given by $\underline{n}: X \to \mathbb{Z}$, where h can compute by substituting each x at any such $\underline{n}$ with the integer $\underline{n}(x)$ in h . In particular, the ring on one variable defined by

$$\mathrm{Int}\left(\mathbb{Z}^{\{x\}}\right) = \{h(X) \in \mathbb{Q}[X] : h(\mathbb{Z}) \subset \mathbb{Z}\}$$

It is called the integer-valued polynomial ring on single variable x.

In particular, the interest for the ring structure of ring $\mathrm{Int}\left(\mathbb{Z}^{\{x\}}\right)$. Polya [6] showed that the binomial polynomial

$$\binom{x}{n}$$

is basis as the Z-module of ring $\mathrm{Int}\left(\mathbb{Z}^{\{x\}}\right)$.

As several kinds of cooperations and operations the ring $\mathrm{Int}\left(\mathbb{Z}^{\{x\}}\right)$ in one variable x and their duals in complex K-theory all arising in algebraic topology. The works in that direction can be seen in [1, 2]. Algebraically this ring $\mathrm{Int}(\mathbb{Z}^X)$ over some variable X is probably one of the interesting examples of a non-Noetherian at least at our paper. (There exist an ideal of $\mathrm{Int}(\mathbb{Z}^X)$. that are not finitely generated) see [7].

DOI: https://doi.org/10.31972/ticma2022

The main point of the paper therefore, to examine all deferent kinds of integer-valued polynomials rings algebraically with their binomial ideals. We establish the new class of Noetherian ring named by binomially Noetherian. These came with a certain kind of finiteness condition, namely, as a binomial all binomial ideals have to be generating finitely. As a main result $\mathrm{Int}(\mathbb{Z}^{\{x_1,x_2\}})$ on two variables x_1 and x_2 given as examples of class of that kind of Noetherian ring. Also, by same way the Int ($F^{\{x_1,x_2\}}$, Z) for a subset $F \subseteq \mathbb{Z}$ on two variables x, x_2 is presented as another example of that class of Noetherian.

This paper is structured by the follow way. The Section 2, start by investigation about binomial rings. It shows that each $\mathrm{Int}(\mathbb{Z}^X)$ rings of integer valued polynomials on finite variables X and the Int (F^X , $\mathbb{Z}$) of a subset $F \subseteq \mathbb{Z}$ and over a finite of variables X. It is another example of binomial ring. Section 3 begin by establishing new notation we called ideal which is closed under binomial for a binomial ring binomial ideal, then the prove of some good properties has been given. The section 4 start with an example to explain that not all principal ideal with set of generators always can be binomial ideal. For that reason, in section 4, we define new class of ideal binomially generated by a set we named by (binomial principal ideal) alongside with some useful theory and properties. Later in this section each binomial ideal in a ring $\mathrm{Int}(\mathbb{Z}^X)$ described by polynomial ideal in ring $\mathbb{Q}[X]$. This result used to define new class of binomial rings called binomially Noetherian ring. In section 5. Then we give the ring $\mathrm{Int}(\mathbb{Z}^{\{x_1,x_2\}})$ on variables x_1 and x_2 is an example of that class of Noetherian ring. With same identical reason we show that for subset F ⊆ Z the ring $\mathrm{Int}(F^{\{x_1,x_2\}}, \mathbb{Z})$ is another example of that class of Noetherian ring.

2. Binomial ring

Recall some notations and definitions from Ya [14]. Then we show that both rings integer-valued polynomials rings $\mathrm{Int}(\mathbb{Z}^X)$ and for particular subset F ⊆ Z the ring $\mathrm{Int}(F^{\{x_1,x_2,\dots,x_i\}}, \mathbb{Z})$ both are binomial rings. This section starts with a definition of Binomial ring.

Definition 2.1

As $\mathbb{Z}-$ module torsion-free ring R with unit is said to be binomial ring if R preserved by binomial symbol (binomial coefficient),

$$\binom{a}{i} = \frac{a(a-1)(a-2)\dots\dots\big(a-(i-1)\big)}{i} \in (R \otimes \mathbb{Q}).$$

In fact, in R for each $a \in R$ and $i \geq 0$.

Example 2.2.

First, we start with some well-known examples of binomial.
The simplest one is the ring $\mathbb{Z}$ of integers.
Any characteristic 0 field R.
Each $\mathbb{Q}$-algebra.

Proposition 2.3.

For a multiplicative closed subset U. The localization ring $U^{-1}R$ of binomial R is binomial ring.

Corollary 2.4.

In ring $\mathbb{Z}$ of integers the p-local integer ring $\mathbb{Z}_{(P)}$ is a binomial ring where, p is prime.

Next began our investigation on special kinds of polynomial rings, which is called integer- valued polynomials. We will see that it is another example of class of binomial ring. The good reference for that you can see [7].

https://conferences.su.edu.krd/su/ticma2022/
DOI: https://doi.org/10.31972/ticma2022

Definition 2.5.
The set of integer-valued polynomials on X that mapping $\mathbb{Z}$ to $\mathbb{Z}$, in the polynomials ring $\mathbb{Q}[X]$ on set X with rational coefficients, expressed by

$$\mathrm{Int}(\mathbb{Z}^X) = \{h(X) \in \mathbb{Q}[X]: h(\mathbb{Z}^X) \subset \mathbb{Z}\}.$$

In particular, integer-valued polynomials in one variable x id denoted by

$$\mathrm{Int}\left(\mathbb{Z}^{\{x\}}\right) = \{h(X) \in \mathbb{Q}[X]: h(\mathbb{Z}) \subset \mathbb{Z}\}$$

It is subring of polynomial ring $\mathbb{Q}[x]$.

Theorem 2.6. [14]
Let X be a set of variables. Then the ring $\mathrm{Int}(\mathbb{Z}^X)$ is an example of class of a binomial ring.
Then we can introduce another kind of polynomial ring, which is integer-valued on kind of subset on $\mathbb{Z}$.

Definition 2.7.
For a subset $F \subseteq \mathbb{Z}$, we named $h \in \mathbb{Q}[X]$ on X with $h(F^X) \in Z$ to be an integer-valued on F, with condition defined by $F^X = \mathrm{Hom}(X, F)$, as in Definition 2.4. We calculate h for any n by substitute all $x \in X$ and $k \in K$ with $n(x)$ in h. The we denoted it by

$\mathrm{Int}(F^X, \mathbb{Z}) = \{h \in \mathbb{Q}[X] : h(K^X) \subseteq \mathbb{Z}\}$, it is actually, define as a subring of $\mathbb{Q}[X]$.

In special case as sub set over the ring of integer, we have

$$\mathrm{Int}\left(F^{\{x\}}, \mathbb{Z}\right) = \{h(x) \in \mathbb{Q}[x]: h(K) \subseteq \mathbb{Z}\}.$$

Consider the ring $\mathrm{Int}(\mathbb{Z}^{\{x\}})$, lead to

$$\mathrm{Int}(\mathbb{Z}^{\{x\}}) = Int(\mathbb{Z}^{\{x\}}, \mathbb{Z}).$$

Example 2.8.
For a special subset $\{0\}$, we can define,

$$\mathrm{Int}\left(\{0\}^{\{x\}}, \mathbb{Z}\right) = \{h(x) \in \mathbb{Q}[x]: h(0) \subseteq \mathbb{Z}\},$$

Specifically, $\mathrm{Int}\left(\{0\}^{\{x\}}, \mathbb{Z}\right)$ is the set of all function (polynomial) in $\mathbb{Q}[x]$ such that constant term is an integer number.

Theorem 2.9.
Consider subset F in the ring $\mathbb{Z}$ of the integers. then the ring $\mathrm{Int}\left(F^{\{x\}}, \mathbb{Z}\right)$ over x is an example of binomial ring.
Proof: First as a subring of the ring $\mathbb{Q}[x]$ the polynomial ring $\mathrm{Int}\left(F^{\{x\}}, \mathbb{Z}\right)$ is clearly $\mathbb{Z}-$ module -torsion free.
To see other statement of a binomial ring, choose $g(x) \in \mathrm{Int}\left(F^{\{x\}}, \mathbb{Z}\right)$. Then

$$\binom{g}{i} = \frac{g(g-1)(g-2)\dots(g-(i-1))}{i!}$$

Select an $\underline{n} \in F^X$, then $g(\underline{n}) \in F$ implies

$$\binom{g}{i}(\underline{n}) = \frac{g(\underline{n})(g(\underline{n})-1)(g(\underline{n})-2)\dots\left(g(\underline{n})-(i-1)\right)}{i!} \in \mathbb{Q}[x], \qquad \text{for i} \geq 0$$
$$= \binom{g(\underline{n})}{i} \in \text{F}.$$

Theorem 2.10.
Let F be a subset in the ring of integeres $\mathbb{Z}$. Then $\mathrm{Int}(F^X, \mathbb{Z})$ is an example of binomial ring.

DOI: https://doi.org/10.31972/ticma2022

Proposition 2.11.
Any $\mathbb{Z}-$ module torsion free homomorphic image ring K onto binomial ring R is also binomial ring. .
Proof: Follow from the following

$$\varphi\binom{a}{i}=\binom{\varphi(a)}{i}=\binom{k}{i}\in K.$$

3. The binomial ideal over binomial rings:

We employ the section to investigate new class of ideal named by binomial ideal over binomial ring.

Definition 3.1.
For binomial ring R. An ideal I of R is said to be binomial ideal if

$$\binom{s}{i}\in I, \text{ for each } s\in I \text{ and } i\geq 1.$$

Example 3.2.
Consider $h(x)\in \mathrm{Int}\left(\mathbb{Z}^{\{x\}}\right)$, then the set define as

$$I_{h(x)}=\left\{I(x)\in \mathrm{Int}\left(\mathbb{Z}^{\{x\}}\right): I(x)=h(x)g(x), \text{for some g(x)}\in \mathbb{Q}[\mathrm{x}]\right\}$$

is binomial ideal of $\mathrm{Int}\left(\mathbb{Z}^{\{x\}}\right)$.

Example 3.3.
For $F\subseteq\mathbb{Z}$ and fixed integer $k\in F$, then the set define as

$$I_k=\left\{h(x)\in \mathrm{Int}\left(F^{\{x\}},\mathbb{Z}\right): h(k)=0\right\},$$

is binomial ideal on $\mathrm{Int}\left(\mathbb{Z}^{\{x\}},\mathbb{Z}\right)$.

Next, we will see some well-known of usual ideal also satisfied by class of binomial ideal will be useful later, when we show the main result.

Proposition 3.4.
The kernel of homomorphism $\varphi: R\to E$ on binomial rings is binomial ideal.
Proof: The proof is follows from the following:

$$\varphi\left(\binom{s}{i}\right)=\binom{\varphi(s)}{i}=\binom{0}{i}=0, \qquad \text{for each } s\in R \text{ and } i\geq 1.$$

Proposition 3.5.
The inverse image of a binomial ideal by a ring homomorphism $\boldsymbol{\varphi: R\to E}$ is a binomial Ideal.
Proof: The proof is clear from the following

$$\varphi^{-1}\left(\binom{e}{i}\right)=\binom{\varphi^{-1}(e)}{i}=\binom{0}{i}=0,$$

for each $e\in E$ and $i\geq 1$.

Theorem 3.6. [8]
The quotient ring R/I for binomial ring R by binomial I is an example of binomial ring.

4. Binomial ideal generated by the set

We start this section with an example it is show that not all usual principal ideal is binomially principal ideal. Thus, we introduce the concept of binomial ideal generated (binomially principal ideal) by a set X.

Example 4.1.
Consider the ideal $2\mathbb{Z}$ in the ring of integers $\mathbb{Z}$, but $2\mathbb{Z}$ not binomial ideal. To see that choose an odd $n\in\mathbb{Z}$. Since $2n\in 2\mathbb{Z}$, but

DOI: https://doi.org/10.31972/ticma2022

$$\binom{2n}{2} = \frac{2n(2n-1)}{2} \notin 2\mathbb{Z}.$$

Commonly a usual ideal is characterized by generators set. So, for each element in the set of generators, we should examine whether it preserved by the binomial symbol. To investigating an ideal J is a binomial ideal.

Proposition 4.2.
The ideal J of ring (binomial ring) R generated by the set $Z = \{b_j\}\, j \in I$ is a binomial ideal if and only if the binomial symbol $\binom{b_j}{i} \in J$, for each $j \in I$ and $i \geq 1$.
Proof: The first part is follows from the Definition 2.1. To see the second direction, consider an element sb_j, for $s \in R$, $b_j \in Z$ and $j \in I$, then as general element we can write it,

$$y = \sum_{k=1}^{m} s_k b_{j_t}.$$

Then finite sum of products rule on $\binom{y}{i}$, we obtain

$$\binom{r_1 b_{j_1}}{p_1}\binom{r_2 b_{j_2}}{p_2}\ldots.\binom{r_m b_{j_m}}{p_m},$$

for $p_1 + p_2 + \cdots + p_m = i$. Thus,

$$\binom{y}{i} \in J.$$

Then it is time to establishing the notion of a binomial ideal, that is came with the set of generate.

Definition 4.3.
Let R be a binomial and S be non-empty subset of R. Then, the binomial ideal generated by the set X, we denote it by $((S))$ and define it by

$$\big((S)\big) = \cap\, \{I : S \subseteq I, I \text{ is a binomial ideal } of\ R\}.$$

So more generally, we can define the notion principal binomial ideal as

Definition 4.4.
The principal binomial ideal of R is denoted by $I = \big((a)\big)$, for some element $a \in R$.

Proposition 4.5.
Consider binomial ring R and the set

$$I = \left(\left\{\binom{s_i}{n} : n \geq 1 \text{ and } i = 1,2,\ldots,k\right\}\right),$$

for $s_i \in R$. Then I is binomial ideal of R generated by the set $\{s_1, s_2, \ldots, s_k\}$.

Proof: The one direction of proof is followed by Definition 4.4,
$((s_1, s_2, \ldots, s_k)) \subseteq I$, for other direction by Definition 2.1,

$$\binom{s_i}{n} \in \big((s_1, s_2, \ldots, s_k)\big),$$

Actually, by definition $((s_1, s_2, \ldots, s_k))$ is an ideal of R. Thus, we have,

$$I \subseteq \big((s_1, s_2, \ldots, s_k)\big).$$

Our first good result, which will be very useful tool, for prove the primary result. That is each binomial ideals of $\mathrm{Int}(\mathbb{Z}^{\{x\}})$ will describe with a polynomial in $\mathbb{Q}[x]$.

DOI: https://doi.org/10.31972/ticma2022

Proposition 4.6.
Consider an ideal J in $\mathbb{Q}[x]$ and define set $I = J \cap \mathrm{Int}(\mathbb{Z}^{\{x\}})$. Thus I is binomial ideal of ring $\mathrm{Int}(\mathbb{Z}^{\{x\}})$.
Proof: To see binomial symbol (operations) condition. Take an element $k(x) \in I$ and $i \geq 1$. Then,

$$\binom{k(x)}{n} = \frac{k(x)(k(x)-1)\dots(k(x)-(i-1))}{i!} = k(x).\left(\frac{(k(x)-1)\dots(k(x)-(i-1)}{i!}\right) \in J$$

Obviously,

$$\binom{k(x)}{i} \in \mathrm{Int}(\mathbb{Z}^{\{x\}})$$

Therefore,

$$\binom{k(x)}{n} \in I.$$

Notice that not each usual ideals of $\mathrm{Int}(\mathbb{Z}^{\{x\}})$ can written as above description.
So, for this suppose we consider an example to see that I cannot write of the form given on Proposition 4.6.

Example 4.7.
In ring $\mathrm{Int}(\mathbb{Z}^{\{x\}})$, choose $I = \left(\frac{x(x-1)(x-2)}{2}\right)$. Then, $\left(\frac{x(x-1)(x-2)}{2}\right).\frac{1}{3} \in J$ and $\left(\frac{x(x-1)(x-2)}{2}\right).\frac{1}{3} = \binom{x}{3} \in \mathrm{Int}(\mathbb{Z}^{\{x\}})$, but $\left(\frac{x(x-1)(x-2)}{6}\right) \notin I$
As particular case of Theorem 3.5, we have.

Proposition 4.8.

Consider binomial ideal $I = ((d\ h(x)))$ in $\mathrm{Int}(\mathbb{Z}^{\{x\}})$, where $d \in \mathbb{Z}$. So $h(x) \in I$ and binomially I also generated the polynomial $h(x)$, that is $I = ((\ h(x)))$. Actually, every binomial ideal of ring $\mathrm{Int}(\mathbb{Z}^{\{x\}})$ can be describe in terms of polynomial ideals in $\mathbb{Q}[x]$ by form

$$I = J \cap \mathrm{Int}(\mathbb{Z}^{\{x\}}),$$

with some ideal J in $\mathbb{Q}[x]$.

Theorem 4.9.
Each binomial ideal I in $\mathrm{Int}(\mathbb{Z}^{\{x\}})$, can characteristic with polynomial ideal in $\mathbb{Q}[x]$ of the style form,

$$I = J \cap \mathrm{Int}(\mathbb{Z}^{\{x\}}),$$

with some ideals define by $J = I \otimes \mathbb{Q}$ in $\mathbb{Q}[x]$.
Proof: We start by setting given ideal by $J = I \otimes \mathbb{Q}$. Then it is clear that J is an ideal of $\mathbb{Q}[x]$. Then to see the equality.

$$I = J \cap \mathrm{Int}(\mathbb{Z}^{\{x\}}).$$

The one side of inclusion is followed $I \subseteq \left(J \cap \mathrm{Int}(\mathbb{Z}^{\{x\}})\right)$.

To see other inclusion $J \cap \mathrm{Int}(\mathbb{Z}^{\{x\}}) \subseteq I$. Pick $h(x) \in \left(J \cap \mathrm{Int}(\mathbb{Z}^{\{x\}})\right)$. Thus, for some $d \in \mathbb{Z} \setminus \{0\}$ and $\bar{h}(x) \in I$, we can write $h(x) = \frac{\bar{h}(x)}{d}$. Since I is binomial ideal, by apply Proposition 3.6, we obtain $h(x) \in I$.

Theorem 4.10.

In the ring $\mathrm{Int}(\mathbb{Z}^{X})$, every binomial ideal I can be written as $I = J \cap \mathrm{Int}(\mathbb{Z}^{X})$, with some ideal given by $J = I \otimes \mathbb{Q}$ in polynomial ring $\mathbb{Q}[X]$.

DOI: https://doi.org/10.31972/ticma2022

proof: The proof is identical to the Theorem 4.9.

Theorem 4.11.
In the ring $\mathrm{Int}(K^X, \mathbb{Z})$, every binomial ideal I can be written as $I = J \cap \mathrm{Int}(K^X, \mathbb{Z})$, with some ideal given by $J = I \otimes \mathbb{Q}$ in polynomial ring $\mathbb{Q}[X]$.

Proof: The Proof is identical to the prove of Theorem 4.9.

In next section we apply the characteristic theorem, to present the prove of primary result of our paper, which is shown that $\mathrm{Int}(\mathbb{Z}^{\{x,y\}})$ is an example of class of binomially Noetherian rings.

5. Binomially Noetherian rings

$\mathrm{Int}(\mathbb{Z}^{\{x_1,x_2\}})$ has many interesting properties and has been extensively investigated. Probably it is referenced as a nice example of non-Noetherian ring. Our main result when introduce new class of Noetherian is based on the truth that the polynomial ring $\mathbb{Q}[x_1, x_2]$ is Noetherian ring.

Definition 5.1.
A binomially Noetherian ring is a binomial ring R in which every binomial ideal I in R can be generated finitely as a binomial ideal.

Theorem 5.2.
The following conditions on binomial ring rare equivalent.

- R is binomially Noetherian: all binomial ideals of Rare finitely generated.
- If each infinite increasing sequence of binomial ideals $I_1 \subseteq I_2 \ldots . \subseteq$ in R eventually stabilizes, $I_n = I_{n+1} = I_{n+2} = \cdots$ for large n.

Proof: The proof is identical to the case in Noetherian ring, you can see [10, Theorem 11.1].

Example 5.3.
The simplest example of class of binomially Noetherian ring is the ring $\mathbb{Z}$ of integers.
Since $\binom{i}{i} = 1$, for $i \geq 1$, then for $i = 0$ and $i = 1$ in $\mathbb{Z}$, we have only 0 = ((0)) and Z = ((1)).

Example 5.4.
By same $\mathbb{Z}_{(P)}$ is also example of class of binomially Noetherian.
Same as Noetherian ring, the following results also satisfied in class of binomially Noetherian.

Proposition 5.5.
Any $\mathbb{Z}-$ module torsion free homomorphic image ring H of binomially Noetherian ring R is also binomially Noetherian ring.
Proof: Set $\phi : R \to H$ as a ring homomorphism . First by Proposition 2.10, H is binomial ring. Now, pick J in H such that $J = \big((\alpha_1, \alpha_2, \ldots, \alpha_n)\big)$, for $\alpha_i \in R$. Then $J = \varphi^{-1}(I)$ by Proposition 3.6 is a binomial ideal in R. Indeed, for all $\alpha \in J$, there exists $\beta \in I$ such that $\varphi(\beta) = \alpha$. Thus, β can be written as a linear combination of the form $\beta = s_1\beta_1 + s_2\beta_1 + \cdots + s_n\beta_n$, for some $s_i \in R$. So,

$$\alpha = \varphi(\beta) = \varphi(s_1\beta_1 + s_2\beta_1 + \cdots + s_n\beta_n) = \varphi(s_1)\beta_1 + \varphi(s_2)\varphi(\beta_2) + \cdots + \varphi(s_n)\varphi(\beta_n).$$

Therefore,

$$I = \big((\varphi(\alpha_1), \varphi(\alpha_2), \ldots, \varphi(\alpha_n))\big).$$

Corollary 5.6.
The quotient of a binomially Noetherian ring is also binomially Noetherian.

DOI: https://doi.org/10.31972/ticma2022

Proposition 5.7.
Any localization of a binomially Noetherian ring is binomially Noetherian.
Proof: First consider homomorphism $\varphi: R \to U^{-1}R$ for multiplicative closed subset U in R. Then by apply Proposition 3.5, we claiming that,

$$\varphi^{-1}(J)(U^{-1}R) = J, \qquad \text{for a binomial ideal in } U^{-1}R.$$

One side of inclusion is followed,

$$\varphi^{-1}(J)(U^{-1}R) \subseteq J.$$

To show another side inclusion,
pick $\frac{a}{s} \in J$. So,

$$\frac{a}{s} = a\left(\frac{1}{s}\right) \in \varphi^{-1}(J)(U^{-1}R).$$

Thus, J is finitely generated.

Proposition 5.8.
Let I be a binomially Noetherian and R/I is binomially Noetherian. Then R must be also binomially Noetherian ring.
Proof: Consider an ascending sequence of binomial ideals in R as

$$J_1 \subseteq J_2 \subseteq \cdots \subseteq J_n \subseteq \cdots$$

Similarly, we obtain

$$J_1 \cap I \subseteq J_2 \cap I \subseteq \cdots \subseteq J_n \cap I \subseteq \cdots$$

and by Proposition 3.7, also we have

$$\frac{J_1}{I} \subseteq \frac{J_2}{I} \subseteq \cdots \subseteq \frac{J_n}{I} \subseteq \cdots$$

Then by hypothesis, there exist M_1, for each $n, m \geq M_1$ and M_2 such that for each $n, m \geq M_2$, we obtain

$$\frac{J_m}{I} = \frac{J_n}{I}.$$

Consequently, for $M = \max\{M_1, M_2\}$ $J_m = J_n$, for each $n, m \geq M$. by [14, Proposition p. 225],

Theorem 5.9.
The ring $\mathrm{Int}(\mathbb{Z}^{\{x_1,x_2\}})$ is an example of class of binomially Noetherian.
Proof: We need see that each ideal J is finitely generated binomial ideal in $\mathrm{Int}(\mathbb{Z}^{\{x_1,x_2\}})$. Apply Theorem 3.6.11, J can be written as,

$$J = K \cap \mathrm{Int}\left(\mathbb{Z}^{\{x_1,x_2\}}\right),$$

for K be an ideal in $\mathbb{Q}[x_1, x_2]$. Consider well-known fact the polynomial $\mathbb{Q}[x_1, x_2]$ is Noetherian. So, $K = (h_1, h_2, \ldots, h_n)$ for $h_i \in \mathbb{Q}[x_1, x_2]$. That is,

$$J = (h_1, h_2, \ldots, h_n) \cap \mathrm{Int}\left(\mathbb{Z}^{\{x_1,x_2\}}\right).$$

Now pick a minimal $b_i \in N$ with

$$b_i h_i \in \mathrm{Int}\left(\mathbb{Z}^{\{x_1,x_2\}}\right),$$

and take $g_i = b_i h_i$. So $K = (g_1, g_2, \ldots, g_n)$ and $J = (g_1, g_2, \ldots, g_n) \cap \mathrm{Int}\left(\mathbb{Z}^{\{x_1,x_2\}}\right)$.
We demanding that $J = ((g_1, g_2, \ldots, g_n))$. Thus, by the Definition 3.1, we have

$$\left((g_1, g_2, \ldots, g_n)\right) \subseteq J.$$

So, to see another side of inclusion. By contradiction, we suppose

$$J \nsubseteq ((g_1, g_2, \ldots, g_n))$$

Then we have,
$((g_1, g_2, \ldots, g_n, E)) \subseteq J$ and $((g_1, g_2, \ldots, g_n, E)) \nsubseteq ((g_1, g_2, \ldots, g_n))$, for another generator E. So,

$$E = \sum_{i=0}^{n} h_i p_i = \sum_{i=0}^{n} g_i \frac{p_i}{b_i},$$

with some $p_i \in \mathbb{Q}[x_1, x_2]$, there exists $\bar{p}_i \in \mathbb{Z}[x_1, x_2]$ and $d_i \in \mathbb{Z} \setminus \{0\}$ with $p_i = \frac{\bar{p}_i}{d_i}$

DOI: https://doi.org/10.31972/ticma2022

So,

$$E = \sum_{i=0}^{n} g_i \frac{p_i}{b_i d_i} \in \mathrm{Int}\left(\mathbb{Z}^{\{x_1,x_2\}}\right).$$

Then we get,

$$NE = \sum_{i=0}^{n} c_i g_i \bar{p}_i \in \mathrm{Int}\left(\mathbb{Z}^{\{x_1,x_2\}}\right),$$

for $c_i \in \mathbb{Z}$ and N to be the least common multiple in the set$\{b_1 d_1, b_2 d_2, \dots, b_n d_n\}$. Thus, NE in ideal of $\mathrm{Int}(\mathbb{Z}^{\{x_1,x_2\}})$ generated with $\{g_1, g_2, \dots, g_n\}$. So, by Definition 4.1,

$$NE \in \left((g_1, g_2, \dots, g_n)\right).$$

Consequently

$$E \in \left((g_1, g_2, \dots, g_n)\right).$$

Which is contradiction and concludes that $J = ((g_1, g_2, \dots, g_n))$.
Next given as generalization of the Theorem 5.9.

Theorem 5.10.
The ring $\mathrm{Int}(\mathbb{Z}^{\{x_1,x_2,\dots,x_n\}})$ is an example of class of binomially Noetherian.
Proof: It is truth that polynomial ring $\mathbb{Q}[x_1, x_2, \dots, x_n]$ on variables $x_1, x_2, \dots, x_n$ is Noetherian. Similarly, each binomial ideal J of $\mathrm{Int}(\mathbb{Z}^{\{x_1,x_2,\dots,x_n\}})$ rewrite as

$$J = K \cap \mathrm{Int}\left(\mathbb{Z}^{\{x_1,x_2,\dots,x_n\}}\right),$$

For ideal K in $\mathbb{Q}[x_1, x_2, \dots, x_n]$. Thus the remain of proof is identical to the Theorem 5.9.

Corollary 5.11.
If J is principal polynomial ideal in $\mathbb{Q}[x_1, x_2, \dots, x_n]$ with set $\{h_1, h_2, \dots, h_n\}$ for some $h_i \in \mathbb{Q}[x_1, x_2, \dots, x_n]$. So principal binomial ideal $K = ((g_1, g_2, \dots, g_n))$ in $\mathrm{Int}(\mathbb{Z}^{\{x_1,x_2,\dots,x_n\}})$ can be rewrite as

$$\left((g_1, g_2, \dots, g_n)\right) = (h_1, h_2, \dots, h_n) \cap \mathrm{Int}\left(\mathbb{Z}^{\{x_1,x_2,\dots,x_n\}}\right),$$

for minimal $b_i \in \mathbb{N}$ with $b_i h_i \in \mathrm{Int}\left(\mathbb{Z}^{\{x_1,x_2,\dots,x_n\}}\right)$.

Theorem 5.12.
The ring $\mathrm{Int}(F^{\{x_1,x_2,\dots,x_n\}}, \mathbb{Z})$ on subset $F \subseteq \mathbb{Z}$ is an example of class of binomially Noetherian.
Proof: Similarly, we can rewrite each binomial ideal J in $\mathrm{Int}(F^{\{x_1,x_2,\dots,x_n\}}, \mathbb{Z})$ as

$$J = K \cap \mathrm{Int}(F^{\{x_1,x_2,\dots,x_n\}}, \mathbb{Z})$$

with some ideal $K \in \mathbb{Q}[x_1, x_2, \dots, x_n]$. So, the remain of proof is identical to the Theorem 5.9.

Proposition 5.13.
Each class of Noetherian ring is class of binomially Noetherian.
Proof: This is follows from binomial ideal is an ideal.
In general, converse of Proposition 5.13, is not right always.

Example 5.14.
The ring $\mathrm{Int}(\mathbb{Z}^{\{x_1,x_2\}})$, is by theorem 5.8, is an example of class of binomially Noetherian, but it is non-Noetherian.

Example 5.15.
By Theorem 5.8., $\mathrm{Int}(\{0\}^{\{x\}}, \mathbb{Z})$ is another example of class of binomially Noetherian. But Strickland in [9, Example 18.3], saw that the ideal $K = xQ[x]$ is not principal in $\mathrm{Int}(\{0\}^{\{x\}}, \mathbb{Z})$.

DOI: https://doi.org/10.31972/ticma2022

6. CONCLUSIONS

In this paper, we introduce Binomially Noetherian, a new class of Noetherian with the property of their binomial ideal. We describe each binomial ideal of $\mathrm{Int}(\mathbb{Z}^X)$, in a team of polynomial ideals of $\mathbb{Q}[X]$.. Use this result to Show that the integer valued polynomial ring $\mathrm{Int}(\mathbb{Z}^{\{x_1,x_2\}})$ on sets of variables X and the integer valued polynomial ring over subset $\mathrm{Int}(F^{\{x\}}, \mathbb{Z})$ for $F \subseteq \mathbb{Z}$ are both examples of Noetherian rings.

Acknowledgments

Firstly, I want to thank the referees for their thorough reading of the paper and for their detailed report containing corrections and suggestions. This a part of my PhD. thesis under supervision prof. Sarah Whitehouse

REFERENCES

[1] Clarke, F., 1981, May. Self-maps of BU. In *Mathematical Proceedings of the Cambridge Philosophical Society* (Vol. 89, No. 3, 491-500). Cambridge University Press.
[2] Clarke, F., Crossley, M.D. and Whitehouse, S., 2001. Bases for cooperations in K-theory. *K-theory*, 23(3), 237-250.
[3] Hall, P., 1969. Nilpotent Groups, Queen Mary College Math. Notes.
[4] Wilkerson, C., 1982. Lambda-rings, binomial domains, and vector bundles over CP (∞). *Communications in Algebra*, 10(3), 311-328.
[5] Elliott, J., 2006. Binomial rings, integer-valued polynomials, and λ-rings. *Journal of pure and applied Algebra*, 207(1), 165-185.
[6] Pólya, G., 1919. Über ganzwertige Polynome in algebraischen Zahlkörpern.
[7] Cahen, P.J. and Chabert, J.L., 1997. *Integer-valued polynomials* (Vol. 48). American Mathematical Soc.
[8] Kareem, S., 2018. *Binomial Rings and their Cohomology* (Doctoral dissertation, University of Sheffield).
[9] S. Neil. *Commutative Algebra Course.* (https://maths-magic.ac.uk/ course.php?id=329, 2013).
[10] Burton, D.M., 1970. *A first course in rings and ideals*. Addison-Wesley.
[11] Richey Xantcha, Q., 2011. Binomial Rings: Axiomatisation, Transfer and Classification. *arXiv e-prints*, arXiv-1104.
[12] Knutson, D., 1973. *l-Rings and the Representation Theory of the Symmetric Group*. Amsterdam, Netherlands: Springer.
[13] Knutson, D., 1975. Binomial λ-rings and a topological corollary. *Proceedings of the American Mathematical Society*, 50(1), 83-84.
[14] Yau, D., 2010. *Lambda-rings*. World Scientific Publishing Company.
[15] Grothendieck, A., 1958. La théorie des classes de Chern. *Bulletin de la société mathématique de France*, 86, 137-154.

Proceeding of 3rd International Conference of Mathematics and its Applications TICMA2022
https://conferences.su.edu.krd/su/ticma2022/
DOI: https://doi.org/10.31972/ticma2022

RESEARCH PAPER

Secure Image Steganography by Utilizing DNA Properties

Yaseen Hikmat Ismael*

Department of Computer sciences College of Computer Sciences and Math University of Mosul

A B S T R A C T:

In the last period, Steganography is commonly used as an alternative to encryption to achieve secret communication between parties. Many methods have emerged to achieve steganography, including the use of spatial domain, spread spectrum, transform domain, and etc.

On the other hand, the methods of attackers have also developed in revealing hidden data and trying to retrieve it. To increase the security of the hiding process, some researchers have found hybrid methods that combine encryption and steganography processes.

The research aims to present a new method in steganography by taking advantage of the properties of DNA, which includes the random sequence of nitrogenous bases (A, C, G, T), the process of hybridization, which occurs between two single strands of DNA to form a double strand of DNA so that the bases in the first strand are complementary to the nitrogenous bases in the second strand.

The research includes the following steps: First, the secret image to be hidden is encrypted by encoding it into a series of nitrogenous bases, and then the XOR process is performed with a nitrogenous bases sequence for a DNA tape agreed upon between the sender and recipient, the hybridization process applied before and after the XOR process. The results show that encrypted image is much different from the original image and thus they added another level of security to the hidden image.

Secondly, the encrypted image resulting from the first step is hidden in the cover image and using a new method based on the use of the agreed-upon DNA tape as a key.

KEY WORDS: DNA Properties, Secure Image Steganography, OTP key.
DOI: https://doi.org/10.31972/ticma22.08

1. INTRODUCTION:

Since it has become possible to store a large amount of information in DNA molecules, then it has become necessary to provide protection and confidentiality for the stored data. DNA Cryptography is a new branch in the field of data encryption that appeared after the discovery of the capabilities of DNA in computing, in which DNA is used as a medium for carrying data and performing calculations with the help of many modern technologies and devices. The DNA consists of two strands wrapped on each other so that they resemble a twisted ladder, and it consists of four types of nitrogenous bases: adenine A, thymine T, cytosine C and guanine G, and these bases are repeated millions or billions of times in all parts of DNA. The process of encoding the DNA tape includes relying on the characteristics or processes that take place on the DNA tape and trying to take advantage of them and combine them with the concepts of alternative and compensatory coding methods to obtain new and efficient coding methods in this field [1] [2].

2. LITERATURE SURVEY

The researchers presented many ideas in DNA cryptography field, as shown in the following researches: Dna cryptography is preferred due to information density and parallelism that are in.herent in any dna molecule, Bevi A. and et al.

*** Corresponding Author:** Yaseen Hikmat Ismael
E-mail: *Yaseen-hikmat@uomosul.edu.iq*
Article History:
Received: 01/08/2022
Accepted: 15/09/2022
Published: 07/12/2022

DOI: https://doi.org/10.31972/ticma2022

[3] introduce dna-based cryptography algorithm depend on feisteal inspired structure with complex operation added to it. Zhang Y. and et al. [4] propose new encryption method depending on characteristics of the biological puzzle, also the method used DNA chip technology to make the cryptography algorithm feasible secure.

Mansi Rathi and etal. [5] present a complex cryptography method by using DNA sequence in encryption. In this research byte-rotation technique with poly- alphabetic substitution are used. The DNA sequence help in generating a random key. In [6] paul and et al. suggest a new approach using chaiotic logistic maps with dna masking and replacement, the researchers used 8 rules to interprets image binary values to the combination of (A,T,C,G) and then perform operations. Kolte S.and et al. [7] introduced a new index-based symmetric DNA cryptography, each characters in plain text encoded to Ascii and to their equivalent binary format. The resulted binary sequence then transformed into DNA sequence and compared to DNA sequence (key), finds the similar sequence, then store the position as a cipher text. Kolate V. and Joshi R. Al-Mahdi Hasan and et al. [8] introduce asymmetric DNA cryptography based on the concept of data dependency, dynamic encoding and RSA cryptosystem. The basic idea of the proposed algorithm is to create a dynamic DNA table, using data dependency for generating 14 dynamic round keys for multilevel security. V. Kolate and R.B. Joshi [9] produce an effective DNA encryption method using a predetermined terminators in the form of {0I1}e to encoding DNA binary strand, also the terminator domains have sticky ends. The secret massage is encrypted in DNA form and mixed in equimolar amounts with dummy DNA strands. The receiver using the key as primers, and PCR is performed, finally Gel-electrophoresis and the amplified sequences used to extract the encrypted strand to decryption it. The attacker must guess the key sequence to differentiate between the dummy and encrypted strands. Samwal Idris and et al. [10] suggested a new DNA cryptography based on one time pad and Caesar cipher, the plain text is first converted to binary format and after that convert to a DNA sequence, using a previously shared DNA sequence as a OTP key, the encryption then implement. Using chaotic map and DNA encoding Aditya Pai and et al. [11] introduce a novel image encryption algorithm, first transform real picture to 2-D matrix, using DNA scrambling method and Chebyshev mapping for confusing image and encryption. The method indicates the best NPCR and UACI scores. Existing DNA cryptography algorithms indicates that the encrypted text has a low avalanche effect of providing a desirable confusion property, therefore Maria Imdad and et al. [12] reassess the security of the DNA cryptography algorithms by modifying the steps in DNA encryption technique. The researchers enhance the overall security by utilizing an existing DNA encoding / decoding table at a selected step in the algorithm. Varsha Hari and R. B. Joshi [13] using DNA based AES security technique to provide multilayer security system. The use of DNA bases (A, T, C, G) for encoding helps to improve the cryptography performance in terms of parallelism and huge capacity to store the data. The researchers find that compression techniques can also be applied te enhance security.

3. DEOXYRIBONUCLEIC ACID (DNA)

Is a nucleic acid that contains the genetic instructions of all proteins used in functioning and the development of any living being. The DNA instructions stored as a code made up of four chemical bases: thymine (T), adenine (A), cytosine (C), and guanine (G). In 1953, Watson and Crick presented a model for DNA consisting of two strands or two coiled strands in the form of a helical ladder in which one of the nitrogenous bases in one slit of the helix is linked with the nitrogen base of the other slit by means of hydrogen bonds, the bonding of the nitrogenous bases between the two slits is restricted “not random”, as the adenine in one of the two strands is always bound with thymine in the other strand by two hydrogen bonds, and the cytosine in one of the two strands is linked with the guanine in the other strand with three hydrogen bonds. DNA Hybridization is the process of combining two complementary single DNA strands to form a double strand of DNA, as the nitrogenous bases in the first chain will be linked by hydrogen bonds with the complementary bases in the second chain [1][2].

4. DEOXYRIBONUCLEIC ACID (DNA)

Is a nucleic acid that contains the genetic instructions of all proteins used in functioning and the development of any living being. The DNA instructions stored as a code made up of four chemical bases:

DOI: https://doi.org/10.31972/ticma2022

thymine (T), adenine (A), cytosine (C), and guanine (G). In 1953, Watson and Crick presented a model for DNA consisting of two strands or two coiled strands in the form of a helical ladder in which one of the nitrogenous bases in one slit of the helix is linked with the nitrogen base of the other slit by means of hydrogen bonds, the bonding of the nitrogenous bases between the two slits is restricted “not random”, as the adenine in one of the two strands is always bound with thymine in the other strand by two hydrogen bonds, and the cytosine in one of the two strands is linked with the guanine in the other strand with three hydrogen bonds. DNA Hybridization is the process of combining two complementary single DNA strands to form a double strand of DNA, as the nitrogenous bases in the first chain will be linked by hydrogen bonds with the complementary bases in the second chain [1][2].

5. THE PROPOSED METHOD

The method includes encrypting the image to be hidden by using a DNA tape agreed upon between the two parties as a key and performing the hybridization process as well as performing the hiding process in a different way also depending on the same key. The mechanism of the proposed method can be clarified through the following points:

A. First, the image data to be hidden is encoded into a sequence of nitrogenous bases using Table 1.

TABLE 1. DNA image encoding

Binary image sequence	DNA nitrogen bases
00	A
01	C
10	G
11	T

TABLE 2. DNA BIO-XOR

BIO-XOR	A	C	G	T
A	C	G	T	A
C	G	T	A	C
G	T	A	C	G
T	A	C	G	T

B. Performing the hybridization process for the series of nitrogenous bases resulting from step A, so that the base A is converted to T and the base C to G and vice versa.
C. Implementation of the BIO-XOR process between the DNA strand produced from step B with the DNA strand (the key) as shown in Table 2.
D. Implementation of the process of hybridization on the chain of bases resulting from the encryption process using BIO-XOR, but in a different way this time where the base A to G and the base T to C and vice versa.
E. To get the encrypted secret image, we convert the resulting series of nitrogen bases from step D into a series of binary numbers using Table 1.
F. After encrypting the secret image to be hidden, the key DNA tape is used to take advantage of the tape's randomness property to achieve an efficient hiding process, as shown in Table 3.

DOI: https://doi.org/10.31972/ticma2022

TABLE 3. Proposed Hiding Rules

DNA sequence	Hiding rules
AA	Do nothing
AC	Hide one bit in bit zero
AG	Hide one bit in bit one
AT	Hide two bits in bit zero & one
CA	Hide one bit in bit zero
CC	Do nothing
CG	Hide one bit in bit one
CT	Hide two bits in bit zero & one
GA	Hide one bit in bit zero
GC	Hide one bit in bit one
GG	Do nothing
GT	Hide two bits in bit zero & one
TA	Hide one bit in bit zero
TC	Hide one bit in bit one
TG	Hide two bits in bit zero & one
TT	Do nothing

6. RESULTS AND DISCUSSIONS

There are many important features of deoxyribonucleic acid (DNA) like the ability to store a large amount of data, possibility of parallel processing of nitrogen bases at the same time, and the randomness property of a sequence of nitrogenous bases, all these features gave the DNA tape great importance for its use in the field of data encryption. The proposed method of image encryption is one of the symmetric encryption methods, where both ends of the communication agree on a DNA strand that is selected from one of the genetic libraries, which is equipped with millions of DNA strands of different organisms.

To accomplish the process of symmetric encryption for digital images, the idea of hybridization process that occurs for the single strand of DNA was used by creating hydrogen bonds to link the complementary nitrogen bases to form the helical DNA strand.

The hybridization process was used initially in its standard form and again in a different manner to add a kind of randomness to the encrypted DNA strand, which represents the image data.

The XOR operation was also used, which is usually done on binary numbers, but here it was used on nitrogenous bases (between two series of bases, one of which represents the image data and the other represents the key), figure 1 show examples of encrypted images and table 4 show the proposed encryption method efficiency measurements.

In table 4 the values of Mean Square error (MSE), Peak Signal to Noise Ratio (PSNR), and Normalized Cross Correlation (NCC), were large, few, and very few, respectively. This indicates, as shown in Figure 1, that the resulting image from the proposed encryption process is more different from the original image, hence, adding another level of security to the hidden image.

After completing the process of encrypting the digital image, in a simple and efficient manner, the DNA tape (the key) was used to hide the encrypted image. The proposed hiding process was characterized by introducing a different method that includes a kind of randomness so that it becomes very difficult for the attacker to retrieve the hidden data.

The hiding process is usually done using the least significant bit, or the two least significant bits, and in a similar format on all the cover data, which gives the attacker the opportunity to retrieve the process, and for this reason, in the proposed method, hiding is done in an arbitrary format.

The randomness of the hiding operation of the proposed method occurs by relying on the DNA bar of the key, which is characterized by being random, depending on the two values of each nitrogen bases of the DNA sequence determines how to perform the hiding operation, which is in four possibilities (1. Hide in bit 0, 2. Hide in bit 1, 3. Hide with bits 0 and 1, 4. Unhide).

DOI: https://doi.org/10.31972/ticma2022

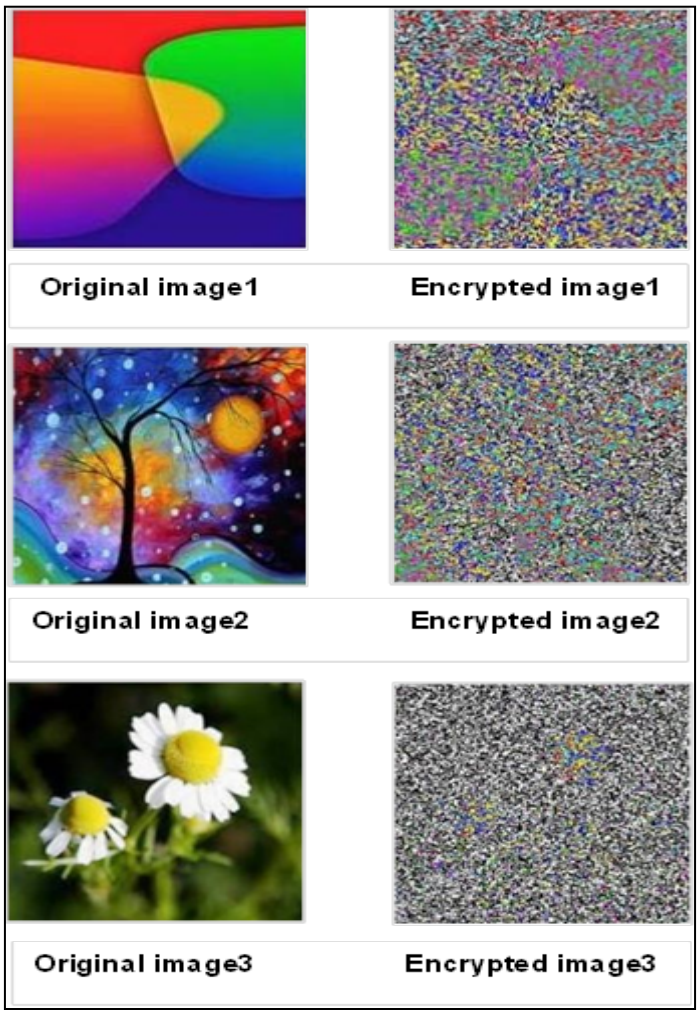

FIGURE 1. Examples of encrypted images

TABLE 4. Efficiency Measurement for Encrypted Images

Original Images	Encrypted Images	MSE	PSNR	NCC
Figure 1 - Original image1	Figure 1 - Encrypted image1	1.5000e+04	6.3698	-0.0059
Figure 1 - Original image2	Figure 1 - Encrypted image2	1.0539e+04	7.9028	0.0153
Figure 1 - Original image3	Figure 1 - Encrypted image3	9.2446e+03	8.4719	-9.6203e-04

7. CONCLUSIONS

1. The methods of encryption and hiding of digital images are based on the secret key, which is the DNA tape that has been agreed upon between the two parties of the connection, and therefore there is no need for the process of key distribution.
2. The tables used in the encryption and hiding operations do not need to be exchanged between the two parties, but only know how to build them.

3. Taking advantage of the randomness of the DNA strand in constructing the encryption and hiding methods gave a high degree of efficiency to the hiding process.
4. The process of encryption using a DNA strand as a key can be thought of as similar to OTP, which according to Shannon's theory is unbreakable.
5. The DNA tape can be used as a key in many modern encryption methods that use the secret key to give it a high degree of efficiency and eliminate the need for the key distribution.

REFERENCES

[1] Das, A., Sarma, S.K. and Deka, S., 2021. Data security with DNA cryptography. In *Transactions on Engineering Technologies* (159-173). Springer, Singapore.

[2] Popovici, C., 2010. Aspects of DNA cryptography. *Annals of the University of Craiova-Mathematics and Computer Science Series*, 37(3), 147-151.

[3] Bevi, A.R., Malarvizhi, S. and Patel, K., 2016. Information Coding and its Retrieval using DNA Cryptography. *Journal of Engineering Science & Technology Review*, *9*(3).

[4] Y. Zhang and Z. Wang and Z. Wang and Y. Karanfil and W. Dai, *A New DNA Cryptography Algorithm Based on the Biological Puzzle and DNA Chip Techniques*-2016, International Conference on Biomedical and Biological Engineering, Atlantis Press, 360-365.

[5] Rathi, M., Bhaskare, S., Kale, T., Shah, N. and Vaswani, N., 2016. Data security using DNA cryptography. *International Journal of Computer Science and Mobile Computing*, 5(10), 123-29.

[6] Paul, S., Dasgupta, P., Naskar, P.K. and Chaudhuri, A., 2017. Secured image encryption scheme based on DNA encoding and chaotic map. *International Information and Engineering Technology Association*, 4, 70-75.

[7] Kolte, N.S., Kulhalli, K.V. and Shinde, S.C., 2017. DNA cryptography using index-based symmetric DNA encryption algorithm. *International Journal of Engineering*, 10(1), 810-813.

[8] Al-Mahdi, H., Alruily, M., Shahin, O.R. and Alkhaldi, K., 2019. Design and analysis of DNA encryption and decryption technique based on asymmetric cryptography system. *International Journal of Advanced Computer Science and Applications*, *10*(2).

[9] Kolate, V. and Joshi, R.B., 2021. An Information Security Using DNA Cryptography along with AES Algorithm. *Turkish Journal of Computer and Mathematics Education*, 12(1S), 183-192.

[10] S. Idris and A. Mathur and A. Hussain, *Novel Enhanced Algorithm Based on DNA Cryptography to Secure Data Transfer over Network*-2021, Journal of Physics: Conference Series, International Conference on Physics and Energy, IOP Publishing, doi:10.1088/17426596/2040/1/012047, 1-7.

[11] Pai, A., Pareek, P.K., Guru Prasad, M.S., Singh, P. and Deshpande, B.K., 2021. Image Encryption Method by Using Chaotic Map and DNA Encoding. *NVEO-NATURAL VOLATILES & ESSENTIAL OILS Journal| NVEO*, 10391-10400.

[12] Imdad, M., Ramli, S.N. and Mahdin, H., 2021. Increasing Randomization of Ciphertext in DNA Cryptography. *International Journal of Advanced Computer Science and Applications*, *12*(10).

[13] Kolate, V. and Joshi, R.B., 2021. An Information Security Using DNA Cryptography along with AES Algorithm. *Turkish Journal of Computer and Mathematics Education*, (1S), 183-192.

Proceeding of 3rd International Conference of Mathematics and its Applications TICMA2022
https://conferences.su.edu.krd/su/ticma2022/
DOI: https://doi.org/10.31972/ticma2022

RESEARCH PAPER

Coherent Dynamics of Quantum Systems with Non-Uniform Fourier Space Excited by Laser Radiation

Sary Banjak[1,*] and Vadim Savva[2]
[1,2]*Department of Higher Mathematics, Belarusian State Technological University, Minsk, Belarus.*

A B S T R A C T:
The algorithm is presented to solve dynamical equations for excitation of molecular models with multiple energy levels. It uses only discrete structures: discrete orthogonal polynomials constructed specially in Fourier space of the probability amplitudes, discrete Fourier transform and leads to exact solution of the differential equations and to discrete distribution of the quantum systems by energy levels.

KEY WORDS: Non-Uniform Fourier Space, Quantum Systems, Coherent Dynamics.
DOI: https://doi.org/10.31972/ticma22.09

1. INTRODUCTION:

The motivation for this work is caused by the fact that Mathematics has significantly changed its appearance in the years after the Second World War. New powerful principles created by discrete mathematics, discrete algorithms, programming, and high–level languages and, of course, computers, computer algebra systems have been added to the former "Mathematical principles of natural science" (as I. Newton called his great book). Newtonian principles (calculus and differential equations, Mathematics of continuous quantities) worked well for 300 years.

Now a rapidly developing branch has been established in mathematics – computer science. The computer algebra system not only performs numerical calculations incredibly quickly, but also performs "analytical calculations", solves algebraic and differential equations. It builds function graphs, works with audio and visual information, competing and collaborating with higher (continuous) Mathematics. Discrete Mathematics can already be considered as Mathematical principles of natural science as well.

Note that the physics of the twentieth century fully recognized the wave-particle duality of the material world. Now this harmony, the unity of the continuous and the discrete, has established itself in mathematics as the language of natural science and technology. Unfortunately, the system of higher education still largely ignores this fact when training most specialists.

The purpose of this work is to apply a discrete algorithm to solve a specific problem - solving a system of differential equations, which, as is known, are usually solved by methods of continuous mathematics, and to show that discrete algorithms give a slightly different perspective, a different view, physically more meaningful.

It was desirable to take a non-"random" problem. As an example, we have chosen one of the fundamental problems of quantum mechanics – the interaction of coherent electromagnetic radiation with quantum systems (models of molecules, atoms, quantum dots and other micro-objects), called the Rabi problem.

It was solved in 1936-37 in a simple, semi-classical version [1, 2], shortly after the creation of quantum mechanics.

*** Corresponding Author: Sary Banjak**
E-mail: bnjk_sary@yahoo.com
Article History:
Received: 01/08/2022
Accepted: 15/09/2022
Published: 07/12/2022

https://conferences.su.edu.krd/su/ticma2022/
DOI: https://doi.org/10.31972/ticma2022

The solution showed that the influence of radiation on quantum systems should be carried out in a different form than classical physics described it: oscillations of the energy level populations of the molecule should appear while the radiation is active. These oscillations are called Rabi oscillations. The problem is included in textbooks of quantum mechanics and has been the subject of numerous scientific studies for more than 80 years, since it underlies many important, diverse and promising areas of physics, chemistry, and technology. Journal of Physics A: Mathematical and Theoretical devoted a special issue of articles to this anniversary [3, 4].

The Rabi problem has two variants – semi-classical and fully quantum; the first describes radiation (usually given) in terms of classical physics, and the molecule is considered in terms of quantum mechanics. In the second variant, both interacting objects, usually located in the resonator, have a quantum description. This is a more complex option, also because the states of both the field and the microsystem change during interaction.

We will very briefly list the scientific and applied research directions for the last decades that have stimulated great interest (analytical, numerical, and experimental) in the Rabi problem. In the early 60s, it was caused by the creation of lasers and the formation of quantum optics. In the 70s - the development of laser isotope separation. In the 80s - the use of ultra-short laser pulses to control chemical reactions, and in spectroscopy - methods for obtaining selectively excited molecules to study the rates of energy redistribution through bonds. A more complex variant - the Rabi quantum problem has become in demand in connection with the development of quantum computers, quantum information transmission networks, modern cryptography and the study of the basics of quantum mechanics.

In our previous works [5-7] devoted to the analytical solution of the semi-classical Rabi problem, in which a discrete spectral algorithm for solving the corresponding equations was proposed, it was shown that it was possible to construct orthogonal discrete polynomials in the corresponding Fourier space of the desired functions and introduce free parameters into their weight function. This opened up an extensive field of use of discrete variable polynomials, which were previously very rarely used in solving physical problems. The presence of free parameters led to a solution for extensive families of quantum systems with various characteristics, including systems with non-equidistant arrangement of energy levels (more real models of molecules and atoms).

In this paper a discrete algorithm for constructing analytical solutions describing the dynamics of excitation is extended to quantum systems with an inhomogeneous Fourier space of the desired functions. It is shown that oscillations of energy level populations can have a more complex form.

They can be non-periodic in time, which is not related to the quantum properties of radiation.

A quantum system with energy levels $E_0, E_1, \dots, E_N$ excited by radiation acting in N transitions between neighbor levels is described with equations:

$$-i\frac{da_n(t)}{dt} = f_{n+1}e^{-i\varepsilon_{n+1}t}a_{n+1}(t) + f_n e^{+i\varepsilon_n t}a_{n-1}(t);$$

$$a_n(t=0) = \delta_{n,0};\ \ n = 0,1,\dots,N. \qquad (1)$$

All variables and coefficients are dimensionless ones. We will consider simple case $N = 2$, two transitions $E_0 \rightleftarrows E_1 \rightleftarrows E_2$, but this is not essential. Coefficients f_1, f_2 describe dipole interaction of radiation with n transition (with normalization $f_1 = 1$); $\varepsilon_1, \varepsilon_2$ are frequency detuning of transition frequency from laser frequency; dimensionless t is time and $a_n(t)$ are functions to be obtained; they are probability amplitudes to find a particle with energy E_n at t moment.

The aim of the paper is to give more general discrete method of solving the equations (1) for quantum systems possessing non-uniform Fourier space of $a_n(t)$ functions in contrast to the method for quantum systems with a homogeneous Fourier space [6].

DOI: https://doi.org/10.31972/ticma2022

3. CONSTRUCTING OBJECTS IN THE DISCRETE FOURIER SPACE OF THE UNKNOWN FUNCTIONS $a_n(t)$

In this example, we define a discrete function $\sigma(x;a,b,c)$ with an argument $x=\{0,1,\sqrt{7}\}$ on an inhomogeneous grid showing another three-level model (irrational, non-periodical dynamics). The function contains free parameters as below:

$$\sigma(x)=\left\{\frac{1}{2}-a,\quad a,\quad \frac{1}{2}\right\},$$

$$x=\{0,1,\sqrt{7}\},\quad 0<a<\tfrac{1}{2} \tag{2}$$

The standard procedure with such a weight function results in a sequence of three discrete orthogonal polynomials $\{\hat{p}(x)\}_{n=0}^{2}$:

- $\hat{P}_0(x)\equiv 1,$
- $\hat{P}_1(x)=\frac{1}{d_1}\left(x-a-\frac{\sqrt{7}}{2}\right),$
- $\hat{P}_2(x)=\frac{1}{d_2}\begin{pmatrix}\frac{1}{4}\left(7-4a\left(-1+\sqrt{7}+a\right)\right)x^2\\+\frac{1}{4}\left(-7\sqrt{7}+2a\left(5+\sqrt{7}+2a\right)\right)x+\left(4\sqrt{7}-7\right)a\end{pmatrix}.$

The polynomial norms are:

- $d_1=\sqrt{\frac{7}{4}-a\left(-1+\sqrt{7}+a\right)}$
- $d_2=\frac{1}{2}\sqrt{\left(\frac{7}{2}\left[-a(-1+2a)\left(-7\left(-4+\sqrt{7}\right)+4a\left(11-5\sqrt{7}+\left(-4+\sqrt{7}\right)a\right)\right)\right)\right]}$

(3)

It is known that orthogonal polynomials satisfy the three-term recurrence relation:

$$\bar{f}_{n+1}\hat{p}_{n+1}(x)+\bar{f}_n\hat{p}_{n-1}(x)=[rx+s_n]\,\hat{p}_n(x);$$
$$n=0,1,2;\quad \bar{f}_0=0\,,\ \bar{f}_1=1,\ \bar{f}_3=0\,. \tag{4}$$

Using the well-known formulas of the theory of orthogonal polynomials [3], one can obtain the coefficients of this relation (4):

$$r=\frac{1}{d_1}=\frac{1}{\sqrt{\frac{7}{4}-a\left(-1+\sqrt{7}+a\right)}},$$
$$\bar{f}_1=1,$$

$$f_2=\frac{4\sqrt{14}\sqrt{-(-a+2a^2)(28-7\sqrt{7}+44a-20\sqrt{7}a-16a^2+4\sqrt{7}a^2)}}{(-7-4a+4\sqrt{7}a+4a^2)^2} \tag{5}$$

DOI: https://doi.org/10.31972/ticma2022

Similarly, one can obtain the other coefficients S_0,S_1, S_2.

Numerical values $f_1 = 1;\quad f_2 \simeq 0.68$; show the corresponding quantum three-level system has two dipole transitions $f_n = \{1.0; 0.68\}$ and non-equidistant energy levels for all values of $0 < a < \frac{1}{2}$.

The Figures below shows frequency detuning and "Force" $f2$ for different quantum systems of a-family.

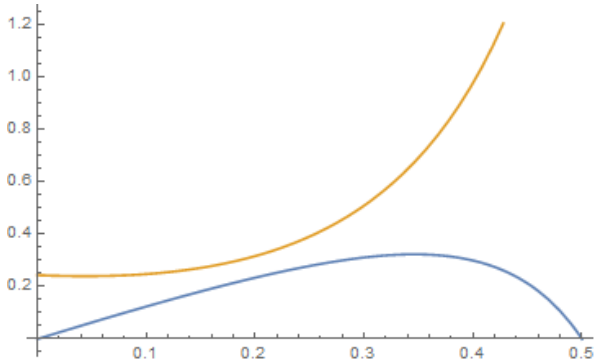

FIGURE 1. The dependence of the frequency tuning of both transitions $(\varepsilon_1, \varepsilon_2)$ for different quantum systems. (ε_2– at the top, ε_1– at the bottom)

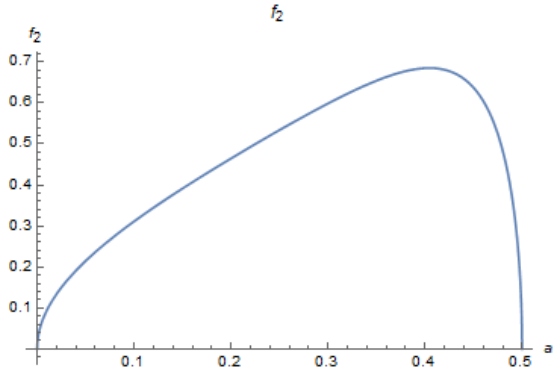

FIGURE 2. The dependence of $f_2(a)$ for different quantum systems of a-family.

4. SOLUTION AND DISCRETE PROBABILITY DISTRIBUTION OF QUANTUM SYSTEMS BY ENERGY LEVELS

Solution of the differential equations (1) is in the form of a discrete Fourier transform:

$$a_n(t) = e^{is_n t} \sum_{x=0}^{2} F_n(x) e^{irxt} \tag{6}$$

where $F_n(x)$ are the Fourier images (spectra) of the amplitudes of the probability of finding a particle at the level E_n at the time t when the radiation is active.

We assume that the Fourier spectra are expressed in terms of the constructed polynomials as follows:

$$F_n(x) = \sigma(x)\hat{p}_0\hat{p}_n(x); \quad n = 0,1,2; \quad x = 0,1,3 \tag{7}$$

The validity of this assumption is proved by substituting (6) and (7) into equations (1), which are satisfied when

$$f_n = \bar{f}_n\,, \quad \varepsilon_n = s_n - s_{n-1}\,, \quad n = 1,2 \tag{8}$$

DOI: https://doi.org/10.31972/ticma2022

This one-to-one correspondence establishes a relationship between the coefficients of the equations (1) – on the right and the coefficients of the recurrence relation (4) – on the left for the constructed polynomials. In other words, it is a correspondence between the characteristics of quantum systems and their exciting radiation, on the one hand, and the spectral properties of the probability amplitudes $a_n(t)$.

All values in (6) and 7) are known and one can calculate the Fourier spectra and construct a solution of equations (1).

5. DISCRETE PROBABILITY DISTRIBUTION OF QUANTUM SYSTEMS BY ENERGY LEVELS

Here we present a discrete statistical distribution of the excited particles over the energy levels. These are time-dependent level populations:

$$\rho_0(t) = \frac{1}{2}\begin{Bmatrix} 1-2a+4a^2-2a(-1+2a)Cos(rt) \\ +(1-2a)Cos(\sqrt{7}rt)+2aCos(rt-\sqrt{7}rt) \end{Bmatrix},$$

$$\rho_1(t) = \frac{1}{-14+8(-1+\sqrt{7})a+8a^2}\begin{Bmatrix} -7+14a-40a^2+16\sqrt{7}a^2 \\ +24a^3-16\sqrt{7}a^3-16a^4+2a(-1+2a) \\ (7-2\sqrt{7}+4(-1+\sqrt{7})a+4a^2)Cos(rt) \\ +(7-14a-4a^2+8a^3)\,Cos(\sqrt{7}rt) \\ +(14a-4\sqrt{7}a+8a^2-8a^3)Cos(rt-\sqrt{7}rt) \end{Bmatrix},$$

$$\rho_2(t)$$

$$= \frac{2a(-1+2a)}{-7(-4+\sqrt{7})+(44-20\sqrt{7})a+4(-4+\sqrt{7})a^2}\begin{Bmatrix} -39+12\sqrt{7} \\ +(35-11\sqrt{7})Cos[rt] \\ +(11-5\sqrt{7})Cos(\sqrt{7}rt) \\ +(-7+4\sqrt{7})Cos(rt-\sqrt{7}rt) \end{Bmatrix} \quad (9)$$

Expression (8) defines all the coefficients of equations (1), i.e. the quantum systems whose dynamics are described by the constructed solution. This is a a family of particle models with different dipole moments of transitions and with a different arrangement of energy levels, including a non-equidistant arrangement, which is typical for molecules. These systems are excited by radiation having different sets of parameters – the carrier frequency and the amplitude.

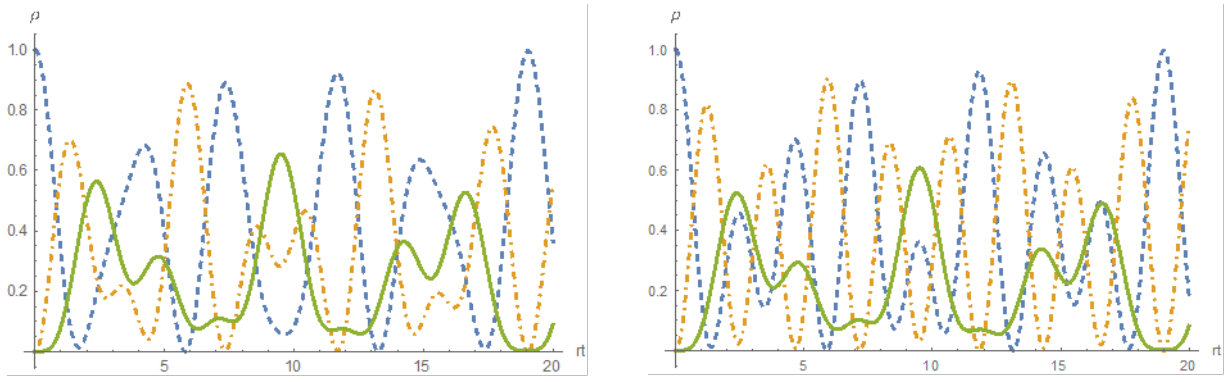

(a) (b)

FIGURE 3. The dependence of populations $\rho_n(rt)$ of the three-level quantum systems on time rt; ρ_0, ρ_1, ρ_2 are dashed, dot-dashed, and thick. (Where a =1/√7 in figure (a) and a =1/5 in figure (b))

DOI: https://doi.org/10.31972/ticma2022

6. CONCLUSIONS:

In this section we welcome you to include a summary of the end results of your research. Font should be Times New Roman, 10 pt. The discrete algorithm allows one to obtain a solution of equations of the form (1) for a variety of quantum systems with both homogeneous and inhomogeneous Fourier space of the desired functions (probability amplitudes of the excited quantum systems). The method is close to the physical content of the problem under consideration and corresponds to the main goal – to obtain a discrete distribution of particles over energy levels. The method does not require searching for already studied polynomials in order to apply them, but allows one to construct a sequence of polynomials for the quantum models under consideration. It is quite simple to introduce additional parameters leading to a solution describing the coherent dynamics of a family of quantum systems.

Note that the simple function $\sigma(x)$ (2) of the discrete argument x defines all the other structures associated with equations (1). It "generates" the corresponding system of orthogonal polynomials in the Fourier space of functions $a_n(t)$.

The work was carried out with the support of the Belarusian State Technological University, Minsk, Belarus and the SABIS® International School, Erbil, Kurdistan- Iraq.

REFERENCES

[1] Rabi, I.I., 1936. On the process of space quantization. *Physical Review*, 49(4), 324.

[2] Rabi, I.I., 1937. Space quantization in a gyrating magnetic field. *Physical Review*, 51(8), 652.

[3] Braak, D., Chen, Q.H., Batchelor, M.T. and Solano, E., 2016. Semi-classical and quantum Rabi models: in celebration of 80 years. *Journal of Physics A: Mathematical and Theoretical*, 49(30), 300301.

[4] Xie, Q., Zhong, H., Batchelor, M.T. and Lee, C., 2017. The quantum Rabi model: solution and dynamics. *Journal of Physics A: Mathematical and Theoretical*, 50(11), 113001.

[5] Banjak, S., 2019. Solving method without integration of some differential equation systems for coherent dynamics of quantum media excited by laser radiation. *Journal of Interdisciplinary Mathematics*, 22(6), 1051-1059.

[6] Banjak S., Savva V. The role of discrete orthogonal polynomials in constructing solutions of the dynamical equations describing coherent excitation of quantum systems in the field of laser radiation. AIP Conference Proceedings 2213, 020189 (2020). DOI 10.1063/5.0000104.

[7] Savva, V.A. and Banjak, S., 2020. Fourier Spectra of Quantum Systems Excited by Laser Radiation and the Exact Solution of their Dynamics Equations without Integration. *Journal of Applied Spectroscopy*, 87(5), 805-811.

Proceeding of 3rd International Conference of Mathematics and its Applications TICMA2022
https://conferences.su.edu.krd/su/ticma2022/
DOI: https://doi.org/10.31972/ticma2022

RESEARCH PAPER

New Results in Bi- Domination in Graphs

M. N. Al-Harere [1, a,*] and Athraa T. Breesam [2, b]
[1] manal.n.alharere@uotechnology.edu.iq
[2] A.T.Breesam@gmail.com
[a, b] *Department of Applied Sciences, University of Technology -Iraq*

A B S T R A C T:
In this paper, some new results are introduced for the bi-domination in graphs. Some properties of bi-domination number and bounds according to maximum, minimum degrees, order, and size have been determined. The effects of removing a vertex and removing or adding an edge are discussed on the bi-domination number of a graph. This study is important to know affected graphs by the deletion or addition of components.

KEY WORDS: domination number, bi-domination number, minimum dominating set.
DOI: https://doi.org/10.31972/ticma22.10

1. INTRODUCTION:

Consider $G = (V, E)$ be a graph without an isolated vertex where V is the vertex set of order n and E is the edge set of size m. the degree of a vertex of any graph G is the number of edges incident on this vertex. It is denoted by $deg(v)$, where $\delta(G)$ and $\Delta(G)$ are the minimum and maximum degrees of vertices in a graph G respectively. The *open* neighborhood of a vertex v is the set $N(v) = \{u \in V,\ uv \in E\}$ while the closed neighborhood is $N[v] = N(v) \cup \{v\}$. Consider a vertex $v \in V$. A set $D \subseteq V(G)$ is called a dominating set (DS) in the graph G *if* $N(v) \cap D \neq \emptyset, \forall v \in V - D$[17]. The domination number of G, denoted by $\gamma(G)$, is the minimum cardinality over all DS in G. Domination deals with various fields in graph theory as a topological graph [5], fuzzy graph [18], labelled graph [15,20]. Also, there is a study of domination polynomial of certain graph as in [8]. Conditions are imposed on the dominant number in order to fit the problems for which it is intended to solve. Some of the conditions mentioned earlier are put on the dominating set as in [6,16]. Or by putting conditions out of the DS as in [4,14]. And some definitions included both methods like [7,9]. Al-Harere and Breesam [1] are introduced a new model of domination under the condition that every vertex dominates exactly two vertices called bi-domination. These vertices do not belong to the DS. In [2] five new definitions of domination have been presented, which they are modified versions of bi-domination: "connected bi-domination", "total bi-domination", "connected independent bi-domination", "restrained domination", and "complementary tree bi-domination". The lower and upper bounds are calculated for the size of graphs having these parameters. In [3] bi- domination in spinner graph is determined. In this paper, some properties for bi- DS set are introduced.
Also, the size of a graph which has bi-domination number is determined. We proved that every bi- DS, is a minimal bi- DS. Moreover, several bounds are founded on this number for a graph G, according to its order, set of pendants, minimum and maximum degrees of its vertices.

Finally, changes that may occur in bi-domination number were discussed when a vertex or an edge is added to a graph, or when it is deleted. For graph theoretic terminology we refer to [11]. An excellent treatment of several topics in domination can be found in [10,12,13].

*** Corresponding Author: M. N. Al-Harere**
E-mail: manal.n.alharere@uotechnology.edu.iq
Article History:
Received: 01/08/2022
Accepted: 15/09/2022
Published: 07/12/2022

Proceeding of 3rd International Conference of Mathematics and its Applications
TICMA2022
https://conferences.su.edu.krd/su/ticma2022/
DOI: https://doi.org/10.31972/ticma2022

2. Bi-dominating sets

Definition 2.1. [1] Consider $G = (V, E)$ be a finite, simple, and undirected graph without isolated vertex. A subset $D \subset V(G)$ is a $bi - DS$, if $\forall\, v \in D$ dominates exactly two vertices in the set $V - D$, such that $|N(v) \cap \{V - D\}| = 2$. The minimum bi-dominating set of G is denoted by $\gamma_{bi}(G)$-set. The minimum cardinality of all $bi - DS$ is called bi-domination number and denoted by $\gamma_{bi}(G)$.

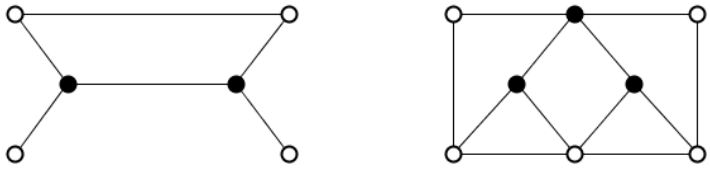

Figure 1: $bi - DS$ in graphs

Observation 2.2. [1] Let G be a finite simple undirected graph of order n with a $bi - DS$ D and γbi(G). We have

- The order of a graph G is $n; n \geq 3$.
- $\delta(G) \geq 1$, $\Delta(G) \geq 2$.
- Every $v \in D$, $deg(v) \geq 2$.
- Every support vertex $v, v \in D$.
- $\gamma(G) \leq \gamma_{bi}(G)$.

Observation 2.3. Assume that a graph G has $bi - DS$, then $\gamma_{bi}(G) \leq n - p$ where p is the number of pendant vertices in G.

Observation 2.4. If there is a component K_2 in a graph G, then G has no $bi - DS$.

Observation 2.5. If G has support vertices adjacent to more than 2 pendants vertices in a graph G, then G has no $bi - DS$.

Proposition 2.6. Let G be any graph which has a $bi - DS$, then $\gamma_{bi}(G) = 1$ if and only if G is an either $P_3 or\ K_3$.

Proof: If $\gamma_{bi}(G) = 1$, then G has a $bi - DS$ contains one vertex, this vertex dominates two vertices in $V - D$. Thus, G is connected and has only three vertices therefore, G is an either $P_3 or\ K_3$. Conversely, it is clear.

Theorem 2.7. Assume that G be a graph having $\gamma_{bi}(G)$ then the size m of G is

$$2\gamma_{bi} \leq m \leq \frac{n^2-n}{2} + {\gamma_{bi}}^2 - n\gamma_{bi} + 2\gamma_{bi}$$

Proof: Consider D to be a γ_{bi} - set of G, so we prove the required by discussing two different cases as follows.

Case 1. Firstly, to prove $2\gamma_{bi} \leq m$, let $G[D]$ and $G[V - D]$ be two null graphs. Hence, G contains as few as possible edges. Now, by the definition of $bi - DS$ there exist exactly two edges incident to all vertices in D. Thus, the number of edges is $2|D| = 2\gamma_{bi}$. Therefore, $m \geq 2\gamma_{bi}$.

Case 2. To prove the upper bound, this case occurs where the two induced subgraphs of the sets D and $V - D$ are complete, so let m_1 *and* m_2 be the number of edges of two induced subgraphs *of the sets* D *and* $V - D$ respectively. Thus,

$$m_1 = \frac{|D|\,|D-1|}{2} = \frac{\gamma_{bi}(\gamma_{bi}-1)}{2} \quad and\ m_2 = \frac{|V-D||V-D-1|}{2} = \frac{(n-\gamma_{bi})(n-\gamma_{bi}-1)}{2} .$$

And according to case 1 we have

$$m_3 = 2|D| = 2\gamma_{bi}$$

So, in this case

$$m = m_1 + m_2 + m_3$$

Hence,

DOI: https://doi.org/10.31972/ticma2022

$$m = 2|D| + \frac{|D|\,|D-1|}{2} + \frac{|V-D||V-D-1|}{2} = 2\gamma_{bi} + \frac{\gamma_{bi}(\gamma_{bi}-1)}{2} + \frac{(n-\gamma_{bi})(n-\gamma_{bi}-1)}{2}.$$

In general

$$m \le m_1 + m_2 + m_3$$

Theorem 2.8. Assume that a graph G has γ_{bi}, then

$$\lceil n/3 \rceil \le \gamma_{bi}(G) \le n-2$$

Proof. Let D be a γ_{bi}- set of G, and let the vertices $v_i, v_j \in D$. Then there are two different cases as the following.

Case1. If $N(v_i) \cap N(v_j) \cap (V-D) = \emptyset$, so each vertex in the set $V-D$ is dominated by exactly one vertex in the set D, and $\gamma_{bi}(G) = n/3$.

Case2. If $N(v_i) \cap N(v_j) \cap (V-D) \neq \emptyset$, this means exists one vertex or more being dominated by the same vertex in D which means $\gamma_{bi}(G) > \lceil n/3 \rceil$.

Thus, $\gamma_{bi}(G) \ge \lceil n/3 \rceil$. The upper bound is obvious.

Corollary 2.9. Consider G be a graph having a γ_{bi}, then

1. $\gamma_{bi}(G) \ge \left\lceil \frac{n}{\delta+2} \right\rceil, \delta \ge 1$.
2. $\gamma_{bi}(G) \ge \left\lceil \frac{n}{\Delta+1} \right\rceil, \Delta \ge 2$.

Theorem 2.10. Every $bi-DS$ is a minimal $bi-DS$.

Proof. Assume that the set D be any $bi-DS$ in a graph G. Assume that the set D is not a minimal $bi-DS$, so there is at least one vertex say $v \in D$ such that $D-\{v\}$ is a $bi-DS$. Now we discuss the deletion cases as follows.

Case 1. Assume that there are two vertices that are dominated by the vertex v is not dominated by the other vertex. Then the set $D-\{v\}$ is not a $bi-DS$ and this is a contradiction.

Case 2. If there are one or more vertices in $D-\{v\}$ which dominate the two vertices in $V-D$ that are adjacent to the vertex v, then we discuss which vertices are dominating vertex v. Now, if the set $D-\{v\}$ has no a vertex dominating the vertex v, then $D-\{v\}$ is not a $bi-DS$, so this is a contradiction too. Otherwise, the vertex v is dominated by at least one vertex say w in the set $D-\{v\}$. Therefore, w dominates at least three vertices in the set $V-(D-\{v\})$. Thus, the set $D-\{v\}$ is not a $bi-DS$ and this is a contradiction. From all cases above, the set $D-\{v\}$ is not a $bi-DS$, so, D is the minimal $bi-DS$.

3. Changing and unchanging of bi-domination number:

Throughout this section the effects on $\gamma_{bi}(G)$ when G is modified by deleting a vertex or deleting or adding an edge are discussed.

If $G-v$ has a $bi-DS$, then the three partitions of the vertices of G are:

$$V^0 = \{v \in V : \gamma_{bi}(G-v) = \gamma_{bi}(G)\}.$$
$$V^+ = \{v \in V : \gamma_{bi}(G-v) > \gamma_{bi}(G)\}.$$
$$V^- = \{v \in V : \gamma_{bi}(G-v) < \gamma_{bi}(G)\}.$$

In the same manner the edge set can be classification into

$$E_*^0 = \{e \in E : \gamma_{bi}(G*e) = \gamma_{bi}(G)\}$$
$$E_*^+ = \{e \in E : \gamma_{bi}(G*e) > \gamma_{bi}(G)\}$$
$$E_*^- = \{e \in E : \gamma_{bi}(G*e) < \gamma_{bi}(G)\}, \text{ where } * = \begin{cases} - & , \ e \in G \\ + & , \ e \in \bar{G} \end{cases}$$

Theorem 3.1. For graph G having a unique γ_{bi}- set, there exists a vertex v such that if $G-v$ has a bi-dominating set then v belongs to $(V^0 \cup V^+ \cup V^-)$

Proof. By assumption there is a unique γ_{bi}- set say D then there are two different cases as follows.

(a) When $v \in D$, vertex v dominates two vertices say w_1 and w_2 in $V-D$ then there are three cases

DOI: https://doi.org/10.31972/ticma2022

Case1. $v \in V^0$, this case occurs in two cases as the following.
i. If vertex v dominates w_1 and w_2 such that only one vertex say $w_1 \in pn[v, D]$ and it is adjacent to exactly two vertices in $V - D$, then we can add this vertex (w_1) to set $D - \{v\}$. It is obvious that $\{D - v \cup \{w_1\}\}$ is a $bi - DS$ and $\gamma_{bi}(G - v) = \gamma_{bi}(G)$. (For example, see Fig. 2).

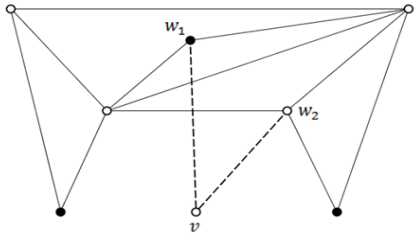

Figure 2: $bi - DS$ of $G - v$

ii. If the both vertices w_1 and $w_2 \in pn[v, D]$, such that w_1 is adjacent to w_2 and to other vertex in $V - D$, then we can add vertex w_1 to set $D - \{v\}$. It is obvious that $D - \{v\} \cup \{w_1\}$ is a minimal $bi - DS$ and $\gamma_{bi}(G - v) = \gamma_{bi}(G)$. (For example, see Fig. 3).

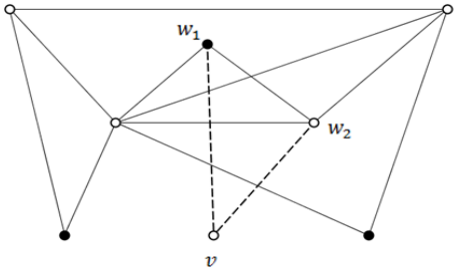

Figure 3: $bi - DS$ of $G - v$

Case 2. A vertex $v \in V^+$ if both vertices w_1 and $w_2 \in pn[v, D]$. So that the two vertices w_1 and w_2 are not dominated by vertices of $D - \{v\}$, and each one of w_1 and w_2 is exactly adjacent to two vertices in $V - (D - \{v\})$ regardless the possibility that they are adjacent to each other or not. Then we can add the vertices w_1 and w_2 to the set $D - \{v\}$ and it is obvious that $\{D - \{v\} \cup \{w_1, w_2\}\}$ is a minimal $bi - DS$ and $\gamma_{bi}(G - v) > \gamma_{bi}(G)$. (For example, see Fig. 4).

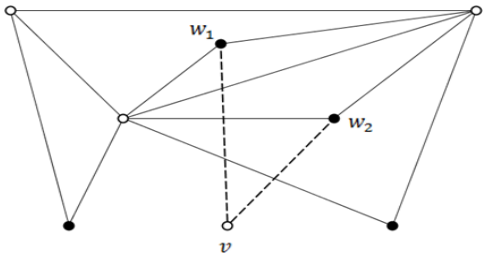

Figure 4: $bi - DS$ of $G - v$

Case 3. A vertex $v \in V^-$ if the two vertices $w_1 and\, w_2$ are dominated by other vertices in D, then $\gamma_{bi}(G - v) < \gamma_{bi}(G)$.
(b) When $v \in V - D$, then there are two cases
Case1. $v \in V^0$
The vertex in D that dominates the vertex v say u dominates another vertex in $V - D$ say w, if w is adjacent to exactly one vertex in $V - D$, then we can take the vertex w instead of the vertex u.
Case 2. $v \in V^-$, if the vertex v is dominated by more one vertex in D say the set $M = \{v_1, v_2, .. v_i, \dots, v_k\}$, and there is a vertex in M say v_i such that all other vertices in M are adjacent to it. G is $bi - DS$ and $v_i \in D$,

Proceeding of 3rd International Conference of Mathematics and its Applications
TICMA2022
https://conferences.su.edu.krd/su/ticma2022/
DOI: https://doi.org/10.31972/ticma2022

thus there is a vertex $v \neq u \in V - D$ which dominates by the vertex v_i and suppose that this vertex is already dominated by another vertex in D, then the vertex v_i will take place the vertex v in the set $V - D$. Therefore, $\gamma_{bi}(G - v) < \gamma_{bi}(G)$. (For example, see Fig. 5).

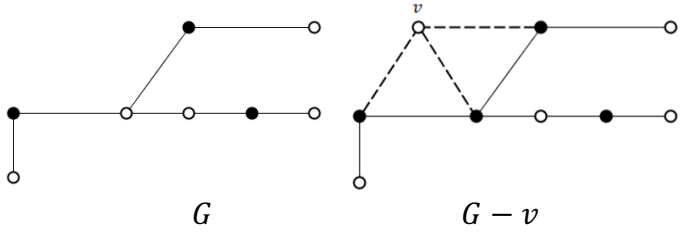

Figure 5: $bi - DS$ in G and $G - v$

Theorem 3.2. Assume that $G = (V, E)$ be a graph with a minimum $bi - DS$, and $e \in \bar{G}$, if $G + e$ has $bi - DS$ then either $e \in E_+^0$ or $e \in E_+^+$.

Proof. Let D be a minimum $bi - DS$. If e is added to $G[D]$or to $G[V - D]$, it is obvious that the set D is not influenced by this addition, which means $\gamma_{bi}(G) = \gamma_{bi}(G + e)$. Thus, $e \in E^0$.
If e is added to G, such that one vertex incident with e say v belongs to D and the other vertex say w belongs to $V - D$ and let u and z are two vertices in $V - D$ which are dominated by to vertex v. When $G + e$ has a $bi - DS$ then there are two cases as the following.
Case 1. $e \in E_+^0$: There are three different cases as the following.
i. If u and $z \in pn[v, D]$ and there is one or more induced subgraph K_3 in G then there are three different cases as the following.
a) If v, u, and z are the vertices of K_3, in $G + e$, where $e = vw$, we can take either u or z instead of the vertex v in D if this vertex of degree two in G (as shown in Fig. 6).
b) If the two vertices u and z are not adjacent and w is a vertex of the induced subgraph K_3 then in $G + e$ we can add w instead of its dominating vertex in D if both of them are of degree two in G.
(as shown in Fig. 7)
c) If there are two induced subgraphs K_3, then we can combine the two cases above.

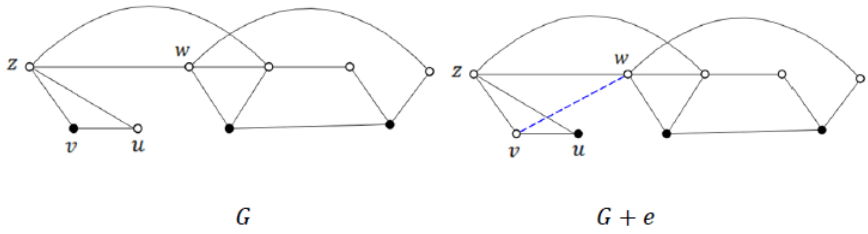

Figure 6: A minimum $bi - DS$ in G and $G + e$

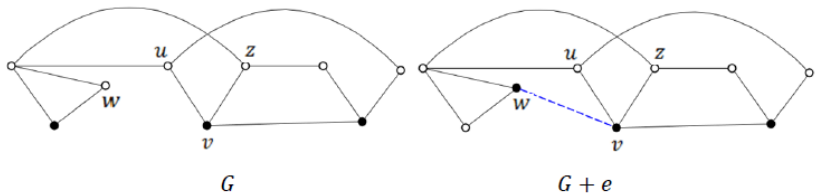

Figure 7: A minimum $bi - DS$ in G and $G + e$
ii. If one of the vertices say z is adjacent to some vertices in D say h, then there are two different cases:
a) if $deg\ (u) = deg\ (v) = 2$ in G, then we can take u instead of v in D. (as shown in following Fig. 8).

Proceeding of 3rd International Conference of Mathematics and its Applications
TICMA2022
https://conferences.su.edu.krd/su/ticma2022/
DOI: https://doi.org/10.31972/ticma2022

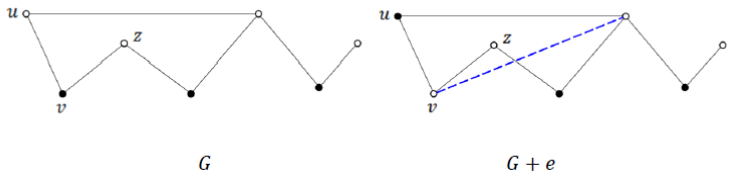

Figure 8: A minimum $bi-DS$ in G and $G+e$

b) If $deg\ (u) = deg\ (w) = 3$ in $G+e$ such that u and w are adjacent then we can take $u\ and\ w$ instead of $v\ and\ h$ respectively if $deg\ (v) = deg\ (h) = 2$ in G. (see Fig. 9).

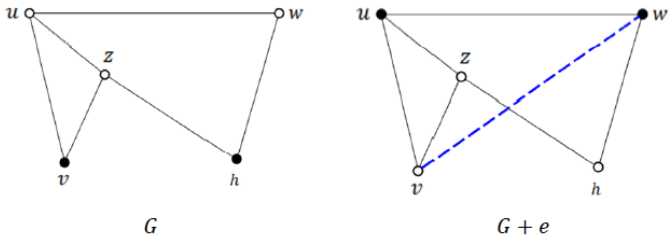

Figure 9: A minimum $bi-DS$ in G and $G+e$

iii. If u and z are dominated by other vertices of D, then four cases are discussed as follows.
a) Add w to set D instead of its dominating vertex, if w is a vertex as in case 1(i)(b)

b) Having a component of G such that v, u, z and, h, are its vertices, where both $v\ and\ h$ dominate u and z. So, we take u and z instead of v and h as the dominating vertices. (as illustrated in Fig. 10).

c) If h and c dominate u and z respectively in addition to v. Also, v and h are isolated vertices in $G[D]$, assume $w \in pn[D,h]$, $deg(w) = 3$ in $G+e$. So, w will replace h in D. (as illustrated in Fig. 11).

d) Assume h dominates both u and x and c dominates z and another vertex, such that $v\ and\ h$ are isolated vertices in $G[D]$and u is an isolated in $G[V-D]$, so $u\ and\ x$ will replace $v\ and\ h$ respectively in D. (as illustrated for example in Fig. 12).
In all sub cases a, b, c,and d $\gamma_{bi}(G) = \gamma_{bi}(G+e)$
So, in case 1 $\gamma_{bi}(G) = \gamma_{bi}(G+e)$.

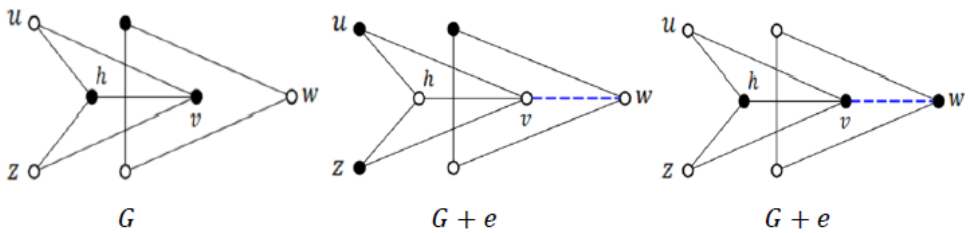

Figure 10: A minimum $bi-DS$ in G and $G+e$

DOI: https://doi.org/10.31972/ticma2022

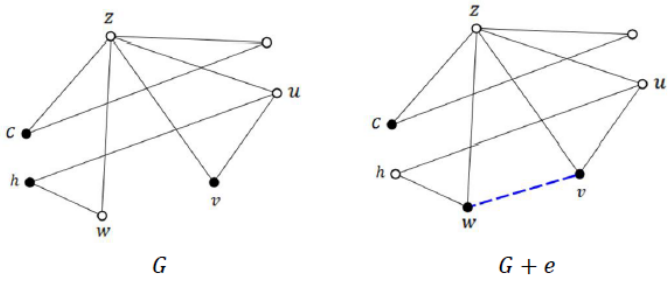

Figure 11: A minimum $bi-DS$ in G and $G+e$

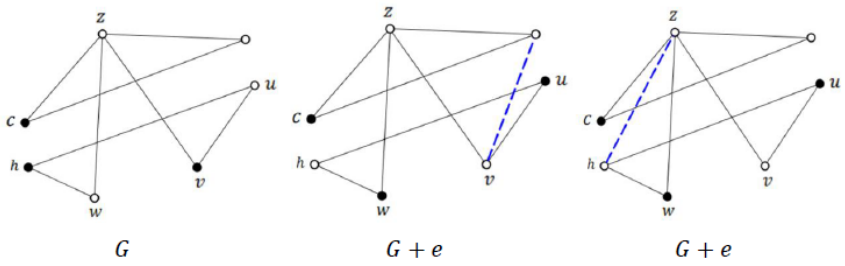

Figure 12: A minimum $bi-DS$ in G and $G+e$

Case 2. $e \in E_+^+$: This case occurs in three different cases below.
i) If both u and $z \in pn[v, D]$ in G , we can add u and z to D instead of the vertex v if u and z are not adjacent to each other and v is isolated in $[D]$. Also, $deg\ (u) = deg\ (z) = 1$ in G$[V-D]$. (as an example, see Fig. 13).

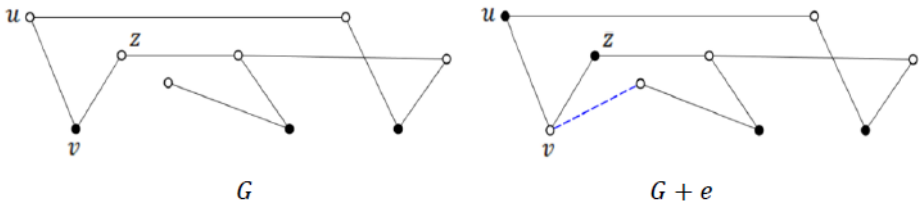

Figure 13: A minimum $bi-DS$ in G and $G+e$

ii) If one of two vertices say u satisfies that $|N(u) \cap (V-D)| = 2$, then in $G+e$, we add vertex u to the set D, so we get the result. (for example, see Fig.14).
Hence, in case 2 $\gamma_{bi}(G+e) > \gamma_{bi}(G)$

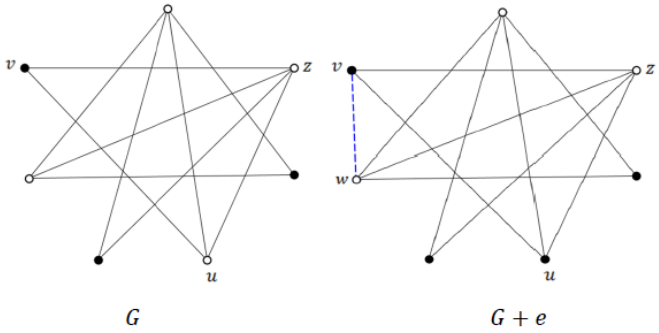

Figure 14: A minimum $bi-DS$ in G and $G+e$

DOI: https://doi.org/10.31972/ticma2022

Theorem 3.3. Let $G = (V, E)$ be a graph with a minimum $bi - DS$, and $e \in E(G)$, if $G - e$ has $bi - DS$ then, $E_{-}^{*} \neq \emptyset, where * = 0\ or\ -, or +$.

Proof. Let D be a *minimum* $bi - DS$ .There are three cases to show the set E_{-}^{*} is not an empty set as follows.
Case 1. $E_{-}^{0} \neq \emptyset$.
If e is deleted from $G[D]$or from $G[V - D]$, it is obvious that the minimum $bi - DS$ is not influenced for this change, which means $\gamma_{bi}(G - e) = \gamma_{bi}(G)$. Thus, $e \in E_{-}^{0}$. Hence, $E_{-}^{0} \neq \emptyset$.
Case 2. $E_{-}^{+} \neq \emptyset$
Let $e = vu$, where $v \in D\ and\ u \in V - D$ and let $v \neq w \in V - D$ that it is dominated by the vertex v and suppose that u and w are adjacent. Also, u is adjacent to exactly two other vertices in $V - D$ and w is adjacent to only one vertex in $V - D$, then $(D - \{v\}) \cup \{u, w\}$ is a minimum $bi - DS$. Thus, we get the result. (see Fig. 15).

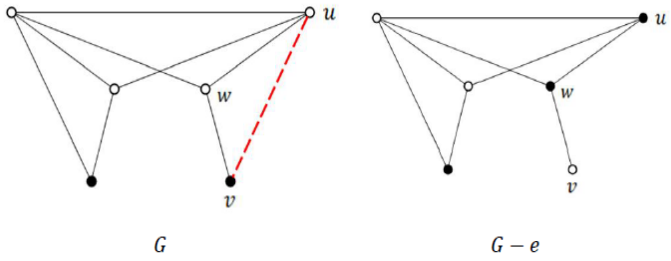

Figure 15: A minimum $bi - DS$ in G and $G - e$

Case 3. $E_{-}^{-} \neq \emptyset$
Let $e = vu$, where $v \in D\ and\ u \in V - D$. In $G - e$, if there is a vertex in D say w such that w is adjacent to only v in set D. So, $(w) \cap D - \{v\} = \emptyset$, and there is a vertex or more in $D - \{w\}$ dominating the two vertices which are dominated by w, then $D - \{w\}$ is a $bi - DS$. Therefore, $E_{-}^{-} \neq \emptyset$ (as an example, see Fig.16).

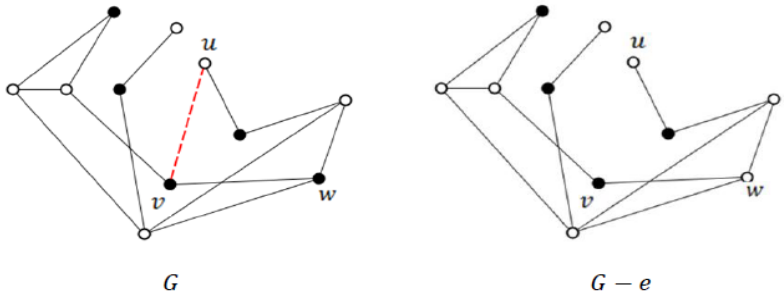

Figure 16: A minimum $bi - DS$ in G and $G - e$

4. CONCLUSIONS

The domination type called bi-domination is one of the domination types can be calculated in a connected and disconnected graph. This definition can be determined if applicable or not depending on graph size. Every bi-dominating set is a minimal bi-dominating set. Also, bi-domination number could be maintained when a vertex is deleted, or when we add or delete an edge from the graph.

REFERENCES

1. Al-Harere, M.N. and Breesam, A.T., 2019, April. Further results on bi-domination in graphs. In *AIP Conference Proceedings* (Vol. 2096, No. 1, 020013). AIP Publishing LLC.
2. Al-Harere, M.N. and Breesam, A.T., 2019. Variant Typesof Domination in Spinner Graph. *Al-Nahrain Journal of Science*, (2), 127-133.
3. M.N. Al-Harere, A.T. Breesam , On bi-domination in graphs, Albahir journal, 10(17-18)(2019),63-68.

DOI: https://doi.org/10.31972/ticma2022

4. Al-Harere, M.N. and Bakhash, K., 2022. Changing and unchanging on Tadpole domination number in G− e, G+ e graphs.
5. Al'Dzhabri, K.S., Omran, A.A. and Al-Harere, M.N., 2021. DG-domination topology in Digraph. *Journal of Prime Research in Mathematics*, 17(2), 93-100.
6. Abed, S.S. and Al-Harere, M.N., 2022. Rings domination in graphs. *International Journal of Nonlinear Analysis and Applications*.
7. Al-harere, M.N., 2022. Some Modified Types of Pitchfork Domination and It's Inverse. *Boletim da Sociedade Paranaense de Matemática*, 40, 1-9.
8. Alwan, I.A. and Omran, A.A., 2020, July. Domination polynomial of the composition of complete graph and star graph. In *Journal of Physics: Conference Series* (Vol. 1591, No. 1, 012048). IOP Publishing.
9. Al-Harere, M.N., Mitlif, R.J. and Sadiq, F.A., 2021. Variant Domination Types for a Complete h-ary Tree. *Baghdad Science Journal*, 18(1), 797-802.
10. C. Berge, The theory of graphs and its applications, Methuen, 1962.
11. F. Harary, Graph Theory, Addison-Wesley Publishing Company, 1969.
12. Haynes, T., 1998. S. hedetniemi, and P. Slater. Fundamentals of domination in graphs.
13. Haynes, T., 2017. *Domination in graphs: volume 2: advanced topics*. Routledge.
14. Kahat, S.S. and Al-Harere, M.N., 2021, May. Inverse equality co-neighborhood domination in graphs. In *Journal of Physics: Conference Series* (Vol. 1879, No. 3, 032036). IOP Publishing.
15. Majeed, S.S., Omran, A.A.A. and Yaqoob, M.N., 2022. Modern Roman domination of corona of cycle graph with some certain graphs. *Computer Science*, 17(1), 317-324.
16. Omran, A.A., Al-Harere, M.N. and Kahat, S.S., 2022. Equality co-neighborhood domination in graphs. *Discrete Mathematics, Algorithms and Applications*, 14(01), 2150098.
17. O. Ore, Theory of graphs, American Mathematical Soc. 1962.
18. Yousif, H.J. and Omran, A.A., 2021, May. Closed fuzzy dominating set in fuzzy graphs. In *Journal of Physics: Conference Series* (Vol. 1879, No. 3, 032022). IOP Publishing.

Proceeding of 3rd International Conference of Mathematics and its Applications TICMA2022
https://conferences.su.edu.krd/su/ticma2022/
DOI: https://doi.org/10.31972/ticma2022

RESEARCH PAPER

Hopf Bifurcation Analysis of a Chaotic System

Rizgar H. Salih[1,a] and Bashdar M. Mohammed[2,b,*]
[1,2] *Department of Mathematics, College of Basic Education, University of Raparin, Raniyah, Kurdistan Region - Iraq.*
[a] *rizgar.salih@uor.edu.krd*
[b] *bashdar.mahmoodmuhamad@uor.edu.krd*

A B S T R A C T:

This paper is devoted to studying the stability of the unique equilibrium point and the occurrence of the Hopf bifurcation as well as limit cycles of a three-dimensional chaotic system. We characterize the parameters for which a Hopf equilibrium point takes place at the equilibrium point. In addition, the system has only one equilibrium point which is $E_0 = (0,0,0)$. It was proved that E_0 is asymptotically stable and unstable when $\alpha < \frac{-13}{7}$ and $\alpha > \frac{-13}{7}$, respectively. Moreover, for studying the cyclicity of the system, two techniques are used which are dynamics on the center manifold and Liapunov quantities. It was shown that at most two limit cycles can be bifurcated from the origin. All the results presented in this paper have been verified by a program via Maple software.

KEY WORDS: Chaotic System, Hopf Bifurcation Analysis, equilibrium point.
DOI: https://doi.org/10.31972/ticma22.11

1. INTRODUCTION:

We consider the following system of differential equations

$$\frac{dU}{dt} = AU + F(U,\mu) \tag{1}$$

where variable $U \in \mathbb{R}^3$, F is an analytic function, parameter $\mu \in \mathbb{R}^k$ and A is the square matrix has two complex eigenvalues $\alpha \pm i\beta$ $(\beta \neq 0)$ and a non-zero eigenvalue γ, such that $F(0;\mu) = D_U(0;\mu) = 0 \ \ \forall\mu$, where $D_U(0;\mu)$ is the determinant of Jacobian matrix of $F(U;\mu)$ $at\ U = 0$.

A sufficient condition of Hopf bifurcation for the three-dimensional system (1) (having a nonzero with two pure imaginary eigenvalues) is illustrated below:

Let

$$\lambda^3 - T\lambda^2 - K\lambda - D = 0 \tag{2}$$

be the characteristic polynomial of the linearized system (1) at the origin, where

$T = \sum_{i=1}^{3} a_{i,i}$ (Trace of the Jacobian matrix of system (1) at the origin),
$D =$ Determinant of the Jacobian matrix of system (1) at the origin,
$K = -(A_1 + A_2 + A_3)$;

where $A_i = a_{j,j}a_{k,k} - a_{j,k}a_{k,j}$, $i,j,k = 1,2,3, i \neq j \neq k$ are elements of the Jacobian matrix of system (1) at the origin [1], [2] and [3]. Then, the Hopf bifurcation takes place at a point (which is called a Hopf point) where

$$TK + D = 0 \quad (T \neq 0 \ \& \ K < 0) \tag{3}$$

*** Corresponding Author: Bashdar M. Mohammed**
E-mail: *bashdar.mahmoodmuhamad@uor.edu.krd*
Article History:
Received: 01/08/2022
Accepted: 15/09/2022
Published: 07/12/2022

Proceeding of 3rd International Conference of Mathematics and its Applications TICMA2022
https://conferences.su.edu.krd/su/ticma2022/
DOI: https://doi.org/10.31972/ticma2022

Moreover, suppose that system (1) has a critical point (u_0, μ_0), then this system has a Hopf bifurcation if $D_u f(u_0, \mu_0)$ has a simple pair of pure imaginary eigenvalues with no other eigenvalues with zero real parts and $\frac{d}{d\mu} Re(\lambda_{2,3}(\mu))|_{\mu=\mu_0} = d \neq 0$ are satisfied, where $Re(\lambda_{2,3}(\mu))$ denotes the real part of the complex eigenvalues which is smooth function of μ. Then, there is a unique three-dimensional center manifold passing through (u_0, μ_0) in $\mathbb{R}^3 \times \mathbb{R}$ and a smooth system of coordinates (preserving the planes $\mu = const.$) for which the Taylor expansion of degree three on the center manifold is given by

$$\begin{pmatrix} \dot{u} \\ \\ \dot{v} \end{pmatrix} = \begin{pmatrix} \left(d\,\mu + a\,(u^2+v^2)\right) u - \left(\omega + c\,\mu + b\,(u^2+v^2)\right) v \\ \\ \left(\omega + c\,\mu + b\,(u^2+v^2)\right) u + \left(d\,\mu + a\,(u^2+v^2)\right) v \end{pmatrix} \tag{4}$$

If $a \neq 0$, there is a surface of periodic solution in the center manifold which has quadratic tangency with the eigenspace of $\lambda(\mu_0)$, $\overline{\lambda(\mu_0)}$ agreeing to second order with the parabolic $\mu = -\frac{a}{d}(u^2+v^2)$. If $a < 0$, then these periodic solutions are stable limit cycles, the bifurcation is of type Supercritical Hopf bifurcation. While if $a > 0$, the periodic solutions are repelling (unstable limit cycles), the bifurcation is of type Subcritical Hopf bifurcation [4] and [5].

By the time rescaling $\tau = \beta t$ and a linear change of coordinates, system (1) can be written in the form

$$\begin{pmatrix} \dot{u} \\ \dot{v} \\ \dot{w} \end{pmatrix} = \begin{pmatrix} \alpha_1 u - v \\ \alpha_1 v + u \\ \lambda\, w \end{pmatrix} + \begin{pmatrix} F_1(u,v,w;\mu) \\ F_2(u,v,w;\mu) \\ F_3(u,v,w;\mu) \end{pmatrix} \tag{5}$$

where $\alpha_1 = \frac{\alpha}{\beta}$, $\lambda = \frac{\gamma}{\beta}$, $F_i(u,v,w;\mu) = \sum_{k=2}^{\infty} {F_i}^k(u,v,w;\mu)$, $i = 1,2,3$ and ${F_i}^k(u,v,w;\mu)$ are polynomials that are homogeneous of degree k. The Hopf point at the origin of equation (5) has two pure imaginary eigenvalues, $\pm i$, and a nonzero eigenvalue λ when $\alpha_1 = 0$. A good source of Hopf bifurcation in $\mathbb{R}^n$ is [6]. At $\alpha_1 = 0$, system (5) can be written of the following form

$$\begin{pmatrix} \dot{u} \\ \dot{v} \\ \dot{w} \end{pmatrix} = \begin{pmatrix} -v \\ u \\ \lambda\, w \end{pmatrix} + \begin{pmatrix} F_1(u,v,w;\mu) \\ F_2(u,v,w;\mu) \\ F_3(u,v,w;\mu) \end{pmatrix} \tag{6}$$

where F_1, F_2 and F_3 are real analytic functions on the neighborhood of the origin in $\mathbb{R}^3$ and with their derivatives vanish at the origin. Since system (6) has two eigenvalues with zero real part $\alpha_1 = 0$, then system (6) has a local 2-dimensional centre manifold, $W^c(0)$ [7]. This manifold is invariant and there exists a function h of class C^K, $k \geq 1$ in a small neighbourhood of the origin such that $h(0,0;\,\mu) = D\,h(0,0;\,\mu) = 0$, where $D\,h(0,0;\,\mu)$ is a Jacobian matrix of h at the origin. The 2-dimensional centre manifold, $W^c(0)$, is defined by

$$W^c(0) = \{(u, v, h(u,v;\,\mu);\,\mu) \in \mathbb{R}^3 : (u,v) \in \text{a small neighborhood of the origin}\}$$

In the third component of equation (6), after inserting $w = h(u,v;\,\mu)$ and using the chain rule, the following equation is obtained, which is useful to find the function h.

DOI: https://doi.org/10.31972/ticma2022

$$D\,h(0,0;\ \mu)\begin{pmatrix}-v+F_1(u,v,h(u,v;\ \mu);\mu)\\ u+F_2(u,v,h(u,v;\ \mu);\mu)\end{pmatrix}=\lambda\,h(u,v;\ \mu)+F_3(u,v,h(u,v;\ \mu);\mu) \tag{7}$$

In the first two components of equation (6), after substituting $w=h(u,v;\ \mu)$, the following reduced system to the center manifold is obtained; its linear part is of center-focus type.

$$\begin{pmatrix}\dot{u}\\ \\ \dot{v}\end{pmatrix}=\begin{pmatrix}-v\\ \\ u\end{pmatrix}+\begin{pmatrix}F_1(u,v,h(u,v;\ \mu);\mu)\\ \\ F_2(u,v,h(u,v;\ \mu);\mu)\end{pmatrix} \tag{8}$$

To find the Liapunov quantities of system (8), we seek a Lyapunov function of the form

$$V(u,v)=u^2+v^2+\sum_{k=3}^{n}V_{\mathrm{k}}(u,v;\mu) \tag{9}$$

where V_{k} is a polynomial in u,v of degree k and the coefficients of V_{k} satisfy

$$\chi(V)=\eta_2\,r^2+\eta_4\,r^4+\eta_6\,r^6+\cdots+\eta_{2i}\,r^{2i} \tag{10}$$

where $r^2=u^2+v^2$ or u^2 or v^2 or $(u^2+v^2)^2$ or other suitable forms and χ is the vector field of system (8). Here, $\eta_{2i},\ i=1,2,3,\ldots$ is a polynomial in the parameter μ of the system also called the i^{th} Liapunov quantity, for more detail see ([8],[9] and [10]).
In this paper, we study the following non-linear system of differential equations

$$\begin{aligned}\dot{x}&=-z,\\ \dot{y}&=-x-z,\\ \dot{z}&=2x-\tfrac{13}{10}\,y+\alpha\,z+x^2+\beta\,z^2-xz,\end{aligned} \tag{11}$$

which was introduced in 2014 by Lao and Sprott, where x,y and z are variables and α,β are parameters in $\mathbb{R}$ [11]. This system is simplest electronic circuit, it is significant and used in mathematics, physics and engineering applications. Lao et al. have explained the simplest electronic circuit design. This circuit design consists of multipliers, integrator, amplifier and inverting amplifier. A new cost function base on Gaussian mixture model has been studied for parameter estimation of system (11) in [11]. Muhammed has investigated the non-integrability of system (11) and have proved that system (11) for any value of the parameters α and β has no polynomial, Darboux, rational and analytic first integrals. Also, system (11) has two exponential factors e^x and e^y with cofactors $-z$ and $-x-z$, respectively and has no invariant algebraic surfaces with nonzero cofactors. In addition, the dynamics at infinity for system (11) is analysed by using the theory of Poincaré compactification in $\mathbb{R}^3$ [12]. According to our knowledge, the Hopf bifurcation and limit cycles for the system have not studded.

In this paper, Hopf bifurcation theorem and Liapunov quantities for finding limit cycles of system (11) are used. It was shown that one stable limit cycle can be bifurcated from the origin when $\beta>\frac{1}{1274}\left(204+\sqrt{204506}\right)$ or $\beta<\frac{1}{1274}\left(204-\sqrt{204506}\right)$. Moreover, by finding Liapunov quantities, it was shown that at most two limit cycles can be bifurcated from the origin when $\beta=\frac{1}{1274}(204\pm\sqrt{204506})$. Of course, it is important to give an analytical proof for this result.

DOI: https://doi.org/10.31972/ticma2022

2. STABILITY ANALYSIS:

In this section, the stability of the unique equilibrium points at the origin of system (11) is presented. It is easy to see that system (11) has a unique equilibrium $E_0 = (0,0,0)$. By linearization around E_0, the Jacobian matrix of system (11) is given by

$$J(E_0) = \begin{pmatrix} 0 & 0 & -1 \\ -1 & 0 & -1 \\ 2 & -\frac{13}{10} & \alpha \end{pmatrix}$$

It's characteristic equation at E_0 is given by

$$\lambda^3 - T\lambda^2 - K\lambda - D = 0 \tag{12}$$

where $T = \alpha,\ D = \frac{-13}{10}$,and $K = \frac{-7}{10}$. The Hurwitz matrix of the characteristic polynomial of system (11) is:

$$H_3 = \begin{pmatrix} -\alpha & 1 & 0 \\ \frac{13}{10} & \frac{7}{10} & -\alpha \\ 0 & 0 & \frac{13}{10} \end{pmatrix}$$

The principal diagonal minors are $\Delta_1 = -\alpha,\ \Delta_2 = \frac{-1}{10}(7\alpha + 13)$ and $\Delta_3 = \frac{-13}{100}(7\alpha + 13)$.

Proposition 1.

I) The equilibrium point E_0 is locally asymptotically stable if and only if $\alpha < \frac{-13}{7}$.

II) The equilibrium point E_0 is unstable if and only if $\alpha > \frac{-13}{7}$.

Proof:

I) Suppose that E_0 is locally asymptotically stable, then equation (12) has no roots with positive real parts [13]. Since $D = \frac{-13}{10} \neq 0$ and $TK + D = 0$ if and only if $\alpha = \frac{-13}{7}$, then equation (12) has no zero roots and has no pure imaginary roots for $\alpha \neq \frac{-13}{7}$, respectively. From above we can obtain that, equation (12) has no roots with zero real parts. Thus, equation (12) has all roots with negative real part when $\alpha \neq \frac{-13}{7}$, then $\Delta_1 > 0,\ \Delta_2 > 0$, and $\Delta_3 > 0$. Therefore $\alpha < \frac{-13}{7}$, is obtained.

Conversely, suppose that $\alpha < \frac{-13}{7}$, this implies that $-\alpha > 0,\ \frac{-1}{10}(7\alpha + 13) > 0$, and $\frac{-13}{100}(7\alpha + 13) > 0$, then $\Delta_1 > 0,\ \Delta_2 > 0$, and $\Delta_3 > 0$. Thus, by Routh-Hurwitz's theorem all roots of equation (12) have negative real parts [14]**.** Therefore, E_0 is locally asymptotically stable (see Fig.1a).

II) Suppose that E_0 is unstable, then at least one roots of equation (12) has positive real part [15]. When $\alpha \not> \frac{-13}{7}$, then $\alpha = \frac{-13}{7}$ or $\alpha < \frac{-13}{7}$.

- If $\alpha = \frac{-13}{7}$, then the roots of equation (12) are $\lambda_1 = \frac{-13}{7}$ and $\lambda_{2,3} = \pm\frac{\sqrt{70}}{10}i$ and non of them are positive, which is contradiction.

Proceeding of 3rd International Conference of Mathematics and its Applications TICMA2022
https://conferences.su.edu.krd/su/ticma2022/
DOI: https://doi.org/10.31972/ticma2022

- If $\alpha < \frac{-13}{7}$, then by Proposition 1(I), E_0 is locally asymptotically stable, which is contradiction.

Therefore $\alpha > \frac{-13}{7}$ (see Fig.1b).

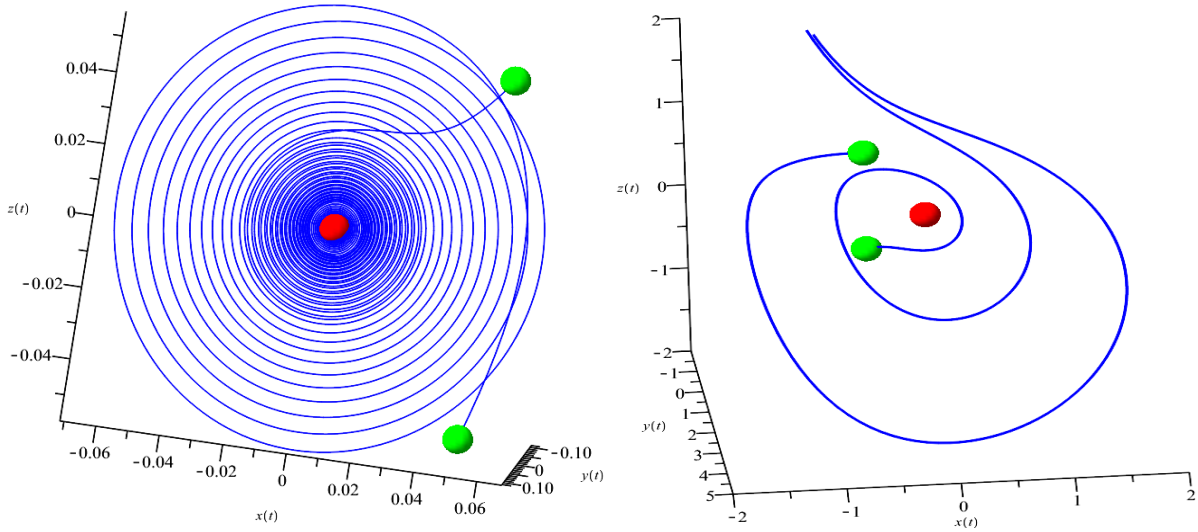

(a) (b)

FIGURE 1. The phase portrait for system (11). (a) when $\alpha = -2$ & $\beta = 1$, E_0 is asymptotically stable. (b) when $\alpha = 2$ & $\beta = 1$, E_0 is unstable. The green and red balls indicate the initial and equilibrium points, respectively.

Conversely, suppose that $\alpha > \frac{-13}{7}$. Since D and $TK + D$ are not equal to zero, then equation (12) has no roots with zero real parts.

The roots of equation (12) are $\lambda_1 = \frac{\Omega_1}{30} - \frac{30\,\Omega_2}{\Omega_1} + \frac{\alpha}{3}$ and $\lambda_{2,3} = \left(-\frac{\Omega_1}{60} + \frac{15\,\Omega_2}{\Omega_1} + \frac{\alpha}{3}\right) \pm i\sqrt{3}\left(\frac{\Omega_1}{60} + \frac{15\,\Omega_2}{\Omega_1}\right)$.Where $\Omega_1 = \sqrt[3]{1000\,\alpha^2 - 3150\,\alpha - 17550 + 30\sqrt{\Omega_3}}$, $\Omega_2 = \frac{7}{30} - \frac{\alpha^2}{9}$ and $\Omega_3 = -3900\,\alpha^3 - 3675\,\alpha^2 + +122850\,\alpha + 352515$.

- When $\Omega_3 > 0$, then the values of $\lambda_1 = \frac{\Omega_1}{30} - \frac{30\,\Omega_2}{\Omega_1} + \frac{\alpha}{3}$ is positive, therefore E_0 is unstable (see Fig. 2 and Figure. 3a).
- When $\Omega_3 = 0$, then the values of $\lambda_1 = \frac{\sqrt[3]{1000\,\alpha^2 - 3150\,\alpha - 17550}}{30} - \frac{30\left(\frac{7}{30} - \frac{\alpha^2}{9}\right)}{\sqrt[3]{1000\,\alpha^2 - 3150\,\alpha - 17550}}$ and it is positive at the value of vanishing Ω_3, in this case $\lambda_1 \approx 2.240$, therefore E_0 is unstable.
- When $\Omega_3 < 0$, then the real part of λ_1 is positive. Thus, E_0 is unstable (see Fig. 2 and Fig. 3b). ■

Proceeding of 3rd International Conference of Mathematics and its Applications TICMA2022
https://conferences.su.edu.krd/su/ticma2022/
DOI: https://doi.org/10.31972/ticma2022

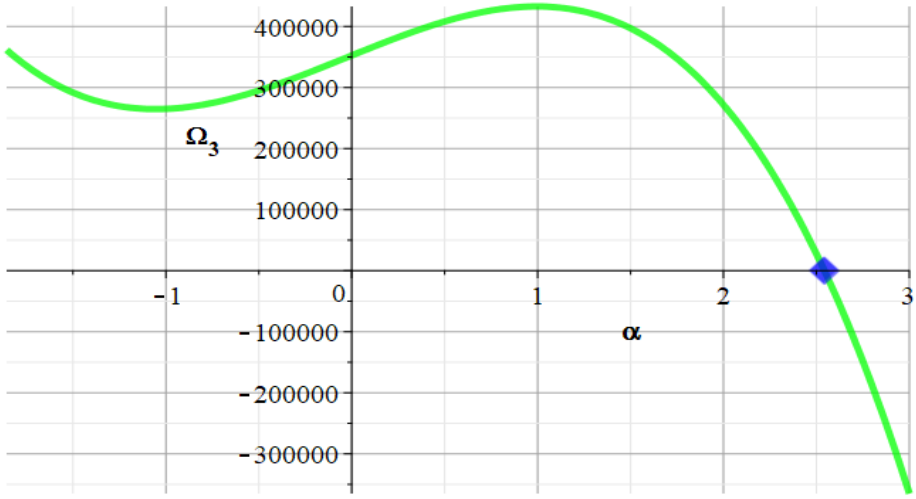

FIGURE 2: The plot of Ω_3, it is positive when $\alpha < 2.5427$, zero at $\alpha = 2.5427$ and negative when $\alpha > 2.5427$, approximately.

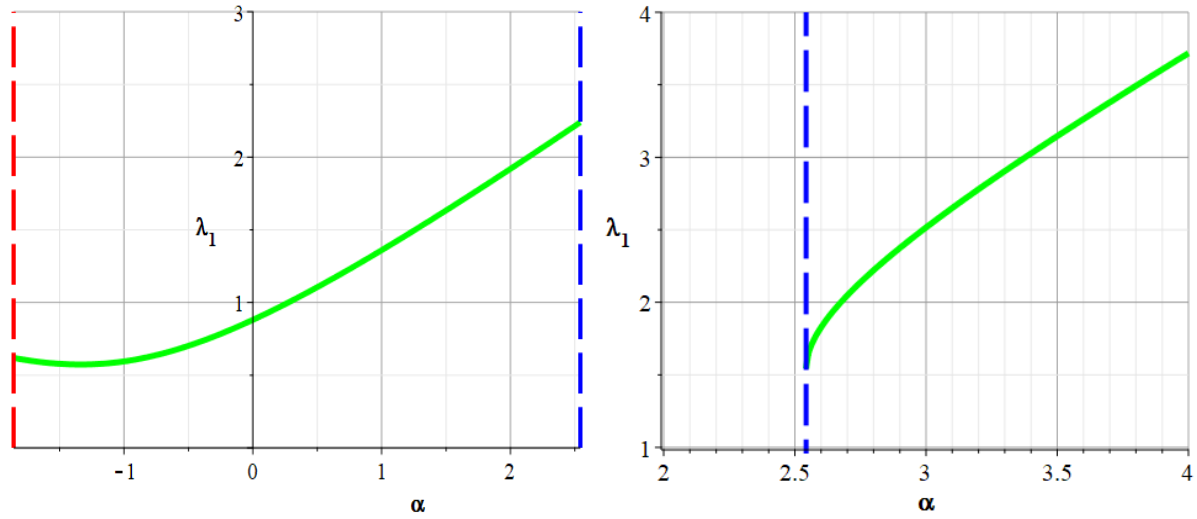

(a) (b)

FIGURE 3. (a) The plot of eigenvalue λ_1 when $\Omega_3 > 0$ which is indicted in a green colour. (b) The plot of real part of λ_1 when $\Omega_3 < 0$, shown in a green colour. The red dash line is the value of $\alpha = -\frac{13}{7}$ and the blue dash lines indicates the value of α which vanishes Ω_3.

3. HOPF BIFURCATION ANALYSIS AND LIMIT CYCLES:

In this section, the occurrence of Hopf bifurcation and bifurcated Limit cycles of system (11) are studied.

Proposition 2. Equation (12) has two pure imaginaries with non-zero eigenvalues if and only if $\alpha = \frac{-13}{7}$. In this case the solutions of equation (12) are $\lambda_1 = -\frac{13}{7}$, $\lambda_{2,3} = \pm i\omega$ where $\omega = \frac{\sqrt{70}}{10}$.

Proof: Suppose that equation (12) has two pure imaginaries with non-zero eigenvalues. Then conditions (3) are satisfied.

From equation (12), $T = \alpha \neq 0, K = \frac{-7}{10} < 0$, $D = \frac{-13}{10} \neq 0$ and $TK + D = \frac{-7}{10}\alpha - \frac{13}{10} = 0$ at $\alpha = \frac{-13}{7}$. Therefore, $\alpha = \frac{-13}{7}$.

Proceeding of 3rd International Conference of Mathematics and its Applications
TICMA2022
https://conferences.su.edu.krd/su/ticma2022/
DOI: https://doi.org/10.31972/ticma2022

Conversely, suppose that $\alpha = \frac{-13}{7}$. Let λ_1 be the real solution and $\lambda_{2,3} = \pm i\omega$ be complex solutions of equation (12).

$$\lambda_1 + \lambda_2 + \lambda_3 = T \implies \lambda_1 = \frac{-13}{7} \quad \text{and} \quad \lambda_1.\lambda_2.\lambda_3 = D \implies \omega = \frac{\sqrt{70}}{10}.$$

Therefore, equation (12) has two pure imaginaries with nonzero eigenvalues (see Fig. 4). ■

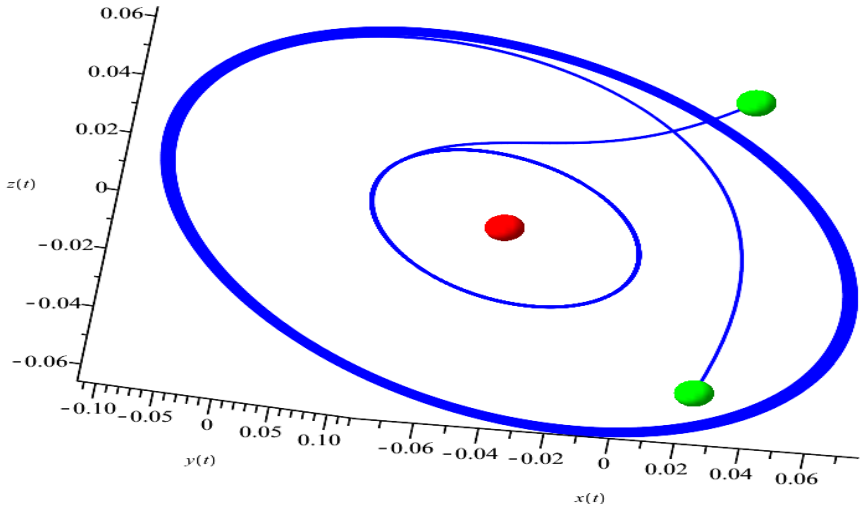

FIGURE 4: The phase portrait for system (11) when $\alpha = \frac{-13}{7}$ & $\beta = 1$, the green and red balls indicate the initial and equilibrium points, respectively.

So, the first Hopf bifurcation theorem condition is fulfilled [4].
Nevertheless, a second condition of the Hopf bifurcation theorem must be fulfilled. In the simple way:

$$\frac{d}{d\alpha} Re\left(\lambda_{2,3}(\alpha)\right) \neq 0,$$

where $Re\left(\lambda_{2,3}(\alpha)\right)$ is the real part of $\lambda_{2,3}$ which is a smooth function of α.

Proposition 3. The derivative of the real part of complex solution of the equation (12) with respect to α at $\alpha = \frac{-13}{7}$ is non-zero and equal to $\frac{343}{4066}$, i.e., $\frac{d}{d\alpha}(Re(\lambda_{2,3}(\alpha)))\Big|_{\alpha=\frac{-13}{7}} = d = \frac{343}{4066} \neq 0$.

Proof: Since $J(E_0)$ has two pure imaginary eigenvalues where $\alpha = \frac{-13}{7}$, then for α near $\frac{-13}{7}$ two of the eigenvalues will be complex conjugates. Let $\lambda_2 = u + iv, \lambda_3 = \overline{\lambda_2} = u - iv$ and λ_1 be eigenvalues and satisfy the following equation

$$\lambda^3 - (2u + \lambda_1)\lambda^2 + (|\lambda_2|^2 + 2u\,\lambda_1)\lambda - |\lambda_2|^2\lambda_1 = 0 \quad \text{(see [16])}$$

Equating coefficients with equation (12) results are

$$2u + \lambda_1 = \alpha,$$

$$|\lambda_2|^2\,\lambda_1 = \frac{-13}{10},$$

$$|\lambda_2|^2 + 2u\,\lambda_1 = \frac{7}{10}.$$

https://conferences.su.edu.krd/su/ticma2022/
DOI: https://doi.org/10.31972/ticma2022

Thus,

$$\frac{13}{20\,u-10\,\alpha}+2u\,(\alpha-2u)=\frac{7}{10},$$

implicitly differentiating $u=u(\alpha)$, the following is obtained:

$$u'=\frac{-20\,\alpha^2u+80\,\alpha u^2-80\,u^3-13}{20\,\alpha^3-160\,\alpha^2u+400\,\alpha u^2-320\,u^3-26},$$

at $\alpha=\frac{-13}{7}$ where $Re(\lambda_{2,3})=u=0$, we obtain:

$$u'=d=\frac{343}{4066}>0\,,where\ \alpha=\frac{-13}{7}.$$ ■

So, the second condition of Hopf bifurcation theorem is fulfilled. Therefore, the Hopf bifurcation theorem holds.

Theorem 1. Under the first and second conditions of Hopf Bifurcation.

I) When $\beta>\frac{1}{1274}(204+\sqrt{204506})$ or $\beta<\frac{1}{1274}(204-\sqrt{204506})$, the bifurcated limit cycle is unstable.
II) When $\beta\in(\frac{1}{1274}(204-\sqrt{204506}),\frac{1}{1274}(204+\sqrt{204506}))$, the bifurcated limit cycle is stable.

Proof: At first, we find the expression for the two-dimensional flow in the center manifold W^c at the bifurcation point.

System (11) is transformed into the Canonical form by the following linear transformation.

$$\begin{pmatrix}x\\y\\z\end{pmatrix}=T\begin{pmatrix}u\\v\\w\end{pmatrix},where\quad T=\begin{pmatrix}\frac{13}{20}&1&1\\1&1-\frac{\sqrt{70}}{7}i&1+\frac{\sqrt{70}}{7}i\\\frac{169}{140}&\frac{\sqrt{70}}{10}i&\frac{-\sqrt{70}}{10}i\end{pmatrix}$$

After some calculations, the following system is obtained.

$$\begin{pmatrix}\dot{u}\\\dot{v}\\\dot{w}\end{pmatrix}=\begin{pmatrix}\frac{-13}{7}u\\-i\frac{\sqrt{70}}{10}\,v\\i\frac{\sqrt{70}}{10}\,w\end{pmatrix}+\begin{pmatrix}\Phi_1u^2+\Phi_2v^2+\overline{\Phi_2}\,w^2+\Phi_3\,uv+\overline{\Phi_3}\,uw+\Phi_4vw\\\Phi_5\,u^2+\Phi_6v^2+\Phi_7\,w^2+\Phi_8\,uv+\Phi_9\,uw+\Phi_{10}\,vw\\\overline{\Phi_5}\,u^2+\overline{\Phi_7}\,v^2+\overline{\Phi_6}\,w^2+\overline{\Phi_9}\,uv+\overline{\Phi_8}\,uw+\overline{\Phi_{10}}\,vw\end{pmatrix}\qquad(13)$$

where

$\Phi_1=\frac{1}{28462}(28561\,\beta-7098)$

$\Phi_2=\frac{1}{2033}\left[(1400-980\,\beta)-140\sqrt{70}\,i\right]$

$\Phi_3=\frac{1}{2033}\left[130+338\left(\beta-\frac{7}{26}\right)\sqrt{70}\,i\right]$

https://conferences.su.edu.krd/su/ticma2022/
DOI: https://doi.org/10.31972/ticma2022

$$\Phi_4 = \frac{1}{2033}(2800 + 1960\,\beta)$$
$$\Phi_5 = \frac{1}{11384800}\left[\,(922740 - 3712930\,\beta) + (49686 - 199927\,\beta)\sqrt{70}\;i\,\right]$$
$$\Phi_6 = \frac{1}{11384800}\left[\,(1783600\,\beta - 3508400\,) + (96040\,\beta + 117600)\sqrt{70}\;i\,\right]$$
$$\Phi_7 = \frac{1}{11384800}\left[\,(1783600\,\beta - 1587600\,) + (96040\,\beta - 392000)\sqrt{70}\;i\,\right]$$
$$\Phi_8 = \frac{1}{11384800}\left[\,(2318680\,\beta - 860860\,) + (152880 - 615160\,\beta)\sqrt{70}\;i\,\right]$$
$$\Phi_9 = \frac{1}{11384800}\left[\,(387660\; - 2318680\,\beta\,) + (615160\,\beta - 178360)\sqrt{70}\;i\,\right]$$
$$\Phi_{10} = \frac{-1}{11384800}\left[\,(3567200\,\beta + 5096000\,) + (192080\,\beta + 274400)\sqrt{70}\;i\,\right]$$

According to the Center manifold theorem, the center manifold W^c is tangent to $E^c = span\{v, w\}$ at the origin [4]. Therefore, W^c can be approximated for the two variables v, w by the following equation:

$$u = h(v, w) = \sigma_1\, v^2 + \sigma_2\, vw + \sigma_3\, w^2 + O(3) \tag{14}$$

With

$$\dot{u} = \frac{\partial h}{\partial v}\,\dot{v} + \frac{\partial h}{\partial w}\,\dot{w} \tag{15}$$

It follows together with system (13) and equation (15) obtain:

$$\frac{-13}{7}\left(\sigma_1 v^2 + \sigma_2\, vw + \sigma_3\, w^2 + 0(3)\right) + \Phi_1\left(\sigma_1 v^2 + \sigma_2\, vw + \sigma_3\, w^2 + 0(3)\right)^2 + \Phi_2\, v^2 + \overline{\Phi_2}\, w^2 + \Phi_3\left(\sigma_1\, v^2 + \sigma_2\, vw + \sigma_3\, w^2 + 0(3)\right) v + \overline{\Phi_3}\,(\sigma_1\, v^2 + \sigma_2\, vw + \sigma_3\, w^2 + 0(3))\, w + \Phi_4\, vw = (2\sigma_1\, v + \sigma_2\, w)\left(-i\frac{\sqrt{70}}{10}\, v + \Phi_5\,(\sigma_1\, v^2 + \sigma_2\, vw + \sigma_3\, w^2 + 0(3))^2 + \Phi_6\, v^2 + \Phi_7\, w^2 + \Phi_8\,(\sigma_1\, v^2 + \sigma_2\, vw + \sigma_3\, w^2 + 0(3))\, v + \Phi_9(\sigma_1\, v^2 + \sigma_2\, vw + \sigma_3\, w^2 + 0(3))\, w + \Phi_{10} vw\right) + (\sigma_2\, v + 2\sigma_3\, w)\left(i\frac{\sqrt{70}}{10}\, w + \overline{\Phi_5}\,(\sigma_1\, v^2 + \sigma_2\, vw + \sigma_3\, w^2 + 0(3))^2 + \overline{\Phi_7}\, v^2 + \overline{\Phi_6}\, w^2 + \overline{\Phi_9}\,(\sigma_1\, v^2 + \sigma_2\, vw + \sigma_3\, w^2 + 0(3))\, v + \overline{\Phi_8}\,(\sigma_1\, v^2 + \sigma_2\, vw + \sigma_3\, w^2 + 0(3))w + \overline{\Phi_{10}}\, vw\right) \tag{16}$$

After comparison of the coefficient for $v^2, vw, and\ w^2$ in equation (16), one can find expressions for $\sigma_1, \sigma_2\ and\ \sigma_3$.

$$\sigma_1 = \frac{1}{3112523}\left[(1117200 - 445900\,\beta) - i\left(63700\sqrt{70} + \frac{7\sqrt{70}}{5}(34300\,\beta - 49000)\right)\right]$$
$$\sigma_2 = \frac{1}{26429}\,(13720\,\beta + 19600)$$
$$\sigma_3 = \frac{1}{3112523}\left[(1117200 - 445900\,\beta) + i\left(63700\sqrt{70} + \frac{7\sqrt{70}}{5}(34300\,\beta - 49000)\right)\right]$$

We substitute the values of σ_1, σ_2 and σ_3 in equation (3.2) and obtain:

$$u = \frac{1}{3112523}\left[(1117200 - 445900\,\beta) - i\,(63700\sqrt{70} + \frac{7\sqrt{70}}{5}(34300\,\beta - 49000)\,)\right] v^2$$

Proceeding of 3rd International Conference of Mathematics and its Applications TICMA2022
https://conferences.su.edu.krd/su/ticma2022/
DOI: https://doi.org/10.31972/ticma2022

$$+\frac{1}{26429}\,(13720\,\beta+19600)\,vw+\frac{1}{3112523}[(1117200-445900\,\beta)+i\,(63700\sqrt{70}$$
$$+\tfrac{7\sqrt{70}}{5}(34300\,\beta-49000)\,)]\,w^2.$$

After inserting the value of u into the equations for v, w in equation (13), an approximated expression for the flow in the centre manifold is obtained:

$$\begin{pmatrix}\dot{v}\\ \\ \dot{w}\end{pmatrix}=\begin{pmatrix}-i\frac{\sqrt{70}}{10}\,v\\ \\ i\frac{\sqrt{70}}{10}\,w\end{pmatrix}+\begin{pmatrix}\Psi_1\,v^2+\Psi_2\,vw+\Psi_3\,w^2\\ \\ \overline{\Psi_3}\,v^2+\overline{\Psi_2}\,vw+\overline{\Psi_1}\,w^2\end{pmatrix}+O(3) \qquad (17)$$

Where

$$\Psi_1=\frac{7}{40660}\left[\,(910\,\beta-1790)+i\,(49\,\beta+60)\,\sqrt{70}\,\right]$$
$$\Psi_2=\frac{-7}{20330}\left[\,(910\,\beta+1300)+i\,(49\,\beta+70)\,\sqrt{70}\,\right]$$
$$\Psi_3=\frac{7}{40660}\left[\,(910\,\beta-810)+i\,(49\,\beta-200)\,\sqrt{70}\,\right]$$

By removing all the redundant non-linear terms of equation (17), the simplified expression for the flow in the centre manifold is obtained. The simplest expression is called the normal form which still contains all information about the qualitative behavior of the system at the bifurcation point. With a further linear coordinate transformation, system (17) can be rewritten into a form which is called standard form.

With

$$\begin{pmatrix}v\\ \\ w\end{pmatrix}=T\begin{pmatrix}\mathrm{p}\\ \\ \mathrm{q}\end{pmatrix},\ where\ T=\begin{pmatrix}1 & -i\\ \\ 1 & i\end{pmatrix}$$

After some calculations, the following system is obtained.

$$\begin{pmatrix}\dot{p}\\ \\ \dot{q}\end{pmatrix}=\begin{pmatrix}-\frac{\sqrt{70}}{10}\,q\\ \\ \frac{\sqrt{70}}{10}\,p\end{pmatrix}+\begin{pmatrix}f(p,q)\\ \\ g(p,q)\end{pmatrix} \qquad (18)$$

where

$$f(p,q)=\varphi_1\,p^2-\frac{\sqrt{70}}{10}\varphi_1\,pq+\varphi_2\,q^2+\varphi_3\,p^3+\sqrt{70}\,\varphi_4\;\,p^2q+\varphi_5\,pq^2+\sqrt{70}\,\varphi_6\,q^3+\varphi_7\,p^4+$$
$$\sqrt{70}\,\varphi_8\,p^3q+\;\varphi_9\,p^2q^2+\sqrt{70}\,\varphi_{10}\,p\,q^3+\;\varphi_{11}\,q^4.$$

$$g(p,q)=\frac{-7\sqrt{70}}{130}\,\varphi_1\,p^2+\frac{49}{130}\,\varphi_1\,pq-\frac{7\sqrt{70}}{130}\varphi_2\,q^2-\frac{7\sqrt{70}}{130}\varphi_3\,p^3-\frac{49}{13}\,\varphi_4\,p^2q-\frac{7\sqrt{70}}{130}\varphi_5\,pq^2-\frac{49}{13}\,\varphi_6\,q^3-$$
$$\frac{7\sqrt{70}}{130}\,\varphi_7\,p^4-\frac{49}{13}\,\varphi_8\,p^3q+\frac{7\sqrt{70}}{130}\,\varphi_9\,p^2q^2-\frac{49}{13}\,\varphi_{10}\,p\,q^3-\frac{7\sqrt{70}}{130}\,\varphi_{11}\,q^4,$$

where

$$\varphi_1=\frac{-1820}{2033}$$

DOI: https://doi.org/10.31972/ticma2022

$$\varphi_2 = \frac{-1274}{2033}\,\beta$$
$$\varphi_3 = \frac{-25480}{6327759259}\,(2401\,\beta + 15065)$$
$$\varphi_4 = \frac{-2548}{6327759259}\,(62426\,\beta^2 + 368513\,\beta - 104805)$$
$$\varphi_5 = \frac{178360}{6327759259}\,(16562\,\beta^2 - 7337\,\beta + 420)$$
$$\varphi_6 = \frac{-17836}{6327759259}\,(35 + 1188\,\beta)(26\,\beta - 7)$$
$$\varphi_7 = \frac{-356720}{19695296232100457}(2401\,\beta + 15065)^2(169\,\beta - 42)$$
$$\varphi_8 = \frac{9274720}{19695296232100457}\,(2401\,\beta + 15065)(49\,\beta - 5)(169\,\beta - 42)$$
$$\varphi_9 = \frac{4994080}{19695296232100457}\,(169\,\beta - 42)\,(4881233\,\beta^2 + 17567205\,\beta + 548400)$$
$$\varphi_{10} = \frac{64923040}{19695296232100457}\,(35 + 1188\,\beta)(49\,\beta - 5)(169\,\beta - 42)$$
$$\varphi_{11} = \frac{-17479280}{19695296232100457}\,(35 + 1188\,\beta)^2(169\,\beta - 42)$$

In [4], a nonlinear coordinate transformation is presented to transform every system with the following system

$$\begin{pmatrix}\dot{p}\\ \\ \dot{q}\end{pmatrix} = \begin{pmatrix}-\omega\, q\\ \\ \omega\, p\end{pmatrix} + \begin{pmatrix}O(|p|,|q|)\\ \\ O(|p|,|q|)\end{pmatrix} \tag{19}$$

Into the system:

$$\begin{pmatrix}\dot{u}\\ \\ \dot{v}\end{pmatrix} = \begin{pmatrix}-\omega\, v\\ \\ \omega\, u\end{pmatrix} + \begin{pmatrix}(au - bv)(u^2 + v^2) + O(4)\\ \\ (au + bv)(u^2 + v^2) + O(4)\end{pmatrix} \tag{20}$$

This is expressed in polar coordinates as:

$$\begin{pmatrix}\dot{r}\\ \\ \dot{\theta}\end{pmatrix} = \begin{pmatrix}a\, r^3\\ \\ \omega + b\, r^2\end{pmatrix} \tag{21}$$

At the Hopf bifurcation point, the sign of "a" determining the stability of the equilibrium point, where

$$a = \frac{1}{16}\left[f_{ppp} + f_{pqq} + g_{ppq} + g_{qqq} + \frac{1}{\omega}\left(f_{pq}(f_{pp} + f_{qq}) - g_{pq}(g_{pp} + g_{qq}) - f_{pp}\, g_{pp} + f_{qq}\, g_{qq}\right)\right] \tag{22}$$

f_{pq} denotes $\frac{\partial^2 f(0,0)}{\partial p \partial q}$,etc. and f, g are the functions containing the nonlinear terms of equation (19). Applying equation (22) to expression (18) which has structure of (19) to obtain:

DOI: https://doi.org/10.31972/ticma2022

$$a = \frac{1}{3112523}(436982\,\beta^2 - 139944\,\beta - 43855)$$

Fig. 5 describes the values of a and the following is obtained.

- When $\beta > \frac{1}{1274}\left(204 + \sqrt{204506}\right)$ or $\beta < \frac{1}{1274}(204 - \sqrt{204506})$, then a is positive i.e. the bifurcated limit cycle is unstable and the type of Hopf bifurcation is Subcritical Hopf bifurcation.
- When $\beta \in (\frac{1}{1274}(204 - \sqrt{204506}), \frac{1}{1274}(204 + \sqrt{204506}))$, then a is negative i.e. the bifurcated limit cycle is stable and the type of Hopf bifurcation is supercritical Hopf bifurcation. ■

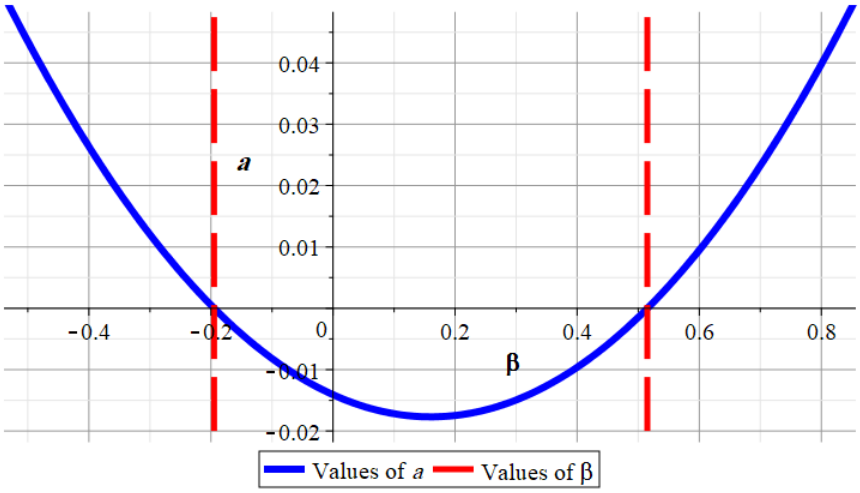

FIGURE 5: The plot of value $a = \frac{1}{3112523}(436982\,\beta^2 - 139944\,\beta - 43855)$ and the roots of a is $\beta = \frac{102}{637} \pm \frac{\sqrt{204506}}{1274}$.

4. MULTIPLE OF HOPF BIFURCATION:

The bifurcation of several limit cycles from a focus is related with the stability of the focus. Andronov have assigned a set of numbers $\eta_2, \eta_4, \eta_6, \ldots$ which they call focal values. The stability of the focus is determined by the sign of the first nonvanishing focal value. Furthermore, the number of limit cycles which may bifurcated from the focus is obtained by the number of vanishing $\eta_i\,(i = 2,4,6,\ldots)$ simultaneously [8]. For more information about this topic, the reader can refer to [17],[18], [19] and [20].

Theorem 2. When $\beta = \frac{1}{1274}(204 \pm \sqrt{204506})$, then at most two limit cycles can be bifurcated from the origin.

Proof: At first, system (11) transforms into the Canonical form by the following linear transformation.

$$\begin{pmatrix} x \\ y \\ z \end{pmatrix} = T \begin{pmatrix} u \\ v \\ w \end{pmatrix}, where \quad T = \begin{pmatrix} -\frac{\sqrt{70}}{7} & 1 & \frac{13}{20} \\ 0 & \frac{17}{7} & 1 \\ -\frac{\sqrt{70}}{10} & -1 & \frac{169}{140} \end{pmatrix}$$

After some calculations, the following system is obtained.

https://conferences.su.edu.krd/su/ticma2022/
DOI: https://doi.org/10.31972/ticma2022

$$\begin{pmatrix} \dot{u} \\ \dot{v} \\ \dot{w} \end{pmatrix} = \begin{pmatrix} -\frac{\sqrt{70}}{10}\, v \\ \frac{\sqrt{70}}{10}\, u \\ -\frac{13}{7}\, w \end{pmatrix} + \begin{pmatrix} \frac{567}{\sqrt{70}}\vartheta_1\, u^2 + 567\sqrt{70}\ \vartheta_2\, v^2 - 13689\sqrt{70}\,\vartheta_3\, w^2 - 39690\,\vartheta_4\, uv + 13689\,\vartheta_5\, uw + \frac{567}{\sqrt{70}}\,\vartheta_6\, vw \\ -140\,\vartheta_1\, u^2 - 9800\,\vartheta_2\, v^2 + 236600\,\vartheta_3\, w^2 + 140\sqrt{70}\,\vartheta_4\, uv - 338\sqrt{70}\,\vartheta_5\, uw - 140\,\vartheta_6\, vw \\ 340\,\vartheta_1\, u^2 + 23800\,\vartheta_2\, v^2 - \vartheta_3\, w^2 - 340\sqrt{70}\ \vartheta_4\, uv + \frac{57460\sqrt{70}}{7}\vartheta_5\, uw + 340\,\vartheta_6\, vw \end{pmatrix} \quad (23)$$

where

$$\vartheta_1 = \frac{1}{34561}\,(30 + 49\,\beta)$$
$$\vartheta_2 = \frac{1}{34561}\,(2 + \beta)$$
$$\vartheta_3 = \frac{1}{96770800}\,(42 - 169\,\beta)$$
$$\vartheta_4 = \frac{1}{34561}\,(23 - 14\,\beta)$$
$$\vartheta_5 = \frac{1}{691220}\,(3 - 14\,\beta)$$
$$\vartheta_6 = \frac{567}{34561\sqrt{70}}\,(52 - 169\,\beta)$$

We introduce the following Lyapunov function

$$V(u,v,w) = u^2 + v^2 + \sum_{k=3}^{n}\sum_{j=0}^{k}\sum_{i=0}^{j} C_{i,j-i,k-j}\ u^i\ v^{j-i}\ w^{k-j} \quad (24)$$

satisfying the following equation

$$\chi(V) = \eta_2\, r^2 + \eta_4\, r^4 + \eta_6\, r^6 + \cdots + \eta_{2i}\, r^{2i} \quad (25)$$

where $r^2 = u^2 + v^2$ and χ is the vector field of system (23). By solving equation (25) and using computer algebra MAPLE, we obtain:

$\eta_2 = 0$,

$\eta_4 = \frac{1}{6225046}(1061242\ \beta^2 - 339864\,\beta\ - 106505)$,

$\eta_6 = \frac{1}{1726726011260711266104}(\,78631416434808830320\,\beta^4 - 74879873077254304750 6\,\beta^3$
$- 99601093143458465694 8\,\beta^2 + 42719147266851158176 5\,\beta$
$+113442500988872872250)$.

Since $\eta_4 = 0$ if and only if $\beta = \frac{1}{1274}\left(204 \pm \sqrt{204506}\right)$. Therefore at $\beta = \frac{1}{1274}\left(204 \pm \sqrt{204506}\right)$, $\eta_4 = 0$, but $\eta_6 = \frac{1}{21728158897809}(-185734059215 \pm 356475635\sqrt{204506})$ non equal zero.

Since $\eta_2 = \eta_4 = 0$ when $\beta = \frac{1}{1274}\left(204 \pm \sqrt{204506}\right)$, then at most two limit cycles can be bifurcated from the origin.

■

5. CONCLUSIONS:

In this paper, system (11) has been investigated. The local stability and the existence of the Hopf bifurcation are studied, in addition to the direction and stability of the bifurcating periodic solutions. It was shown that the origin of system (11) is asymptotically stable and unstable when $\alpha < \frac{-13}{7}$ and $\alpha > \frac{-13}{7}$, respectively. it was proved that the bifurcated limit cycle at the bifurcation value, $\alpha = \frac{-13}{7}$, is unstable and the type of Hopf bifurcation is subcritical Hopf bifurcation when $\beta > \frac{1}{1274}\left(204 + \sqrt{204506}\right)$ or $\beta <$

DOI: https://doi.org/10.31972/ticma2022

$\frac{1}{1274}(204 - \sqrt{204506})$ and it is stable and the type of Hopf bifurcation is supercritical Hopf bifurcation when $\beta \in (\frac{1}{1274}(204 - \sqrt{204506}), \frac{1}{1274}(204 + \sqrt{204506}))$. Furthermore, it was also verified that at most two limit cycles can be bifurcated from the origin when $\beta = \frac{1}{1274}(204 \pm \sqrt{204506})$.

REFERENCES:

[1] Salih, R. and Hasso, M. 2017. Centre bifurcations of periodic orbits for some special three dimensional systems. *Electronic Journal of Qualitative Theory of Differential Equations*, 2017(19), 1-10.
[2] Salih, R.H., 2015. Hopf bifurcation and centre bifurcation in three dimensional Lotka-Volterra systems.
[3] Liu, W.M. 1994. Criterion of Hopf bifurcations without using eigenvalues. *Journal of Mathematical Analysis and Applications*, 182(1), 250-256.
[4] Guckenheimer, J. and Holmes, P., 2013. *Nonlinear oscillations, dynamical systems, and bifurcations of vector fields* (Vol. 42). Springer Science & Business Media.
[5] Lynch, S., 2009. *Dynamical systems with applications using MapleTM*. Springer Science & Business Media.
[6] Marsden, J.E. and McCracken, M., 2012. *The Hopf bifurcation and its applications* (Vol. 19). Springer Science & Business Media.
[7] Carr, J., 2012. *Applications of centre manifold theory* (Vol. 35). Springer Science & Business Media.
[8] Andronov, A.A., 1971. *Theory of bifurcations of dynamic systems on a plane*. Israel Program for Scientific Translations;[available from the US Department of Commerce, National Technical Information Service, Springfield, Va.].
[9] Wang, D., 1991. Mechanical manipulation for a class of differential systems. *Journal of symbolic computation*, *12*(2), pp.233-254.
[10] Lu, Z. and Luo, Y.O.N.G., 2002. Two limit cycles in three-dimensional Lotka-Volterra systems. *Computers & Mathematics with Applications*, *44*(1-2), pp.51-66.
[11] Lao, S.K., Shekofteh, Y., Jafari, S. and Sprott, J.C., 2014. Cost function based on Gaussian mixture model for parameter estimation of a chaotic circuit with a hidden attractor. *International Journal of Bifurcation and Chaos*, *24*(01), p.1450010.
[12] Muhammed S. F., 2020. *Darboux and Analytic First Integrals of a Family of a Chaotic Three Dimensional Differential Systems*, MSc. Thesis, Salahaddin University-Erbil.
[13] Pushpavanam, S., 1998. *Mathematical methods in chemical engineering*. PHI Learning Pvt. Ltd.
[14] Arrowsmith, D.K. and Place, C.M., 1982. *Ordinary Differential Equations: A qualitative approach with applications* (No. 517.38 A7).
[15] Rao, M.R.M., 1980. Ordinary differential equations, Theory and Applications, East.
[16] Merrill, S.J., 1978. A model of the stimulation of B-cells by replicating antigen—II. *Mathematical Biosciences*, *41*(1-2), pp.143-156.
[17] Buică, A., García, I.A. and Maza, S. 2012. Existence of inverse Jacobi multipliers around Hopf points in R3: emphasis on the center problem. *Journal of Differential Equations*, *252*(12), 6324-6336.
[18] Göbber, F. and Willamowski, K.D., 1979. Ljapunov approach to multiple Hopf bifurcation. *Journal of mathematical analysis and applications*, 71(2), 333-350.
[19] Lestandi, L., Bhaumik, S., Avatar, G.R.K.C., Azaiez, M. and Sengupta, T.K., 2018. Multiple Hopf bifurcations and flow dynamics inside a 2D singular lid driven cavity. *Computers & Fluids*, 166, 86-103.
[20] Rionero, S., 2019. Hopf bifurcations in dynamical systems. *Ricerche di Matematica*, 68(2), 811-840

Proceeding of 3rd International Conference of Mathematics and its Applications TICMA2022
https://conferences.su.edu.krd/su/ticma2022/
DOI: https://doi.org/10.31972/ticma2022

RESEARCH PAPER

ω_p-Open and ω_p-Closed Functions

Halgwrd Mohammed Darwesh[1, a] And Shagull Hossein Mahmood[2, b,*]
[1,2] *Department of Mathematics, College of Science, University of Sulaimani, 46001 Sulaimani, Kurdistan Region, Iraq*

[a]*halgwrd.darwesh@univsul.edu.iq*
[b]*shagull.mahmmod@univsul.edu.iq*

A B S T R A C T: In this *work*, we study and define two new concepts of functions named ω_p-open and $\omega_p-closed$ functions by using the concepts of $\omega_p - open$ and $\omega_p -closed$ sets. The concept of $\omega_p - open$ function strictly located between both the concepts of $open$ and $preopen$ functions. We obtain a few properties of these functions, however, the connections between them are examined.

KEYWORDS: ω_p-$closed$ set, ω_p-$open$ set, ω_p-$continuous$ $function$, $\omega_p - closed$ $function$, ω_p-open function.
DOI: https://doi.org/10.31972/ticma22.12

1. INTRODUCTION:

In 1963, Levine [2] defined a new class of $open$ sets called semi-$open$ sets, also he introduced a new class of functions named $semi$-$continuous$ and semi-$open$ functions in the space of topology. Mashhour et al. [3] presented pre-$continuous$, $weak\ pre$-$continuous$ and pre-$open$ functions. The concepts of $\alpha-continuous$ and α-$open$ functions are investigated and defined by Mashhour et al. [4].

Abd El-Monsef et el. [5] represented a new class of sets called $\beta - open$ sets, and they described β-$continuous$ and β-$open$ functions. The notion of the γ-$open$ function is investigated by El-Atik [6]. However, Raychaudhuri and Mukherjee [7] defined $\delta-preopen$ sets, also they present $\delta-almost$ $continuous$ and δ-$preopen$ functions.

The purpose of the $paper$ is, we apply the notions of ω_p-open and $\omega_p-closed$ set to describe the new types of functions denoted by $\omega_p - open$ and $\omega_p - closed$ functions. In addition, the basic properties and the relation between these functions are presented.

2. PRELIMINARIES

All through the present paper (X, τ) and $(Y, \Im)$ express the $spaces$ of $topology$ on which no $separation$ axioms are considered otherwise is clarified, also Fun means function. If $\mathcal{D} \subseteq$ X, then the $interior$ (resp. $\omega - interior, \delta - interior, \omega_p - interior$) of $\mathcal{D}$ is the union of all $open$ (resp. $\omega - open, \delta - open, \omega p - open$) sets in X contained in $\mathcal{D}$ represented by $Int(\mathcal{D})$ (resp. $\omega Int(\mathcal{D})$, $Int_\delta(\mathcal{D})$, $\omega_p Int(D)$. The $closure$ (resp. $\omega - closure, \delta - closure, \omega_p - closure$) of $\mathcal{D}$ is the $intersection$ of all $closed$ (resp. $\omega - closed$, $\delta - closed, \omega_p - closed$) sets of X containing $\mathcal{D}$. A subset $\mathcal{D}$ in X is called $semi - open$ [2] (resp. $regular - open$ [8], $preopen$ [3], $\alpha-open$ [9], $\beta - open$, [5], $\gamma - open$ [6], $\delta-preopen$ [7], $\omega_p - open$ [1]) if $\mathcal{D} \subseteq Cl(Int(\mathcal{D}))$ (resp. $\mathcal{D} = Int(Cl(\mathcal{D}))$, $\mathcal{D} \subseteq Int(Cl(\mathcal{D}))$, $\mathcal{D} \subseteq Int(Cl(Int(\mathcal{D})))$, $\mathcal{D} \subseteq Cl(Int(Cl(\mathcal{D})))$, $\mathcal{D} \subseteq Int(Cl(\mathcal{D})) \cup Cl(Int(\mathcal{D}))$, $G \subseteq Int(Cl_\delta(\mathcal{D}))$, $\mathcal{D} \subseteq Int(\omega Cl(\mathcal{D}))$.

*** Corresponding Author: Shagull Hossein Mahmood**
E-mail: shagull.mahmmod@univsul.edu.iq
Article History:
Received: 01/08/2022
Accepted: 15/09/2022
Published: 07/12/2022

DOI: https://doi.org/10.31972/ticma2022

Also, a subset $\mathcal{D}$ of X is called $\delta - open$ [10] if $\mathcal{D}$ is the $union$ of all $regular - open$ subset of X, and a subset $\mathcal{D}$ is called $\omega - open$ [11] if for $each\ x \in A$, $there\ exits$ an $open$ set $\mathcal{U}$ in X containing x such that $\mathcal{U} - D$ is $countable$. The family of all $semi - o$pen (resp. $regular - open$, $preopen$, $\alpha - open$, $\beta - open$, $\gamma - open$, $\delta - open$, $\delta - open$, $\omega - open$, $\omega_p - open$) subsets of X represented by $SO(X)$ (resp. $RO(X)$, $PO(X)$, α-$O(X)$, β-$O(X)$, γ-$O(X)$, δ-$O(X)$, δ-$PO(X)$, $\omega O(X)$, $\omega_p O(X)$). The complement of $semi - open$ (resp. $regular - open$, $preopen$, $\alpha - open$, $\beta - open$, $\gamma - open$, $\delta - preopen$, $\omega - open$, $\omega_p - open$) set is called $semi - closed$ (resp. $regular - closed$, $preclosed$, $\alpha - closed$, $\beta - closed$, $\gamma - closed$, $\delta - preclosed$, $\omega - closed$ $\omega_p - closed$), also their family is represented by $SC(X)$ (resp. $RC(X)$, $PC(X)$, $\alpha - C(X)$, $\beta - C(X)$, $\gamma - C(X)$, $\delta - C(X)$, $\delta - PC(X)$, $\omega C(X)$, $\omega_p C(X)$).

Definition 2.1. Let $\mathfrak{h}: X \to Y$ be a Fun. If $\mathfrak{h}(\mathcal{D})$ is $open$ (resp. $semi - open$, $preopen$, $\alpha - open$, $\beta - open$, $\delta - preopen$, $\gamma - open$) in Y, each $open$ subset $\mathcal{D}$ of X, thus, $\mathfrak{h}$ is called $open$ (resp. $semi - open$ [12], $preopen$ [3], $\alpha - open$ [4], $\beta - open$ [5], $\gamma - open$ [6], $\delta - preopen$ [7]) Fun.

Definition 2.2. Let $\mathfrak{h}: X \to Y$ be a Fun. If $\mathfrak{h}^{-1}(\mathcal{D})$ is $open$ ($\omega_p - open$) in X, each $open$ subset $\mathcal{D}$ of Y, thus, $\mathfrak{h}$ is called $continuous$ [13] ($\omega_p - continuous$ [1]) Fun.

Definition 2.3. ([14]) Let (X, τ) be a $space$ of $topology$. Then, a $space$ X is said to be:
1. $Locally$ $countable$, if each $point$ $x \in X$ has a $countable$ $open$ $neighborhood$.
2. $Submaximal$, if every $preopen$ set is $open$, equivalently if every dense subset of X is $open$ in X.

Lemma 2.4. ([1]) For a set $\mathcal{D}$ in space X, the $followings$ are true:
1. Let $\mathcal{D}$ be an $open$ set. Then it is $\omega_p - open$.
2. Let $\mathcal{D}$ be an $\omega_p - open$. Then it is $pre - open$, $pre - \omega - open$ and $\delta - preopen$.

Theorem 2.5. ([16]) Let (X, τ) be a $locally\ countable\ space$. Then, $\tau^{\omega} = \tau_{dis}$.

Proposition 2.6. ([1]) A subset $\mathcal{D}$ of $space$ X is $\omega_p - open$ ($\omega_p - closed$) $\Leftrightarrow \omega_p Int(\mathcal{D}) = \mathcal{D}$ ($\omega_p Cl(\mathcal{D}) = \mathcal{D}$).

3. MORE PROPERTIES OF ω_p-OPEN SETS

Theorem 3.1. Let (X, τ) be a $locally\ countable\ space$. Then, a set $\mathcal{D}$ in X is $\omega_p - open \Leftrightarrow$ its $open$.
Proof: If $\mathcal{D}$ is an $\omega_p - open$ subset of a $locally\ countable\ space$ X, so $\omega Cl(\mathcal{D}) = \mathcal{D}$, by Theorem 2.5, so $A \subseteq Int(\omega Cl(\mathcal{D})) = Int(\mathcal{D})$. This means that, $\mathcal{D}$ is an $open$ set. Conversely, let $\mathcal{D}$ be an $open$ set in X. Then, $\mathcal{D} = Int(\mathcal{D})$, so $\mathcal{D} \subseteq Int(\omega Cl(\mathcal{D}))$. Hence, $\mathcal{D}\ is$ an $\omega_p - open$ set.

Theorem 3.2. If (X, τ) is a $submaximal\ space$, then a set $\mathcal{D}$ of X is $\omega_p - open \Leftrightarrow$ its $preopen$.
Proof: Let $\mathcal{D}$ be an $\omega_p - open$ set in X. Then, by Lemma 2.4, $\mathcal{D}$ is $preopen$. Conversely, assume $\mathcal{D}$ is a $preopen$ set in $a\ submaximal\ space$ X. Then, $\mathcal{D}$ is $open$. By part (1) of Lemma 2.4, $\mathcal{D}$ is $\omega_p - open$.

$$\int_0^t W^m(t)dW(t) = \frac{1}{m+1}W^{m+1}(t) + \sum_{j=0}^{m-2}(-1)^{j+1}\frac{m!}{2^{j+1}(m-j)!}w^{m-j}(t) + (-1)^m\frac{m!}{2^m}\frac{t}{2} \quad (8)$$

Proceeding of 3rd International Conference of Mathematics and its Applications TICMA2022
https://conferences.su.edu.krd/su/ticma2022/
DOI: https://doi.org/10.31972/ticma2022

4.ω_p-Open Functions

Definition 4.1. A Fun $\mathfrak{h}: X \longrightarrow Y$ is $said\ to$ be $\omega_p - open$, if the $image$ of $each\ open$ set in X is $\omega_p - open$ in Y.

Theorem 4.2. Let $\mathfrak{h}: X \longrightarrow Y$ be a Fun. Then, $\mathfrak{h}$ is an $\omega_p - open \Leftrightarrow$ for $each\ x \in X$ and $each\ open$ set $\mathcal{U}$ in X containing x, there $exists\ an\ \omega_p - open\ set\ \mathcal{V}$ in Y containing $\mathfrak{h}(x)$ such that $\mathcal{V} \subseteq \mathfrak{f}(\mathcal{U})$.

Proof: Suppose $\mathcal{U}$ is an $open$ set in X such that $x \in \mathcal{U}$. Then, $\mathfrak{h}(\mathcal{U})$ is $\omega_p -\ open\ in\ Y$, and $\mathfrak{h}(x) \in \mathfrak{f}\ (\mathcal{U})$. Put $\mathcal{V} = \mathfrak{h}(\mathcal{U})$ is $\omega_p - open$, $\mathfrak{h}(x) \in \mathcal{V}$ and $\mathcal{V} = \mathfrak{h}(\mathcal{U})$. Conversely, let $\mathcal{U}$ be an $open\ set\ in\ X$. To show $\mathfrak{h}$ is $\omega_p - open$. We must show $\mathfrak{h}(\mathcal{U})$ is $\omega_p - open$. If $\mathfrak{h}(\mathcal{U}) = \emptyset$, then its $\omega_p - open$. Otherwise, let $y \in \mathfrak{h}(\mathcal{U})$. Then, there $exists\ x \in \mathcal{U}$ such that $\mathfrak{h}(x) = y$. Since $x \in \mathcal{U}$, so by hypothesis, there $exists$ an $\omega_p - open$ subset $\mathcal{V}$ of X such that $\mathfrak{h}(x) \in \mathcal{V} \subseteq \mathfrak{h}(\mathcal{U})$ that is, $y \in \mathcal{V} \subseteq \mathfrak{h}(\mathcal{U})$. Therefore, $y \in \omega_p Int(\ \mathfrak{h}(\mathcal{U}))$. This implies that, $\mathfrak{h}(\mathcal{U}) = \omega_p Int(\ \mathfrak{h}(\mathcal{U}))$ which by Proposition 2.6, means $\mathfrak{h}(\mathcal{U})$ is $an\ \omega_p - open$ set in Y. Hence $\mathfrak{h}$ is $\omega_p - open$.

Theorem 4.3. The $following$ conditions are $equivalent$ for that Fun $\mathfrak{h}$ from a space X to space Y:

1. $\mathfrak{h}$ is an $\omega p{-}open$;
2. $\mathfrak{h}\ (Int(\mathcal{D})) \subseteq \omega_p Int(\mathfrak{h}(\mathcal{D}))$, for $each\ \mathcal{D} \subseteq X$;
3. $Int(\mathfrak{h}^{-1}(\mathcal{D})) \subseteq \mathfrak{h}^{-1}(\omega_p Int(\mathcal{D}))$, for $each\ \mathcal{D} \subseteq Y$;
4. $\mathfrak{h}^{-1}(\omega_p Cl(\mathcal{D})) \subseteq Cl(\mathfrak{h}^{-1}(\mathcal{D}))$, for $each\ \mathcal{D} \subseteq Y$.

Proof: (1) ⇒ (2) Let $\mathcal{D} \subseteq X$. Then, $Int(\mathcal{D})$ is $open$ in X. By (1), $\mathfrak{h}\ (Int(\mathcal{D}))$ is $\omega_p - open$ in Y, implies that,

$$\omega_p Int(\mathfrak{h}\ (Int(\mathcal{D}))) = \mathfrak{h}\ (Int(\mathcal{D})) \quad (*)$$

$Since$, $\mathfrak{h}\ (Int(\mathcal{D})) \subseteq \mathfrak{h}\ (\mathcal{D})$, then, $\omega_p Int(\mathfrak{h}\ (Int(\mathcal{D}))) \subseteq \omega_p Int(\mathfrak{h}(\mathcal{D}))$, thus by $(*)$, $\mathfrak{h}\ (Int(\mathcal{D})) \subseteq \omega_p Int(\mathfrak{h}\ (\mathcal{D}))$.

(2) ⇒ (3) Suppose $\mathcal{U}\ is\ any\ subset\ of\ Y$. Then, $\mathfrak{h}^{-1}(\mathcal{U}) \subseteq X$, so by (2), $\mathfrak{h}\ (Int(\mathfrak{h}^{-1}(\mathcal{U}))) \subseteq \omega_p Int(\mathfrak{h}\ (^{-1}(\mathcal{U}))) \subseteq \omega_p Int(\mathcal{U})$. Therefore, $Int(\mathfrak{h}^{-1}(\mathcal{U})) \subseteq \mathfrak{h}^{-1}(\omega_p Int(\mathcal{U}))$.

(3) ⇒ (4) Let $\mathcal{U} \subseteq Y$. Then, $Y - \mathcal{U} \subseteq Y$. Thus by (3), $Int(\mathfrak{h}^{-1}(Y - \mathcal{U})) \subseteq \mathfrak{h}^{-1}(\omega_p Int(Y - \mathcal{U}))$. So, $X - Cl(\mathfrak{h}^{-1}(\mathcal{U})) \subseteq X - \mathfrak{h}^{-1}(\omega_p Cl(\mathcal{U}))$. That is, $\mathfrak{h}^{-1}(\omega_p Cl(\mathcal{U})) \subseteq Cl(\mathfrak{h}^{-1}(\mathcal{U}))$.

(4) ⇒ (1) Let $\mathcal{D}$ be an $open$ subset of X. Then, by (3), $Int(\mathfrak{h}^{-1}(\mathfrak{h}\ (\mathcal{D}))) \subseteq \mathfrak{h}^{-1}(\omega_p Int(\mathfrak{h}\ (\mathcal{D})))$. Since $Int(\mathfrak{h}\ (\mathfrak{h}^{-1}(\mathcal{D}))) \subseteq \mathfrak{h}^{-1}(\omega_p Int(\mathfrak{h}\ (\mathcal{D})))$, so $Int(\mathcal{D}) \subseteq Int(\mathfrak{h}^{-1}(\mathfrak{h}\ (\mathcal{D})))$, implies that $Int(\mathcal{D}) \subseteq \mathfrak{h}^{-1}(\omega_p Int(\mathfrak{h}(\mathcal{D})))$, but since $\mathcal{D}$ is $open$, then $\mathcal{D} \subseteq \mathfrak{h}^{-1}(\omega_p Int(\mathfrak{h}\ (\mathcal{D})))$. Thus, $\mathfrak{h}(\mathcal{D}) \subseteq \mathfrak{h}\ (\mathfrak{h}^{-1}(\omega_p Int(\mathfrak{h}(\mathcal{D})))) \subseteq \omega_p Int(\mathfrak{h}(\mathcal{D}))$. Therefore, $\mathfrak{h}(\mathcal{D})$ is $\omega_p{-}open$. Hence, $\mathfrak{h}$ an is $\omega_p - open\ Fun$.

Proceeding of 3rd International Conference of Mathematics and its Applications TICMA2022
https://conferences.su.edu.krd/su/ticma2022/
DOI: https://doi.org/10.31972/ticma2022

Remark 4.4. The *following* implications show the *relationship between* $\omega_p - open\ Fun$ and other types of *open Fun*.

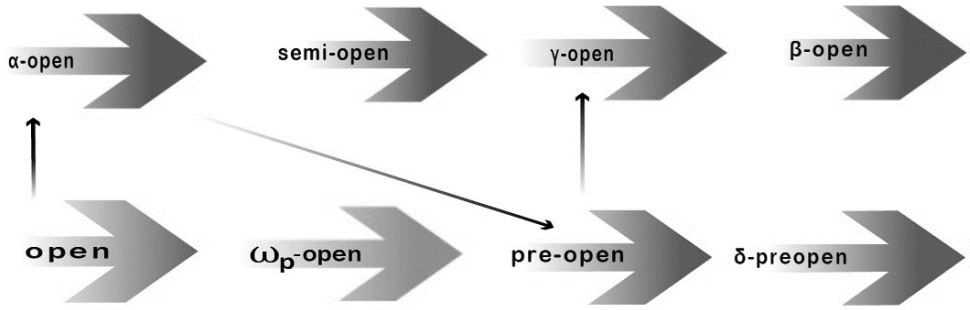

FIGURE 1. *shows the relationship between* $\omega_p - open\ Fun$ *and other types of open Fun*

The f*ollowing* examples show that the converse of the implications in Figure 1 is not *true* in *general*.

Example 4.5. If $X = Y = \{1,2,3\}$, and $\tau = \Im = \{\emptyset, X, \{1\}, \{1,2\}\}$, then the *Fun* $\mathfrak{f} : (X,\tau) \to (Y,\rho)$ is *defined* by, $\mathfrak{f}(1) = 1, \mathfrak{f}(2) = 3$ *and* $\mathfrak{f}(3) = 2$ is *preopen*, but not $\omega_p - open$. Since, $PO(Y) = \{\emptyset, Y, \{1\}, \{1,2\}, \{1,3\}\}$ and $\omega_p O(Y) = \{\emptyset, Y, \{1\}, \{1,2\}\}$. Thus, $\mathfrak{f}(\{1,2\}) = \{1,3\}$ is not $\omega_p - open$ in Y.

Example 4.6. Consider $X = \mathbb{R}$ with the *usual topology* $\Im_u$ and $Y = \mathbb{R}$ *with* the $co - countable\ topology$ τ_{coc}. The *identity Fun* $\iota: (X,\Im_u) \to (Y,\tau_{coc})$ is $\omega_p - open\ but$ not *open*. Since $(0,1)$ is *open* in $(\mathbb{R},\Im_u)$, but $\iota((0,1)) = (0,1)$ is not $(\mathbb{R},\tau_{coc})$, so it is not *open* while for any *open* subset $\mathcal{D}$ of $(\mathbb{R},\Im_u)$, there is an *open* interval (a,b) subset of $\mathcal{D}$, and $\iota(\mathcal{D}) = \mathcal{D} \subseteq \mathbb{R} = Int(Cl((a,b))) = Int(\omega Cl((a,b))) \subseteq Int(\omega Cl(\mathcal{D})) = Int(\omega Cl(\iota(\mathcal{D})))$ which is $\omega_p - open$ in $(\mathbb{R},\tau_{coc})$, hence its $\omega_p - open\ Fun$.

Theorem 4.7. If $\zeta: X \to Y$ is an *open Fun* and $\eta: Y \to Z$ is an $\omega_p - open\ Fun$, then $\eta \circ \zeta$ is an $\omega_p - open$ *Fun*.
Proof: Let $\mathcal{V}$ be an *open* subset of X. Then, by *hypothesis*, $\zeta(\mathcal{V})$ is *open* in Y. Since η is $\omega_p - open$, thus $\eta(\zeta(\mathcal{V}))$ is $\omega_p - open$ in Z. Therefore, $\eta \circ \zeta$ is $\omega_p - open$.

Proposition 4.8. Let $\mathfrak{h}$ be a *Fun* from any space (X,τ) to a *locally countable space* (Y,ρ). Then, $\mathfrak{h}$ is $\omega_p - open \Leftrightarrow$ its *open*.
Proof: Let $\mathfrak{h}$ be an $\omega_p - open\ Fun$. Then, for *each open* set $\mathcal{U}$ in X, thus $\mathfrak{h}(\mathcal{U})$ is $\omega_p - open$ in Y. Since, Y is *locally countable*, thus by *Theorem* 3.1, $\mathfrak{h}(\mathcal{U})$ *open* in Y. Therefore, $\mathfrak{h}$ is *open*. Conversely, *it* follows *from Lemma* 2.4.

Proposition 4.9. Let $\mathfrak{h}$ be a *Fun* from any *space* (X,τ) to a *submaximal space* (Y,ρ). Then, $\mathfrak{h}$ is *preopen* $\Leftrightarrow$ its $\omega_p - open$.
Proof: It follo*ws* from *Proposition* 3.2.

Theorem 4.10. For the *Funs* $\mathfrak{g} : X \to Y$ and $\mathfrak{h} : Y \to Z$, the f*ollowing conditions* are *true*:

1. If $\mathfrak{h} \circ \mathfrak{g}$ is an *open Fun* and $\mathfrak{h}$ is an *injective* $\omega_p - continuous\ Fun$, then $\mathfrak{g}$ is $\omega_p - open$.
2. If $\mathfrak{h} \circ \mathfrak{g}$ is an $\omega_p - open\ Fun$ and $\mathfrak{g}$ is an *surjective continuous Fun*, then $\mathfrak{h}$ is $\omega_p - open$.

Proof:

1. Let $\mathcal{U}$ be any *open* subset of X. Then, by *hypothesis*, $\mathfrak{h}(\mathfrak{g}(\mathcal{U}))$ is *open* in Z. Since $\mathfrak{h}$ is *injective* $\omega_p - continuous$, thus, $\mathfrak{h}^{-1}(\mathfrak{h}(\mathfrak{g}(\mathcal{U}))) = \mathfrak{g}(\mathcal{U})$ is $\omega_p - open$ in Y. Hence, $\mathfrak{g}$ is $\omega_p - open$.

https://conferences.su.edu.krd/su/ticma2022/
DOI: https://doi.org/10.31972/ticma2022

2. Suppose $\mathcal{U}$ is an *open* subset of Y. By *hypothesis*, $\mathfrak{g}^{-1}(\mathcal{U})$ is *open* in X. Since, $\mathfrak{h} \circ \mathfrak{g}$ is $\omega_p - open$, $\mathfrak{h} \circ \mathfrak{g}(\mathfrak{g}^{-1}(\mathcal{U}))$ is $\omega_p - open$ in Z. Since, $\mathfrak{g}$ is *surjective*, so $\mathfrak{h}(\mathcal{U}) = \mathfrak{h}\,(\mathfrak{g}(\mathfrak{g}^{-1}(\mathcal{U})))$. Hence, $\mathfrak{h}$ is an $\omega_p - open\ Fun$.

Theorem 4.11. Let $\mathfrak{h} : X \to Y$ be an $\omega_p - open\ Fun$. If $\mathcal{K}$ is an *open subspace* of X, then the *restriction* $Fun\ \mathfrak{h}_{/\mathcal{K}} : \mathcal{K} \to Y$ is $\omega_p - open$.

Proof: Let $\mathcal{D}$ be any *open* subset of $\mathcal{K}$. Since $\mathcal{K}$ is *open* in X, implies that $\mathcal{D}$ is *open* in X. By *hypothesis*, $\mathfrak{h}(\mathcal{D})$ is $\omega_p - open$ in Y. But, $\mathfrak{h}_{/\mathcal{K}}(\mathcal{D}) = \mathfrak{h}(\mathcal{D})$. Therefore, $\mathfrak{h}_{/\mathcal{K}}$ is $\omega_p - open$ an Fun.

5. ω_p-CLOSED FUNCTIONS

Definition 5.1. A $Fun\ \mathfrak{h} : X \to Y$ is *said* to be an $\omega_p - closed\ Fun$, if the *image* of *each closed* set in X is $\omega_p - closed$ in Y.

Theorem 5.2. Let $\mathfrak{h} : X \to Y$ be a Fun. Then, $\mathfrak{h}$ is $\omega_p - closed \iff \omega_p Cl(\mathfrak{h}(\mathcal{D})) \subseteq \mathfrak{h}(Cl(\mathcal{D}))$, for *each* $\mathcal{D} \subseteq X$.
Proof: Let $\mathfrak{h}$ be an $\omega_p - closed\ Fun$ and $\mathcal{D} \subseteq X$. Then, $Cl(\mathcal{D})$ is a *closed* subset of X. By *hypothesis*, $\mathfrak{h}(Cl(\mathcal{D}))$ is $\omega_p - closed$ in Y. That is, $\omega_p Cl(\mathfrak{h}(Cl(\mathcal{D}))) = \mathfrak{h}(Cl(\mathcal{D}))$. Since, $\mathfrak{h}(\mathcal{D}) \subseteq \mathfrak{h}(Cl(\mathcal{D}))$, then $\omega_p Cl(\mathfrak{h}(\mathcal{D})) \subseteq \omega_p Cl(\mathfrak{h}(Cl(\mathcal{D}))) = \mathfrak{h}(Cl(\mathcal{D}))$. Therefore, $\omega_p Cl(\mathfrak{h}(\mathcal{D})) \subseteq \mathfrak{h}(Cl(\mathcal{D}))$. Conversely, we must show that $\mathfrak{h}$ is $\omega_p - closed$. Let $\mathcal{D}$ be a *closed* subset of X. By *hypothesis*, $\omega_p Cl(\mathfrak{h}(\mathcal{D})) \subseteq \mathfrak{h}(Cl(\mathcal{D})) = \mathfrak{h}(\mathcal{D})$. That is, $\mathfrak{h}(\mathcal{D})$ is $\omega_p - closed$ in Y.

Theorem 5.3. The *following statement* are *equivalent*, for a *bijective Fun* $\mathfrak{h} : X \to Y$:
1. $\mathfrak{h}$ is an $\omega_p - closed$;
2. $\mathfrak{h}^{-1}(\omega_p Cl(\mathcal{D})) \subseteq Cl(\mathfrak{h}(\mathcal{D}))$, for *each* $\mathcal{D} \subseteq Y$;
3. $Int(\mathfrak{h}^{-1}(\mathcal{D})) \subseteq \mathfrak{h}^{-1}(\omega_p Int(\mathcal{D}))$, for *each* $\mathcal{D} \subseteq Y$.

Proof:
$(1) \Rightarrow (2)$ Let $\mathfrak{h}$ be a $\omega_p - closed$ and $\mathcal{D} \subseteq Y$. Then, $Cl(\mathfrak{h}(\mathcal{D}))$ is *closed* in X. By *hypothesis*, $\mathfrak{h}(Cl(\mathfrak{h}^{-1}(\mathcal{D})))$ is $\omega_p - closed$ in Y, this implies that,

$$\omega_p\, Cl\left(\mathfrak{h}\left(Cl(\mathfrak{h}^{-1}(\mathcal{D}))\right)\right) = \mathfrak{h}\left(Cl(\mathfrak{h}^{-1}(\mathcal{D}))\right) \qquad (**)$$

Since $\mathfrak{h}$ is *bijective*, thus $\mathcal{D} = \mathfrak{h}(\mathfrak{h}^{-1}(\mathcal{D})) \subseteq \mathfrak{h}(Cl(\mathfrak{h}^{-1}(\mathcal{D})))$. By $(**)$ $\omega_p Cl(\mathcal{D}) \subseteq \omega_p Cl(\mathfrak{h}(Cl(\mathfrak{h}^{-1}(\mathcal{D})))) = \mathfrak{h}(Cl(\mathfrak{h}^{-1}(\mathcal{D})))$. Therefore, $\mathfrak{h}^{-1}(\omega_p Cl(\mathcal{D})) \subseteq Cl(\mathfrak{h}^{-1}(\mathcal{D}))$.

$(2) \Rightarrow (3)$ Let $\mathcal{U} \subseteq Y$. Then, $Y - \mathcal{U} \subseteq Y$, by (2), $\mathfrak{h}^{-1}(\omega_p Cl(Y - \mathcal{U})) \subseteq Cl(\mathfrak{h}^{-1}(Y - \mathcal{U}))$. Thus, $X - \mathfrak{h}^{-1}(\omega_p Int(\mathcal{U})) \subseteq X - Int(\mathfrak{h}^{-1}(\mathcal{U}))$, this means that $Int(\mathfrak{h}^{-1}(\mathcal{U})) \subseteq \mathfrak{h}^{-1}(\omega_p Int(\mathcal{U}))$.

$(3) \Rightarrow (1)$ Let $\mathcal{D}$ be a *closed* subset of X. To show that, $\mathfrak{h}$ is $\omega_p - closed$. Since, $\mathfrak{h}(X - \mathcal{D}) \subseteq Y$, so by (3), $Int((\mathfrak{h}(X - \mathcal{D}))) \subseteq \mathfrak{h}^{-1}(\omega_p Int(\mathfrak{h}(X - \mathcal{D}))$. By *bijective* of $\mathfrak{h}$, $X - Cl(\mathcal{D}) \subseteq X - \mathfrak{h}^{-1}(\omega_p Cl(\mathfrak{h}(\mathcal{D})))$, then $\omega_p Cl(\mathfrak{h}(\mathcal{D})) \subseteq (\mathfrak{h}(Cl(\mathcal{D})))$. But $\mathcal{D}$ is *closed*, thus $\omega_p Cl(\mathfrak{h}(\mathcal{D})) \subseteq \mathfrak{h}(\mathcal{D})$, and $\mathfrak{h}\,(\mathcal{D})$ is *closed* in Y. Hence, $\mathfrak{h}$ *is* $\omega_p - closed$.

Theorem 5.4. Let $\mathfrak{h}: X \to Y$ be an $\omega_p - closed\ Fun$. If $\mathcal{K}$ is a *closed subspace* in X, then the *restriction*
$Fun\ \mathfrak{h}_{/\mathcal{K}} : \mathcal{K} \to Y$ is $\omega_p - closed$.
Proof: Let $\mathcal{D}$ be any *closed* subset of $\mathcal{K}$. Since $\mathcal{K}$ is *closed* in X, implies that $\mathcal{D}$ is *closed* in X.
By hypothesis,

DOI: https://doi.org/10.31972/ticma2022

$\mathfrak{h}(\mathcal{D})$ is $\omega_p -$ $closed$ in Y. But, $\mathfrak{h}_{/\mathcal{K}}(\mathcal{D}) = \mathfrak{h}(\mathcal{D})$. Therefore, $\mathfrak{h}_{/\mathcal{K}}$ is $\omega_p -$ $closed\ Fun$.

Theorem 5.5. Let $\zeta: X \to Y$ be a $closed$ Fun and $\eta: Y \to Z$ be an $\omega_p - closed\ Fun$. Then, $\eta \circ \zeta$ is an $\omega_p -$ $closed\ Fun$.
Proof: Let $\mathcal{D}$ be any $closed$ subset of X. Then, by $hypothesis$, $\zeta(\mathcal{D})$ is $closed$ in Y. Since η is $\omega_p - closed$, thus $\eta(\zeta(\mathcal{D}))$ is $an\ \omega_p - closed\ set$ in Z. Therefore, $\eta \circ \zeta$ is $\omega_p - closed$.

Theorem 5.6. The $following\ conditions$ are $true$, for the $Funs$ $\mathfrak{g}: X \to Y$ and $\mathfrak{h}: Y \to Z$:

1. If $\mathfrak{h} \circ \mathfrak{g}$ is a $closed\ Fun$ and $\mathfrak{h}$ is an $injective\ \omega_p - continuous\ Fun$, then $\mathfrak{g}$ is $\omega_p - closed$.
2. If $\mathfrak{h} \circ \mathfrak{g}$ is an $\omega_p - closed\ Fun$ and $\mathfrak{g}$ is an $surjective$ continuous Fun, then $\mathfrak{h}$ is $\omega_p - closed$.

$Proof$.

1. Let $\mathcal{D}$ be any $closed$ subset of X. Then, by $hypothesis$, $\mathfrak{h}(\mathfrak{g}(\mathcal{D}))$ is $closed$ in Z. Since $\mathfrak{h}$ is $injective$

$\omega_p - continuous$, $\mathfrak{h}^{-1}\left(\mathfrak{h}\left(\mathfrak{g}(\mathcal{D})\right)\right) = \mathfrak{g}(\mathcal{D})$ is $\omega_p - closed$ in Y. Hence, $\mathfrak{g}\ is\ \omega_p - open$.

2. Suppose $\mathcal{D}$ is a $closed$ subset of Y. Since $\mathfrak{g}$ is $continuous$, then, $\mathfrak{g}^{-1}(\mathcal{D})$ is $closed$ in X. By $hypothesis$,

$\mathfrak{h}\left(\mathfrak{g}\left(\mathfrak{g}^{-1}(\mathcal{D})\right)\right) = \mathfrak{h}(\mathcal{D})$ is $an\ \omega_p - closed$ set in Z. Therefore, $\mathfrak{h}$ is $\omega_p - closed$.

Theorem 5.7. The $following$ conditions are $equivalent$, for a $bijective\ Fun$ $\mathfrak{h}: X \to Y$:

1. h is $\omega_p - continuous$;
2. h is $\omega_p - open$;
3. h is $\omega_p - closed$.

Proof:

$(1) \Rightarrow (2)$ Let $\mathcal{D}$ be any $open$ set in X. Since $\mathfrak{h}^{-1}$ is $\omega_p - continuous$, thus, $(\mathfrak{h}^{-1})^{-1}(\mathcal{D}) = \mathfrak{h}(\mathcal{D})$ is $\omega_p -$ ope

in Y. Therefore, $\mathfrak{h}$ is $\omega_p - open$.

$(2) \Rightarrow (3)$ Let $\mathfrak{h}$ be an $\omega_p - open\ Fun$, and $\mathcal{D}$ be a $closed$ set in X. Then, $X - \mathcal{D}$ is $open$. By $hypothesis$, $\mathfrak{h}(X - \mathcal{D}) = Y - \mathfrak{h}(\mathcal{D})$ is $\omega_p - open$ in Y. Thus, $\mathfrak{h}(\mathcal{D})$ is $\omega_p - closed$.

$(3) \Rightarrow (1)$ Let $\mathcal{D}$ be any $open$ set in X. Then, $X - \mathcal{D}$ is $closed$. Since $\mathfrak{h}$ is $bijective$ and by (3), $\mathfrak{h}(X - \mathcal{D}) =$

$Y - \mathfrak{h}(\mathcal{D})$ is $\omega_p - closed$ in Y. Thus, $(\mathfrak{h}^{-1})^{-1}(\mathcal{D}) = \mathfrak{h}(\mathcal{D})$ is $\omega_p - open$. Hence, $\mathfrak{h}^{-1}$ is $\omega_p - open$.

6. CONCLUSION:

In this $paper$, we showed that every $\omega_p - open$ set in $locally\ countable$ space is $open$. We used the $notions$ of $\omega_p - open$ and $\omega_p - closed$ sets to describe $\omega_p - open$ and $\omega_p - closed\ Fun$. Also, there is a relationship between $open$ and $preopen\ Funs$ via $\omega_p - open\ Funs$. We acquired some $fundamental\ theorems$ and properties of these $Funs$. However, there are combined $\omega_p - continuous\ Funs$ with $\omega_p -$ $open$ and $\omega_p - closed\ Fun$.

ACKNOWLEDGMENTS

I'd like to thank the referees for their constructive $feedback$. as well as manuscript suggestions.

DOI: https://doi.org/10.31972/ticma2022

REFERENCES

1. Darwesh, H. M. 2013. Between Preopen and Open Sets in Topological Spaces, *Thai Journal of Mathematics* 11(1), 143-55.
2. Levine, N. 1963. Semi-Open Sets and Semi-Continuity in Topological Spaces, *Amer. Math. Monthly*, 70, 36-41.
3. Mashhour, A. S., Abd El-Monsef, M. E. and El-Deep S. N. 1982. On Precontinuous and Weak Precontinuous Mappings, *Proc. Math. Phys. Soc. Egypt*, 53, 47–53.
4. Mashhour, A. S., Hassanien I. A. and EL-Deeb S. N. 1983. α −Continuousand α −Open Mappings, *Acta Mathematica Hungarica*, 41, 213–218.
5. Abd EL-Monsef, M. E., El-Deeb S. N. and Mahmoud R. A. 1983. β −Open Sets and β −Continuous Mappings, *Bulletin of the Faculty of Science A. Physics and Mathematics*, 12, 77–90.
6. El-Atik, A. A. 1997. *A Study on Some Types of Mappings on Topological Spaces*, M.Sc. Thesis, Tanta Uni., Egypt.
7. Raychaudhuri, S. and Mukherjee, N. 1993. On δ −Almost Continuity and δ −Preopen Sets, *Bulletin of the Institute of Mathematics Academia Sinica*, 21, 357–366.
8. Stone, M. 1937. Applications of The Theory of Boolean Ring to General Topology, *Trans. Amer. Math. Soc.*, 41, 375–481.
9. Njastad, O. 1965. On Some Classes of Nearly Open Sets, *Pacific Journal of Mathematics*, 15, 961–970.
10. Velicko, N. V. 1968. H − Closed Topological Spaces, *Transactions of the American Mathematical Society*, 78, 103–118.
11. Hdeib, H. Z. 1982. ω − Closed Mapping, *Revista Colombiana de Mathematics*, 16, 65–78.
12. Biswas, N. 1969. On Some Mappings in Topological Spaces, *Bulletin of Calcutta Mathematical Society*, 61, 127–135.
13. Sharma, J. N. 1979, *Krishna's Topology*, Krishna Prakashan Media $1^{st}ed$., India.
14. Al-Zoubi, K. and Al-Nashef, B. 2003. The Topology of $\omega - Open$ Subsets, *Al-Manarah J.*, 9, 169-179.
15. Reilly, I. L. and Vamanamurthy M. K. 1990. On Some Questions Concerning Preopen Sets, *Kyungpook Math. J.,* 30, 87-93.
16. Darwesh, H. M. 2009. *Some Types of Separation Axioms and Dimension Functions in Topological Spaces*, PhD thesis, Sulaimani University, Sulaimani Kurdistan Region.

Proceeding of 3rd International Conference of Mathematics and its Applications TICMA2022
https://conferences.su.edu.krd/su/ticma2022/
DOI: https://doi.org/10.31972/ticma2022

RESEARCH PAPER

Studying Some Stochastic Differential Equations with trigonometric terms with Application

Abdulghafoor Jasim Salim[1,*] Ali A. Asmael[2]

[1,2]Department of Mathematics, college of computer science and Mathematics, University of Mosul.

[1]drabdul_salim@uomosul.edu.iq
2ali.20csp132@student.uomosul.edu.iq

A B S T R A C T: In this paper we look at several (trigonometric) stochastic differential equations, we find the general form for such nonlinear stochastic differential equation by using the I'to formula. Then we find the exact solution for the different trigonometric stochastic differential equations by the use of stochastic integrals. Ilustrate the approach with various examples. (Precise solution using the Ito integral formula) and approximate solution (numerical approximation (the Euler-Maruyama technique and the Milstein method) were compared to the exact solutions with the error of those approaches

KEYWORDS: Trigonometric stochastic differential equations, Euler-Maruyama technique, Milstein method.
DOI: https://doi.org/10.31972/ticma22.13

1. INTRODUCTION:

The most common applications are modeled using stochastic differential equations and ordinary differential equations. Many phenomena including unexpected (uncertain) consequences are typically described by adding a random or stochastic component to the ordinary differential equation, resulting in stochastic(random) differential equations (SDEs), and the word stochastic(random) is referred to as the noise term [1]. Then, an SDE is a differential equation in which one or more of the terms are stochastic (random) processes, and the solution is also stochastic as a result of the stochastic process [2] . suppose we have the following ordinary differential equation.

$$y\,(t) = G(t, y(t)) \quad ; \quad t > 0 \qquad (1)$$

$$Y(0) = y_0$$

If G(.) is any smooth function and y0 is any initial(fixed) point y0 ∈ Rn, if equation (1) contain the stochastic effects (wiener process) to describe random behavior known as Brownian motion, such equation has the form:

$$\dot{y}(t) = G(t, y(t)) + F(t, y(t))\delta(t) \quad ; \quad t > 0 \qquad (2)$$

Where $\delta(t)$ represents the white noise (random) process (which is the formal derivative of the).
Equation (2) can also be written as:

$$\frac{dy(t)}{dt} = G(t, y(t)) + F(t, y(t)\ \frac{dW(t)}{dt} \qquad (3)$$

*** Corresponding Author: Abdulghafoor Jasim Salim**
E-mail: drabdul_salim@uomosul.edu.iq
Article History:
Received: 01/08/2022
Accepted: 15/09/2022
Published: 07/12/2022

DOI: https://doi.org/10.31972/ticma2022

Where $\frac{dW(t)}{dt} = \delta(t)$, $dW(t)$ indicates the derivative of the Weiner process. multiply both side of equation (3) by dt , we get

$$dy(t) = G(t, y(t))dt + F(t, y(t))\, dW(t) \qquad (4)$$

$$y(0) = y_0$$

The drift and diffusion coefficients are denoted by G (.) and F(.) correspondingly.
Then we obtain a stochastic differential equations (eq.(4)).

In 2019 Junteng Jia and Austin R. Benson introduced Neural Jump Stochastic Differential Equations that provide a data-driven approach to learning continuous and discrete dynamic behavior [3], and Xuechen Li et.al generalized the adjoint sensitivity method stochastic differential equations, allowing time-efficient and constant-memory computation of gradients with high-order adaptive solvers [4], and in 2020 M. M. Vas'kovskii studied mixed-type stochastic differential equations driven by standard and fractional Brownian motions with Hurst indices greater than 1/3 [5], and in 2020 Saeed and Salim studied the exact and approximate solution for some harmonic stochastic differential equations, by using Ito integral formula and numerical approximation [6].

We identify the general form and investigate some product (SDE) in this article, as well as the precise solution of that equation and compare it to the exact solution of the suggested model using numerical methods.

2.MAIN RESULTS:

Definition (1) :(The random variable) [7]
The random variable Y(.) is a one to one function that maps from sample space μ to the real number R (i.e. Y:$\mu \rightarrow$ R).

Definition 2: (stochastic(random) process) [8]
A stochastic process, often known as a random process, is a mathematical object consisting of a set of random variables represented by {Y(t)} where t belonging to T (sorted by index set T where T⊆ R.)

Definition 3: (Wiener process) [8]
$\{W(t)\}$ is a Wiener process (Brownian motion) over the interval [0, T] which is a continuous-time stochastic process satisfying: the following conditions: 1: $W(0) = 0$
2: suppose t, s ≥ 0, then W (t)- W (s) is distributed normally, with zero mean and variance $|t - s|$.
3: For $0 \le s < t < u < v \le T$, $W(t) - W(s)$ *and* $W(v) - W(u)$ are independent.

3.STOCHASTIC INTEGRAL [9] [10]

A stochastic integral is an integral which is defined as a sum more than an integration and it is increased by the rise in time on the Wiener process trajectory (Dumas and Luciano, 2017). That is :

$$\int_a^b c(t)\, dw(t) = \sum_{i=0}^{k-1} \delta i\, (W_{t_{i+1}} - W_{t_i}) \qquad (5)$$

Where c(t) is a real-valued stochastic process, $c = \{c(t)\}_{a \le t < b}$ and {w(t)}is a Wiener process.
We can write equation (4) in the integral form, that is,

$$Y(t) = y(0) + \int_0^t G\ (s, Y(s))\ ds + \int_0^t F\ (s, Y(s))\ dW(s) \qquad (6)$$

The first integral is determistic and the second are stochastic which need much attension to be solved:

https://conferences.su.edu.krd/su/ticma2022/
DOI: https://doi.org/10.31972/ticma2022

That's need The following requirements for G(s, Y(s)) and F(s, Y(s)).

$$E \quad \int_0^t F^2(s,Y(s)) \ ds < \infty$$

and nearly certainly for all t ≥ 0

$$\int_0^t \left| G\ (s,Y(s)) \right| ds < \infty$$

The stochastic integral has one of the most essential properties:

$$\int_0^t W(S)\ dW(s) = \tfrac{1}{2}\int_0^t d(W^2(S)) - \tfrac{1}{2}\int_0^t ds \qquad (7)$$
$$= \tfrac{1}{2}W^2(t) - \frac{t}{2}$$

And the general form's are: (see for example […])

$$\int_0^t W^m(t)dW(t) = \frac{1}{m+1}W^{m+1}(t) + \sum_{j=0}^{m-2}(-1)^{j+1}\frac{m!}{2^{j+1}(m-j)!}w^{m-j}(t) + (-1)^m\frac{m!}{2^m}\frac{t}{2} \qquad (8)$$

lemma: [11]

Consider the process $E_t = G(t)F(W_t)$ with differentiable G and F. By using the product rule for differentiation to E_t, the following results are obtained

$$dE_t = \ dG(t)\ f(W_t)\ + G(t)\ dF(W_t)$$

$$= \ G'(t)\ F(W_t)\ dt\ +\ G(t)\ (F'(W_t)dWt\ +\ 1/2\ F''(W_t)\ dt)$$

$$= \ G'(t)\ F(W_t)\ dt\ +\ 1/2\ a(t)\ F''(W_t)\ dt\ +\ G(t)\ F'(W_t)dW_t.$$

Using integration by parts which is obtained by writing the connection in integral form, then we have:

$$\int_n^m G(t)F'(W_t)d(W_t) = G(t)F(W_t)|\frac{m}{n} - \int_n^m G'(t)F(W_t)dt\ - \frac{1}{2}\int_n^m G(t)F''(W_t)dt \qquad (9)$$

Suppose we have a product between two functions (of t and W_t) for which an antiderivative is known, use this formula. The two examples below are both essential and useful in our applications.

1. The aforementioned formula assumes the simple form if b(W_t) = W_t.

$$\int_n^m G(t)d(W_t) = G(t)W_t|\frac{t=m}{t=n} - \int_n^m G'(t)W_t dt \qquad (10)$$

It is worth noting that the left side is a Wiener integral.

1. If a(t) = 1, then the formula becomes

DOI: https://doi.org/10.31972/ticma2022

$$\int_n^m F'(W_t)d(W_t) = F(W_t)|\frac{t=m}{t=n} - \frac{1}{2}\int_n^m F''(Wt)dt \qquad (11)$$

Ito's integral formula: [1]

Consider Ito's stochastic differential equation, which has the following form:

$$dy(t) = G\big(t,y(t)\big)dt + F\big(t,y(t)\big)dW(t) \qquad (12)$$

for $0 \le t \le T$ let $X\big(t,Y(t)\big)$ be a smooth function if we use the Taylor expansion rule, then we get:

$$dX\big(t,Y(t)\big) = \left(\frac{\partial x}{\partial t} + G\big(t,Y(t)\big)\frac{\partial x}{\partial y} + \frac{1}{2}F^2\big(t,Y(t)\big)\frac{\partial^2 x}{\partial y^2}\right)dt + F\big(t,Y(t)\big)\frac{\partial x}{\partial y}dW(t) \qquad (13)$$

eq.(13) is called ito formula where y(t) is the solution of a stochastic differential equation (12). If the requisite partial derivatives are present, the mixed differentials can be joined according to the requirements.

$$dt.dW = dW.dt = (dt)^2 = 0 \quad \& \quad (dW)^2 = dt$$

Proposition: Let X(t,Y(t)) satisfies equation (14), i.e. the solution of equation (12), we can find the general form to $X\big(t,Y(t)\big) = (Y(t))^n$.where y(t) any trigonometric function.

i) y(t)= sin(x(t))

Here $X(t) = U\big(t,sin(x(t)\big)$, Then: by using ito-formula we have:

$$d\big(X(t)\big) = d(sin(x(t))^n = \left(n\big(sin(x(t))\big)^{n-1}G(x(t),t) + \tfrac{1}{2}n(n-1)\left(sin(x(t))\right)^{n-2}F^2(y(t),t)\right)dt + \left(n\big(sin(x(t))\big)^{n-1}F(y(t),t)\right)dW(t) \qquad (14)$$

we obtain the prove for equation (14) recursively:

- let $m = 1$

$$dX(t) = \frac{\partial U(y(t),t)}{\partial t}dt + \frac{\partial U(y(t),t)}{\partial y}dx + \frac{1}{2}F^2(y(t),t)\frac{\partial^2 U(y(t),t)}{\partial y^2}dt$$

$$dX(t) = \frac{\partial U(y(t),t)}{\partial t}dt + \frac{\partial U(y(t),t)}{\partial y}\big(G(y(t),t)dt + F(y(t),t)dW_{(t)}\big) + \frac{1}{2}F^2(y(t),t)\frac{\partial^2 U(y(t),t)}{\partial y^2}dt$$

$$dX(t) = \left(\frac{\partial U(y(t),t)}{\partial t} + G(y(t),t)\frac{\partial U(y(t),t)}{\partial y} + \frac{1}{2}F^2(y(t),t)\frac{\partial^2 U(y(t),t)}{\partial y^2}\right)dtG(y(t),t)\frac{\partial U(y(t),t)}{\partial y}dW(t) \qquad (15)$$

But, $X(t) = U(y(t),t) = sin(x(t))$ Then,

$$dX(t) = d(sin\,(x(t))) = cos\,(x(t))dx + \frac{1}{2}sin\,(x(t))F^2(y(t),t)dt$$

DOI: https://doi.org/10.31972/ticma2022

$$d(sin\ sin\ (x(t)\ ) = \big(cos\ (x(t))(G(y(t)\ ,t)\ dt + F(y(t),t\ )\ dW(t)\big) + \frac{1}{2} sin\ (x(t))F^2(y(t),t)dt$$

$$d(sin\ sin\ (x(t)\ ) = \left(cos\ cos\ (x(t))\ G(y(t),t) + \frac{1}{2\ sin\ sin\ \big(x(t)\big)\ F^2(y(t),t)}\right)dt$$
$$+ (cos\ (x(t))F(x(t),t))dW(t) \qquad (16)$$

$$sin\ (t) = sin(0) + \int_0^t \left(cos\ cos\ (s)\ G(y(s),s) + \frac{1}{2} sin\ sin\ (s)\ F^2(y(s),s)\right)ds$$
$$+ \int_0^t cos\ (ws)dW(s) \qquad (17)$$

- $m = 2$, we have:

$$dX(t) = d\big(sin(x(t))\big)^2$$
$$= \big(2\ sin\ sin\ \big(x(t)\big)\ cos\ cos\ \big(x(t)\big)\ G(y(t),t) + [sin^2(x(t)) - cos^2(x(t))]F^2(Y(t),t)\big)\ dt$$
$$+\ (2\ sin\ sin\ (x(t))\ cos\ ((xt))F(Y(t),t))dW(t)$$

proof:

$$d(sin(x(t)))^2 = \ 2\ sin\ sin\ (x(t))\ \ cos\ cos\ (x(t))\ dx + [sin^2\big(x(t)\big) - cos^2(x(t)]F^2(y(t),t)dt$$

$$d(sin(x(t)))^2 = 2\ sin\ sin\ (x(t))\ \ cos\ cos\ (x(t))\ \big(G(y(t),t)dt + F(y(t),t)dW(t)\big) + [sin^2(x(t))$$
$$- cos^2(x(t))F^2(Y(t),t)dt$$

$$d(sin(x(t)))^2 = \ (2\ sin\ sin\ (x(t))\ \ cos\ cos\ (x(t))\ G(y(t),t) + [sin^2(x(t)) - cos^2(x(t))]F^2(Y(t),t))dt$$
$$+\ (2\ sin\ sin\ (x(t))\ cos\ (x(t))F(Y(t),t))dW(t) \qquad (18)$$

By integrating from zero to t, we get

$$sin^2(t) = sin^2(0) + \int_0^t \ (2\ sin\ sin\ (s)\ \ cos\ cos\ (s)\ G(y(s),s) + [sin^2(s) - cos^2(s)F^2(y(s),s))]ds$$
$$+ \int_0^t \ \big((2\ sin\ sin\ (ws)\ cos\ (ws)F(Y(t),t))\big)dW(s) \qquad (19)$$

- The solution for the general form ($m = n$):

$$X(t) = d(sin(x(t)))^n$$

$$= \left(n\ (sin\ (x(t)))^{n-1}G(y(t),t) + \frac{1}{2}n\ (n-1)(sin\ (x(t)))^{n-2}F^2(y(t),t)\right)dt$$
$$+ (n\ (sin\ (x(t)))^{n-1}F\ (y(t),t)dW(t)$$

proof:

$$d(sin\ (x(t)))^n = n(sin(x(t)))^{n-1}dx + \frac{1}{2}n(n-1)(sin(x(t)))^{n-2}F^2(y(t),t)dt$$

DOI: https://doi.org/10.31972/ticma2022

$$d(sin\,(x(t))^n = n(sin(x(t)))^{n-1}\big(G\,(t\,,y(t))dt + F(t\,,y(t))dW(t)\big) + \frac{1}{2}n(n-1)(sin(x(t)))^{n-2}\,F^2(y(t),t)dt$$

$$d(sin(x(t)))^n = \left(n(sin(x(t)))^{n-1}G(y(t),t) + \frac{1}{2}n(n-1)\,(sin(x(t)))^{n-2}F^2(y(t),t)\right)dt + (n(sin(x(t)))^{n-1}F(y(t),t))dW(t) \quad (20)$$

By integrating from zero to t, we get

$$sin(t) = sin(0) + \int_0^t \left(n\big(sin(s)\big)^{n-1}G(y(s),s) + \frac{1}{2}n(n-1)\big(sin(s)\big)^{n-2}F^2(y(s),s)\right)ds + \int_0^t \left(n\big(sin(s)\big)^{n-1}F(y(s),s)\right)dW(s) \quad (21)$$

ii) suppose that Y(t)= cos(x(t)), then as before we obtain

$$X(t) = d(cos(x(t)))^n = \left(n(cos(x(t)))^{n-1}G(y(t),t) + \frac{1}{2}n(n-1)\,(cos(x(t)))^{n-2}F^2(y(t),t)\right)dt + (n(cos(x(t)))^{n-1}F(y(t),t))dW(t) \quad (22)$$

By integrating from zero to t, we get

$$cos(t) = cos(0) + \int_0^t \left(n\big(cos(s)\big)^{n-1}G(y(s),s) + \frac{1}{2}n(n-1)\big(cos(s)\big)^{n-2}F^2(y(s),s)\right)ds + \int_0^t \left(n\big(cos(s)\big)^{n-1}F(y(s),s)\right)dW(s) \quad (23)$$

iii) Y(t)= tan(x(t)), then:

$$X(t) = d(tan\,(x(t)))^n = \left(n(tan(x(t)))^{n-1}G(y(t),t) + \frac{1}{2}n(n-1)\,(tan(x(t)))^{n-2}F^2(y(t),t)\right)dt + (n(tan(x(t)))^{n-1}F(y(t),t))dW(t) \quad (24)$$

By integrating from zero to t, we get

$$tan(t) = tan(0) + \int_0^t \left(n\big(tan(s)\big)^{n-1}G(y(s),s) + \frac{1}{2}n(n-1)\big(tan(s)\big)^{n-2}F^2(y(s),s)\right)ds + \int_0^t \left(n\big(tan(s)\big)^{n-1}F(y(s),s)\right)dW(s) \quad (25)$$

EXAMPLES:

In this paragraph we explain the method by introducing some examples.
Let equation (12) be given. i. e.

$$dY(t) = G\,\big(t,y(t)\big)dt + F\,\big(t\,,y(t)\big)dW(t)$$

Example 1:

DOI: https://doi.org/10.31972/ticma2022

find the exact solution for equation (16), where $G = 0$ and $F = 1, X(t) = t$, then $dY(t) = dt + dW(t)$. and let the initial condition $X(0) = 0.1$
From equation (18) we get

$$d(sin\ sin\ (x(t))\ ) = \left(-\frac{1}{2}sin(x(t))\right)dt + cos\big(x(t)\big)\ dW(t) \quad (26)$$

and therefore, the exact solution is found:

$$sin(t) = sin\ sin\ (0)\ - sin\ sin\ (W_t - W0) \quad (27)$$

Example 2:
find the exact solution for equation (18), where $G = 1$ and $F = 1,\ X(t) = t$, then $dY(t) = dt + dW(t)$. and also let the initial condition $x(0) = 0.1$
From equation (18) we get.

$$d\big(sin(t)\big)^2 = \big(2\ sin\ sin\ (t)\ \ cos\ cos\ (t)\ - sin^2(t) + cos^2(t)\big)dt + 2\ sin\ sin\ (t)\ cos\ cos\ (t)\ dW(t) \quad (28)$$

and therefore, the exact solution is found:

$$sin^2(t) = sin(t)cos(t) + \frac{1}{2}exp(2t) - \frac{1}{2}cos(2W_t) \quad (29)$$

4. NUMERICAL SOLUTION:

We employ numerical approximations such as the Euler-Maruyama and Milstein methods, as well as calculating the error to explain solution convergence (exact and approximation).

Suppose we have the following stochastic differential equation:

$$dY(t)\ =\ G_n\big(t, Y(t)\big)dt\ + F_n\ \big(t, Y(t)\big)dW(t)\ , \qquad y(t0) = x0$$

Euler Maruyama method has the form [15] :-

$$y_{t_{n+1}} = y_{t_n} + G_n(t_{n+1} - t_n) + F_n\big(W_{t_{n+1}} - W_{t_n}\big) \quad (30)$$

$$Y_{t_{i+1}} = Y_{t_i} + G_n\Delta t + F_n\sqrt{\Delta t}\eta_i \quad (31)$$

With y(0) = 0.1 and , $t_i = i\Delta t \Rightarrow \Delta t = \frac{1}{N}$, ηi~(0,1) ,t ∈ [0,1]
Equation (31) is called Euler-Maruyama method.

5.MILSTEIN'S METHOD HAS THE FORM [15] :

In the 1-dimensional case with d = m =1, we add to the Euler scheme the term $\frac{1}{2}F_{y_t}[(dW_t)^2 - dt]$
Therefore, we have from the Ito-Taylor expansion the Milstein method given below

$$y_{t_{n+1}} = y_{t_n} + G_n(t_{n+1} - t_n) + F_n\big(W_{t_{n+1}} - W_{t_n}\big) + \frac{1}{2}F_nF_{x_n}[(dW_t)^2 - dt] \quad (32)$$

In the multi-dimension case with m =1 and d ≥1 the $j\ th$ component of the Milstein method is given by :

$$y^j_{t_{n+1}} = y^j_{t_n} + G^j_n(t_{n+1} - t_n) + F^j_n\big(W_{t_{n+1}} - W_{t_n}\big) + \frac{1}{2}\sum_{i=1}^{d} F^j_nF^j_{x_n}[(dW_t)^2 - dt] \quad (33)$$

Proceeding of 3rd International Conference of Mathematics and its Applications
TICMA2022
https://conferences.su.edu.krd/su/ticma2022/
DOI: https://doi.org/10.31972/ticma2022

$$y_{t_{i+1}} = y_{t_i} + \Delta t + \sqrt{\Delta t}\eta_i + \frac{1}{4}({\eta_i}^2 - 1)\Delta t \qquad (34)$$

6. Results:

1: Suppose we have equation (26), that is

$$d(sin\ sin\ (y(t))\ ) = \left(-\frac{1}{2}sin(y(t))\right)dt + cos\ cos\ \left(y(t)\right)\ dW(t) \qquad (26)$$

and therefore, the exact solution is found:

$$sin(t) = sin\ sin\ (0)\ - sin\ sin\ (W_t - W0) \qquad (27)$$

The following graphs were obtained from the $Matlab$™ program implementing the algorithm: see [9]

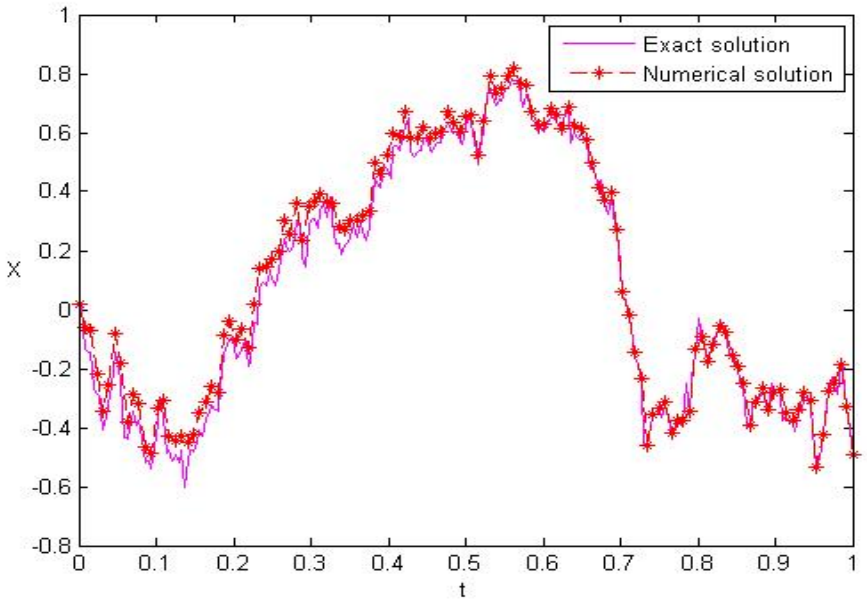

Figure 1: Exact solution charts vs numerical solutions produced using the Euler Maruyama method. With N=2^8 & R=2

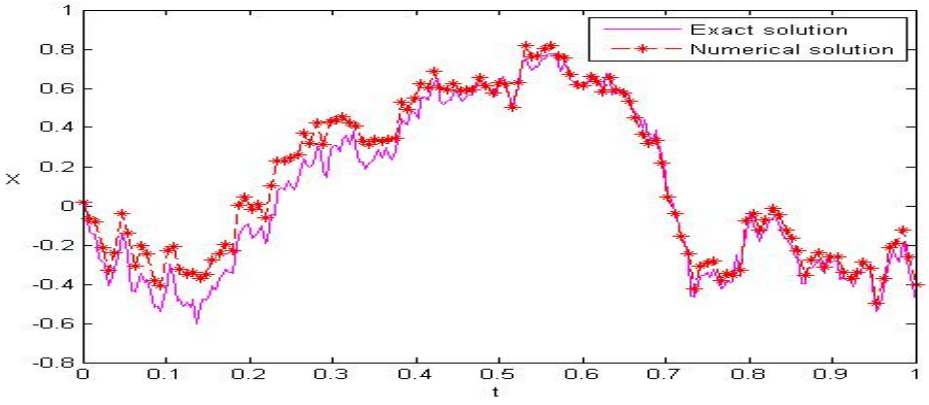

Figure 2 shows a comparison of precise answers to numerical solutions produced using Milstein's technique. With N=2^8 & R=2

DOI: https://doi.org/10.31972/ticma2022

Table1 shows the comparison of the Euler-Maruyama and Millstein's Method outcomes.

Error	N	R	numerical method
0.0040	2^8	2	Euler Maruyama method
0.0846	2^8	2	Milstein's method

The numerical solution is relatively near to the precise answer, and Euler-Maruyama is more accurate than Millstein's Method, as seen in the above figures and table.

2: The following graphs are for example two equations (28)

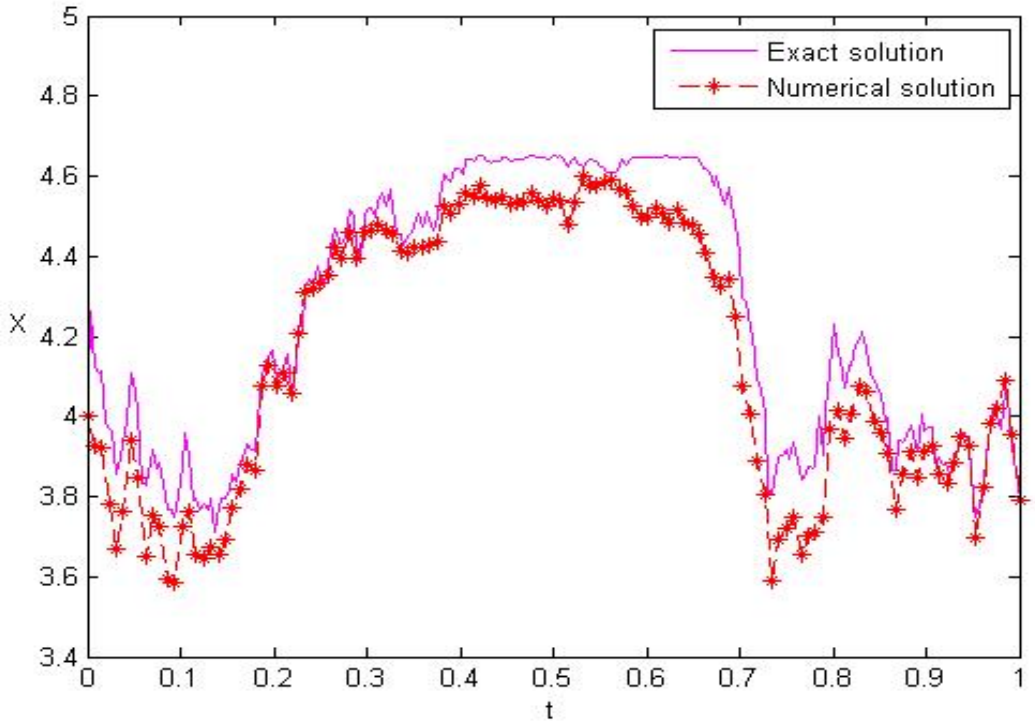

Figure 3: Comparison of precise and numerical solutions derived using the Euler Maruyama technique. With N=2^8 & R=2

DOI: https://doi.org/10.31972/ticma2022

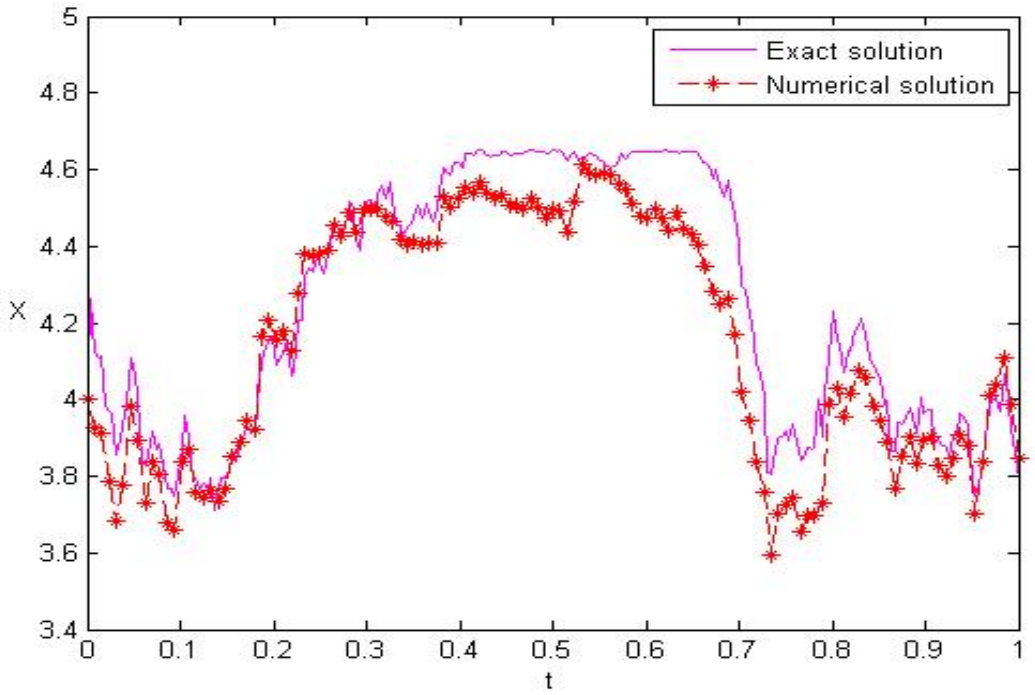

Figure 4: Exact solution vs numerical solutions produced using Millstein's Method. With N=2^8 & R=2

Table 2: Analysis of the Euler-Maruyama and Millstein's Method outcomes in comparison.

Error	N	R	numerical method
0.0023	2^8	2	Euler Maruyama method
0.0568	2^8	2	Milstein's method

The error between the Euler Maruyama approach and Milstein's method is explained in the table above (See for example [15]).

We can also see that the Euler Maruyama method is closer to the Exact Solution than the Milstein method when N = 2^8 .

6. CONCLUSION:

In this paper, we find the general form of a stochastic differential equation with limits of trigonometric functions using the ito formula and its solutions, and we have applied those results byusing some examples to explain the methods and use one of the simplest numerical methods (Euler-Maruyama and Milstein methods)to find approximate solutions. We see that Euler-Maruyama is better than the Milstein method's convergence of micro-stochasticity.

REFERENCE:

[1] Oksendal, B., 2013. *Stochastic differential equations: an introduction with applications*. Springer Science & Business Media.

[2] Kloeden, P. E., Platen, E., Gelbrich M. and Romisch W. 1995. Numerical Solution of Stochastic Differential Equations, *SIAM Review*, 37, 272-274.

[3] Jia J. and Benson A. R. 2019. Neural jump stochastic differential equations, *Advances in Neural Information Processing Systems*, 32.

[4] Li X., Wong, T.-K. L. Chen, R. T. and Duvenaud D. 2020. Scalable gradients for stochastic differential equations, *International Conference on Artificial Intelligence and Statistics*, 3870-3882.
[5] Vas'kovskii, M. 2020. Mixed-type stochastic differential equations driven by standard and fractional Brownian motions with Hurst indices greater than 1/3, *Proceedings of the National Academy of Sciences of Belarus. Physics and Mathematics Series*, 56, 36-50.
[6] Saeed, W. A. and Salim, A. J. 2020. Convergence solution for some Harmonic Stochastic Differential Equations with Application, *Tikrit Journal of Pure Science*, 25, 119-123.
[7] Charles, W.M. and van der Weide, J.A.M., 2011. Stochastic differential equations. Introduction to Stochastic Models for pollutant, Dispersion, Epidemic and Finance. *Lappennranta University Finland*.
[8] Evans, L.C., 2012. *An introduction to stochastic differential equations* (Vol. 82). American Mathematical Soc.
[9] Fadilah, M.U.H.Y.I.A.T.U.L., Permanasari, A.N.N.A., Riandi, R. and Maryani, E., 2020. The Level of disaster literacy of earthquake-experienced students in mathematics and science faculty of state university in Indonesia. *Journal of Engineering Science and Technology (JESTEC) on AASEC2019, Februari*, *2020*, 30-38.
[10] Alnafisah, Y.A., 2016. First-order numerical schemes for stochastic differential equations using coupling.
[11] Klebaner, F. C. 2012, *Introduction to stochastic calculus with applications*, World Scientific Publishing Company.
[12] Allen, E., 2007. *Modeling with Itô stochastic differential equations* (Vol. 22). Springer Science & Business Media.
[13] Särkkä, S. and Solin, A., 2019. *Applied stochastic differential equations* (Vol. 10). Cambridge University Press.
[14] Liu, S., 2019. Stochastic Calculus And Stochastic Differential Equations.
[15] Fadugba, S. E., Adegboyegun, B. J. and Ogunbiyi, O.T. 2013. On the convergence of euler maruyama method and milstein scheme for the solution of stochastic differential equations. *International Journal of Applied Mathematics and Modeling*, 1, p.1.

Proceeding of 3rd International Conference of Mathematics and its Applications TICMA2022
https://conferences.su.edu.krd/su/ticma2022/
DOI: https://doi.org/10.31972/ticma2022

RESEARCH PAPER

New Applications of Coding Theory in The Projective Space of Order Three

Hajir Hayder Abdullah[1,a,*] and Nada Yassen Kasm Yahya[2,b]

[1]*Department of Mathematics, College of Education for Pure Science, University of Mosul, Mosul, Iraq*

[2]*Department of Mathematics, College of Education for Pure Science, University of Mosul, Mosul, Iraq*

[a]hajar.20esp13@student.uomosul.edu.iq
[b]drnadaqasim1@gmail.com, drnadaqasim3@uomosul.edu.iq

A B S T R A C T:

The main aim of this paper is to introduce the relationship between the topic of coding theory and the projective space in field three and test the code. The maximum value of size of code over finite field of order three and an incidence matrix with the parameters, *n* (length of code), *d* (minimum distance of code) and *e* (error-correcting of code) have been constructed. With a theorem and a result that test the code if it is perfect or not.

KEY WORDS: Coding Theory, Projective Space, finite field.
DOI: https://doi.org/10.31972/ticma22.14

1. INTRODUCTION:

In 2018 Al-Saraji and Al-Hamidi [5],[6], applied the coding theory to the projective plane of field 3., so I did this expanding the work of Al-Saraji, where the coding theory was applied to field 3 in projective space, and there were several differences. In order to expand the work further and as a new work.

2. Coding Theory in The PG (3,3):

Theorem 1.1: [3],[4]

Every line in PG (3,3) contains exactly q+1 points.

Theorem 1.2:[9]

Every plane in PG (3,3) contains exactly $q^2+ q+1$ point (line).

Theorem 1.3: [10]

There exist $q^3+q^2+ q+1$ points in PG(3,3).

*** Corresponding Author: Hajir Hayder Abdullah**
E-mail: hajar.20esp13@student.uomosul.edu.iq
Article History:
Received: 01/08/2022
Accepted: 15/09/2022
Published: 07/12/2022

DOI: https://doi.org/10.31972/ticma2022

Theorem 1.5:[6]

(n, M, d)-code C satisfies

$M\{\binom{n}{0}+\binom{n}{1}(q-1)+\ldots+\binom{n}{e}(q-1)^e\}\leq q^n$

Corollary 1.6:[6]

(n, M ,d)-code C is perfect if and only if $M\{\binom{n}{0}+\binom{n}{1}(q-1)+\ldots+\binom{n}{e}(q-1)^e\}=q^n$

Now let's talk about the fields of order three of the projective space of the three -dimensions. And let us have the following points generated from a generated matrix: $\{T_1=[1,0,0,0], T_2=[0,1,0,0], T_3=[1,1,0,0], T_4=[2,1,0,0], T_5=[0,1,1,0], p_6=[1,1,1,0], T_7=[2,1,1,0], T_8=[0,2,1,0], T_9=[0,0,1,0], T_{10}=[1,0,1,0], T_{11}=[2,0,1,0], T_{12}=[1,2,1,0], T_{13}=[2,2,1,0], T_{14}=[0,0,0,1], T_{15}=[1,0,0,1], T_{16}=[2,0,0,1], T_{17}=[0,1,0,1], T_{18}=[1,1,0,1], T_{19}=[2,1,0,1], T_{20}=[0,2,0,1], T_{21}=[1,2,0,1], p_{22}=[2,2,0,1], T_{23}=[0,0,1,1], T_{24}=[1,0,1,1], T_{25}=[2,0,1,1], T_{26}=[0,1,1,1], T_{27}=[1,1,1,1], T_{28}=[2,1,1,1], T_{29}=[0,2,1,1], T_{30}=[1,2,1,1], T_{31}=[2,2,1,1], T_{32}=[0,0,2,1], T_{33}=[1,0,2,1], T_{34}=[2,0,2,1], T_{35}=[0,1,2,1], T_{36}=[1,1,2,1], T_{37}=[2,1,2,1], T_{38}=[0,2,2,1], T_{39}=[1,2,2,1], T_{40}=[2,2,2,1]\}$

Table of planes for field 3:

π_1	π_2	π_3	π_4	.	.	.	π_{37}	π_{38}	π_{39}	π_{40}
2	1	4	3	.	.	.	3	1	3	4
5	9	7	6	.	.	.	5	8	7	6
8	10	9	9	.	.	.	11	12	8	8
9	11	12	13	.	.	.	12	13	10	11
14	14	14	14	.	.	.	15	17	16	15
17	15	19	18	.	.	.	19	18	17	17
20	16	21	22	.	.	.	20	19	21	22
23	23	23	23	.	.	.	23	23	23	23
26	24	28	27	.	.	.	27	24	27	28
29	25	30	31	.	.	.	31	25	31	30
32	32	32	32	.	.	.	34	38	33	34
35	33	37	36	.	.	.	35	39	37	36
38	34	39	40	.	.	.	39	40	38	38

https://conferences.su.edu.krd/su/ticma2022/
DOI: https://doi.org/10.31972/ticma2022

It is obvious that space contains a table of lines and plans and a table of planes now we will create a table for the planes and planes that will be obtained according to the following equation: $x_1 y_1 + x_2 y_2 + x_3 y_3 + x_4 y_4 = 0$, when $T_i = [x_1, x_2, x_3, x_4]$ and $T_j = [y_1, y_2, y_3, y_4]$

1	2	5	8	9	14	17	20	23	26	29	32	35	38
	5	14	14	14	2	5	5	2	8	9	2	9	8
	8	26	29	23	17	29	23	26	20	20	35	17	17
	9	38	35	32	20	32	35	29	32	38	38	26	23
2	1	9	10	11	14	15	16	23	24	25	32	33	34
	9	14	14	14	1	9	9	1	16	10	1	10	11
	10	23	24	25	15	24	25	24	11	15	33	16	15
	11	32	34	33	16	33	34	25	32	32	34	23	23
. . .	.	.	.	.	.	.	.	.	.	.	.	.	.
	.	.	.	.	.	.	.	.	.	.	.	.	.
	.	.	.	.	.	.	.	.	.	.	.	.	.
40	4	6	8	11	15	17	22	23	28	30	34	36	38
	6	15	17	17	4	6	6	4	8	11	11	8	4
	8	28	23	28	17	30	23	28	22	22	15	15	34
	11	38	38	36	22	34	36	30	34	38	23	30	36

Theorem 1.7

The projective space of in field three is a code with a parameters [n = 40,d=13,e =6, $M=3^{36}$]

proof: The space $\pi_3$has an incidence matrix $A=(a_{ij})$,where

$a_{ij} = 1$ if $T_j \in \pi_i$ And also condition $a_{ij} = 0$ if $T_j \notin \pi_i$

After applying the theorem we will have a table of the planes on which the point lie and which do not and in field 3we have 0,1,2 where z=[0,0,0,0,0,0,0,0,0,0,0,0,0,0,0…,0,0,0,0,0] and u=[1,1,1,1,1,1,1…,1,1,1,1,1,1,1,1,1] and w =[2,2,2,2,2,2,2,2,2,2,2…,2,2,2,2,2,2,2] and then we have the table m from the law $m_i = u + l_i$ and table V from $v_i = w + l_i$ and then find these values $d(z, \pi_i)$and $d(u,\pi_i), d(w,\pi_i), d(\pi_i,\pi_j), d(m_i,\pi_i), d(\pi_i,v_i), d(z,m_i), d(u,m_i), d(w,m_i), d(m_i,m_j), d(m_i,v_j), d(z,v_i), d(u,v_i), d(w,v_i), d(v_i,v_j)$ and $i \neq j$ in the following tables of the planes .

	T_1	T_2	T_3	T_4	.	.	.	T_{37}	T_{38}	T_{39}	T_{40}
$\boldsymbol{\pi_1}$	0	1	0	0	.	.		0	1	0	0
$\boldsymbol{\pi_2}$	1	0	0	0	.	.		0	0	0	0
$\boldsymbol{\pi_3}$	0	0	0	1	.	.		1	0	1	0
$\boldsymbol{\pi_4}$	0	0	1	0	.	.		0	0	0	1
.	.	.	.	.	.	.		.	.	.	.
.	.	.	.	.	.	.		.	.	.	.
.	.	.	.	.	.	.	.	.	.	.	.
$\boldsymbol{\pi_{37}}$	0	0	1	0	.	.	.	0	0	1	0
$\boldsymbol{\pi_{38}}$	1	0	0	0	.	.	.	0	1	1	1
$\boldsymbol{\pi_{39}}$	0	0	1	0	.	.	.	1	1	0	0
$\boldsymbol{\pi_{40}}$	0	0	0	1	.	.	.	0	1	0	0

Now the table of m_i

$\mathbf{m_1}$	1	2	1	1	.	.	.	1	2	1	1
$\mathbf{m_2}$	2	1	1	1	.	.	.	1	1	1	1
$\mathbf{m_3}$	1	1	1	2	.	.	.	2	1	2	1
$\mathbf{m_4}$	1	1	2	1	.	.	.	1	1	1	2
.	.	.	.	.	.	.	.	.	.	.	.
.	.	.	.	.	.	.	.	.	.	.	.
.	.	.	.	.	.	.	.	.	.	.	.
$\mathbf{m_{37}}$	1	1	2	1	.	.	.	1	1	2	1
$\mathbf{m_{38}}$	2	1	1	1	.	.	.	1	2	2	2
$\mathbf{m_{39}}$	1	1	2	1	.	.	.	2	2	1	1
$\mathbf{m_{40}}$	1	1	1	2	.	.	.	1	2	1	1

DOI: https://doi.org/10.31972/ticma2022

The table of v_i

$\mathbf{v_1}$	2	0	2	2	.	.	.	2	0	2	2
$\mathbf{v_2}$	0	2	2	2	.	.	.	2	2	2	2
$\mathbf{v_3}$	2	2	2	0	.	.	.	0	2	0	2
$\mathbf{v_4}$	2	2	0	2	.	.	.	2	2	2	0
.	.	.	.	.	.	.	.	.	.	.	.
.	.	.	.	.	.	.	.	.	.	.	.
.	.	.	.	.	.	.	.	.	.	.	.
$\mathbf{v_{37}}$	2	2	0	2	.	.	.	2	2	0	2
$\mathbf{v_{38}}$	0	2	2	2	.	.	.	2	0	0	0
$\mathbf{v_{39}}$	2	2	0	2	.	.	.	0	0	2	2
$\mathbf{v_{40}}$	2	2	2	0	.	.	.	2	0	2	2

these values d(z,π_i)=13 and d(u,π_i)=27,d(w,π_i)=40,d(π_i,π_j) =18,d(m_i,π_i) =40 d(π_i,v_i)=40,d(z,m_i)=40,d(u,m_i)=13,d(w,m_i)=27,d(m_i,m_j)=18,d(m_i,v_i)=40,d(z,v_i)=27,d(u,v_i)=40,d(w,v_i)=13,d(v_i,v_j) =18.If we substitute the values of n = 40,d= 13,e =6,Hence C is a(40,3^{36},13)-code .And applying the theorem 2.2.3 we gets that :

$3^{36}\{\binom{40}{0}+\binom{40}{1}(2)+\binom{40}{2}(4)+\binom{40}{3}(8)+\binom{40}{4}(16)+\binom{40}{5}(32)+\binom{40}{6}(64)\}$

$= 3^{36}(1+80+3120+79040+1462240+21056256+245656320)$

$= 3^{36}(1+80+3120+79040+1462240+21056256+245656320)$

$\neq q^n$, n = 40 By corollary 1.6 therefore C is not perfect

3. CONCLUSIONS

The application of the coding theory to certain fields in space and plane, we summarize them in the following table:

Acknowledgments

The research is supported by the department of Mathematics, College of Education for Pure Science, University of Mosul, Mosul, Iraq.The authors declare that there are no conflicts of interest regarding this work.

DOI: https://doi.org/10.31972/ticma2022

REFERENCES

[1] Abdulla, A.A.A. and Yahya, N.Y.K., 2021, May. A Geometric Construction of Surface Complete (k, r)-cap in PG (3, 7). In *Journal of Physics: Conference Series* (Vol. 1879, No. 2, p. 022112). IOP Publishing.
[2] Abdullah, F.N. and Yahya, N.Y.K., 2020. Bounds on minimum distance for linear codes over GF (q). *Italian Journal of Pure and Applied Mathematics*, p.894.
[3] Al-Mukhtar, A.S., 2008. *Complete Arcs and Surfaces in three Dimensional Projective Space Over Galois Field* (Doctoral dissertation, Ph. D. Thesis, University of Technology, Iraq).
[4] Al-Mukhtar, Sh. 2012. On Projective 3-Space Over Galois Field. Ibn AL-Haitham J. Pure and App. Sci., 25(1), 239-265.
[5] AL-Seraji, N.A. and Ajaj, H.L. 2019. Some Applications of Coding Theory in the Projective Plane of Order Four. *Al-Mustansiriyah Journal of Science*, 30(1), 152-157.
[6] Al-Zangana, E.B. and Yahya, N.Y.K., 2022. Subgroups and Orbits by Companion Matrix in Three Dimensional Projective Space. *Baghdad Science Journal*, 0805-0805.
[7] Hirschfeld, J. W. P., 1998. *Projective Geometries Over Finite Field. 2nd Edition*, Oxford Mathematical Monograph, The Clarendon press, Oxford University press, New York.
[8] Hirschfeld, J. W. P., 2014. Coding Theory, *Lectures*, Sussex University, UK.
[9] Hirschfeld, J.W. and Storme, L., 2001. The packing problem in statistics, coding theory and finite projective spaces: update 2001. In *Finite geometries* (pp. 201-246). Springer, Boston, MA.
[10] Yahya, N.Y.K., 2022. Applications geometry of space in PG (3, P). *Journal of Interdisciplinary Mathematics*, 25(2), 285-297.
[11] Yahya, N.Y.K. and Al-Zangana, E.B., 2021. The Non-existence of [1864, 3, 1828] 53 Linear Code by Combinatorial Technique. *Computer Science*, 16(4), pp.1575-1581.
[12] Sulaimaan, A.E.M. and Yahya, N.Y.K., 2020, July. The Reverse construction of complete (k, n)-arcs in three-dimensional projective space PG (3, 4). In *Journal of Physics: Conference Series* (Vol. 1591, No. 1, p. 012078). IOP Publishing.
[13] Khalaf, H.M. and Yahya, N.Y.K., 2022, August. A Geometric Construction of (ℜ, r)-cap in PG (3, q) for q prime, 2≤ q≤ 997. In *Journal of Physics: Conference Series* (Vol. 2322, No. 1, p. 012043). IOP Publishing.

Proceeding of 3rd International Conference of Mathematics and its Applications TICMA2022
https://conferences.su.edu.krd/su/ticma2022/
DOI: https://doi.org/10.31972/ticma2022

RESEARCH PAPER

A New Transformation Technique to Solve Multi-Objective Linear Programming Problems

Zhian M. Mahmood[1,a,*] and Nejmaddin A.Sulaiman[1,b]

[1]*Department of Mathematics, College of Education, Salahaddin University, Erbil, 44001, Iraq*

[a]zhian.m.mahmood@su.edu.krd
[b]nejmaddin.sulaiman@su.edu.krd

A B S T R A C T:

In this paper Standard Error of Mean (SEM), as a new technique, is used for transforming multi-objective linear programming problems (MOLPPs) to the single objective linear programming problems (SOLPPs). To this end, an algorithm has been proposed and suggested to solve MOLPPs, which have been tested through numerical examples by employing Excel Solver. However, the study compares the results of other techniques like (Chandra Sen, Optimal Average of Minimax and Maximin, New Arithmetic Average, New Geometric Average, New Harmonic Average, and Advanced Transformation) with the results of this new technique SEM. The numerical results indicate that a new technique in general is promising.

KEY WORDS: Multi-Objective Linear Programming, Geometric Average, Harmonic Average.
DOI: https://doi.org/10.31972/ticma22.15

1. INTRODUCTION:

A single objective function has frequently been optimized (maximized or minimized) using linear programming under certain restrictions. It can be challenging to maximize two or more objectives at once, and this challenge increases if the objectives are incompatible. It was decided to investigate the potential of coming up with a compromise solution that meets all the objectives. Many techniques have been utilized for the purpose of resolving multi-objective optimization problems. In 1983, [1] was the first to introduce the problem of multi-objective linear programming. Following that, several alternative statistical methods were developed that are now followed by numerous intellectuals and specialists.

Many strategies have been presented, particularly in the last four decades. For example, [2] proposed an approach for solving multi-objective fractional programming problems. The algorithm's computer application was tested on a variety of numerical problems, and the technique was improved by employing mean and median values for objective function values [3].

To tackle the challenges of the multi-objective programming, the Chandra Sen method has been enhanced since then. [4] proposed a new approach based on the optimum average technique that was a development of the Chandra Sen [1] and [3] techniques. Moreover, regarding mean and median, [5] offered the harmonic average (mean) technique to turn MOLPPs into single-objective linear programming problems.

*** Corresponding Author: Zhian M. Mahmood**
E-mail: zhian.m.mahmood@su.edu.krd
Article History:
Received: 01/08/2022
Accepted: 15/09/2022
Published: 07/12/2022

https://conferences.su.edu.krd/su/ticma2022/
DOI: https://doi.org/10.31972/ticma2022

[6] also proposed a novel strategy for solving multi-objective linear fractional programming issues utilizing a novel geometric averaging method that outperformed other methods. The newly suggested harmonic averaging approach outperforms all other averaging methods in terms of performance. [7] developed an enhanced transformational strategy for solving MOPP, claiming that the strategy was very simple to compute.

To expand on the previous work, the current research is an attempt to solve the MOLPP as a single linear programming problem using an unproven approach called standard error of mean. Because of its more reasonable and efficient implementations, multi-objective programming has gained popularity among many scholars. The present work describes a MOLPP and proposes a standard error of mean approach to optimize the objective function, where a single objective function is formed from multi-objective functions. The outcome is compared to that of optimization utilizing average and the most current methodologies by implementing Excel solver. The new approach used in the present work and its results outperforms the outcomes of all the other aforementioned techniques.

2. DEFINITIONS:

MULTI-OBJECTIVE LINEAR PROGRAMMING PROBLEMS

The mathematical form of MOLPP is given as follows:

$$Max\ \mathcal{K}_1 = C_1^t x$$
$$Max\ \mathcal{K}_2 = C_2^t x$$
$$\vdots$$
$$Min\ \mathcal{K}_{r+1} = C_{r+1}^t x$$
$$\vdots$$
(1)
$$Min\ \mathcal{K}_s = C_s^t x$$

s/t :-

$$AX\ (\geq, =, or \leq)\ b$$
$$X \geq 0$$

where, b is m-dimensional vector of constants, x is n dimensional vector of decision variables and A is $m \times n$ matrix of constants.

3. ARITHMETIC AVERAGE [8]:

Arithmetic average (AA) which is sometimes referred to as mean, is the most commonly used central value of a distribution. The AA is calculated by the sum of the values of all the observations $y_1, y_2, \dots, y_n$ and this total is divided by the number of observations: AA = $\frac{y_1+y_2+\cdots+y_n}{n}$, where n is the total number of observations.

4. GEOMETRIC AVERAGE [9]:

The geometric average (GA) of n positive observation values $y_1, y_2, \dots, y_n$ is defined as the nth positive root of the product of the values: GA = $\sqrt[n]{y_1 y_2 \dots y_n}$, where n is the total number of observations.

5. HARMONIC AVERAGE [9]:

The harmonic average (HA) is another type of averages of observation values $y_1, y_2, \dots, y_n$: HA= $\frac{n}{\frac{1}{y_1}+\frac{1}{y_2}+\cdots+\frac{1}{y_n}}$, where n is the total number of observations.

DOI: https://doi.org/10.31972/ticma2022

6. STANDARD ERROR OF MEAN [10]:

The standard error of mean (SEM) of n positive observation values $y_1, y_2, \dots, y_n$ is defined mathematically as the standard deviation (SD) of $y_1, y_2, \dots, y_n$ that is divided by the square root of n; $SEM = \frac{SD}{\sqrt{n}}$, where standard deviation SD = $\sqrt{\frac{\sum_{i=1}^{n}(y_i - \text{AA})^2}{n-1}}$, and AA is the arithmetic average of $y_1, y_2, \dots, y_n$.

7. APPLIED TECHNIQUES OF CONVERTING MULTI-OBJECTIVE OPTIMIZATION PROBLEMS INTO SINGLE OPTIMIZATION PROBLEM:

Various strategies are presented in the literature to resolve the MOLPP. Initially, Chandra Sen's approach was employed to solve multi-objective optimization problems, yielding a somewhat poor outcome for the objective function. Then, to solve it, additional known and recommended strategies are applied. These strategies are concisely detailed below.

8. CHANDRA SEN'S (CS) TECHNIQUE [1]:

Using simplex method to solve MOLPP in equation (1), a single value corresponding to each of the objective functions is obtained which are in equation (2).

$$Max\ \mathcal{K}_1 = Л_1$$
$$Max\ \mathcal{K}_2 = Л_2$$
$$\vdots$$
(2)
$$Max\ \mathcal{K}_r = Л_r$$
$$Min\ \mathcal{K}_{r+1} = Л_{r+1}$$
$$\vdots$$
$$Min\ \mathcal{K}_s = Л_s$$

Where $Л_1$, $Л_2$,…, $Л_s$ are values of the objective functions. These values are utilized in Chandra Sen's technique to obtain a single objective function as shown in equation (3).

$$\text{Max } \mathcal{K} = \sum_{i=1}^{r} \frac{\mathcal{K}_i}{|Л_i|} + \sum_{i=r+1}^{s} \frac{\mathcal{K}_i}{|Л_i|}, \quad (3)$$

where $Л_i \neq 0$, i=1, …,s subject to the constraints of equation (1), and the optimum value of the objective functions $Л_i$ may be positive or negative.

9. OPTIMAL AVERAGE OF MINIMAX AND MAXIMIN (OAXN)TECHNIQUE [11]:

m_1 =min { $|Л_i|$ }, i = 1, 2, …, r.
m_2 =max { $|Л_i|$ }, $i = r + 1, \dots, s$.
OAXN = $\frac{m_1+m_2}{2}$. The MOLPP becomes Max $\mathcal{K} = \frac{\sum_{i=1}^{r} Max\ \mathcal{K}_i - \sum_{i=r+1}^{s} Min\ \mathcal{K}_i}{OAXN}$.

10. NEW ARITHMETIC AVERAGE (NAA) TECHNIQUE [12]:

m_1 =min { $|Л_i|$ }, i = 1, …, r.
m_2 =min { $|Л_i|$ }, $i = r + 1, \dots, s$.
NAA = $\frac{m_1+m_2}{2}$. The MOLPP becomes Max $\mathcal{K} = \frac{\sum_{i=1}^{r} Max\ \mathcal{K}_i - \sum_{i=r+1}^{s} Min\ \mathcal{K}_i}{\text{NAA}}$.

11. NEW GEOMETRIC AVERAGE (NGA) TECHNIQUE [12]:

m_1 =min { $|Л_i|$ }, i = 1, …, r.
m_2 =min { $|Л_i|$ }, $i = r + 1, \dots, s$.
NGA= $\sqrt{m_1 m_2}$. The MOLPP becomes Max $\mathcal{K} = \frac{\sum_{i=1}^{r} Max\ \mathcal{K}_i - \sum_{i=r+1}^{s} Min\ \mathcal{K}_i}{\text{NGA}}$.

12. NEW HARMONIC AVERAGE (NHA) TECHNIQUE [7]:

m_1 =min { $|Л_i|$ }, i = 1, …, r.
m_2 =min { $|Л_i|$ }, $i = r + 1, \dots, s$.

DOI: https://doi.org/10.31972/ticma2022

NHA=$\frac{2}{\frac{1}{m_1}+\frac{1}{m_2}}$. The MOLPP becomes Max $\mathcal{K} = \frac{\sum_{i=1}^{r} Max\ \mathcal{K}_i - \sum_{i=r+1}^{s} Min\ \mathcal{K}_i}{NHA}$.

13. ADVANCED TRANSFORMATION (AT) TECHNIQUE [7]:

m_1 =min { $|\Lambda_i|$ }, $i = 1, \ldots, r$.
m_2 =min { $|\Lambda_i|$ }, $i = r + 1, \ldots, s$.
m= min { m_1, m_2 }. The MOLPP becomes Max $\mathcal{K} = \frac{\sum_{i=1}^{r} Max\ \mathcal{K}_i - \sum_{i=r+1}^{s} Min\ \mathcal{K}_i}{m}$.

14. NEW TRANSFORMATION TECHNIQUE: STANDARD ERROR OF MEAN (SEM) TECHNIQUE:

The standard error of mean technique is a proposed technique which is used to come up with a single optimization problem from multi-objective optimization problems. It is denoted by $EM = \frac{SD}{\sqrt{s}}$, SD is the standard deviation of $|\Lambda_i|$, $\forall\ i = 1, \cdots, s$; SD=$\sqrt{\frac{\sum_{i=1}^{s}(|\Lambda_i| - \mathrm{AA})^2}{s-1}}$, and AA is the arithmetic average of $|\Lambda_i|$, $\forall\ i = 1, \cdots, s$.
The MOLPP becomes Max $\mathcal{K} = \frac{\sum_{i=1}^{r} Max\ \mathcal{K}_i - \sum_{i=r+1}^{s} Min\ \mathcal{K}_i}{SEM}$, subject to the same constraints.

3. ALGORITHM:

The following algorithm is followed to obtain the optimal solution for the MOLP problems defined previously via using SEM technique can be summarized through the following steps:

1. Find the value of optimal solution of all the objectives individually by simplex method via Excel solver, which is to be maximized or minimized.
2. Calculate the SEM of the optimal values; $|\Lambda_i|$, $i = 1, \ldots, s$.
3. Construct the combined objective function by subtracting weighted minimization objective function from weighted maximization objective function; $\sum_{i=1}^{r} Max\ \mathcal{K}_i - \sum_{i=r+1}^{s} Min\ \mathcal{K}_i$.
4. Divide the result of step (3) by SEM; $\frac{\sum_{i=1}^{r} Max\ \mathcal{K}_i - \sum_{i=r+1}^{s} Min\ \mathcal{K}_i}{SEM}$.
5. Solve the result (4) by simplex method via employing Excel solver, then the solution of the problem is obtained.

4. NUMERICAL EXAMPLES:

Consider the following multi-objective linear programming problems. The following two examples are solved for the analysis purposes of the present study; the results of the two examples are also compared for the purposes of making a distinction between CS, OAXN, NAA, NGA, NHA and AT techniques and SEM as a more effective technique.

EXAMPLE 1

$$\text{Max } \mathcal{K}_1 = 3x_1 + 2x_2$$
$$\text{Max } \mathcal{K}_2 = 4x_1 + x_2$$
$$\text{Max } \mathcal{K}_3 = 4x_1 - 2x_2$$
$$\text{Max } \mathcal{K}_4 = 15x_1 + 4x_2$$
$$\text{Min } \mathcal{K}_5 = -6x_1 + 2x_2$$
$$\text{Min } \mathcal{K}_6 = -9x_1 + 3x_2$$
$$\text{Min } \mathcal{K}_7 = -5x_1 + 2x_2$$
s/to: -
$$x_1 + x_2 \leq 4$$
$$x_1 - x_2 \leq 2$$
$$x_1, x_2 \geq 0$$

DOI: https://doi.org/10.31972/ticma2022

SOLUTION:
After finding the value of each of the individual objective functions by simplex method employing Excel solver; the results are as below in Table 1:

TABLE 1: Results of Example 1

i	$\mathcal{K}_i$	(x_1, x_2)	$\lvert\mathcal{K}_i\rvert$
1	11	(3,1)	11
2	13	(3,1)	13
3	10	(3,1)	10
4	49	(3,1)	49
5	-16	(3,1)	16
6	-24	(3,1)	24
7	-13	(3,1)	13

EXAMPLE 2

$$\text{Max } \mathcal{K}_1 = 0.5x_1 + 0.66x_2 + 0.833x_3$$
$$\text{Max } \mathcal{K}_2 = 0.25x_1 + 0.33x_2 + 0.415x_3$$
$$\text{Min } \mathcal{K}_3 = 0.2x_1 - 0.34x_2 - 0.3x_3$$
$$\text{Min } \mathcal{K}_4 = 0.3x_1 - 0.32x_2 - 0.32x_3$$
s/to: -
$$3x_1 + 4x_2 + 2x_3 \leq 60$$
$$2x_1 + x_2 + 2x_3 \leq 40$$
$$x_1 + 3x_2 + 2x_3 \leq 80$$
$$x_1, x_2, x_2 \geq 0$$

SOLUTION:

After finding the value of each of the individual objective functions by simplex method employing Excel solver, the results are as below in Table 2:

TABLE 2: Results of Example 2

i	$\mathcal{K}_i$	(x_1, x_2, x_3)	$\lvert\mathcal{K}_i\rvert$
1	18.283	(0,6.667,16.667)	18.283
2	9.12	(0,6.667,16.667)	9.12
3	-7.27	(0,6.667,16.667)	7.27
4	-7.47	(0,6.667,16.667)	7.47

5. RESULTS AND DISCUSSION:

Table 3 summarizes the solutions of the MOLPP using techniques. It shows that the solution of the objective functions is improved when used the proposed new transformation technique SEM is used.

TABLE 3. Comparison between the results of techniques

Techniques	**Example1**				**Example2**			
	$\mathcal{K}$	(x_1, x_2)	**Time**	N. Iterations	$\mathcal{K}$	$(x_1, x_{2,} x_3)$	**Time**	N. Iterations

DOI: https://doi.org/10.31972/ticma2022

CS	7	(3,1)	0.062	2	3.999	(0, 6.667, 16.667)	0.063	2
OAXN	8	(3,1)	0.063	2	5.077	(0, 6.667, 16.667)	0.063	2
NAA	11.826	(3,1)	0.062	2	5.141	(0, 6.667, 16.667)	0.078	2
NGA	11.928	(3,1)	0.047	2	5.174	(0, 6.667, 16.667)	0.078	2
NHA	12.031	(3,1)	0.078	2	5.208	(0, 6.667, 16.667)	0.063	2
AT	13.6	(3,1)	0.078	2	5.796	(0, 6.667, 16.667)	0.062	2
SEM	**23.7**	(3,1)	**0.047**	**2**	**16.114**	(0, 6.667, 16.667)	**0.078**	**2**

It can be seen that in Example 1, the values of x_1, x_2 and the number of iterations do not change in all the techniques; however, the value of objective functions is improved and increased in the techniques successively. As Table 3 shows, the difference in the value of $\mathcal{K}$ is significantly higher using the SEM technique compared to all the previously used techniques. This indicates that the SEM technique is more effective than such techniques as CS, OAXN, NAA, NGA, NHA and AT. There is time difference in solving each problem using each technique as presented in the table. The CS and OAXN techniques needed 0.062 seconds only for the solution of the problem. However, for the transformation of the Example 1, the maximum time required is 0.078 seconds for the NHA and AT techniques; their results are better than OAXN, NAA, NGA and SEM. Interestingly, although the value of $\mathcal{K}$ differs in NGA and SEM techniques, with 11.928 and 23.7, respectively- the required time for solving is the same in the first example. Thus, the highest value of $\mathcal{K}$ does not take the least time.

In Example 2, the less consuming time technique goes for the AT, whereas the most consuming time is needed for NAA, NGA and SEM but with the optimize value 5.141, 5.174 and 16.114, respectively. This reveals that in Excel solver, the required time changes depending on the technique being used and ensures that two different techniques with big differences of optimal values may take the same time. Just like Example 1, in Example 2 also the results of $x_1,\ x_2, x_3$ and the number of iterations remain the same in all the techniques used in the present study. The result of SEM in Example 2 proves to be better than all the other techniques, namely, CS, OAXN, NAA, NGA, NHA and AT.

6. CONCLUSION AND FUTURE WORK:

Different techniques such as CS, OAXN, NAA, NGA, NHA and AT are used to solve MOLPP, and the results are compared in Table 3. As a new transformation technique, SEM is used to transform MOLPP into single linear programming problem. As the obtained results reveal, for transforming MOLPP, SEM is better suited for optimizing MOLPP compared to such techniques as CS, OAXN, NAA, NGA, NHA and AT.

The results show the importance of the proposed SEM as a new transformation technique for the optimizing MOLPP using standard error of mean for the very first time. In Example 1, the consumed time for NGA and SEM is the same although value of $\mathcal{K}$ is remarkably different with 11.928 and 23.7, respectively. Similarly, for solving Example 2, NAA, NGA and SEM takes the same time with 0.078 seconds only despite the great difference in their $\mathcal{K}$ value with 5.141, 5.174 and 16.114, respectively. This reveals that whether the value of $\mathcal{K}$ is greater or not, the required time to solve the MOLPPs remains the same. It cannot be generalized that the greater the value of $\mathcal{K}$ is, the more or less time it will require to solve.

The future studies should compare SEM with techniques other than CS, OAXN, NAA, NGA, NHA and AT to reinforce the results and come up with better results.

DOI: https://doi.org/10.31972/ticma2022

References

[1] Sen, C., 1983. A new approach for multi-objective rural development planning. *The Indian Economic Journal*, 30(4), 91-96.

[2] Abdil-Kadir, M.S. and Sulaiman, N.A. 1993. An Approach for Multi-objective Fractional programming problem. *Journal of the College of Education, University of Salahaddin-Erbil\Iraq*, 3(1), 1-5.

[3] Sulaiman, N.A. and Sadiq, G.W. 2006. Solving the Multi Objective Programming Problem Using Mean and Median Value. *AL-Rafidain Journal of Computer Sciences and Mathematics*, 3(1), 69-83.

[4] Sulaiman, N.A. and Hamadameen, A.Q.O. 2008. Optimal transformation technique to solve multi-objective linear programming problem (MOLPP). *Kirkuk University Journal-Scientific Studies*, 3(2), 96-106.

[5] Sulaiman, N.A. and Mustafa, R.B. 2016. Using harmonic mean to solve multi-objective linear programming problems. *American journal of operations Research*, 6(1), 25-30.

[6] Nahar, S. and Alim, M.A. 2017. A new geometric average technique to solve multi-objective linear fractional programming problem and comparison with new arithmetic average technique. *IOSR Journal of Mathematics (IOSR-JM)*, 13, 39-52.

[7] Yesmin, M. and Alim, M.A. 2021. Advanced Transformation Technique to Solve Multi-Objective Optimization Problems. *American Journal of Operations Research*, 11(3), 166-180.

[8] Huntington, E.V., 1927. Sets of independent postulates for the arithmetic mean, the geometric mean, the harmonic mean, and the root-mean-square. *Transactions of the American Mathematical Society*, 29(1), 1-22.

[9] Forman, E. and Peniwati, K., 1998. Aggregating individual judgments and priorities with the analytic hierarchy process. *European journal of operational research*, 108(1), 165-169.

[10] Barde, M.P. and Barde, P.J. 2012. What to use to express the variability of data: Standard deviation or standard error of mean?. *Perspectives in clinical research*, 3(3), p.113.

[11] Suleiman, N.A. and Nawkhass, M.A. 2013. Transforming and solving multi-objective quadratic fractional programming problems by optimal average of maximin & minimax techniques. *American Journal of Operational Research*, *3*(3), 92-98.

[12] Nahar, S. and Alim, M.A., 2017. A new statistical averaging method to solve multi-objective linear programming problem. *International Journal of Science and Research*, 6, 623-629.

Proceeding of 3rd International Conference of Mathematics and its Applications TICMA2022
https://conferences.su.edu.krd/su/ticma2022/
DOI: https://doi.org/10.31972/ticma2022

RESEARCH PAPER

Combinations of L-Complex Fuzzy t-Norms and t-Conorms

Pishtiwan O. Sabir[1,a] and Aram N. Qadir[2,b,*]
[1]*Department of Mathematics, College of Science, University of Sulaimani, Sulaymaniyah 46001, Iraq.*
[2]*Department of Mathematics, College of Education, University of Garmian, Kalar 46021, Iraq.*

[a]*pishtiwan.sabir@univsul.edu.iq*
[b]*aram.nory89@gmail.com*

A B S T R A C T:
This paper investigates the study of L-complex fuzzy sets. The L-complex fuzzy set, where L is a completely distributive lattice, is a generalization of the complex fuzzy set. The fundamental set theoretic operations on L-complex fuzzy sets are discussed properly, including L-complex fuzzy complement, union and intersection. New procedures are presented to combine the novel concepts of L-complex fuzzy t-norms and t-conorms and look into the conditions that lead to a comparable representation theorem. We have used the axiomatic method, in the sense that our underlying assumptions, especially about L, are abstract; it can thus be ascertained to what extent our results apply to some new problem. On the other hand, our method shows that if mathematics, as we use it, is consistent, so is fuzziness, as we formulate it.

KEY WORDS: Fuzzy set; Complex fuzzy set; L-complex fuzzy set; Fuzzy t-norm; Fuzzy t-conorm.
DOI: https://doi.org/10.31972/ticma22.16

1. INTRODUCTION:

Zadeh developed the notion of fuzzy sets in [1]. Many basic ideas held by scholars at the time were called into question by this unique way of portraying uncertainty. Fuzzy sets, in particular, created a problem for probability theory. Proposing a new instrument for modeling uncertainty, and its core foundation: Aristotelian two-valued logic [2]. As a result, the new theory came under attack. On the other hand, fuzzy sets have grown in popularity in recent years. Have proved to be a popular approach for portraying uncertainty. They're beneficial in a variety of situations. A few decades have passed following Zadeh's landmark paper. There has been a lot of research into fuzzy sets.

Ramot *et al*. [3] were among the first to propose the concept of a complex fuzzy set. As a result, a complex fuzzy set has a range that extends from the closed interval $[0, 1]$ to a disk of radius one on the complex plane. They introduce set-theoretic operations on complex fuzzy sets such as, intersection, union, complement, rotation, and reflection.

Also, provides De Morgan's laws for complex fuzzy sets and complex fuzzy relationships. The phase component of complex fuzzy set memberships, according to Ramot *et al*., may be used to depict periodic issues or recurrent problems considerably more accurately, such as reflecting the influence of financial indicators from two nations on each other over time. He suggested that signal processing is another sector where a complex fuzzy set may be useful. Furthermore, one of the desired uses of complex fuzzy sets, according to Dick [4], is to depict events with roughly periodic activity.

*** Corresponding Author: Aram N. Qadir**
E-mail: aram.nory89@gmail.com
Article History:
Received: 01/08/2022
Accepted: 15/09/2022
Published: 07/12/2022

DOI: https://doi.org/10.31972/ticma2022

Congestion in a large metropolis is a periodic phenomenon that never repeats itself. As a result, sophisticated fuzzy logic, rather simply fuzzy logic, can be utilized to answer certain types of problems more efficiently and precisely.

The significance of this work may lie more in its point of view than in any particular results. The theory is still young, and no doubt many concepts have yet to be formulated, while others have yet to take their final form. However, it should now be possible to visualize the outlines of the theory. One reason for this is the natural feeling that probability theory is not appropriate for treating the kind of uncertainty that appears in study fuzzy systems; this uncertainty seems to be more of an ambiguity than a statistical variation. Similar difficulties arise in a wide variety of problems. It is characteristic of attempts to apply probability theory to them that it is difficult or impossible to estimate the distributions assumed to be involved, that there is uncertainty about the nature of the statistical independence, or that certain parameters are ignored, taken as given, or found difficult to estimate. Under these circumstances, the chief use of L theory has been to partially justify intuitively appealing procedures, to suggest procedures already found useful in complex fuzzy sets, or to provide some sort of insight into the nature of things. This paper develops a basic language, and some combination properties, mainly formal and algebraic, and prepares for new points of view. However, there are related topics of greater mathematical depth. These include an information theory for complex fuzzy sets, the fuzzification of various mathematical structures, and a more detailed treatment of the lattice problem.

The paper has been divided into three sections: In section two, we go through the topic's definitions and ideas, as well as the notations that will be used in the rest of the paper. In section three, we generalize the complex fuzzy set to the L-complex fuzzy set where L is a completely distributive lattice. In addition, we describe various additional operations and laws for an L-complex fuzzy concerning the L-complex fuzzy union, intersection, and complement function, such as distributive property, idempotent property, absorption rule, and so on. In section four, we offer some fundamental L-complex fuzzy set findings for L-complex fuzzy union, L-complex fuzzy intersection, and L-complex fuzzy complement and examine specific instances of these. The last section contains our key results conclusions.

2. PRELIMINARIES

Fuzzy subsets are defined by their membership function but their values can be any number in the unit interval [0,1]. We will use the notation of placing a "bar" over a letter to denote a fuzzy subset. As a consequence, when we replace the requirement that membership functions must be in the unit interval [0, 1] to represented by symbols of an arbitrary set L, that is, at least partially ordered, we obtain fuzzy sets of another generalized type. They are called L-fuzzy sets [5], and their membership grades are from universal set X into L (set L with its ordering is most frequently a lattice).

To study the algebra of fuzzy sets of X, we have to specify union and intersection. Let $\tilde{x} = \tilde{x}_1 \cup \tilde{x}_2$ or $\tilde{x} = \tilde{x}_1 \cap \tilde{x}_2$. The value of $\tilde{x}(x)$ will be a function of the two values $\tilde{x}_1(x)$ and $\tilde{x}_2(x)$ so that $\tilde{x}(x) = u(a,b)$ for union and $\tilde{x}(x) = i(a,b)$ for intersection, with $a = \tilde{x}_1(x)$, $b = \tilde{x}_2(x)$ in the interval [0,1].

Choices for u could be $u(a,b) = a + b - ab$, $u(a,b) = \max(a,b)$, and $u(a,b) = \min\left(1, \sqrt{a^2 + b^2}\right)$. Choices for i are $i(a,b) = ab$, $i(a,b) = \min(a,b)$, and $i(a,b) = \sqrt{\max(0, a^2 + b^2 - 1)}$.

A function C: [0,1] × [0,1] → [0,1] is a t-conorm satisfying the following four axioms:

(1) $C(a,0) = a$,
(2) $C(a,b) = C(b,a)$,
(3) $C(a, C(b,c)) = C(C(a,b), c)$,
(4) $a \le b$ and $c \le d$ implies $C(a,c) \le C(b,d)$.

Axiom 1 is a boundary condition that implies $C(1,1) = 1$, $C(1,0) = 1$. Axiom 2 is symmetric condition and we see that $C(0,1) = 1$ too. Axiom 3 and 4 then says that C is associative and $0 = C(0,0) \le C(0,1)$.

A t-norm T is a function $y = T(a,b)$, $y, a, b \in [0,1]$ satisfying the following axioms:

(1) $T(a,1) = a$,

DOI: https://doi.org/10.31972/ticma2022

(2) $T(a,b) = T(b,a)$,
(3) $T(a,T(b,c)) = T(T(a,b),c)$,
(4) $a \le b$ and $c \le d$ implies $T(a,c) \le T(b,d)$.

Axioms 1, 2 and 4 give $T(1,1) = 1$, $T(0,1) = T(1,0) = T(0,0) = 0$. In sum, T is associative (Axiom 3) which we will need in later sections. section may be divided by subheadings. It should provide a concise and precise description of the experimental results, their interpretation, as well as the experimental conclusions that can be drawn.

3. OPERATIONS OF *L*-COMPLEX FUZZY SETS

The following L-Complex fuzzy complement intersection, and union special operations are utilized in this section.

3.1. *L*-Complex Fuzzy Complement

Let $\tilde{Z}$ be a L-complex fuzzy set on a universal set S and let $\mu(\tilde{Z}|x)$ be x's complex grade of membership in $\tilde{Z}$. Let $C\tilde{Z}$ denote the L-complex fuzzy complement of $\tilde{Z}$ of type C, defined by the function $C: \hat{z}_1 := \{z_1 | z_1 \in \mathbb{C}, |z_1| < k, k = supL\} \longrightarrow \hat{z}_2 := \{z_2 | z_2 \in \mathbb{C}, |z_2| < k, k = supL\}$, which assigns $C\left(\mu(\tilde{Z}|x)\right) = C\mu(\tilde{Z}|x)$, for all $x \in S$. The L-complex fuzzy complement, function C must satisfy at least two of the following requirements:

(1) $|z_1| = 0$ implies $|C(z_1)| = 1$ and $|z_1| = 1$ implies $|C(z_1)| = 0$.
(2) For all $z_1, z_2 \in \hat{z}$ if $|z_1| \le |z_2|$, then $|C(z_1)| \ge |C(z_2)|$.

In most cases, C should satisfy various additional requirements:

(3) C is a continuous function,
(4) For all $z_1 \in \hat{z}$, then $C\big(C(z_1)\big) = z_1$.

Theorem 3.1.1. For all $z \in \hat{z}$ and $\alpha > 0$ The function $|C(z)| = \frac{\alpha^2(1-|z|)}{|z|+\alpha^2(1-|z|)}$ is an L-complex fuzzy complement.

Proof: To prove that function is an L-complex fuzzy complement, we have to show that it satisfies properties (1) and (2) of L-complex fuzzy complement C.

(1) For any $z \in \hat{z}$, if $|z| = 0$, then $|C(z)| = \frac{\alpha^2(1-|z|)}{|z|+\alpha^2(1-|z|)} = \frac{\alpha^2(1-0)}{0+\alpha^2(1-0)} = 1$, and let $|z| = 1$, then clear that

$$|C(z)| = \frac{\alpha^2(1-|z|)}{|z|+\alpha^2(1-|z|)} = \frac{\alpha^2(1-1)}{1+\alpha^2(1-1)} = 0.$$

Hence, $|C(z)| = \frac{\alpha^2(1-|z|)}{|z|+\alpha^2(1-|z|)}$ is as properties (1).

(2) For all $z_1, z_2 \in \hat{z}$, if $|z_1| \le |z_2|$, then

$$|C(z_1)| = \frac{\alpha^2(1-|z_1|)}{|z_1|+\alpha^2(1-|z_1|)} \ge \frac{\alpha^2(1-|z_2|)}{|z_2|+\alpha^2(1-|z_2|)} = |C(z_2)|$$

Hence, $|C(z)| = \frac{\alpha^2(1-|z|)}{|z|+\alpha^2(1-|z|)}$ satisfies properties (2). So that it is a L-fuzzy complexities complement.

Definition 3.1.2. For any L-complex fuzzy complement C, we say $z_e \in \hat{z}$ is the equilibrium of C, if $|C(z_e)| = |z_e|$.

Theorem 3.1.3. For any L-complex fuzzy complement C, the absolute value of equilibrium of C is unique.

Proof: Suppose that z_{e_1} and z_{e_2} are any two equilibrium of L-complex fuzzy complement of C, such that $|z_{e_1}| < |z_{e_2}|$. Then by Definition 3.1.2, we conclude that $|C(z_{e_1})| - |z_{e_1}| = 0$ and $|C(z_{e_2})| - |z_{e_2}| = 0$, that is $|C(z_{e_1})| - |z_{e_1}| = |C(z_{e_2})| - |z_{e_2}|$, and by axiom (2) we now C is non increasing, this means that

DOI: https://doi.org/10.31972/ticma2022

$|C(z_{e_1})| \geq |C(z_{e_2})|$, this implies that $|C(z_{e_1})| - |z_{e_1}| > |C(z_{e_2})| - |z_{e_2}|$, which is a contradiction of our assumption.

Theorem 3.1.4. Suppose that C, is any L-complex fuzzy complement and has an equilibrium z_e, then
$|z| \leq |C(z)|$ if and only if $|z| \leq |z_e|$, $|z| \geq |C(z)|$ if and only if $|z| \geq |z_e|$
for all $z \in \hat{z}$.
Proof: Suppose $|z| > |z_e|$, $|z| = |z_e|$ and $|z| < |z_e|$ in turn. Then, since C is non increasing, so that by (2), $|C(z)| \leq |C(z_e)|$, for $|z| > |z_e|$, $|C(z)| = |C(z_e)|$, for $|z| = |z_e|$ and $|C(z)| \geq |C(z_e)|$, for $|z| < |z_e|$. Since clearly by definition equilibrium $|C(z_e)| = |z_e|$. So that, by substitution, we can say $|C(z)| \leq |z_e|$, $|C(z)| = ||z_e||$ and $|C(z)| \geq ||z_e||$, respectively. From our assumption we can additional rewrite these as $|C(z)| > |z|$, $|C(z)| = |z|$, and $|C(z)| < |z|$, respectively. So that if $|z| \leq |z_e|$ by above inequality ($|C(z)| \geq |z_e|$), we get $|z| \leq |C(z)|$, also when, $|z| \geq |z_e|$, by inequality $|C(z)| \leq |z_e|$, we get $|z| \geq C(z)$. Conversely, similar form.

Definition 3.1.5. For each L-complex fuzzy complement C, we called $z_d \in \hat{z}$ is dual point of $z \in \hat{z}$, such that $|C(z_d)| - |z_d| = |z| - |C(z)|$.

Theorem 3.1.6. If z_e is the equilibrium of complement C, then $(z_e)_d = z_e$.
Proof: If we assume that $z_e = z \in \hat{z}$ then by Definition of equilibrium $|C(z_e)| - |z_e| = 0$. Moreover, if $z_e = z_d$, then $|C(z_d)| - |z_d| = 0$. So, it is clear that the equation $|C(z^d)| - |z^d| = |z| - |C(z)|$ holds when $z_d = z_e = z$.

Theorem 3.1.7. For all $z \in \hat{z}$, $z_d = C(z)$ if and only if $|C(C(z))| = |z|$.
Proof: Suppose that $z_d = C(z)$, By Definition 3.1.5, we get $|C(C(z))| - |C(z)| = |z| - |C(z)|$. So that $|C(C(z))| = |z|$. Conversely, let $|C(C(z))| = |z|$, then by substation $|C(C(z))|$ for $|z|$, in Definition 3.1.5, we get $|C(z_d)| - |z_d| = |C(C(z))| - |C(z)|$, This implies that $z_d = C(z)$.

3.2 *L*-Complex Fuzzy Intersection *t*-Norms

Let $\tilde{Z}_1$ and $\tilde{Z}_2$ be any two L-complex fuzzy sets with complex-valued membership functions $\mu(\tilde{Z}_1|x)$ and $\mu(\tilde{Z}_2|x)$, respectively. The intersection between them is defined by a function of form $I: \hat{z}_1 \times \hat{z}_1 \longrightarrow \hat{z}_2$, which returns the membership function of $\tilde{Z}_1 \cap \tilde{Z}_1$ assigns $\mu(\tilde{Z}_1 \cap \tilde{Z}_1|x) = I(\mu(\tilde{Z}_1|x), \mu(\tilde{Z}_2|x))$, for all $x \in S$. A fuzzy intersection I is a binary operation satisfied that s at least four of the following properties for all $z_1, z_2, z_3, z_4 \in \hat{z}$}:

(1) If $|z_2| = 1$, then $|I(z_1, z_2)| = |z_1|$;
(2) $|z_2| \leq |z_3|$ implies $|I(z_1, z_2)| \leq |I(z_1, z_3)|$;
(3) $I(z_1, z_2) = I(z_2, z_1)$;
(4) $I(z_1, I(z_2, z_4)) = I(I(z_1, z_2), z_4)$.

In most cases, I should satisfy various additional requirements:

(5) I is a continuous function;
(6) $|I(z_1, z_1)| < |z_1|$;
(7) $|z_1| \leq |z_3|$ and $|z_2| \leq |z_4| \Longrightarrow |I(z_1, z_2)| \leq |I(z_3, z_4)|$.

We have the following examples that can be used as an L-complex fuzzy intersection, each defined for all $z_1, z_2 \in \hat{z}$,
(1) $I_m(z_1, z_2) = \min(|z_1|, |z_2|)$.
(2) $I_P(z_1, z_2) = |z_1| \cdot |z_2|$.
(3) $I_b(z_1, z_2) = \max\{|z_1| + |z_2| - 1, 0\}$.

DOI: https://doi.org/10.31972/ticma2022

$$(4)\ I_d(z_1,z_2)=\begin{cases}|z_1| & \text{when } |z_2|=1\\ |z_2| & \text{when } |z_1|=1.\\ 0 & \text{otherwIse}\end{cases}$$

Proposition 3.2.1. For all $z_1, z_2 \in \hat{z}$, $I_d(z_1,z_2) \le |I(z_1,z_2)| \le I_m(z_1,z_2)$.
Proof: First we prove the left-hand right inequality, if $|z_2|=1$ then by boundary condition $|I(z_1,z_2)|=|z_1|$ and if $|z_1|=1$ by the same condition, we get $|I(z_1,z_2)|=|z_2|$. On the other hand, we have $|I(z_1,z_2)| \le \min(|z_1|,|z_2|)$, so that $|I(z_1,0)| \le min(|z_1|,0)=0$ and $|I(0,z_1)| \le min(0,|z_1|)=0$. This is enough to say $|I(z_1,0)|=|I(0,z_2)|=0$. Therefore, by monotonicity condition we obtain that $|I(z_1,z_2)| \ge |I(z_1,0)|=|I(0,z_2)|=0$.
Now, we prove of the second inequality. By the monotonicity condition we have $|I(z_1,z_2)| \le |I(z_1,1)|$, and by boundary condition we have to get $|I(z_1,z_2)| \le |I(z_1,1)|=|z_1|$. Next by commutatively $|I(z_1,z_2)|=|I(z_2,z_1)| \le |I(z_2,1)|=|z_2|$. Hence, $|I(z_1,z_2)|$ is less than or equal to $|z_1|$ and $|z_2|$, and this implies that $|I(z_1,z_2)| \le min(|z_1|,|z_2|)$.

Proposition 3.2.2. For all $z_1, z_2 \in \hat{z}$, $I_p(z_1,z_2) \le I_m(z_1,z_2)$.
Proof: At first, if $|z_1|=0$ or $|z_2|=0$, then $I_p(z_1,z_2)=I_m(z_1,z_2)=0$. Next, if $|z_1|=1$ (resp. $|z_2|=1$), then $I_p(z_1,z_2)=I_m(z_1,z_2)=|z_2|$ (resp. $I_p(z_1,z_2)=I_m(z_1,z_2)=|z_1|$). Finally, if $(|z_1|,|z_2|<k, k=supL)\backslash\{0,1\}$, then we obtain that $|z_1|\cdot|z_2| \le |z_1|$ and $|z_1|\cdot|z_2| \le |z_2|$. In other words, $|z_1|\cdot|z_2| \le \min(|z_1|,|z_2|)$, implies that $I_p(z_1,z_2) \le I_m(z_1,z_2)$.

Proposition 3.2.3. For all $z_1, z_2 \in \hat{z}$, $I_b(z_1,z_2) \le I_p(z_1,z_2)$.
Proof: In the case of $|z_2|$ equals one or zero, then $I_b(z_1,z_2)=I_p(z_1,z_2)$. But if $(|z_1|,|z_2|<k, k=supL)\backslash\{0,1\}$, then $I_b(z_1,z_2)=\max\{0,|z_1|+|z_2|-1\} \le I_p(z_1,z_2)$ because of $|z_1|+|z_2|-1 \le |z_1|\cdot|z_2|$.

Proposition 3.2.4. For all $z_1, z_2 \in \hat{z}$, $I_d(z_1,z_2) \le I_b(z_1,z_2)$.
Proof: First, if $|z_1|=1$ (resp. $|z_2|=1$), then $I_d(z_1,z_2)=|z_2|=I_b(z_1,z_2)$ (resp. $I_d(z_1,z_2)=|z_1|=I_b(z_1,z_2)$). Next, if at least one of $|z_1|$, $|z_2|$ is zero, $\forall z_1,z_2 \in \hat{z}$ then $I_b(z_1,z_2)=0=I_d(z_1,z_2)$. Finally, if $(|z_1|,|z_2|<k, k=supL)\backslash\{0,1\}$, then $I_b(z_1,z_2)=\max\{0,|z_1|+|z_2|-1\} \ge I_d(z_1,z_2)=0$. Hence, $I_d(z_1,z_2) \le I_b(z_1,z_2)$.

Corollary 3.2.5. For all $z_1, z_2 \in \hat{z}$, $I_d(z_1,z_2) \le I_b(z_1,z_2) \le I_p(z_1,z_2) \le I_m(z_1,z_2)$.
Proof: The proof follows from Proposition 3.2.1, Proposition 3.2.2, Proposition 3.2.3 and Proposition 3.2.4.

Theorem 3.2.6. If I is an L-complex fuzzy intersection t-norms then $I(z_1,z_2+z_3)=I(z_1,z_2)+I(z_1,z_3)$ if I is an algebraic product that is $I=I_p$, $\forall\ z_1,z_2,z_3 \in \hat{z}$ and $|z_2+z_3| \in L$.
Proof: By t-norms I is an algebraic product we can say that

$$\begin{aligned} I(z_1,z_2+z_3) &= |z_1|\cdot|z_2+z_3| \\ &= |z_1\cdot(z_2+z_3)| = |z_1||z_2|+|z_1||z_3| \\ &= I(z_1,z_2)+I(z_1,z_3). \end{aligned}$$

Theorem 3.2.7. If I is an algebraic product, then $I\big(I(z_1,z_2),I(z_3,z_4)\big)=I\big(I(z_1,z_3),I(z_2,z_4)\big)$ For all $z_1,z_2,z_3,z_4 \in \hat{z}$.
Proof: Since I be an algebraic product so that

$$\begin{aligned} I\big(I(z_1,z_2),I(z_3,z_4)\big) &= |I(z_1,z_2)|\cdot|I(z_3,z_4)| = \big||z_1|\cdot|z_2|\big|\cdot\big||z_3|\cdot|z_4|\big| \\ &= \big||z_1|\cdot|z_2|\cdot|z_3|\cdot|z_4|\big| = \big||z_1|\cdot|z_3|\cdot|z_2|\cdot|z_4|\big| \\ &= \big||z_1|\cdot|z_3|\big|\cdot\big||z_2|\cdot|z_4|\big| = |I(z_1,z_3)|\cdot|I(z_2,z_4)| \\ &= I\big(I(z_1,z_3),I(z_2,z_4)\big). \end{aligned}$$

DOI: https://doi.org/10.31972/ticma2022

3.3 L-Complex Fuzzy Union t-Conorms

Let $\tilde{Z}_1$ and $\tilde{Z}_2$ be any two L-complex fuzzy sets with complex-valued membership functions $\mu(\tilde{Z}_1|x)$ and $\mu(\tilde{Z}_2|x)$, respectively. The union of $\tilde{Z}_1$ and $\tilde{Z}_2$ is defined by a function of the form $U: \hat{z}_1 \times \hat{z}_1 \longrightarrow \hat{z}_2$, which returns the membership function of $\tilde{Z}_1 \cup \tilde{Z}_1$ assigns $\mu(\tilde{Z}_1 \cup \tilde{Z}_1|x) = U\big(\mu(\tilde{Z}_1|x), \mu(\tilde{Z}_2|x)\big)$, for all $x \in S$. The L-complex fuzzy union U is a binary operation that satisfies at least four of the following properties for all $z_1, z_2, z_3, z_4 \in \hat{z}$:

(1) If $|z_2| = 0$, then $|U(z_1, z_2)| = |z_1|$;
(2) $|z_2| \leq |z_3|$ implies $|U(z_1, z_2)| \leq |U(z_1, z_3)|$;
(3) $U(z_1, z_2) = U(z_2, z_1)$;
(4) $U\big(z_1, U(z_2, z_4)\big) = U(U(z_1, z_2), z_4)$.

In most cases, it is desirable that U should satisfy various additional requirements:

(5) U is a continuous function;
(6) $|U(z_1, z_1)| > |z_1|$;
(7) $|z_1| \leq |z_3|$ and $|z_2| \leq |z_4| \Longrightarrow |U(z_1, z_2)| \leq |U(z_3, z_4)|$.

We have some examples that can be used for the L-complex fuzzy union as the following, each defined for all $z_1, z_2 \in \hat{z}$,

(1) $U_m(z_1, z_2) = \max(|z_1|, |z_2|)$.
(2) $U_P(z_1, z_2) = |z_1| + |z_2| - |z_1| \cdot |z_2|$.
(3) $U_b(z_1, z_2) = \min\,(|z_1| + |z_2|, 1)$.
(4) $U_d(z_1, z_2) = \begin{cases} |z_1| \; when \; |z_2| = 0 \\ |z_2| \; when \; |z_1| = 0. \\ 1 \quad otherwIse. \end{cases}$

Proposition 3.3.1. For all $z_1, z_2 \in \hat{z}$ then $U_m(z_1, z_2) \leq |U(z_1, z_2)| \leq U_d(z_1, z_2)$.
Proof: First we prove the left-hand right inequality. By the monotonicity condition, we have $|U(z_1, z_2)| \geq |U(z_1, 0)|$, and by boundary condition, we have to get $|U(z_1, z_2)| \geq |U(z_1, 0)| = |z_1|$. Next by commutatively, $|U(z_1, z_2)| = |U(z_2, z_1)| \geq |U(z_2, 0)| = |z_2|$. Hence, $|U(z_1, z_2)|$ is greater than or equal to $|z_1|$ and $|z_2|$, and this implies that $|U(z_1, z_2)| \geq max(|z_1|, |z_2|)$.
Now, we prove the second inequality, if $|z_2| = 0$ then by the boundary condition $|U(z_1, z_2)| = |z_1|$ and if $|z_1| = 0$ by the same condition, we get $|U(z_1, z_2)| = |z_2|$. Moreover, we have $|U(z_1, z_2)| \geq \max(|z_1|, |z_2|)$, so that $|U(z_1, 1)| \geq max(|z_1|, 1) = 1$ and $|U(1, z_1)| \geq max(1, |z_1|) = 1$. This is enough to say $|U(z_1, 1)| = |U(1, z_2)| = 1$. Therefore, by monotonicity condition, we get that $|U(z_1, z_2)| \leq |U(z_1, 1)| = |U(1, z_2)| = 1$.

Proposition 3.3.2. For all $z_1, z_2 \in \hat{z}$, then $U_b(z_1, z_2) \leq U_d(z_1, z_2)$.
Proof: First, if $|z_1| = 0$ (resp. $|z_2| = 0$), then $U_b(z_1, z_2) = U_d(z_1, z_2) = |z_1|$ (resp. $U_b(z_1, z_2) = U_d(z_1, z_2) = |z_2|$) respectively. Next, if $|z_1| = 1$ or $|z_2| = 1$, then $U_b(z_1, z_2) = U_d(z_1, z_2) = 1$. Finally, if $(|z_1|, |z_2| < k, k = supL) \backslash \{0,1\}$, then we say that $\min\{1, |z_1| + |z_2|\} \leq 1 = U_d(z_1, z_2)$. This implies that $U_b(z_1, z_2) \leq U_d(z_1, z_2)$.

Proposition 3.3.3. For all $z_1, z_2 \in \hat{z}$ then $U_m(z_1, z_2) \leq U_s(z_1, z_2)$.
Proof: At first, if $|z_1| = 1$ or $|z_2| = 1$, then $U_m(z_1, z_2) = U_s(z_1, z_2) = 1$. Next, if $|z_1| = 0$ (resp. $|z_2| = 0$), then $U_m(z_1, z_2) = U_s(z_1, z_2) = |z_2|$, (resp. $U_m(z_1, z_2) = U_s(z_1, z_2) = |z_1|$). Finally, if $(|z_1|, |z_2| < k, k = supL) \backslash \{0,1\}$, then we illustrate that $|z_1| + |z_2| - |z_1| \cdot |z_2| \geq |z_1|$, and $|z_1| + |z_2| - |z_1| \cdot |z_2| \geq |z_2|$, so that $|z_1| + |z_2| - |z_1| \cdot |z_2| \geq \max\,(|z_1|, |z_2|)$, implies that $U_m(z_1, z_2) \leq U_s(z_1, z_2)$.

Proposition 3.3.4. For all $z_1, z_2 \in \hat{z}$ then $U_s(z_1, z_2) \leq U_b(z_1, z_2)$.

DOI: https://doi.org/10.31972/ticma2022

Proof: In the case of $|z_1|$ or $|z_2|$ equals one or zero, $U_s(z_1, z_2) = U_b(z_1, z_2)$. But if $(|z_1|, |z_2| < k, k = supL)\backslash\{0,1\}$, then $U_s(z_1, z_2) = |z_1| + |z_2| - |z_1| \cdot |z_2| \leq U_b(z_1, z_2)$, because of $|z_1| + |z_2| - |z_1| \cdot |z_2| \leq |z_1| + |z_2|$.

Corollary 3.3.5. For all $z_1, z_2 \in \hat{z}$, $U_m(z_1, z_2) \leq U_s(z_1, z_2) \leq U_b(z_1, z_2) \leq U_d(z_1, z_2)$.
Proof: The proof follows from Proposition 3.3.1, Proposition 3.3.2, Proposition 3.3.3, and Proposition 3.3.4.

4. COMBINATIONS OF OPERATIONS

L-complex fuzzy sets satisfy the generalization of De Morgan's laws if and only if $|C(z)| = |z|$. That is

$$C\big(I(z_1, z_2)\big) = U\big(C(z_1), C(z_2)\big) \text{ and } C\big(U(z_1, z_2)\big) = I\big(C(z_1), C(z_2)\big)$$

for all $z, z_1, z_2 \in \hat{z}$.

Theorem 4.1. The operations I_d, U_d and L-complex fuzzy complement are satisfied with the De Morgan's laws if $|C(z)| = |z|$, for all $z \in \hat{z}$.
Proof: First suppose $|z_1| = 0$, then by properties (1) of C, we have $|C(z_1)| = 1$, for all $z_1, z_2 \in \hat{z}$, so that we have two Cases,
Case (1); If $|z_2| = 1$, then by properties (1) of C we get $|C(z_2)| = 0$, so that

$$C\big(U_d(z_1, z_2)\big) = C(|z_2|) = |C(z_2)| = I_d\big(C(z_1), C(z_2)\big)$$

and,

$$C\big(I_d(z_1, z_2)\big) = C(|z_1|) = |C(z_1)| = U_d\big(C(z_1), C(z_2)\big)$$

Case (2); If $|z_2|$ is not equal to one, implies that $|C(z_2)|$ not equal to zero, so that

$$C\big(I_d(z_1, z_2)\big) = C(0) = 1 = U_d\big(C(z_1), C(z_2)\big)$$

and,

$$C\big(U_d(z_1, z_2)\big) = C(|z_2|) = |C(z_2)| = I_d\big(C(z_1), C(z_2)\big)$$

Next, If $|z_2| = 0$, then $|C(z_2)| = 1$, for all $z_1, z_2 \in \hat{z}$, so that we have two cases
Case (i); If $|z_1| = 1$, then by properties (1) of C we get that $|C(z_1)| = 0$, so that

$$C\big(U_d(z_1, z_2)\big) = C(|z_1|) = |C(z_1)| = I_d\big(C(z_1), C(z_2)\big)$$

and,

$$C\big(I_d(z_1, z_2)\big) = C(|z_2|) = |C(z_2)| = U_d\big(C(z_1), C(z_2)\big)$$

Case (ii) If $|z_1|$ is equal to one, implies that $|C(z_1)|$ is not equal to zero, so that

$$C\big(I_d(z_1, z_2)\big) = C(0) = 1 = U_d\big(C(z_1), C(z_2)\big)$$

and,

$$C\big(U_d(z_1, z_2)\big) = C(|z_1|) = |C(z_1)| = I_d\big(C(z_1), C(z_2)\big)$$

Finally, If $(|z_1|, |z_2| < k, k = supL)\backslash\{0,1\}$, then clear that $(C(z_1), C(z_2) < k, k = supL)\backslash\{0,1\}$.

$$C\left(I_p(z_1, z_2)\right) = C(0) = 1 = U_d\big(C(z_1), C(z_2)\big)$$

and,

$$C\big(U_d(z_1, z_2)\big) = C(1) = 0 = I_d\big(C(z_1), C(z_2)\big)$$

Hence, they satisfy De Morgan's laws.

Theorem 4.2. The operations I_m, U_m and L-complex fuzzy complement C are satisfies the De Morgan's laws if $|C(z)| = |z|$. For all $z \in \hat{z}$.
Proof: Suppose that $|z_1| \leq |z_2|$ for all $z_1, z_2 \in \hat{z}$, then by property (2) of C, clear that $|C(z_1)| \geq |C(z_2)|$, so that

$$C\big(I_m(z_1, z_2)\big) = C(\min(|z_1|, |z_2|)) = C(|z_1|) = |C(z_1)|, \quad by\ |C(z)| = |z|$$
$$= \max\big((|C(z_1)|, |C(z_2)|)\big) = U_m\big(C(z_1), C(z_2)\big).$$

and

$$C\big(U_m(z_1, z_2)\big) = C(\max(|z_1|, |z_2|)) = C(|z_2|) = |C(z_2)|, \quad by\ |C(z)| = |z|$$

DOI: https://doi.org/10.31972/ticma2022

$$= \min\big((|C(z_1)|, |C(z_2)|)\big) = I_m\big(C(z_1), C(z_2)\big).$$

This implies they satisfy the De Morgan's laws.

Theorem 4.3. For a t-conorm U and L-complex fuzzy complement C, the binary operation I on $\hat{z}$ defined by $I(z_1, z_2) = C\left(U\big(C(z_1), C(z_2)\big)\right)$, is a t-norm if $|C(z)| = C|z|$, for all $z, z_1, z_2 \in \{z \mid z \in \mathbb{C}, |z| < k, k = supL\}$.

Proof: To prove that theorem we have to show that $I(z_1, z_2) = C\left(U\big(C(z_1), (z_2)\big)\right)$ is satisfied all conditions I.

(1) Let $|z_2| = 1$ then by properties (1) of C we get $|C(z_2)| = 0$, so that by definition I we have

$$\begin{aligned} |I(z_1, z_2)| &= \left|C\left(U\big(C(z_1), (z_2)\big)\right)\right| \\ &= C\big(\left|U\big(C(z_1), C(z_2)\big)\right|\big), \quad \text{by } |C(z)| = C|z|, \\ &= C(|C(z_1)|) = \left|C\big(C(z_1)\big)\right|, \text{by properties (2) } of\ I \text{ and } |C(z)| = C|z|, \\ &= |z_1|, \quad \text{by properties (4) of } C. \end{aligned}$$

Hence, I satisfy property (1).

(2) for all $z_1, z_2, z_3 \in \hat{z}$. If $|z_2| \leq |z_3|$ then by monotonicity of C, $|C(z_2)| \geq |C(z_3)|$. Moreover, by monotonicity of U

$$\left|U\big(C(z_1), C(z_2)\big)\right| \geq \left|U\big(C(z_1), C(z_3)\big)\right|,$$

Hence,

$$\begin{aligned} |I(z_1, z_2)| = \left|C\big(U(C(z_1), |C(z_2)|)\big)\right| &= C\left|\big(U(C(z_1), |C(z_2)|)\big)\right| \\ \leq C\left|\big(U(C(z_1), |C(z_3)|)\big)\right| &= \left|C\left(U\big(C(z_1), C(z_3)\big)\right)\right| = |I(z_1, z_3)|. \end{aligned}$$

This implies that I satisfies property (2).

(3) By commutativity of U we have

$$I(z_1, z_2) = C\left(U\big(C(z_1), C(z_2)\big)\right) = C\left(U\big(C(z_2), C(z_1)\big)\right) = I(z_1, z_2)$$

So that, I satisfies property (3).

(4) For any $z_1, z_2, z_3 \in \hat{z}$. Then

$$\begin{aligned} I\big(z_1, I(z_2, z_3)\big) &= C\left(U\left(C(z_1), C\big(I(z_2, z_3)\big)\right)\right) \\ &= C\left(U\left(C(z_1), C\left(C\left(U\big(C(z_2), C(z_3)\big)\right)\right)\right)\right) \\ &= C\left(U\left(C(z_1), \left(U\big(C(z_2), C(z_3)\big)\right)\right)\right), \text{by property (4)of } C \\ &= C\left(U\left(U\big(C(z_1), C(z_2)\big), C(z_3)\right)\right), \text{by property (4)of } U \\ &= C\left(U\left(C\left(C\left(U\big(C(z_1), C(z_2)\big)\right)\right), C(z_3)\right)\right), \text{by property (4)of } C \\ &= I(I(z_1, z_2), z_3) \end{aligned}$$

Hence, I satisfys property (4), so that it is a L-complex fuzzy t-norm.

Theorem 4.4. L-complex fuzzy t-norm $I(z_1, z_2) = C\left(U\big(C(z_1), C(z_2)\big)\right)$ is satisfies the De morgan's laws, for any $z_1, z_2 \in \hat{z}$.

Proof: By definition I we have

$$\begin{aligned} C\big(I(z_1, z_2)\big) &= C\left(C\left(U\big(C(z_1), C(z_2)\big)\right)\right) \\ &= U\big(C(z_1), C(z_2)\big), \text{by property (4) of } C. \end{aligned}$$

https://conferences.su.edu.krd/su/ticma2022/
DOI: https://doi.org/10.31972/ticma2022

$$I\big(C(z_1), C(z_2)\big) = C\left(U\left(C\big(C(z_1)\big), C\big(C(z_2)\big)\right)\right)$$
$$= C\big(U(z_1, z_2)\big), \text{By property (4) of } C.$$

Theorem 4.5. For a t-norm I and an L-complex fuzzy complement C, the binary operation U on $\hat{z}$ defined by $U(z_1, z_2) = C\left(I\big(C(z_1), C(z_2)\big)\right)$, is t-conorm if $|C(z)| = C|z|$, for all $z, z_1, z_2 \in \hat{z}$.

Proof: Similar steps with Theorem 4.3.

Hence, U satisfies properties (4), so that it is L-complex fuzzy t-conorm.

Theorem 4.6. L-complex fuzzy t-conorm $U(z_1, z_2) = C\big(I(C(z_1), |C(z_2)|)\big)$ is satisfies the De morgan laws, for any $z_1, z_2 \in \hat{z}$.

Proof: Analogous to the proof of Theorem 4.4.

5. CONCLUSIONS:

This work introduced a new form of set, the L-complex fuzzy set, where L is a completely distributive lattice. This is an extension of the notion of a complex fuzzy set. This work also proposed various applications for the idea of an L-complex fuzzy set. The research started with a look at the basic set-theoretic operations of complement, union and intersection, as well as how these apply to the complicated L-complex fuzzy set. On L-complex fuzzy sets, basic operations and properties were developed derived.

REFERENCES

[1] Zadeh, L.A. 1965. Fuzzy sets. *Information and control*, 8(3), 338-353.

[2] Klir, G.J., St. Clair, U. and Yuan, B., 1997. *Fuzzy set theory: foundations and applications*. Prentice-Hall, Inc..

[3] Ramot, D., Milo, R., Friedman, M. and Kandel, A., 2002. Complex fuzzy sets. *IEEE Transactions on Fuzzy Systems*, 10(2), 171-186.

[4] Dick, S., 2005. Toward complex fuzzy logic. *IEEE Transactions on Fuzzy Systems*, 13(3), 405-414.

[5] Goguen, J.A. 1967. L-fuzzy sets. *Journal of mathematical analysis and applications*, 18(1), 145-174.